



DOUTORAMENTO

CIÊNCIAS BIOMÉDICAS

Portuguese seaweeds, a marine treasure of Actinobacteria producing novel bioactive compounds

Mariana Girão Silva Martins



Portuguese seaweeds, a marine treasure of Actinobacteria producing novel bioactive compounds Mariana Girão Silva Martins



MARIANA GIRÃO SILVA MARTINS

PORTUGUESE SEAWEEDS, A MARINE TREASURE OF ACTINOBACTERIA PRODUCING NOVEL BIOACTIVE COMPOUNDS

Tese de Candidatura ao grau de Doutor em Ciências Biomédicas

Programa Doutoral da Universidade do Porto (Instituto de Ciências Biomédicas de Abel Salazar)

Orientador

Doutora Maria de Fátima Magalhães Carvalho

Investigadora Principal no Centro Interdisciplinar de Investigação Marinha e Ambiental da Universidade do Porto

Professora Auxiliar Convidada no Instituto de Ciências Biomédicas Abel Salazar da Universidade do Porto

Co-orientador (es)

Doutor Pedro Nuno da Costa Leão

Investigador Principal no Centro Interdisciplinar de Investigação Marinha e Ambiental da Universidade do Porto

Doutor Ralph Urbatzka

Investigador Principal no Centro Interdisciplinar de Investigação Marinha e Ambiental da Universidade do Porto

DECLARAÇÃO DE HONRA

Declaro que a presente tese é de minha autoria e não foi utilizada previamente noutro curso ou unidade curricular, desta ou de outra instituição. As referências a outros autores (afirmações, ideias, pensamentos) respeitam escrupulosamente as regras da atribuição, e encontram-se devidamente indicadas no texto e nas referências bibliográficas, de acordo com as normas de referenciação. Tenho consciência de que a prática de plágio e autoplágio constitui um ilícito académico.

Mariana Girão Silva Martins

Moniana Gras Silva Rantins

Within the scope of this Thesis, the following scientific articles and book chapters have been prepared:

PUBLISHED ARTICLES

Girão, M., Alexandrino D.A.M., Weiwei C., Costa I., Zhongjun J., & Carvalho M.F. (2024) Revealing the culturable and non-culturable actinobacterial diversity in two macroalgae species from the northern Portuguese coast. Environmental Microbiology, 26(4), e16620. DOI: 10.1111/1462-2920.16620

This article was fully integrated in Chapter 2 and was not used in another thesis.

Open Access Licensing and Copyright

© 2024 The Authors. Environmental Microbiology published by John Wiley & Sons Ltd. This is an open access article under the terms of the Creative Commons Attribution-NonCommercial License, which permits use, distribution and reproduction in any medium, provided the original work is properly cited and is not used for commercial purposes.

Girão, M., Freitas, S., Martins, T. P., Urbatzka, R., Carvalho, M. F., & Leão, P. N. (2024). Decylprodigiosin: a new member of the prodigiosin family isolated from a seaweed-associated *Streptomyces*. Frontiers in Pharmacology, 15, 1347485. DOI: 10.3389/fphar.2024.1347485

This article was fully integrated in Chapter 5 and was not used in another thesis.

Open Access Licensing and Copyright

© 2024 Girão, Freitas, Martins, Urbatzka, Carvalho and Leão. This is an open-access article distributed under the terms of the Creative Commons Attribution License (CC BY). The use, distribution or reproduction in other forums is permitted, provided the original author(s) and the copyright owner(s) are credited and that the original publication in this journal is cited, in accordance with accepted academic practice. No use, distribution or reproduction is permitted which does not comply with these terms.

PUBLISHED BOOK CHAPTERS

Girão, M., Ribeiro, I., & Carvalho, M.F. (2022). Actinobacteria from Marine Environments: A Unique Source of Natural Products. In Natural Products from Actinomycetes: Diversity, Ecology and Drug Discovery (pp. 1-45). Singapore: Springer Singapore.

SUBMITTED ARTICLES - UNDER REVIEW

Girão M., Lequint Z., Rego A., Costa I., Proença D.N., Morais P.V., & Carvalho M.F. *Nocardiopsis codii* sp. nov. and *Rhodococcus algaerubra* sp. nov., two novel actinomycetes species isolated from macroalgae collected in the northern Portuguese coast. [Under review for publication in the International Journal of Systematic and Evolutionary Microbiology]

This article was fully integrated in Chapter 3 and was not used in another thesis.

Girão, M., Rego, A., Fonseca A.C., Weiwei C., Zhongjun J., Urbatzka, R., Leão, P. N. & Carvalho, M. F. *Bioactive potential of macroalgae-associated Actinomycetota revealed through culture-dependent and -independent approaches.* [Under review for publication in Microbial Biotechnology Journal]

This article was fully integrated in Chapter 4 and was not used in another thesis.

Girão, M., Murillo-Alba J., Martín J., Pérez-Victoria I., Urbatzka, R., Leite R.B., Leão, P. N., Carvalho, M. F., & Reyes F. Cellulamides: new family of marine-sourced peptides from the unexplored *Cellulosimicrobium* Actinomycetota genus. [Under review for publication in Marine Drugs Journal]

This article was fully integrated in Chapter 6 and was not used in another thesis.

Part of the results obtained within the scope of this Thesis were presented in the following national and international conferences/meetings:

ORAL COMMUNICATIONS

Girão, M., Murillo-Alba J., Martín J., Pérez-Victoria I., Urbatzka, R., Leão, P. N., Carvalho, M. F., & Reyes F. "Novel chemistry from a seaweed-associated Actinomycetota" European transdisciplinary networking platform for marine biotechnology COST Action CA18238 (Ocean4Biotech) meeting, 5-7th March 2024, Riga, Latvia

Girão M., Santos M., Gomes M.S., Silva T., Azevedo I.C., Urbatzka R., Leão P.N., & Carvalho M.F. "Seaweed-associated Actinobacteria: a hub of diversity and bioactive metabolites" Blue Think Conference Share Science, Spread Knowledge (BTC), 13th September 2023, Porto, Portugal

Girão M., Azevedo I.C., Urbatzka R., Leão P.N., & Carvalho M.F. "Exploring seaweed-associated Actinobacteria for the discovery of novel bioactive compounds" Trends in Natural Products Research: A PSE Young Scientists' Meeting, 23-26th May 2022, Crete, Greece

Girão M., Azevedo I.C., Urbatzka R., Leão P.N., & Carvalho M.F. "Seaweed-associated Actinobacteria: a hotspot for biotechnology-relevant compounds discovery" XII European Conference on Marine Natural Products, 30th August - 1st September 2021, Galway, Ireland

Girão M., Azevedo I.C., Urbatzka R., Leão P.N., & Carvalho M.F. "Macroalgae-associated Actinobacteria: a hotspot for the discovery of clinically-relevant compounds" 10th International Conference on Marine Biotechnology (BIOPROSP'21), 9-10th March 2021, TromsØ, Norway

Girão M., Azevedo I.C., Urbatzka R., Leão P.N., & Carvalho M.F. "Algae associated Actinobacteria: unveiling their diversity and potential to produce novel bioactive compounds" Blue Think Conference Share Science, Spread Knowledge (BTC), 17th September 2020, Porto, Portugal

POSTER COMMUNICATIONS

Girão, M., Murillo-Alba J., Martín J., Pérez-Victoria I., Urbatzka, R., Leão, P. N., Carvalho, M. F., & Reyes F. "Cellulamides, a new family of marine-sourced peptides from a seaweed-associated *Cellulosimicrobium*" [accepted for poster communication] International Congress on Natural Products Research, 13-17th July 2024, Kraków, Poland

Girão M., Santos M., Gomes M.S., Silva T., Azevedo I.C., Urbatzka R., Leão P.N., & Carvalho M.F. "Seaweed-associated Actinobacteria: a hotspot for biotechnology-relevant compounds discovery" XVII International Symposium on Marine Natural Products | XIII European Conference on Marine Natural Products, 3-8th September 2023, Granada, Spain

Girão M., Azevedo I.C., Urbatzka R., Leão P.N., & Carvalho M.F. "Mining seaweed-associated Actinobacteria secondary metabolism to uncover novel bioactive compounds" 11th International Conference on Marine Biotechnology (BIOPROSP'23), 14-16th March 2023, TromsØ, Norway

Girão M., Azevedo I.C., Urbatzka R., Leão P.N., & Carvalho M.F. "Unlocking the diversity and bioactive potential of seaweed-associated Actinobacteria" 2nd FEMS Conference on Microbiology, 30th June - 2nd July 2022, Belgrade, Serbia

Girão M., Azevedo I.C., Urbatzka R., Leão P.N., & Carvalho M.F. "Mining seaweed associated Actinobacteria for biotechnologically relevant compound discovery" MICROBIOTEC, 23-26th November 2021, Lisbon, Portugal

Girão M., Azevedo I.C., Urbatzka R., Leão P.N., & Carvalho M.F. "Actinobacteria from seaweeds: Unveiling their diversity and bioactive potential" Blue Think Conference Share Science, Spread Knowledge (BTC), 23rd September 2021, Porto, Portugal

Within the scope of the work developed in this Thesis, the following awards and distinctions have been garnered:

Short-Term Scientific Missions (STSM) grant to support a one-month working visit to Fundación MEDINA, under the supervision of Dr. Fernando Reyes, 1-30th September 2023, Granada, Spain

Awarded by: European Cooperation in Science and Technology (COST; Ocean4Biotech COST action)

Travel bursary to PhD students to attend the BIOPROSP_23 conference, 14-16th March 2023, TromsØ, Norway

Awarded by: The Norwegian Society of Graduate Technical and Scientific Professionals (TEKNA)

Travel bursary to PhD oral speakers to attend the "Trends in Natural Products Research: A PSE Young Scientists' Meeting", 23-26th May 2022, Crete, Greece Awarded by: Phytochemical Society of Europe (PSE)

1st place in the contest "Science Communication in Microbiology", 2021 Awarded by: Portuguese Society of Microbiology (SPC)

Best oral presentation in the Marine Biotechnology session of the Blue Think Conference (BTC), 17th September 2020, Porto, Portugal

Awarded by: International Society for Microbial Ecology (ISME)

ACKNOWLEDGEMENTS

The past four and a half years of work that culminated in the present Thesis would not have been possible without the mentorship, guidance, encouragement, and support of a very special group of individuals, to whom I would like to express my heartfelt gratitude.

First and foremost, to my supervisor Fátima Carvalho. Thank you for your kind guidance, wisdom, trust, and unwavering belief in my abilities. It was a true pleasure to have had the opportunity to be a part of and evolve with your team for so many years. Your mentorship has shaped not only my research but also my growth as a scholar and individual. I truly believe that I could not have chosen a better person to lead me in such an important step of my career.

To my co-supervisor Pedro Leão, thank you for welcoming me to your group and making me feel truly a part of it. Many of the outputs of this thesis would not have been possible without your valuable guidance, teaching, availability, and dedication. To my co-supervisor Ralph Urbatzka, thank you for your guidance and availability that so well contributed to the success of this work.

A sincere acknowledgment also to Fernando Reyes and his team from Fundación MEDINA, for welcoming me with open arms to their institute and the valuable collaboration in critical tasks of this thesis, and to Diogo Proença, curator of the University of Coimbra Bacteria Culture Collection, for his assistance on the taxonomic studies.

I extend my acknowledgement to all the CIIMAR community, especially fellow researchers, and peers from ECOBIOTEC and CNP laboratories, who always helped me and shared their expertise and feedback throughout this journey. In particular to my colleagues and friends from the "small room above the chemistry lab", thank you for providing the best work environment, for your words of motivation, for all the laughs and exciting discussions. I wish you all the best for your undoubtedly bright future.

Finally, I want to express my deepest appreciation to my family, to whom I dedicate, and always will, all of my achievements. Your unconditional love, understanding, and patience have always sustained me through all the ups and downs. To my friends, who provided much-needed moments of laughter, distraction, and encouragement, thank you for being there for me, in particular Diogo, Rita, Teresa, Beatriz, Catarina, Pedro, José, and my entire JD family.

If there is the idea that doing a PhD might be a lonely journey, I am grateful to say that I never felt alone in mine.

I also acknowledge CIIMAR for ensuring that all the conditions were met for the unfolding of my research, and ICBAS for the financial support which allowed me to participate in various international scientific conferences, internships and training schools.

This Doctoral Thesis received the support of Fundação para a Ciência e a Tecnologia, I.P. (FCT), through the PhD fellowship FRH/BD/145646/2019, and of School of Medicine and Biomedical Sciences Abel Salazar (ICBAS), which provided financial support for the participation in scientific conferences, advanced courses and acquisition of services that were essential for this work. The research work produced in the scope of this Thesis was also funded by the project ATLANTIDA (NORTE-01-0145-FEDER-000040), supported by the Norte Portugal Regional Operational Programme (NORTE 2020) under the PORTUGAL 2020 Partnership Agreement and through the European Regional Development Fund (ERDF), as well as by the Strategic Funding UIDB/04423/2020 and UIDP/04423/2020 through national funds provided by FCT and ERDF; European Union's Horizon 2020 research and innovation programme under grant agreement No 952374; Fundo Social Europeu and Programa Operacional Potencial Humano; WP9 - Portuguese Blue Biobank under the Blue Economy Pact, Grant/Award Number: C644915664-00000026.











ABSTRACT

Mining microbial secondary metabolism from untapped marine sources represents a valuable route to uncover novel biotechnologically relevant chemistry. Actinomycetota, firstclass producers of bioactive natural products, often establish symbiotic associations with marine organisms, as macroalgae, prompting a prolific – yet poorly explored – hotspot for the synthesis of unique molecules that can portray novel drug leads against human and animal health disorders. In this context, the primary objective of this Thesis was to study the macroalgae-associated Actinomycetota community from two native species inhabiting the northern Portuguese coast, Codium tomentosum and Chondrus crispus, to uncover novel bioactive natural products, using both culture-dependent and independent approaches. A combination of classic cultivation techniques and metagenomic analysis was employed to survey Actinomycetota diversity associated with the two macroalgae under study. A collection of 380 Actinomycetota strains was obtained and taxonomically identified, being distributed across 12 orders, 15 families, and 25 genera affiliated to the Actinomycetia class, composed of around 60% of Streptomyces, and representing the largest published collection of macroalgae-associated Actinomycetota to date. Metagenomic data showed Acidimicrobiales as the dominant Actinomycetota order in both macroalgae, but no strain affiliated with this taxonomic group was successfully isolated. The synergistic use of both approaches proved to be beneficial, enabling the identification and recovery of not only abundant but also rare taxonomic members and a better understanding of the whole macroalgae-associated Actinomycetota community. Furthermore. Actinomycetota species, Nocardiopsis codii sp. nov., and Rhodococcus algaerubra sp. nov., were identified in this collection and taxonomically described. The 380 strains were screened for the production of antibacterial, antifungal, anticancer and lipid-reducing metabolites, with nearly 43% of the crude extracts displaying activity in at least one of the screenings performed. Dereplication data pinpointed potential novel mass features in the metabolome of several strains, highlighting the opportunity for biodiscovery. Metagenomics was used to explore the biosynthetic machinery of the macroalgae-associated Actinomycetota communities, providing added insights into the abundance, functional diversity and novelty of encoded biosynthetic gene clusters. In total, 91 biosynthetic gene cluster families were identified, 83 of which showed less than 30% of similarity to database entries, thus confirming macroalgae-symbiotic Actinomycetota as a hub of chemical novelty deserving further exploration. Both bioactivity and mass-guided approaches were successfully conducted to isolate novel natural products from the secondary metabolism of selected strains from this collection. Decylprodigiosin, a new analogue of the red-pigmented family of the antibiotics prodigiosins, was retrieved from the culture of Streptomyces violaceoruber CT-F61 and cellulamides A and B, a new family of linear peptides, from Cellulosimicrobium funkei CT-R177. Cellulamides represent the first natural product reported from the metabolism of the Cellulosimicrobium genus. Other likely novel compounds, produced by Streptomyces violaceoruber CT-F61 and Micromonospora sp. CC-R88, were also identified, isolated, and partially chemically characterized. The work conducted in this Thesis provides a multidisciplinary and comprehensive survey on the Actinomycetota diversity and biosynthetic potential associated with two unexplored algae species (one green and one red) native to the Portuguese coast. Here, we provide a large and chemically diverse collection of Actinomycetota strains, including new taxa, and three chemically characterized new compounds, thus contributing to push forward the state-of-the-art on this scientific topic.

Keywords: Actinomycetota; Bioactivity; *Codium tomentosum*; *Chondrus crispus*; Macroalgae; Natural Products; Secondary metabolism

RESUMO

A investigação do metabolismo secundário microbiano a partir de fontes marinhas inexploradas representa uma rota valiosa para descobrir novos compostos químicos relevantes na área da biotecnologia. Os microrganismos do filo Actinomycetota, produtores de excelência de produtos naturais bioativos, estabelecem frequentemente associações simbióticas com organismos marinhos, como macroalgas, criando um nicho ecológico prolífico – mas ainda pouco explorado – para a síntese de moléculas únicas que podem representar novas soluções terapêuticas eficazes na saúde humana e animal. Neste contexto, o objetivo principal desta Tese foi estudar a comunidade de Actinomycetota associada a duas espécies de macroalgas nativas da costa norte de Portugal, Codium tomentosum e Chondrus crispus, para descobrir novos produtos naturais bioativos, utilizando para isso abordagens dependentes e independentes de cultivo. A combinação de técnicas clássicas de cultivo e análise metagenómica foi usada para estudar a diversidade de Actinomycetota associada às duas macroalgas em estudo. Uma coleção de 380 estirpes foi obtida e taxonomicamente identificada, distribuída por 12 ordens, 15 famílias e 25 géneros afiliados à classe Actinomycetia, composta por cerca de 60% de Streptomyces, e representando a maior coleção de Actinomycetota associada a macroalgas até ao momento publicada. Os dados independentes do cultivo mostraram que a ordem Acidimicrobiales é a mais dominante em ambas as macroalgas, mas nenhuma estirpe afiliada a este grupo taxonómico foi isolada com sucesso. O uso sinérgico de ambas as abordagens mostrou-se benéfico, permitindo a identificação e recuperação não apenas de membros taxonómicos abundantes, mas também raros, e uma melhor compreensão da comunidade de Actinomycetota associada às macroalgas em estudo. Além disso, duas novas espécies de Actinomycetota, Nocardiopsis codii sp. nov. e Rhodococcus algaerubra sp. nov., foram identificadas nesta coleção e descritas taxonomicamente. As 380 estirpes isoladas foram testadas para a produção de metabolitos com propriedades antibacterianas, antifúngicas, anticancerígenas e redutoras de lípidos, com cerca de 43% dos extratos brutos exibindo atividade em pelo menos um dos testes realizados. Os dados de desreplicação destacaram potenciais novas massas no metaboloma de várias estirpes, mostrando assim a oportunidade para a bio-descoberta. A maquinaria biosintética da comunidade de Actinomycetota associada às duas macroalgas foi também explorada através de uma análise de metagenómica, fornecendo informação adicionais sobre a abundância, diversidade funcional e novidade dos grupos de genes biosintéticos presentes. No total, 91 famílias de grupos de genes biosintéticos foram identificadas, das quais 83 mostraram menos de 30% de similaridade com os registos em bases de dados, confirmando assim que as bactérias do filo Actinomycetota que vivem em simbiose com macroalgas são uma promissora fonte de novidade química digna de exploração adicional. O isolamento de metabolitos secundários guiado pela bioatividade e por espectrometria de massa foi realizado para algumas estirpes selecionadas da coleção. Um novo análogo da família de antibióticos de coloração vermelha prodigiosinas, designado decilprodigiosina, foi isolado da cultura da estirpe Streptomyces violaceoruber CT-F61 e uma nova família de péptidos lineares, celulamidas A e B, foi obtida da cultura da estirpe Cellulosimicrobium funkei CT-R177. As celulamidas representam os primeiros produtos naturais obtidos do metabolismo secundário do género Cellulosimicrobium. Outros compostos potencialmente novos produzidos pelas estirpes Streptomyces violaceoruber CT-F61 e Micromonospora sp. CC-R88 foram também identificados, isolados e parcialmente caracterizados quimicamente. O trabalho realizado nesta Tese compreende uma abordagem multidisciplinar e abrangente para explorar a diversidade e o potencial biosintético de bactérias do filo Actinomycetota associadas a duas espécies de macroalgas nativas da costa portuguesa nunca antes exploradas para este fim. Como resultado deste trabalho é apresentada uma grande e diversificada coleção de estirpes afiliadas a este filo, incluindo novas espécies, e três novos compostos quimicamente caracterizados, contribuindo assim para o avanço do estado da arte nesta área de investigação científica.

Palavras-chave: Actinomycetota; Bioactividade; *Codium tomentosum*; *Chondrus crispus*; Macroalga; Metabolismo secundário; Produtos Naturais

TABLE OF CONTENTS

LIST OF FIGURES	25
LIST OF APPENDIX FIGURES	31
LIST OF TABLES	35
LIST OF APPENDIX TABLES	37
LIST OF ABBREVIATIONS	40
CHAPTER 1 General Introduction	
1.1. Microbial Natural Products in Drug Discovery	46
1.2. The Phylum Actinomycetota	48
1.3. Underexplored Environments as Key to Novel Chemistry: the Ocean	, 49
1.4. Macroalgae-associated Actinomycetota: Overview of a Prolific Symbiosis	,,, 49
1.4.1. Abundance and Diversity	51
1.4.2. A Hotspot of Bioactivity	52
1.4.3. Novel Chemistry	57
1.5. Cultivation-Independent Methods: Taking Advantage of the Genomic Era to	0
Boost the Discovery of NP	64
1.6. Current Challenges and Opportunities	65
1.7. Aim and outline of this Thesis	66
CHAPTER 2 Unveiling the culturable and non-culturable actinobacterial diver	•
Codium tomentosum and Chondrus crispus macroalgae collected from the no	rthern
Portuguese coast	
2.1. Introduction	71
2.2. Materials and Methods	
2.2.1. Macroalgae Sampling	73
2.2.2. Actinomycetota Isolation	73
2.2.3. Identification of the Isolates and Phylogenetic Analysis	74
2.2.4. DNA Extraction and Quantification for Metagenomic Analysis	75
2.2.5. Metagenomic Sequencing and Analysis	75
2.3. Results and Discussion	

2.3.1. Isolation, diversity, and phylogeny of culturable macroalgae-associ	ated Actinomycetota76
2.3.2. Macroalgae-associated Actinomycetota community accessed by	
2.4. Conclusion	
CHAPTER 3 Nocardiopsis codii sp. nov., and Rhodococcus algaer	ubra sp. nov., two novel
actinomycetes species isolated from macroalgae collected in the nor	thern Portuguese coast
3.1. Introduction	92
3.2. Materials and Methods	
3.2.1. Bacterial Isolation	94
3.2.2. Phylogenetic and Phylogenomic analysis	94
3.2.3. Genome Mining	95
3.2.4. Physiology and Chemotaxonomy	95
3.3. Results and Discussion	
3.3.1. Phylogenetic and Phylogenomic Identification	97
3.3.2. Genomic Features and Biosynthetic Potential	101
3.3.3. Physiology and Chemotaxonomy	102
3.4. Conclusion	109
CHAPTER 4 Bioactive potential of macroalgae-associated Action through culture-dependent and -independent approaches	·
4.1. Introduction	114
4.2. Materials and Methods	
4.2.1. Samples Analysed in this Study	116
4.2.2. Preparation of the Crude Extract's Library	116
4.2.3. Antimicrobial Assay	116
4.2.4. Anticancer Assay	117
4.2.5. Lipid-reducing Assay	117
4.2.6. Statistics	118
4.2.7. Evolutionary Relationship of the Bioactive Strains	118
4.2.8. Dereplication and Metabolic Profiling of Active Extracts	119
4.2.9. Recovery and Mining of Actinobacterial Contigs and MAGs	119
4.3. Results and Discussion	
4.3.1. Bioactivity Screening	
4.3.1.1. Antimicrobial Activity	121
4.3.1.2. Anticancer Activity	121

4.3.2. Dereplication, Metabolic and Taxonomic Profiling of Active Extracts	128
4.3.3. Actinobacterial Biosynthetic Potential Assessed Through Metagenomes	132
4.4. Conclusion	136
CHAPTER 5 Decylprodigiosin: a new member of the prodigiosin family isolate	d from a
seaweed-associated Streptomyces	-
5.1. Introduction	140
5.2. Materials and Methods	
5.2.1. Sampling and Bacterial Isolation	142
5.2.2. Taxonomic and Phylogenetic Analysis of Streptomyces violaceoruber CT-F61	142
5.2.3. Bioactivity Screenings	142
5.2.4. Decylprodigiosin Isolation and Structure Elucidation	143
5.2.5. Streptomyces violaceoruber CT-F61 Genome Sequencing	144
5.3. Results and Discussion	
5.3.1. Streptomyces violaceoruber CT-F61 Isolation and Taxonomic Identification	145
5.3.2. Bioactivity Screening	146
5.3.3. Bioactivity-guided Isolation and Structure Elucidation of Decylprodigiosin	147
5.3.4. Prodigiosins as Product of Seaweed-associated Actinobacterial Metabolism	151
5.4. Conclusion	152
CHAPTER 6 Cellulamides: a new family of marine-sourced linear peptides	from the
unexplored <i>Cellulosimicrobium</i> genus	
6.1. Introduction	156
6.2. Materials and Methods	
6.2.1. Sampling and Bacterial Isolation	158
6.2.2. Taxonomic and Phylogenetic Analysis of <i>Cellulosimicrobium funkei</i> CT-R177	
6.2.3. Fermentation and Organic Extraction of <i>Cellulosimicrobium funkei</i> CT-R177	
6.2.4. Bioactivity Screening and Dereplication of CT-R177 Crude Extract	
6.2.5. Mass Spectrometry Guided Isolation and Structure Elucidation of Cellulamides	
6.2.6. Marfey's Analysis of Cellulamide A	
6.2.7. Cellulosimicrobium funkei CT-R177 Genome Sequencing	
6.2.8. Bioactivity Screening of Cellulamide A	161
6.2.9. General Experimental Procedures	162
6.3. Results and Discussion	
6.3.1. Cellulosimicrobium funkei CT-R177 Isolation and Taxonomic Identification	163
6.3.2. Bioactivity Screening and Dereplication of Cellulosimicrobium funkei CT-R177 Crud	de Extract
	164

6.3.3. Mass Spectrometry Guided Isolation and Structural Elucidation of Cellulamides	
6.3.4. Genomic Analysis	
6.3.5. Bioactivity Screening of Cellulamide A	
6.4. Conclusion	171
CHAPTER 7 Bioactivity-guided isolation of novel natural products from the	secondary
metabolism of Streptomyces violaceoruber CT-F61 and Micromonospora sp. nov	•
7.1. Introduction	175
7.2. Materials and Methods	
7.2.1. Bacterial Isolation and Taxonomic Identification	176
7.2.2. Up-scaling and Organic Extraction	176
7.2.3. Bioactivity-guided Isolation of NP from Streptomyces violaceoruber CT-F61	176
7.2.4. Bioactivity-guided Isolation of NP from <i>Micromonospora</i> sp. CC-F88	
7.2.5. Genome Mining	178
7.3. Results and Discussion	
7.3.1. Bioactivity-guided Isolation of NP from Streptomyces violaceoruber CT-F61	179
7.3.1. Bioactivity-guided Isolation of NP from <i>Micromonospora</i> sp. CC-F88	
7.3.3. Genome Mining	187
7.4. Conclusion	189
CHAPTER 8 General Conclusions and Future Perspectives	191
REFERENCES	197
APPENDIX	
Appendix I	233
Appendix II	250
Appendix III	
Appendix IV	
Appendix V	
Appendix VI	
Appendix vi	305

LIST OF FIGURES

Figure 1. Macroalgae-associated Actinomycetota described worldwide. Information
regarding each sampling site, the macroalgae species collected, the number of reported
Actinomycetota strains, the bioactivity screening results, and novel NP elucidated is
presented. (•) Phaeophyta (•) Rhodophyta (•) Chlorophyta
procented. (-) i nacepriyta (-) i nacepriyta (-) e nacepriyta (-)
Figure 2. Examples of the morphological diversity of Actinomycetota strains isolated from
C. crispus and C. tomentosum macroalgae.
Figure 3. Actinomycetota recovered from <i>C. crispus</i> (■) and <i>C. tomentosum</i> (□). The
number of isolates recovered from the holdfast and blade of each macroalgae species, and
the respective isolation media (NPS: Nutrient-poor Sediment Extract agar; AIA:
Actinomycete Isolation Agar; SCN: Starch-Casein-Nitrate agar; SA: Seaweed Agar), are
presented (A) as well as the distribution of the genera recovered (B). The taxonomic
distribution of the strains - order, family, and genus, from the inside to the outside of the
circle, respectively - is presented according to the part of the macroalgae from which they
were isolated. Numbers in brackets indicate the number of isolates retrieved from each
genus. Genera exclusively obtained from a macroalgae species are highlighted in bold (C).
80
Figure 4. Dhula gapatia trea hagad on the 400 gDNA gapa, abtained by Maying ye Likelih and
Figure 4. Phylogenetic tree based on the 16S rRNA gene, obtained by Maximum Likelihood
analysis of Actinomycetota isolates recovered from C. crispus (■) and C. tomentosum (□)
affiliated to the genus Streptomyces. Genomic data from strains CT-R87 and CT-F145 were
not considered due to the small size of their consensus sequences. The tree was generated
using an alignment of 1522 bp and 1000 bootstraps. The order-level affiliation of the strains
is coloured indicated as described in the picture caption. Strains representing potential
novel taxa (•) are pointed out as well. 81
Figure 5. Phylogenetic tree based on the 16S rRNA gene, obtained by Maximum Likelihood
analysis of Actinomycetota isolates recovered from C. crispus (■) and C. tomentosum (□)
affiliated to non-Streptomyces genera. Genomic data from strains CC-F55 and CT-R135
were not considered due to the small size of their consensus sequences. The tree was
generated using an alignment of 1345 bp and 1000 bootstraps. The order-level affiliation of
the strains is coloured indicated as described in the picture caption. Strains representing
potential novel taxa (•) are pointed out as well.
Figure 6. Phylogenetic trees for strains CT-R113, CC-R104, CT-R125 and CT-R113,

representing potential novel Actinomycetota species recovered from C. crispus (■) and C.

tomentosum (\square). The trees were obtained by Maximum Likelihood analysis of the 16S rRNA gene sequences of the 15 closest related type strains associated to each of the potential novel species. The phylogeny test used was the bootstrap method with 1000 replications. Bacillus subtilis ABQL01000001 was used as outgroup. Numbers at nodes represent bootstrap values when higher than 50%. Accession numbers are indicated in brackets.
Figure 7. Relative distribution of classified reads from <i>C. crispus</i> (■) and <i>C. tomentosum</i> (□) shotgun metagenomic dataset at (A) phylum-level, with each circle corresponding to 1%, (B) actinobacterial order-level and (C) actinobacterial genus-level. Taxonomic groups retrieved from cultivation are indicated with a bacteria symbol. 87 Figure 8. ML phylogenetic tree based on 16S rRNA gene sequences (1,302 nt), showing the relationship between strain CT-R113 ^T and the closest related type strains within the genus <i>Nocardiopsis</i> . Accession numbers are indicated in brackets. Values at the nodes indicate bootstrap values of 50% and above, obtained based on 1000 resampling events. <i>Bacillus subtilis</i> NCIB 3610 ^T was used as outgroup. Scale bar, 2 inferred nucleotide
substitution per 100 nucleotides. 98 Figure 9. ML phylogenomic tree based on 400 universal marker genes, showing the relationship between strain CT-R113 ^T and the closest related type strains within the genus Nocardiopsis. Accession numbers are indicated in brackets. Values at the nodes indicate bootstrap values of 50% and above obtained based on 1000 resampling events. Bacillus subtilis NCIB 3610 ^T was used as outgroup. Scale bar, 10 inferred nucleotide substitution per 100 nucleotides.
Figure 10. ML phylogenetic tree based on 16S rRNA gene sequences (1,283 nt), showing the relationship between strain CC-R104 ^T and the closest related type strains within the genus <i>Rhodococcus</i> . Accession numbers are indicated in brackets. Values at the nodes indicate bootstrap values of 50% and above, obtained based on 1,000 resampling events. <i>Bacillus subtilis</i> NCIB 3610 ^T was used as outgroup. Scale bar, 2 inferred nucleotide substitution per 100 nucleotides.
Figure 11. ML phylogenomic tree based on 400 universal marker genes, showing the relationship between strain CC-R104 ^T and the closest related type strains within the genus <i>Rhodococcus</i> . Accession numbers are indicated in brackets. Values at the nodes indicate bootstrap values of 50% and above, obtained based on 1,000 resampling events. <i>Bacillus subtilis</i> NCIB 3610 ^T was used as outgroup. Scale bar, 10 inferred nucleotide substitution

.....126

Figure 12. Distribution, number, and type of BGCs detected in (A) strain CT-R113 ^T and the two closest related type strains, 66/93 ^T and VKM Ac-1457 ^T , and (B) strain CC-R104 ^T and the closest related type strain DSM 45380 ^T , as predicted by antiSMASH.
Figure 13. Morphology of strain CT-R113 ^T colonies in TSA medium, observed using a binocular magnifier (Leica ZOOM 2000) with magnifications of (A) 10x and (B) 30x103
Figure 14. Morphology of colonies of strain CC-R104 ^T on TSA medium, observed using a binocular magnifier (Leica ZOOM 2000) with magnifications of (A) 10x and (B) 30x
Figure 15. Antimicrobial screening of Actinomycetota isolated from C. crispus (CC) and C. tomentosum (CT). (A) Strains with bioactivity in the antimicrobial assay. Only strains active towards at least one reference microorganism are presented. Data displayed as average measurement (mm) of the inhibition halos (IH) diameter from two independent experiments. Strains highlighted in bold presented inhibitory effect toward the growth of at least one human and fish health-relevant reference microorganism. (B) Distribution of active and non-active strains retrieved from CC and CT. (C) Distribution of active strains according to their fermentation medium. (D) Genus-level taxonomic distribution of active strains. Taxonomic groups highlighted in bold were found in both macroalgae. The source of isolation, holdfast (●) or blade (▲), is indicated in all graphs. ■ 123
Figure 16. Anticancer screening of Actinomycetota isolated from <i>C. crispus</i> (CC) and <i>C. tomentosum</i> (CT). (A1) Strains with bioactivity in the MTT assay (15 μg mL ⁻¹). Only the most active strains (p value < 0.001) are presented. Data displayed as mean of cellular viability (%) from two independent experiments (n = 6) and significant differences compared to the SC (solvent control: 0.5% DMSO), after 48 h of exposure. Results for the two cancer cell lines (HCT116 and T47D) and the non-cancer cell line (hCMEC/D3) are presented. Extracts with selective activity in cancer cells are red-bordered, with the ones highlighted in bold presenting cytotoxicity towards both cancer cell lines tested. (A2) Most active extracts in each cancer cell line compared to SC and PC (positive control: 15 μg mL ⁻¹ Staurosporine). Extracts with selective activity in cancer cells are red-bordered. *** p value < 0.001. (B)
Distribution of active and non-active strains retrieved from CC and CT. (C) Distribution of

Figure 17. Anti-obesity screening of Actinomycetota isolated from *C. crispus* (CC) and *C. tomentosum* (CT). (A1) Strains with bioactivity in the Nile Red fat metabolism assay. Data displayed as mean fluorescence intensity (MFI) relative to DMSO (dimethylsulfoxide 0.1%,

active strains according to their fermentation medium. (**D**) Genus-level taxonomic distribution of active strains. Taxonomic groups highlighted in bold were found in both macroalgae. The source of isolation, holdfast (\bullet) or blade (\blacktriangle), is indicated in all graphs.

solvent control) from two independent experiments (n = 6). Statistical differences are shown as asterisks, ** p value < 0.01 and *** p value < 0.001. (A2) Representative images of the tebrafish larvae (overlay of brightfield picture and red fluorescence channel), showing andividuals exposed to DMSO, REV (positive control; 50 μM) and the crude extract of strain CC-F68. (B) Distribution of active and non-active strains retrieved from CC and CT. (C) Distribution of active strains according to their fermentation medium. (D) Genus-level axonomic distribution of active strains. The source of isolation, holdfast (•) or blade (Δ), indicated.
Figure 18. ML phylogenetic tree based on 16S rRNA gene sequences (1,311 nt), showing the evolutionary relationship between all 165 bioactive strains. The results of the bioactivities are provided for every strain. Strains encoding putative new compounds an andicated as well.
Figure 19. Taxonomic classification of actinobacterial contigs from which BGCs were dentified through the antiSMASH analysis. (A) Taxonomic classification of actinobacterial contigs at order level. (B) Heat tree plot of taxonomic classification of contigs. Only contiguous which it was possible to obtain a taxonomic classification at genus level are depicted n=51).
Figure 20. ML phylogenomic tree of the MAGs recovered in this study. Information completeness (bar represented from 50.7 to 97%), total length (bar represented from 2.4 to 5.1 Mb) and the number of BGCs by class for each MAG is included. <i>Bacillus subtili</i> GCF_000009045.1) was used as outgroup.
Figure 24. Actinohoptorial CCFs apposinted with Continue (CC) and Cotomontorum (CT)
A) SSN of all BGC classes recovered from MIBiG. The different colours correspond the distinct GCFs identified by BiG-SCAPE. BGCs recovered from MAGs are represented by ectangle, from contigs associated to CT sample by a triangle, from contigs associated to CC sample by a round rectangle, and MIBiG BGCs are represented by a circle. (B) Total number of GCFs by BGC class. (C) Upset intersection plot for the GCFs by sample typicontigs CT sample, contigs CC sample, MAGs) and the GCFs for MIBiG BGCs

Figure 23. Antimicrobial and cytotoxic activities of CT-F61 crude extract, obtained from the small-scale (SS) and large-scale (LS) cultivation ($\bf A$), C18 VLC fractions of CT-F61 LS crude extract ($\bf B$) and CT-F61 KL C18 HPLC fractions tested at 15 µg mL ⁻¹ and 1.5 µg mL ⁻¹ in HCT116 cell line ($\bf C$). Antimicrobial results presented as mean of the diameter of the inhibition halos measured from two independent experiments. Only reference strains affected by at least one tested sample are presented. Cytotoxic results presented as percentage of cellular viability after 48h of exposure, measured as mean from two independent MTT experiments, performed with triplicates to each sample. Significant differences compared to the solvent control (*p < 0.05; **p < 0.01; ***p < 0.001). The
percentage of cellular viability for the positive control (PC: Staurporine 15 μg mL ⁻¹) is indicated, as well as the samples activity on the non-carcinogenic cell line hCMEC/D3.
Figure 24. EICs of Undecylprodigiosin and Butylcyclohexylprodigiosin, detected in KL_9 and KL_10 fractions, alongside with the mass feature corresponding to 1
Figure 25. Structure elucidation of 1 by comparison of HRESIMS/MS spectra of undecylprodigiosin (in black) and 1 (in pink) (A). Proposed chemical structure of 1 and molecular formula (B).
Figure 26. ML phylogenetic tree based on 16S rRNA gene sequences (1,395 nt), showing the relationship between strain CT-R117 and the closest related type strains according to EzBiocloud database. Accession numbers are indicated in brackets. Values at the nodes indicate bootstrap values of 50% and above, obtained based on 1,000 resampling events. <i>Bacillus subtilis</i> NCIB 3610 ^T was used as outgroup. Type strains affiliated to <i>Cellulosimicrobium</i> genus are blue shaded.
Figure 27. (A) Cytotoxic activity of strain CT-R177 crude extract in HCT116, T47D and hcMEC/d3 human cell lines, tested at 15 μg mL ⁻¹ . Results presented as percentage of cellular viability after 48h of exposure, measured as mean from two independent MTT experiments, each performed in triplicate. Significant differences are compared to the solvent control (**p < 0.01; ****p < 0.001). The percentage of cellular viability for the positive control (PC: Staurosporine 15 μg mL ⁻¹) and solvent control (SC: 99.9% DMSO) are indicated as well. (B) Zoom of the HRMS spectrum displaying the <i>m/z</i> 803.3929 [M+H] ⁺ mass feature in strain CT-R177 crude extract.
Figure 28. (A) Structure of cellulamides A and B (B) Key COSY and HMBC correlations observed in the structure of cellulamide A.

Figure 29. Tandem MS/MS spectra of (A) cellulamide A (2) and (B) cellulamide B (3) 169
Figure 30. Bioactivity screening of CT-F61 samples. Antimicrobial activity of (A) C18 VLC fractions of CT-F61 crude extract, (B) FC fractions of CT-F61 FJ sample, (C) C18 semi-preparative (SP) HPLC fractions of sample FJ_2 and (D) C18 analytical HPLC fractions of samples FJ_2_G, FJ_2_H and FJ_2_I. Antimicrobial results presented as mean of the diameter of the inhibition halos measured from two independent experiments using the agar-based disk diffusion method. Fractions highlighted on bold were selected to the next chromatographic step.
Figure 31. EICs of 4 for fractions generated from sample FJ_2_I. The mass features searched in both NPA and DNP databases are presented, as well as the retrieved results (0 hits).
Figure 32. EICs of 5. The mass features searched in both NPA and DNP databases are presented, as well as the retrieved results (0 hits).
Figure 33. Chemical substructure elucidated of 5 with the indication of key HMBC (arrows) and $^{1}H^{-1}H$ COSY (blue lines) correlations, as well as proton (δ_{H}) and carbon (δ_{C}) resonance values.
Figure 34. Bioactivity screening fractionation of CC-F88 samples. Antimicrobial and cytotoxic activity of (A) C18 VLC fractions of CC-F88 crude extract, (B) FC fractions of CC-F88 HL sample, (C) C18 FC fractions of sample HL_69 and (D) C18 semi-preparative (SP) HPLC fractions of sample HL_69_HL. Antimicrobial results (left pannel) presented as mean of the diameter of the inhibition halos measured from two independent experiments using the agar-based disk diffusion method. Cytotoxic results (right pannel) presented as percentage of cellular viability after 48h of exposure, measured as mean from two independent MTT experiments, performed with triplicates to each sample. Significant differences compared to the solvent control (*p < 0.05; **p < 0.01; ***p < 0.001). The percentage of cellular viability for the positive control (PC: Staurporine 15 μg mL ⁻¹) is indicated. Fractions highlighted on bold were selected to the next chromatographic step.
Figure 35. EICs of 6 . The mass features searched in both NPA and DNP databases are presented, as well as the retrieved results (0 hits).
Figure 36. Chemical substructures elucidated of 6 with the indication of key HMBC (arrows) and $^1H-^1H$ COSY (blue lines) correlations, as well as proton (δ_H) and carbon (δ_C) resonance values.
Figure 37. Number of BGCs annotated by antiSMASH in the genome of CT-F61 and CC-F88 strains and their similarity (%) with MIBiG database188

LIST OF APPENDIX FIGURES

Figure S1. NJ phylogenetic tree based on 16S rRNA gene sequences (1,302 nt), showing the relationship between strain CT-R113 ^T and the closest related type strains within the genus <i>Nocardiopsis</i> . Accession numbers are indicated in brackets. Values at the nodes indicate bootstrap values of 50% and above, obtained based on 1,000 resampling events. <i>Bacillus subtilis</i> NCIB 3610 ^T was used as outgroup. Scale bar, 2 inferred nucleotide substitution per 100 nucleotides.
Figure S2. NJ phylogenomic tree based on 400 universal marker genes, showing the relationship between strain CT-R113 ^T and the closest related type strains within the genus <i>Nocardiopsis</i> . Accession numbers are indicated in brackets. Values at the nodes indicate bootstrap values of 50% and above obtained based on 1,000 resampling events. <i>Bacillus subtilis</i> NCIB 3610 ^T was used as outgroup. Scale bar, 10 inferred nucleotide substitution per 100 nucleotides.
Figure S3. NJ phylogenetic tree based on 16S rRNA gene sequences (1,283 nt), showing the relationship between strain CC-R104 ^T and the closest related type strains within the genus <i>Rhodococcus</i> . Accession numbers are indicated in brackets. Values at the nodes indicate bootstrap values of 50% and above, obtained based on 1,000 resampling events. <i>Bacillus subtilis</i> NCIB 3610 ^T was used as outgroup. Scale bar, 2 inferred nucleotide substitution per 100 nucleotides.
Figure S4. NJ phylogenomic tree based on 400 universal marker genes, showing the relationship between strain CC-R104 ^T and the closest related type strains within the genus <i>Rhodococcus</i> . Accession numbers are indicated in brackets. Values at the nodes indicate bootstrap values of 50% and above obtained based on 1,000 resampling events. <i>Bacillus subtilis</i> NCIB 3610 ^T was used as outgroup. Scale bar, 10 inferred nucleotide substitution per 100 nucleotides.
Figure S5. GNPS molecular networking using MS/MS data from the 22 crude extracts without any hit in the GNPS dereplication tools. The value indicated in each node corresponds to the precursor ion. Detailed information regarding each highlighted cluster is presented in Table 9.
Figure S6. Reverse-phase HPLC chromatogram of CT-F6_KL sample with the indication of the recovered fractions.
Figure S7. ¹ H NMR (Chloroform- d , 600 MHz) spectrum of fraction KL_9 containing semipurified 1 , highlighting the typical prodigiosin signals δ_H 7.5-6.20, associated to the

pyrrole rings (A1) and δ_H 1.29-1.25, consistent with a large methylene envelope (A2). NMR (Chloroform-d, 600 MHz) spectrum of the most purified fraction (KL_9-10_	
containing 1 (B).	88
Figure S8. UV and (+)-ESI-TOF spectra of cellulamide A (2).	91
Figure S9. ¹ H-NMR (500 MHz, CD ₃ OD) spectrum of cellulamide A (2)2	92
Figure S10. ¹³ C-NMR (125 MHz, CD ₃ OD) spectrum of cellulamide A (2)2	93
Figure S11. HSQC (CD ₃ OD) spectrum of cellulamide A (2).	94
Figure S12. HMBC (CD ₃ OD) spectrum of cellulamide A (2).	95
Figure S13. COSY (CD ₃ OD) spectrum of cellulamide A (2).	96
Figure S14. UV and (+)-ESI-TOF spectra of cellulamide B (3).	97
Figure S15. ¹ H-NMR (500 MHz, CD ₃ OH) spectrum of cellulamide B (3)2	98
Figure S16. ¹³ C-NMR (125 MHz, CD ₃ OH) spectrum of cellulamide B (3)2	99
Figure S17. HSQC (CD ₃ OH) spectrum of cellulamide B (3).	00
Figure S18. HMBC (CD₃OH) spectrum of cellulamide B (3)3	01
Figure S19. COSY (CD₃OH) spectrum of cellulamide B (3)3	02
Figure S20. HPLC traces at 210 nm of the D-FDVA derivatives of Ser3	03
Figure S21. HPLC traces at 210 nm of the D-FDVA derivatives of Pro3	03
Figure S22. HPLC traces at 210 nm of the D-FDVA derivatives of Phe3	03
Figure S23. HPLC traces at 210 nm of the D-FDVA derivatives of Leu3	04
Figure S24. HPLC traces at 210 nm of the D and L-FDVA derivatives of <i>cis</i> and <i>trans</i> Hyp	
Figure S25. HPLC trace at 210 nm of the D-FDVA derivatives of the hydrolyzate cellulamide A (2).	

Figure S26. Reverse-phase semi-preparative HPLC chromatogram of CT-F61 FJ_2 sample with the indication of the recovered fractions. The darkest shaded zone corresponds to the baseline, collected separately.
Figure S27. Reverse phase HPLC chromatogram of CT-F61 (A) FJ_2_G, (B) FJ_2_H and (C) FJ_2_I samples with the indication of the recovered fractions. The darkest shaded zone corresponds to the baseline, collected separately.
Figure S28. ¹ H-NMR (600 MHz, CD ₃ O) spectrum of fraction FJ_2_I_5 containing the putative novel compound <i>m/z</i> 539.35605 [M+Na] ⁺ (4).
Figure S29. ¹ H-NMR (600 MHz, CD ₃ OH) spectrum of fraction FJ_2_I_4 containing the pure putative novel compound <i>m/z</i> 387.18048 [M+H] ⁺ (5)306
Figure S30. ¹³ C-NMR (600 MHz, CD ₃ OH) spectrum of fraction FJ_2_I_4 containing the pure putative novel compound <i>m/z</i> 387.18048 [M+H] ⁺ (5).
Figure S31. HSQC (600 MHz, CD ₃ OH) spectrum of fraction FJ_2_I_4 containing the pure putative novel compound <i>m/z</i> 387.18048 [M+H] ⁺ (5). 308
Figure S32. HMBC (600 MHz, CD ₃ OH) spectrum of fraction FJ_2_I_4 containing the pure putative novel compound <i>m/z</i> 387.18048 [M+H] ⁺ (5).
Figure S33. COSY (600 MHz, CD ₃ OH) spectrum of fraction FJ_2_I_4 containing the pure putative novel compound <i>m/z</i> 387.18048 [M+H] ⁺ (5)310
Figure S34. Reverse-phase semi-preparative HPLC chromatogram of CC-F88 HL_69_HL sample with the indication of the recovered fractions. The darkest shaded zone corresponds to the baseline, collected separately.
Figure S35. Reverse phase HPLC chromatogram of CC-F88 (A) HL_69_HL_2, (B) HL_69_HL_6 and (C) HL_69_HL_10 samples with the indication of the recovered fractions. The darkest shaded zone corresponds to the baseline, collected separately311
Figure S36. 1 H-NMR (600 MHz, CD $_{3}$ OD) spectra of fractions (A) HL $_{6}$ 9_HL $_{2}$, (B) HL $_{6}$ 9_HL $_{3}$ 10
Figure S37. ¹ H-NMR (600 MHz, CD ₃ OD) spectrum of fraction HL_69_HL_6_B containing the pure putative novel compound m/z 635.41809 [M-H] ⁻ (6).
Figure S38. ¹³ C-NMR (600 MHz, CD ₃ OH) spectrum of fraction HL_69_HL_6_B containing the pure putative novel compound <i>m/z</i> 635.41809 [M-H] ⁻ (6).

Figure S39. HSQC (600 MHz, CD ₃ OH) spectrum of fraction HL_69_HL_6_B conta	aining the
pure putative novel compound <i>m/z</i> 635.41809 [M-H] ⁻ (6).	315
Figure S40. HMBC (600 MHz, CD ₃ OH) spectrum of fraction HL_69_HL_6_B contagure putative novel compound m/z 635.41809 [M-H] ⁻ (6).	· ·
Figure S41. COSY (600 MHz, CD ₃ OH) spectrum of fraction HL_69_HL_6_B conta	aining the
pure putative novel compound <i>m/z</i> 635.41809 [M-H] ⁻ (6).	317

LIST OF TABLES

Table 1. Actinomycetota genera recovered from Phaeophyta, Rhodophyta and Chlorophyt macroalgae. 5
Table 2. Bioactive Actinomycetota isolated from macroalgae. The macroalgae species an corresponding sampling site are indicated, as well as the recovered Actinomycetota general bioactivity recorded, and the number of strains reported in each study.
Table 3. Novel NP retrieved from macroalgae-associated Actinomycetota. The compounname, type of molecule and corresponding molecular formula are indicated, as well as the producing strain and reported bioactivity.
Table 4. Formulation of the selective culture media used for the isolation of Actinomycetota 7.
Table 5. Fatty acids composition of strains CT-R113 ^T , <i>Nocardiopsis tropica</i> VKM Ac-1457 and <i>Nocardiopsis umidischolae</i> 66/93 ^T . Strains: 1, CT-R113 ^T ; 2, <i>Nocardiopsis tropica</i> VKM Ac-1457 ^T , 3, <i>Nocardiopsis umidischolae</i> 66/93 ^T . All data is from this study. The major cellular fatty acids are in bold. TR, trace amount (fatty acids amounting to < 1%)
Table 6. Differentiating phenotypic, chemotaxonomic and genomic characteristics of strai CT-R113 ^T and the closest related type strains <i>Nocardiopsis tropica</i> VKM Ac-1457 ^T an <i>Nocardiopsis umidischolae</i> 66/93 ^T ; Strains: 1, CT-R113 ^T ; 2, <i>Nocardiopsis tropica</i> VKM Ac 1457 ^T , 3, <i>Nocardiopsis umidischolae</i> 66/93 ^T .
Table 7. Fatty acids composition of strain CC-R104 ^T and <i>Rhodococcus artemisiae</i> DSM 45380 ^T . Strains: 1, CC-R104 ^T ; 2, DSM 45380 ^T . All data is from this study. The major cellula fatty acids are in bold. TR, trace amount (fatty acids amounting to < 1% 107 107 107 107 107 107 107 107 107 107
Table 8. Differentiating phenotypic, chemotaxonomic and genomic characteristics of strai CC-R104 ^T and its closest related type strain DSM 45380 ^T ; Strains: 1, CC-R104 ^T ; 2, DSN 45380 ^T .
Table 9. Single-strain clusters retrieved from the GNPS molecular networking built wit MS/MS data from crude extracts without any hit in the GNPS dereplication tools. Manual dereplication for major peaks detected in each cluster (green-colored nodes) was performe using DNP and NPA databases. The value indicated in each node corresponds to the precursor ion.

Portuguese seaweeds, a mari	ne treasure of Actinobacteria	producing novel bioactive compounds
-----------------------------	-------------------------------	-------------------------------------

Table 10. NMR Data of cellulamides A (1) and B (2) in CD ₃ OD (1) or CD ₃ OH (2)167
Table 11. Secondary metabolite BGCs identified by antiSMASH in the genome of C. funkei
CT-R177

LIST OF APPENDIX TABLES

Table S1. Taxonomic identification of the Actinomycetota isolates recovered from <i>C. crispus</i> and <i>C. tomentosum</i> , collected in the intertidal area of the northern Portuguese rocky shore Information regarding culture media and genomic data, including the GenBank accession
number, is presented. Potential novel species are indicated as well (**).
Table S2. Prokaryotic taxonomic profiles produced from the metagenomes of tomentosum and C. crispus. The abundance of each taxonomic group, as well as the number of reads, are presented. 248
Table S3. ANI (%) of the genome of strain CT-R113 ^T and the closest related type strains within the genus <i>Nocardiopsis</i> . Query genome: <i>Nocardiopsis</i> sp. CT-R113 (JAUZMY00000000).
Table S4. ANI (%) between the genome of strain CC-R104 ^T and the closest related type strains within the genus <i>Rhodococcus</i> . Query genome: <i>Rhodococcus</i> sp. CC-R104 (JAUTXY000000000).
Table S5. BGCs identified by antiSMASH (version 7.1.0) in the genomes of strains CT R113 ^T , VKM Ac-1457 ^T and 66/93 ^T . Relaxed detection settings and all extra features were selected.
Table S6. BGCs identified by antiSMASH (version 7.1.0) in the genomes of strains CC R104 ^T and DSM 45380 ^T . Relaxed detection settings and all extra features were selected
Table S7. Bioactivity profiling of all active actinobacterial crude extracts. Information regarding the fermentation medium used for each strain is also presented. 26
Table S8. Actinomycetota-sourced compounds identified in the active crude extracts using GNPS dereplication tools. Data presented only for hits with score >10 and for compounds of actinobacterial origin with described bioactive properties, which are indicated in the Table. Crude extracts with no hit in any of the dereplication tools are highlighted (bold and grey shaded).
Table S9. List of BGCs recovered from C. crispus sample. 283
Table S10. List of BGCs recovered from <i>C. tomentosum</i> sample.

Table S11. Reverse-phase VLC conditions used to fractionate CT-F61 crude extract. The solvent mixture used to obtain each fraction is shown as well as the yielded mass (mg).
Table S12. Reverse-phase semi-preparative HPLC conditions used to fractionate CT-F61 KL sample. 289
Table S13. Reverse-phase analytical HPLC conditions used to fractionate CT-F61 KL_9- 10 sample. 290
Table S14. Normal-phase FC conditions used to fractionate CT-F61 FJ sample. The solvent mixture is presented, as well as the volume used and the corresponding collection tubes. 318
Table S15. Normal-phase FC conditions used to fractionate CT-F61 FJ sample. The solvent mixture is presented, as well as the volume used and the corresponding collection tubes. 318
Table S16. Reverse-phase semi-preparative HPLC conditions used to fractionate CT-F61 FJ_2 sample. 319
Table S17. Reverse-phase HPLC fractions of CT-F61 FJ_2 sample with the indication of the yielded mass (mg). 319
Table S18. Reverse-phase HPLC fractions of CT-F61 FJ_2_G, FJ_2_H and FJ_2_I samples with the indication of the yielded mass (mg). 319
Table S19. Reverse-phase VLC conditions used to fractionate CC-F88 crude extract. The solvent mixture used to obtain each fraction is shown, as well as the yielded mass (mg).
Table S20. Normal-phase FC conditions used to fractionate CC-F88 HL sample. The solvent mixture used to obtain each fraction is shown as well, as the yielded mass (mg).
Table S21. Reverse-phase FC conditions used to fractionate CC-F88 HL_69 sample.
Table S22. Reverse-phase FC fractions of CC-F88 HL_69 sample, with the indication of the corresponding collection tubes and yielded mass (mg). 321
Table S23. Reverse-phase semi-preparative HPLC conditions used to fractionate CC-F88 HL_69_HL sample. 321
Table S24. Reverse-phase semi-preparative HPLC fractions of CC-F88 HL_69_HL sample, with the indication of the corresponding yielded mass (mg)321

Table S25. Reverse-phase analytical HPLC conditions used to fractionate	CC-F88
HL_69_HL_2, HL_69_HL_6 and HL_69_HL_10 samples.	322
Table S26. Reverse-phase analytical HPLC fractions of HL_69_HL_2, HL_69_HL	6 and
HL_69_HL_10 samples with the indication of the yielded mass (mg).	322

LIST OF ABBREVIATIONS

(v/v) – Volume-to-volume ratio

(w/v) – Weight-to-volume ratio

°C - Degree Celsius

μL – Microlitre

1D - One-dimensional

2D - Two-dimensional

AC - Acetone

AIA – Actinomycete Isolation Agar

ANI - Average Nucleotide Identity

ATCC – American Type Culture Collection

BGC – Biosynthetic Gene Cluster

bp – Base Pair

C - carbon

Calcd - calculated

CC - Chondrus crispus

CDS – Coding Sequence

CT - Codium tomentosum

Da - Dalton

DCM – Dichloromethane

D-FDVA – Nα-(2,4-Dinitro-5-fluorophenyl)-D-valinamide~

bmDKP – (6S,3S)-6-benzyl-3-methyl-2,5-diketopiperazine

DMSO – Dimethyl sulfoxide

DNA – Deoxyribonucleic acid

DNP – Dictionary of Natural Products

DPF – Days post-fertilization

Dpm – 2,6-diaminopimelic acid

DSMZ – The Leibniz Institute - German Collection of Microorganisms and Cell Cultures GmbH

EC – European Union

eDNA - Environmental deoxyribonucleic acid

EIC – Extracted Ion Chromatogram

ESI-QTOF – Electrospray Ionisation Quadrupole-time-of-flight

FAME - Fatty Acid Methyl Ester

FC – Flash Chromatography

FWHM – Full Width at half maximum

g – Gram

G+C - Guanine plus Cytosine

GCF – Gene Cluster Family

gDNA - Genomic deoxyribonucleic acid

GNPS – Global Natural Products Social Molecular Networking

GTDB – Genome Taxonomy Database

GYM - Glycerol Yeast Malt Extract agar

H – Hydrogen

hCMEC/D3 - Human brain capillary endothelial cells

HCT116 - Colorectal carcinoma

HPLC – High-performance Liquid Chromatography

HQ – High-quality

HRMS – High-Resolution Mass-Spectrometry

HTS – High-Throughput Sequencing

Hyp – Hydroxyproline

IH - Inhibition Halo

imDKP - (6S,3S)-6-isobutyl-3-methyl-2,5-diketopiperazine

IPA – Isopropanol

ISP – International Streptomyces Project

J – Coupling constant

JCM – Japan Collection of Microorganisms

LC-DAD – Liquid Chromatography Diode Array Detector

LC-HRESIMS/MS – Liquid Chromatography High Resolution Electrospray Ionization Mass Spectrometry coupled to tandem Mass Spectrometry

Leu - Leucine

L-FDVA – Nα-(2,4-Dinitro-5-fluorophenyl)-L-valinamide

LS - Large-scale

m - Multiplicity

m/z - Mass-to-charge ratio

MA - Marine agar

MAG – Metagenome Assembled Genomes

MB - Marine Broth

Mb – Megabyte

MDR-TB – Multidrug-resistant Tuberculosis

MFI - Mean Fluorescence Intensity

Mg - Magnesium

MHz – Megahertz

min - Minute

MK - Menaquinone

ML - Maximum Likelihood

mL - Millilitre

mm – Milimeter

mM – Milimolar

mol% - Mole percentage

MRSA – Methicillin-Resistant Staphylococcus aureus

MS/MS - Tandem Mass Spectrometry

MSA - Multiple Sequence Alignment

MTT – [3-(4,5-dimethylthiazol-2-yl)-2,5-diphenyltetrazolium bromide]

N - Normality

NCBI – National Center for Biotechnology Information

NJ - Neighbor Joining

NMR - Nuclear Magnetic Resonance

NP – Natural Products

NPA - Natural Products Atlas

NPS – Nutrient-poor Sediment extract agar

NRPS – Non-Ribosomal Peptide Synthetase

O – Oxygen

OD – Optical Density

PC – Positive Control

PCR - Polymerase Chain Reaction

PDA – Potato-Dextrose Agar

Phe - Phenylalanine

PKS - Polyketide Synthase

ppm - Parts per million

Pro – Proline

PTU - 1-phenyl-2-thiourea

REV – Resveratrol

RiPP - Post-translationally modified peptide

RPM – Rotations per minute

rRNA – Ribosomal ribonucleic acid

RT - Retention Time

SA - Seaweed Agar

SC - Solvent Control

SCN – Starch-Casein-Nitrate agar

Ser - Serine

SS - Small-scale

SSN – Sequence Similarity Network

^T – Type strain

T47D - Breast ductal carcinoma

TLC – Thin-Layer Chromatography

tRNA - Transfer ribonucleic acid

TSA – Tryptic Soy Agar

TSB - Tryptic Soy Broth

UV – Ultraviolet

VLC – Vacuum Liquid Chromatography

δ – Chemical shift

λmax – Lambda max

1

General Introduction

Nature has always been a wealthy supplier of biotechnologically relevant molecules, both in the pharmaceutical and industrial fields [1, 2]. In an era marked by escalating health crises, as the emergence of multi drug-resistant pathogens and the intensification of diseases like cancer, the quest for new therapeutic solutions has never been more critical. One effective strategy to address these pressing societal issues is the discovery and study of new bioactive natural products (NP). These molecules encode a vast reservoir of chemical diversity sharpened by millions of years of evolutionary refinement. Actinomycetota are recognized as number one producers of bioactive compounds in the Bacteria domain [1]. Members affiliated to this phylum can be found both in terrestrial and aquatic environments, and can establish symbiotic associations with diverse organisms, including macroalgae [2]. Bioprospecting the metabolism of strains thriving in such highly dynamic symbiotic associations represents a promising approach to uncovering valuable chemical novelty.

1.1. Microbial Natural Products in Drug Discovery

NP are small molecules, both descendant from primary and secondary metabolism, produced by any living organism. Strolling through the records of human knowledge in illnesses and diseases treatment, NP and their derivatives have been an unmatched source for therapeutic agents [3]. If at the dawn of medicine most of these substances were achieved from plants and animals, today microbial specialized NP metabolites represent the backbone of most currently used drugs [4]. The history of microbial NP drug discovery is portrayed by highs and lows and can be briefly summarized in three key points: (i) the "Golden Age", (ii) the pharmaceutical industry desertion and (iii) the re-emergence enhanced by the genomic era. The starting point may be established in the 1940s, with the discovery of actinomycin, streptothricin and streptomycin, all metabolites produced by the Actinomycetota genus Streptomyces, with the following 30 years representing the so-called "Golden Age" of NP discovery, development, and commercialization which achieved its peak between 1970 and 1980 [3, 5]. The ensuing years witnessed significant improvements in screening methods sophistication but were short in the successful output of novel compounds. In fact, it has been more than 30 years since a new class of antibiotics have entered the clinical pipeline [6]. Notwithstanding the importance of microbial NP, so wellproved along the ages, pharmaceutical companies have started dropping their interest in these compounds, favouring more tractable alternatives [4]. Alongside with the known compounds' re-discovery issue, perhaps the major bottleneck in the field, the lack of compatibility between traditional NP extract libraries and high-throughput screening was also a drawback [3]. In the early 2000s, this misconception that NP bioprospecting was no

longer a fruitful approach to novel drug discovery began to change. Genome sequencing truly prompted the tide turning, with the first *Streptomyces* genome sequences revealing a treasure of formerly undiscovered biosynthetic gene clusters (BGCs), unmasking the real – challenging, but still existing - opportunities for microbial NP discovery [7, 8]. As never before, the knowledge and tools to better understand NP biosynthesis, biochemistry and engineering are available and rapidly upgrading, allowing to take full benefit of the unique properties of these molecules and their producers [4].

Over the past few decades, more than 200 000 NP have been reported [4], many mined from microbial secondary metabolism and exhibiting a wide-range spectrum of bioactivities, with the chemical scaffolds derived from microbial NP being specially distributed among antibiotics. Doxorubicin, rapamycin, penicillin or avermectin exemplify broadly used drugs, with anticancer, immune-suppressing, antimicrobial and antiparasitic properties, illustrating the importance of NP in human and animal health [4, 9-11]. From 1981 to 2019, 1881 new NP and NP-derivative drugs were approved, headed by anticancer, antiviral and antibacterial entities [12]. Examples of clinically-relevant specialized metabolites uncovered in this time frame include aplidine, a new anticancer agent that induces cell growth inhibition and apoptosis in the human leukemia cell line MOLT-4 [13] and delamanid, a well-tolerated and safe drug effective in the treatment of pulmonary multidrug-resistant tuberculosis (MDR-TB) [14]. The ability to produce biotechnologically relevant NP is particularly noteworthy for the phylum Actinomycetota, and so more for the members of the order Actinomycetales, commonly referred as actinomycetes. These microorganisms are recognized as an unrivalled source of not only clinically-relevant bioactive secondary metabolites (e.g., antimicrobials, antifungals, antitumor, anti-inflammatory, antiviral and immunosuppressive agents), but also NP that contribute for a more sustainable agriculture (e.g. insecticides, herbicides and plant growth promoters) [15, 16] and molecules that benefit other industry fields (e.g. antifouling, biofuels, enzymes) [17, 18]. Roughly, 45% of all bioactive metabolites currently known are actinomycetes-sourced, with the genus Streptomyces by itself being responsible for the production of more than 70% of these compounds [19]. Although actinomycetes represent an undeniable source for drug discovery, during many years bioprospecting screening programs have focused their attention on terrestrial sources, thereby managing the isolation and exploration of these bacteria to reach an exhaustion point. This translated in a slowdown on novel bioactive molecules discovery and enforced the necessity to explore distinct alternatives, such as the marine environment [20].

1.2. The Phylum Actinomycetota

The phylum Actinomycetota, until recently named as Actinobacteria [21], represents one of the largest taxonomic units within the Bacteria domain, both in number and diversity [22]. Members associated with this phylum are Gram-positive, typically characterized by a high quanine and cytosine (G+C) content in their genomes, which can reach over 70% in some species. These bacteria exhibit a remarkable variety of morphologies, from coccoid to fragmenting hyphal forms or highly differentiated branched mycelium, with several species being able to reproduce by sporulation. With some exceptions [23], the majority are aerobic and either chemoheterotrophic or chemoautotrophic, being able to degrade and use a wide variety of nutritional sources, including various complex polysaccharides [24, 25]. Most Actinomycetota are free-living organisms and are widely distributed in both terrestrial and aquatic ecosystems, including extreme habitats, as well as in the microbiomes of higher eukaryotes [26]. As classic soil-dwelling microorganisms, they play a vital role in nutrient and organic matter recycling, as well as in the bioremediation of polluted substrates [27]. Species living in association with other organisms, as plants [28] or animals [29], usually protect and benefit the host, boosting its growth and survival. Nonetheless, particular Actinomycetota are described as human pathogens [30].

This enormous taxon's physiological and ecological plasticity strongly reflects on Actinomycetota metabolism, making these bacteria powerful and versatile producers of a wide range of bioactive NP [31]. Remarkably, about two thirds of all known antibiotics used in the clinic today, as well as a vast array of anticancer compounds, immunosuppressants, anthelmintics, herbicides and antiviral compounds, in addition to extracellular enzymes, are Actinomycetota sourced [26]. This biosynthetic arsenal is especially noteworthy for species affiliated to the Streptomyces genus that can contain in their genome 20-40 distinct BGCs encoding specialized metabolites, warranting for decades their place in drug discovery programs spotlight. Nearly 80 years ago, from the culture of three soil-dwelling strains, the first antibiotics from Actinomycetota were discovered: actinomycin from a culture of Streptomyces antibioticus in 1940 [32], streptothricin from Streptomyces lavendulae in 1942 [33] and streptomycin from Streptomyces griseus in 1944 [34]. Since then, thousands of structural diverse bioactive NP have been uncovered from the secondary metabolism of actinomycetes [31], making them undisputably the major microbial source of NP. Although Actinomycetota continue to fuel the biotechnology and medicine sectors with new biomolecules, uncovering novel compounds may be a challenge, with the discovery rate no longer keeping up with the demand for novelty. This trend might be due to several reasons, such as exhaustion and over-reliance on particular taxa or environments, and the lack of innovation in culture conditions or techniques, but it is certainly not consistent with genomic

data, which estimates that only 3% of the NP potentially encoded in bacterial genomes have been experimentally characterized [35]. One profitable strategy to overcome this problematic relies on retrieving new actinomycetes from untapped habitats and ecological niches, as the marine environment [36] and bioprospecting their secondary metabolism.

1.3. Underexplored Environments as Key to Novel Chemistry: the Ocean

The ocean represents the largest environment on earth and host a remarkable and underexplored microbial diversity. Marine microorganisms are exposed to singular light, salinity, pressure, and/or temperature conditions, which fosters the development of exclusive adaptation mechanisms that translate into the production of unique NP [20]. During decades Actinomycetota were considered exclusively soil-dwelling microorganisms, only later being recognized as true inhabitants of marine environments: in 1984, Rhodococcus marinonascens was officially reported as the first marine actinomycete [37] and 20 years later, Salinispora was described as the first genus with mandatory salt requirements to grow [38]. Marine Actinomycetota can be found in numerous ecological niches: from coastal and intertidal areas to deep-sea zones, inhabiting sediments, water or establishing association with higher organisms (as sponges, corals and macroalgae), and their distribution spans across Arctic regions to the tropics [39]. Due to their unique traits, different from their terrestrial counterparts, these bacteria gained the attention of the scientific community in drug discovery field, with hundreds of NP with several bioactive properties been described to date from their metabolism [40], in a continuously upward trend [41]. Perhaps the most illustrative example is the hybrid polyketide salinosporamide A (Marizomib/NPI-0052), a highly cytotoxic proteasome inhibitor isolated from Salinospora tropica [42], now in phase 3 of clinical trials to treat patients with glioblastoma [43]. Still, the diversity and bioactive potential of marine Actinomycetota are still largely unknown and require further study. This is especially noteworthy for species living in symbiosis with other organisms, which association might trigger the synthesis of unique specialized NP [44].

1.4. Macroalgae-associated Actinomycetota: Overview of a Prolific Symbiosis

Macroalgae, also known as seaweeds or marine algae, represent a diverse group of photosynthetic marine organisms that play crucial roles in ocean ecosystems, namely in nutrient cycling, oxygen production and by providing habitat for several other organisms. They can be found distributed in waters across the world and are classified in three main groups based on their pigmentation: brown algae (Phaeophyta), red algae (Rhodophyta), and green algae (Chlorophyta) [45]. Macroalgae offer a favorable habitat for several

microorganisms, both epiphytic and endophytic, including Actinomycetota, that functionally regulate and assist on their health, performance and protection [46, 47]. Bacteria affiliated to other phyla, as Pseudomonadota, Bacteroidota and Firmicutes, are also frequently encountered in macroalgae holobiont, as well as fungal taxa, as Ascomycota and Basidiomycota, viruses, especially bacteriophages, and Archaea. NP resulting from hostmicrobes symbiotic association play key roles as chemical mediators that, besides their specific ecological roles, can also have a pivotal importance for the development of new pharmaceuticals [48]. Life in the ocean is characterized by highly refined relationships among the different life forms. Selective pressures over time have shaped these symbiotic associations, which for the case of microorganisms, can be translated in the production of highly specialized molecules with bioactive properties that impact the host and the surrounding environment. Therefore, exploring the communities of marine actinomycetes living in association with macroalgae holds great promise for uncovering structurally unique bioactive NP with diverse applications. Apart from their associated microbiome, macroalgae also represent by itself a valuable bioresource for many industries and have been explored for centuries for their numerous applications: they are used in human and animal diets due to their nutritional value, which includes essential vitamins, minerals, and antioxidants [49]: based on their bioactive properties, some species are used as pharmaceuticals and incorporated into cosmetics formulations [50, 51]; in agriculture they are used as fertilizers [52]; several macroalgae-derived substances such as agar, carrageenan, and alginate are indispensable in many industries, acting as essential gelling agents and stabilizers [53]; renewable energy production and biofuel development are being explored from macroalgae biomass [54]. The likely correlation between some of these macroalgae biotechnological properties and their associated microbial community requires further investigation, but it is reasonable that these bacteria, and in special Actinomycetota, are in the origin of many of the associated bioactive compounds. In fact, it has been shown that many marine metabolites, previously considered as being produced by higher organisms, are in fact of microbial origin. Examples include bryostatins, polyketides with unique structural features and exhibiting anticancer and neurological activities, that were isolated from the marine bryozoan Bugula neritina, which recent studies indicate that they are actually produced by the uncultured symbiotic bacterium "Candidatus Endobugula sertula" ("E. sertula") [55]. Therefore, exploring the microbiota, particulaly Actinomycetota, associated with such biotechnological relevant organisms as macroalgae stands as a promising avenue to uncover new relevant NP.

1.4.1. Abundance and Diversity

Despite representing a scarcely explored ecological niche, previous studies have demonstrated the presence of Actinomycetota in brown, red and green macroalgae. To the moment, 25 Actinomycetota genera have been successfully isolated from macroalgae species, with a higher prevalence of strains affiliated to Brachybacterium, Microbacterium, Micrococcus, Nocardiopsis and Streptomyces (Table 1). The diversity and abundance of Actinomycetota, similarly to the remaining macroalgae microbiome, can change depending on factors such as the host species, geographic location, environmental conditions, and seasonal variations [56, 57]. It is almost certain that a much broader diversity of actinomycetes can be found in association with macroalgae, apart from the described taxa. To gain access to them, broader sampling campaigns could be conducted, involving the collection of various macroalgae species across diverse biogeographic and seasonal ranges, along with the development of tailor-made culture conditions. Apart from cultured isolates, hight throughput sequencing-based studies can provide deeper insights regarding the distribution of actinomycetes on macroalgae, adding knowledge about the overall composition and dynamics of the microbiome beyond what can be captured through culturomics alone [58]. Overall, more studies have targeted members of the Phaeophyta group towards Actinomycetota isolation, when comparing to Rhodophyta and Chlorophyta, with specimens collected from sampling sites worldwide (Table 2, Fig. 1).

Table 1. Actinomycetota genera recovered from Phaeophyta, Rhodophyta and Chlorophyta macroalgae.

Isolation Source	Actinomycetota Genera	Ref
	Aeromicrobium, Amycolatopsis, Arthrobacter,	
	Brachybacterium, Brevibacterium, Isoptericola,	
	Kocuria, Labedella, Leifsonia, Leucobacter,	
Phaeophyta (Brown macroalgae)	Microbacterium, Microbispora, Micrococcus,	[59-69]
	Micromonospora, Nocardiopsis, Nonomurae,	
	Pseudarthrobacter, Rhodococcus, Sanguibacter,	
	Streptomyces, Tessaracoccus	
	Aeromicrobium, Brachybacterium, Citricoccus,	
Rhodophyta (Red macroalgae)	Janibacter, Microbacterium, Micrococcus,	[59, 60, 63- 65, 70, 71]
Knodopnyta (Ned macroalgae)	Nocardiopsis, Salinibacterium, Streptomyces	05, 70, 71]
	Allokutzneria, Brachybacterium, Brevibacterium,	[E0 60 67
Chlorophyta (Croop magraalgae)	Kocuria, Microbacterium, Micrococcus,	[59, 60, 67,
Chlorophyta (Green macroalgae)	Nocardiopsis, Streptomyces	72, 73]

1.4.2. A Hotspot of Bioactivity

The vast majority of the studies reported on macroalgae-associated Actinomycetota are motivated by NP discovery. Even representing a much less targeted ecological niche when compared with other isolation sources as sediments, sponges or corals, macroalgae have proven to be a true hotspot of bioactive Actinomycetota. Many actinomycetes retrieved from macroalgae specimens collected worldwide have demonstrated biotechnological properties, mostly antimicrobial and anticancer/cytotoxic, but also antiinflammatory, antiviral, antifouling, enzymatic and iron-chelating (Table 2). Although headed by Streptomyces, the affiliation of the active strains is not restricted to this genus, with many others proving their value as source of bioactive compounds: Agrococcus, Amycolatopsis, Arthrobacter, Brachybacterium, Brevibacterium, Isoptericola, Kocuria, Leifsonia, Microbacterium, Microbispora, Micromonospora, Nocardiopsis, Micrococcus, Nonomuraeae, Pseudarthrobacter, Pseudonocardia, Salinibacterium, Sanguibacter and Tessaracoccus. It has been briefly discussed how symbiosis might trigger the synthesis of specialized metabolites and how these benefit the host. The fact that macroalgae, especially specimens inhabiting intertidal coastal areas, like the northern Portuguese rocky shore, are able to thrive under such highly dynamic and competitive environment - with daily oscillations of UV radiation, temperature, salinity, immersion during high tides and drought during low tides, limitations of nutrients and space - showcase how resistant and adaptable these organisms are [74-77]. It is reasonable to assume that their symbiotic Actinomycetota contribute to this resilience through the production of bioactive NP that aid in defence against environmental stressors and competition for resources [78], and which properties can be repurposed to meet our society needs. The number of studies bioprospecting macroalgae-associated actinomycetes is still scarce, most exploring specimens from Atlantic, Pacific and Baltic Sea Coasts, Asia-Pacific and Antarctica regions (Table 2, Fig. 1), but these studies have already proven that these microbes represent a great source of metabolites with relevant applications in many sectors or our society. Also, several novel bioactive NP have been uncovered from their metabolism.

Table 2. Bioactive Actinomycetota isolated from macroalgae. The macroalgae species and corresponding sampling site are indicated, as well as the recovered Actinomycetota genera, bioactivity recorded, and the number of strains reported in each study.

Macroalgae Species		Macroalgae Species		Macroalgae Species Sampling Site		Bioactivity	Number of strains reported	Ref
Phaeophyta (•)	Laminaria ochroleuca	Intertidal rocky shore, Mindelo beach,	Isoptericola	Anticancer	90	[79]		
		Portugal	Microbacterium	Antimicrobial				
			Microbispora	Cytotoxic				
			Nocardiopsis					
			Nonomuraeae					
			Rhodococcus					
			Streptomyces					
	Laminaria saccharina	Kiel Fjord, Baltic Sea, Germany	Amycolatopsis	Antimicrobial	36	[69]		
			Arthrobacter					
			Leifsonia					
			Micrococcus					
			Streptomyces					
	Egregia menziesii	Baja California Ensenada, Mexico	Brachybacterium	Anticancer	6	[67]		
	Sargassum muticum		Brevibacterium	Antibacterial				
			Kocuria					
	Fucus vesiculosus	Kiel Fjord, Baltic Sea, Germany	Brevibacterium	Antimicrobial	15	[63]		
			Nocardiopsis					
			Salinibacterium					
			Streptomyces					
	Adenocystis utricularis	Intertidal rocky shore, King George	Aeromicrobium	Antimicrobial	51	[59]		
		Island, Antarctica	Amycolatopsis					
			Arthrobacter					

		Brachybacterium			
		Labedella			
		Microbacterium			
		Micrococcus			
		Kocuria			
		Pseudarthrobacter			
		Rhodococcus			
		Sanguibacter			
		Tessaracoccus			
Cystoseira baccata	Intertidal coast, Central Cantabrian Sea,	Streptomyces	Antibiotic	14	[60]
Fucus spiralis	Spain		Cytotoxic		
Pelvetia canaliculata					
Bifurcaria bifurcata					
Sargassum horneri	Coast of Nanhuangcheng Island, China	Isoptericola	Alginate lyase	1	[68]
Sargassum thunbergii	Coast of Chungsapo, Busan, Kangnung,	Streptomyces	Anti-inflammatory	163	[73]
Undaria pinnatifida	Korea				
Undaria pinnatifida	Coast of Kangnung, Korea	Streptomyces	Antifouling	1	[80]
Undaria pinnatifida	Coast of Kangnung, Korea	Streptomyces	Antimicrobial	87	[61]
Analipus japonicus	Charatsunai beach, Muroran, Japan	Streptomyces	Iron-chelating	68	[81]
Stypopodium zonale	Bahamas Islands	Micromonospora	Anticancer	1	[64]
Durvillaea potatorum	Rivoli Bay, Beachport, South Australia	Streptomyces	Alginate lyase	80	[82]
Turbinaria ornata	Gulf of Mannar, Southeast coast of Tamil	Nocardiopsis	Antimicrobial	100	[65]
Sargassum wightii	Nadu, India				

ICBAS
Portuguese seaweeds, a marine treasure of Actinobacteria producing novel bioactive compounds

	Fucus sp.	Bejaia coast, Algeria	Streptomyces	Antibacterial	1	[83]
	Lobophora variegata	Gallow's Point, Belize	Not-identified	Anti-inflammatory	1	[84]
	Carpodesmia tamariscifolia	Nocrthwestern Atlantic coast of Morocco	Streptomyces	Antibacterial	4	[85]
	Undaria pinnatifida	Coast of Korea	Streptomyces	Antifouling	1	[86]
	Pelvetia canaliculata	Rocky shore of Sonmiani Beach,	Kocuria	Antimicrobial	1	[66]
		Karachi, Pakistan				
Rhodophyta (•)	Delesseria sanguínea	Kiel Fjord, Baltic Sea, Germany	Nocardiopsis	Antimicrobial	12	[63]
			Microbacterium			
			Salinibacterium			
			Brevibacterium			
			Streptomyces			
	Iridaea cordata	Intertidal rocky shore, King George	Aeromicrobium	Antimicrobial	51	[59]
		Island, Antarctica	Brachybacterium			
			Citricoccus			
			Janibacter			
			Micrococcus			
			Salinibacterium			
			Streptomyces			
	Pachymeniopsis lauceolata	Intertidal zone of Esaki, Iwaya port and	Microbacterium	Antimicrobial	1	[87]
		Oiso, Awaji Island, Hyogo, Japan		Antifouling		
	Gelidiella acerosa	Drini Gunungkidul Yogyakarta, Indonesia	Streptomyces	Antivibrio	14	[88]
			Nocardiopsis			
	Plocamium cartilagineum	Intertidal coast, Central Cantabrian Sea,	Streptomyces	Antibiotic	14	[60]
	Halopteris scoparia	Spain		Cytotoxic		
	Mesophyllum lichenoides					

ICBAS
Portuguese seaweeds, a marine treasure of Actinobacteria producing novel bioactive compounds

	Eucheuma cottonii	Intertidal coast, Gulf of Mannar, India	Brachybacterium	Lignocellulolytic	13	[70]
			Brevibacterium			
			Kocuria			
			Micrococcus,			
			Nocardiopsis			
			Streptomyces			
Chlorophyta (•)	Monostroma hariotii	Intertidal rocky shore, King George	Agrococcus	Antimicrobial	51	[59]
		Island, Antarctica	Arthrobacter			
			Brachybacterium			
			Janibacter			
			Rhodococcus			
			Salinibacterium			
			Streptomyces			
			Pseudonocardia			
	Ulva australis	Intertidal rocky shore, Sharks Point,	Micrococcus	Antimicrobial	3	[89]
		Australia				
	Ulva sp.	Intertidal coast, Central Cantabrian Sea,	Streptomyces	Antibiotic	1	[90]
		Spain		Anticancer		
	Ulva pertusa	South China Sea, China	Streptomyces	Antimicrobial	1	[91,
				Anticancer		92]
	Enteromorpha prolifera	Zhanqiao beach, China	Streptomyces	Anticancer	1	[93]
				Antiviral		
	Blidingia minima	Intertidal coast, Central Cantabrian Sea,	Streptomyces	Antibiotic	14	[60]
		Spain		Cytotoxic		

1.4.3. Novel Chemistry

Some of the reported studies summarized in Table 2 have led to the isolation of novel NP, proving not only that macroalgae are a hub of bioactive actinomycetes living in association with them, but also that these microorganisms are a source of chemical novelty. According to the literature, 32 new NP and one novel enzyme have been described so far from the secondary metabolism of macroalgae-associated Actinomycetota (Table 3). These NP are structurally diverse, with many holding significant pharmaceutical and/or industrial applications. Near 70% are polyketides, many classified as macrolides, followed by peptides (19%), in particular siderophores. The remaining ones are classified as alkaloids, furanones, carboxylic acid and benzaldehyde derivatives. Around 90% of these metabolites were uncovered from the metabolome of *Streptomyces* species, showcasing once again the remarkable biosynthetic machinery of this particular taxon. The remaining were isolated from *Nocardiopsis*, *Micromonospora* and *Kocuria* strains, underscoring the potential for finding novel chemistry by exploring a broader range of actinomycetes beyond the well-studied *Streptomyces* genus.

Polyketides constitute one of the major classes of NP exhibiting a wide range of biological properties with pharmaceutical and industrial applications. They are synthesized by polyketide synthases (PKS) and assembled from simple acyl building blocks derived from acyl-CoA precursors. These enzymes catalyze a series of decarboxylative condensation reactions, leading to the production of a linear or cyclic polyketide chain. This chain may undergo modifications such as reduction, dehydration, and cyclization to generate structurally diverse molecules [94]. Examples of novel bioactive polyketides obtained from macroalgae-associated Actinomycetota include streptoarylpyrazinone A, a N-arylpyrazinone derivative existing as a zwitterion, a type of compounds rarely found from natural resources, and 23-O-butyrylbafilomycin D, a novel bafilomycin. Both molecules were retrieved from a culture of the actinomycete Streptomyces sp. HZP-2216E, isolated from the Chlorophyta Ulva pertusa, and inhibited the proliferation of different glioma cell lines and the growth of methicillin-resistant Staphylococcus aureus [92]. Other example are wailupemycins H-L, new α-glucosidase inhibitors obtained from Streptomyces sp. OUCMDZ-3434 isolated from the Clorophyta Enteromorpha prolifera, which biological properties can be applied towards the treatment of diabetes. In particular, α-glucosidase inhibitors aid in the control of blood sugar levels by slowing down the digestion and absorption of carbohydrates, thereby reducing postprandial (after-meal) hyperglycemia in individuals with type 2 diabetes. Additionally,

wailupemycins exhibit an unusual carbon skeleton and aromatic dimers with a methylene linkage, a rare feature in NP, possessing anticancer and antiviral properties [93, 95]. Macrolides belong to the polyketide class of NP and represent some of the most successful clinically-relevant molecules used to treat infectious and immune diseases [96]. Lobophorins A and B exemplify two anti-inflammatory macrolides that have been isolated from the fermentation broth of an actinomycete isolated from the surface the Caribbean brown alga Lobophora 58issue58te [84]. Other examples include 21,22-enbafilomycin D, 21,22-en-9-hydroxybafil D and 23-O-butyrylbafilomycin D, three macrolide antibiotics with antibacterial and anticancer properties isolated from Streptomyces sp. HZP-2216E, retrieved from a Ulva pertusa specimen collected in China [91, 92]. Also desertomycin G represents a new macrolide with strong inhibitory activity towards several Gram-positive and Gram-negative human pathogens, including Mycobacterium tuberculosis clinical isolates, affecting as well the viability of tumor cells lines without deleterious effects on non-carcinogenic ones [90]. This metabolite was isolated from a culture of Streptomyces althioticus MSM3, obtained from the tissues of the intertidal Chlorophyta Ulva sp. Another example of a polyketide-derived macrolide is the neaumycin B, a potent inhibitor of glioblastoma, the most malignant type of glioma with poor survival rates, produced by the marine Micromonospora sp. CNY-010, isolated from the surface of the brown alga Stypopodium zonale [64].

Siderophores are small, high-affinity iron-chelating compounds secreted by several microorganisms, including bacteria, that are synthesized by non-ribosomal peptide synthetases (NRPS) [97]. Streptobactin, dibenarthin and tribenarthin represent three novel siderophores uncovered from the metabolism of the macroalgae-associated actinomycete *Streptomyces* sp. YM5-799, a symbiont of the Phaeophyta *Analipus japonicus* [81]. Bacterial siderophores and their derivatives have large applications in medicine, being used, for example, to improve drug delivery selectivity in the treatment against resistant bacteria. Additionally, they are used in agriculture to increase the soil fertility and to reduce the level of metal contamination, specifically from soil and water [98].

Apart from polyketides and siderophores, other structurally interesting compounds on this list include the two novel antifouling diketopiperazines, (6S,3S)-6-benzyl-3-methyl-2,5-diketopiperazine (bmDKP) and (6S,3S)-6-isobutyl-3-methyl-2,5-diketopiperazine (imDKP), obtained from a culture of *Streptomyces* praecox 291-11, an actinomycete isolated from the rhizosphere of the kelp *Undaria pinnatifida* [80]. Diketopiperazines represent the smallest known class of cyclic peptides and, even mostly produced by Gram-negative bacteria, they can also be synthesized by Gram-positive strains, fungi

and higher organisms [99]. These two compounds - bmDKP and imDKP - showed the ability to inhibit zoospore settlement of the fouling macroalga Ulva pertusa and the diatom Navicula annexa. Displaying the same bioactivity, the furanone derivatives omF and omF2 were isolated from Streptomyces violaceoruber SCH-09, collected from the thallus of the green alga Undaria pinnatifida [86]. Members of this class of NP have also been reported to exhibit various biological activities, as anti-inflammatory, anticancer and antimicrobial. Fouling organisms are the cause of considerable damage to the surfaces of immersed structures as ships, fishnets, and aquaculture facilities, leading to large economic losses. Most techniques employed to combat this problematic rely on synthetic coats containing toxic compounds that cause detrimental effects on the environment and non-target species, making it critical to explore alternative, sustainable methods [100]. In this regard, Actinomycetota-sourced NP pose as a promising solution to this problematic. From the rhizosphere of the brown macroalgae Undaria pinnatifida, Streptomyces atrovirens PK288-21 was isolated and positively screened for antimicrobial activity against bacterial fish pathogens. Two compounds, 2-hydroxy-5-(3methylbut-2-enyl)benzaldehyde and 2-hepta-1,5-dienyl-3,6-dihydroxy-5-(3-methylbut-2enyl)benzaldehyde, were identified from the culture extract of this strain, with the first one representing a new benzaldehyde derivative [61]. Benzaldehyde derivatives are organic compounds containing a benzaldehyde moiety with additional functional groups attached to it, and over the years many have been isolated and reported from fungi and bacteria due to their biological activity [101-103]. Both compounds were effective against the growth of Edwardsiella tarda and Streptococcus iniae, two economic aquaculturerelevant pathogenic species responsible for high mortality rates and decreased production in fish and shellfish farms worldwide [104, 105]. The novel benzoic acid derivative kocumarin, was isolated from the culture of Kocuria marina CMG S2, retrieved from the thallus tissues of the Phaeophyta Pelvetia canaliculate [66]. Benzoic acids are a group of organic compounds with a benzene ring and a carboxylic acid group. These molecules can either be nature-sourced or industrially synthetized, having a wide range of applications, from antimicrobials to food stabilizers and plastic production [106, 107]. Kocumarin displayed strong inhibition effect against a set of fungi and pathogenic bacteria, including methicillin-resistant Staphylococcus aureus (MRSA). Infections caused by antibiotic-resistant bacteria stands as one of the major global health challenges of our time, making the discovery of novel active chemical entities with antibacterial properties critical [108].

Enzymes are biological molecules, typically proteins, that due to their ability to catalyze specific chemical reactions with high efficiency and selectivity under mild

conditions are essential for numerous industrial processes, from the production of phamarceuticals to biofuels [109]. From the macroalgae-associated *Streptomyces luridiscabiei DS44*, a novel alginate lyase, AlyDS44, was purified and characterized. Based on the highly conserved regions of its amino acid sequences, this enzyme was identified as part of the polysaccharide lyase family that is responsible for breaking down complex polysaccharides, such as those found in macroalgae cell walls. AlyDS44 holds the potential for efficient production of alginate oligosaccharides with low degrees of polymerization wich can be relevant in many sectors - biomedical, pharmaceutical, feeding and cosmetics – due to the bioactive properties of these molecules, improved solubility and ease of processing [82]. The producing strain was isolated from the decomposing tissues of the brown macroalga *Durvillaea potatorum*.

Even scarce, the exploration of macroalgae-associated Actinomycetota has unveiled a treasure trove of novel NP with unique structures, highlighting both the richness of bioactive compounds harbored by these microorganisms and the chemical diversity encoded within their genomes. Interestingly, so far, no NP was described from a Rhodophyta-associated Actinomycetota. Figure 1 summarizes all the information on bioactive macroalgae-associated Actinomycetota, and novel NP discovered from their metabolism.

Table 3. Novel NP retrieved from macroalgae-associated Actinomycetota. The compound name, type of molecule and corresponding molecular formula are indicated, as well as the producing strain and reported bioactivity.

Compound Name	Type of Molecule	Molecular Formula	Producing Strain	Bioactivity	Ref
Streptoarylpyrazinone A	Polyketide	C ₂₂ H ₂₂ N ₂ O ₄	Streptomyces sp. HZP-2216E	Antibacterial	[02]
23-O-butyrylbafilomycin D		C ₄₈ H ₇₄ NO ₁₄	Streptomyces sp. HZP-2216E	Anticancer	[92]
Wailupemycin H		C43H30O11			
Wailupemycin I		$C_{43}H_{30}O_{11}$			
Wailupemycin J	Dabdadda	C ₂₀ H ₁₆ O ₄		α-glucosidase inhibitor,	[93,
Wailupemycin K	Polyketide	C ₁₇ H ₁₆ O ₄	Streptomyces sp. OUCMDZ-3434	Cytotoxic, Antiviral	95]
Wailupemycin L		C ₁₈ H ₁₆ O ₆			
3-O-methylwailupemycin G		C ₂₂ H ₁₆ O ₅			
2-hydroxy-5-((6-hydroxy-4-oxo-4H-pyran-2-		Streptomyces sundarbansensi	Streptomyces sundarbansens	A (1) (1)	[00]
yl)methyl)-2-propylchroman-4-one	Polyketide	C ₁₈ H ₁₆ O ₅	WR1L1S8	Antibacterial	[83]
Zoumbericin A		C ₂₀ H ₁₅ O ₅			
Zoumbericin B	Dolykotido	Polyketide C ₁₃ H ₁₂ O ₄ Streptomyces ambofaciens BI0048 No bioactivity	No biogotivity described	[440]	
Germicidin K	Polyketide		Streptomyces ambolaciens Bi0048	No bioactivity described	[110]
Germicidin L		$C_{10}H_{14}O_4$			
4-amino-6-methylsalicylic acid		C ₈ H ₉ NO ₃	Nacardianaia an ASOOC	No biogeticity described	[444]
5-methylresorcinol	Pokyketide	$C_7H_8O_2$	Nocardiopsis sp. AS23C	No bioactivity described	[111]
Lobophorin A	Delederide	C ₆₁ H ₉₂ N ₂ O ₁₉	Astinance to OND 007	A 4: : #1	[0.4]
Lobophorin B	Pokyketide	$C_{61}H_{90}N_2O21$	Actinomycete CNB-837	Anti-inflammatory	[84]
21,22-en-bafilomycin D	Pokyketide	C ₃₅ H ₅₆ O ₈	0(A - til t i - 1	[04]
21,22-en-9-hydroxybafil D		C ₃₅ H ₅₆ O ₉	Streptomyces sp. HZP-2216E	Antibacterial, Anticancer	[91]
Desertomycin G	Pokyketide	C ₆₂ H ₁₀₉ NO ₂₁	Streptomyces althioticus MSM3	Antituberculosis, Anticancer, Antimicrobial	[90]

ICBAS
Portuguese seaweeds, a marine treasure of Actinobacteria producing novel bioactive compounds

Neaumycin B	Pokyketide	C ₅₀ H ₈₂ O ₁₂	Micromonospora sp.	Anticancer	[64]
Desferrioxamine B2	Siderophore	$C_{24}H_{46}N_6O_8$	Streptomyces albidoflavus KC180	Antibacterial	[85]
Streptobactin		C ₅₁ H ₆₉ N ₁₅ O ₁₈			
Dibenarthin	Siderophore	$C_{34}H_{48}N_{10}O_{13} \\$	Streptomyces sp. YM5-799	Iron-chelating	[81]
Tribenarthin		$C_{51}H_{71}N_{15}O_{19}$			
bmDKP	Peptide	C ₁₂ H ₁₄ N ₂ O ₂	Strontomyggg progggy 201 11	Antifouling	[00]
imDKP	replide	$C_9H_{16}N_2O_2$	Streptomyces praecox 291-11	Antilouling	[80]
Streptopertusacin A	Alkaloid	$C_{22}H_{28}N_2O_5S$	Streptomyces sp. HZP-2216E	Antibacterial	[91]
omF	Furanone	C ₁₃ H ₁₈ O ₂	Streptomyces violaceoruber SCH-09	Antifouling	[86]
omF2	Fulatione	$C_{13}H_{20}O_2$	Streptomyces violaceoruber SCI 1-09	Antilouling	[00]
Kocumarin	Carboxylic acid	C ₁₅ H ₁₂ O ₂	Kocuria marina CMG S2	Antimicrobial	[66]
2-hydroxy-5-(3-methylbut-2-	Benzaldehyde	C ₉ H ₁₂ O ₂	Streptomyces atrovirens PK288-21	Antibacterial	[61]
enyl)benzaldehyde	Denzaldenyde		Sueptomyces audvitens FN200-21	Antibacterial	ניין
AlyDS44	Enzyme	Not avaiable	Streptomyces luridiscabiei DS44	Alginate degradating	[82]

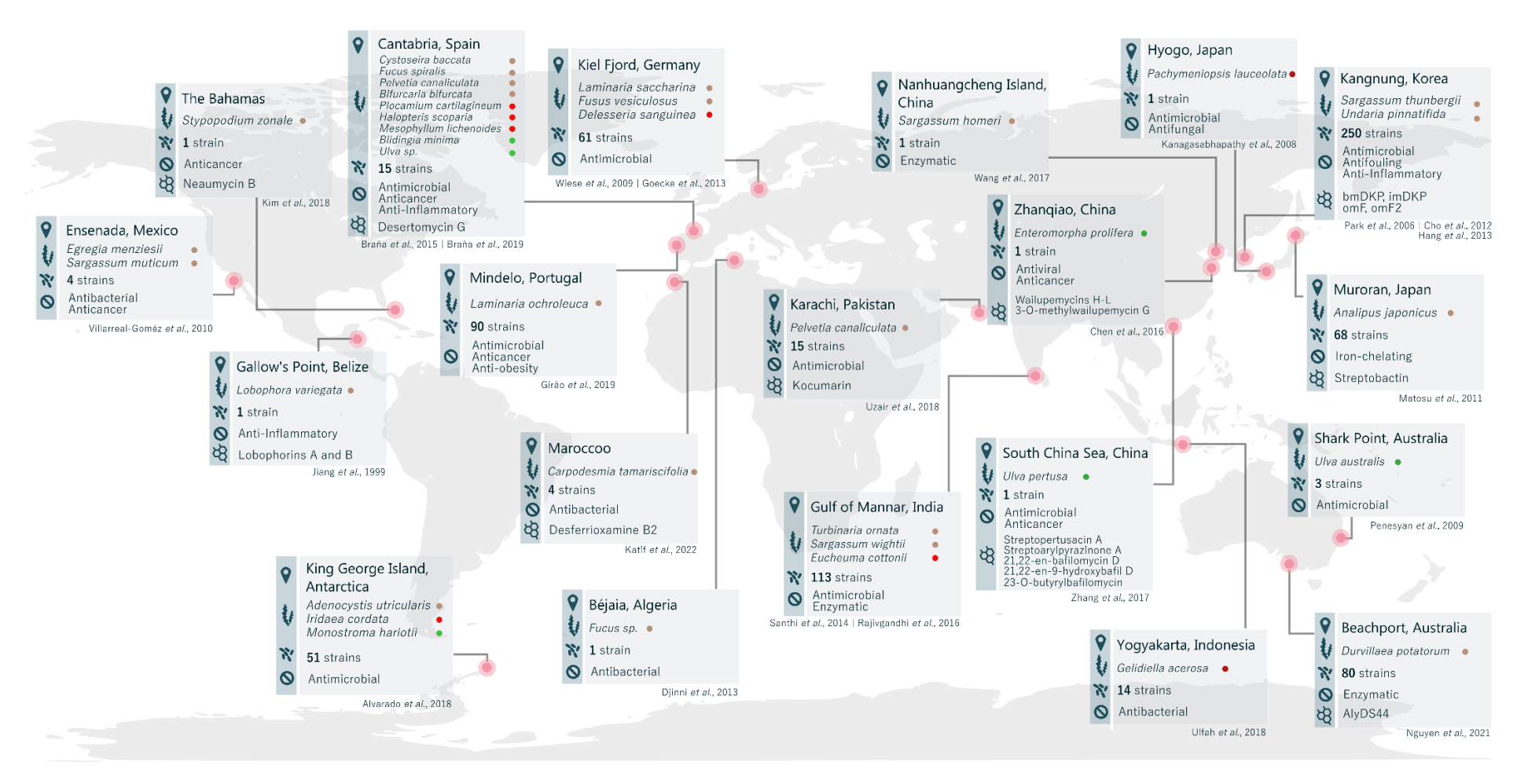


Figure 1. Macroalgae-associated Actinomycetota described worldwide. Information regarding each sampling site, the macroalgae species collected, the number of reported Actinomycetota strains, the bioactivity screening results, and novel NP elucidated is presented. (•) Phaeophyta (•) Rhodophyta (•) Chlorophyta.

1.5. Cultivation-Independent Methods: Taking Advantage of the Genomic Era to Boost the Discovery of NP

Traditionally, the primary methods for studying microbial diversity and their biosynthetic assets, namely involved in NP production and drug discovery, relied solely on strain isolation and cultivation. However, this classical approach has limitations particularly in capturing the full spectrum of microbes present in complex environmental samples, since many species are recalcitrant to cultivation or unable to be cultured at all. In fact, it is estimated that 85-99% of bacteria and archaea cannot be grown under laboratorial conditions, radically limiting our knowledge of microbial life, and holding back NP discovery [112]. Cultivation-independent methods, such as metagenomics and metabolomics, rely on high-throughput sequencing (HTS) technologies to directly examine the collective genetic material of entire microbial communities present in an environmental sample, bypassing the need for cultivation. Emerging as powerful tools to circumvent the limitations of culture-dependent approaches, these ever-evolving omics tools provide a more comprehensive understanding of microbial communities, offering a new window of knowledge and a pathway to harness the so-called microbial dark matter, unlocking information on their diversity and full biosynthetic potential that would otherwise remain inaccessible [113]. Metagenomic data can be used to reconstruct genomes of uncultured microorganisms (metagenome-assembled genomes - MAGs), providing insights into their metabolic capabilities and allowing the identification and analysis of cryptic BGCs that can later be expressed in heterologous hosts, bringing biosynthetic diversity from the environment into drug discovery pipelines. While metagenomics offers various advantages over conventional techniques, certain limitations should also be taken into consideration, such as bias classification depending on databases completeness and curation, non-availability of quality DNA samples and difficulties associated to synthetic biology [114]. Yet, the benefits of cultivationindependent methodologies for studying both marine Actinomycetota diversity [115] and unlocking novel bioactive molecules [114], namely from symbiotic strains [116], have been shown before.

Metagenomics and other *in silico* tools have been also employed in some studies to analyse macroalgae holobiont. Examples include the recovery of bacterial MAGs from the microbiome of the Rhodophyta *Pyropia haitanensis*, 8 of them from Actinomycetota, that have been explored to gain insights into the metabolic functions of these symbionts to the host [117]. Using metagenomics, coupled with amplicon sequencing and imaging techniques, the surface microbiome and metabolome of the Phaeophyta *Fucus*

vesiculosus has been mapped, with results showing both the presence of Actinomycetota and the production of 50 microbial secondary metabolites, only 37 of them previously reported [58]. Also, from a metagenomic library constructed from microorganisms associated to the brown macroalgae $Ascophyllum\ nodosum$, a halotolerant cold-active marine endo- β -1,4-glucanase was identified and characterized, showing the opportunity for enzymatic discovery [118].

The use of culture-independent strategies undoubtedly represent more than ever a promising avenue for the discovery of novel NP, providing direct access to the genetic potential of microbial communities in complex environmental samples. However, studies combining both culture-dependent and independent approaches are advantageous for a more comprehensive understanding of microbial diversity and functional capabilities, representing a good approach to harness the full biotechnological potential of prolific drug producers, as macroalgae-associated Actinomycetota.

1.6. Current Challenges and Opportunities

Microbial specialized NP encode diverse and unique scaffolds and biological properties, making them valuable resources for drug discovery, biotechnology, and environmental applications. This is especially noteworthy for members of the Actinomycetota phylum. In the hunt for novel chemistry, bioprospecting actinomycetes from underexplored marine ecological niches, as macroalgae symbionts, has proven to be a profitable approach. Diverse actinobacterial taxa encoding a wide range of biological properties, mostly antimicrobials, have been uncovered so far from this prolific spot, highlighting the opportunity for discovery. In what concerns the isolation of macroalgae-associated Actinomycetota strains, conducting broader biogeographic and seasonal sampling campaigns, with the collection of various algae species, and the employment of tailor-made culture conditions could facilitate the establishment of larger and more diverse actinobacterial collections for advancing bioprospecting efforts. The combination of culture-dependent and independent approaches can successfully lead to the comprehensive exploration of the full microbial diversity associated with macroalgae, thus promoting the likely discovery of novel taxa and its encoded biosynthetic potential. Furthermore, prioritizing the screening, isolation, and chemical characterization of novel NP from these microbes should be a focal point. Combining classic chemical analytical tools with genomic and bioinformatic approaches can streamline the identification of unique BGCs, expediting new metabolites discovery and providing insights into biosynthetic pathways involved. By exploring the chemical output of the synergistic interactions between macroalgae and symbiotic Actinomycetota new NP able to feed our society needs and challenges can be uncovered.

In summary, bioprospecting macroalgae-associated Actinomycetota represent a significant opportunity for NP discovery.

1.7. Aim and Outline of this Thesis

This Thesis is focused on the study of the diversity and potential of Actinomycetota associated with two common native macroalgae from the Portuguese coast -C. tomentosum and C. crispus - to produce bioactive compounds with relevant biotechnological applications, using both culture-dependent and -independent approaches. The specific objectives of this Thesis consisted in:

- (i) Isolate and taxonomically identify Actinomycetota associated with two specimens of macroalgae from the northern Portuguese coast, *C. tomentosum* and *C.crispus*;
- (ii) Perform the description of novel Actinomycetota taxa;
- (iii) Screen the collection of actinomycetes isolates for the production of bioactive compounds with anticancer, antimicrobial and anti-obesity properties;
- (iv) Isolate and chemically elucidate novel molecules;
- (v) Explore the diversity and biosynthetic potential of the non-cultured macroalgaeassociated Actinomycetota community using in silico tools (metagenomics and genome mining).

The present thesis starts with a comprehensive overview of the state-of-the-art in microbial NP and their relevance for drug discovery, focusing on Actinomycetota-sourced compounds, with particular emphasis on those obtained from strains associated with macroalgae (Chapter 1). The ecological and biotechnological properties of these strains, the newly discovered chemistry associated to them, and current challenges and opportunities in the field are discussed. Following this framework, a sequence of six chapters is presented, each detailing a particular section of the experimental work. Chapter 2 provides the study of the culturable and non-culturable actinobacterial diversity associated to *C. tomentosum* and *C. crispus*, collected from the northern Portuguese coast. Chapter 3 describes the novel taxa *Nocardiopsis codii* sp. nov., and *Rhodococcus algaerubra* sp. nov., two new species isolated from the collected macroalgae. Chapter 4 includes the investigation of the bioactive potential of the

actinomycetes collection obtained from both macroalgae, by performing screening tests for anticancer, antimicrobial and anti-obesity activities, as well as metagenomics analysis. **Chapter 5** provides the description of decylprodigiosin, a new member of the prodigiosin family isolated from *Streptomyces violaceoruber* CT-F61 obtained from the frond tissues of *C. tomentosum*. **Chapter 6** is dedicated to cellulamides, a new family of peptides discovered from *Cellulosimicrobium funkei* CT-R177, a strain isolated from the holdfast tissues of *C. tomentosum*. **Chapter 7** comprises the bioactivity-guided isolation of novel chemistry from the secondary metabolism of *Streptomyces violaceoruber* CT-F61 and *Micromonospora* sp. CC-F88, the latter strain isolated from the frond tissues of *C. crispus*. To finalize, **Chapter 8** summarizes the main conclusions of this Thesis, highlighting the main findings of this thesis, needs, and opportunities for future research.

2

Unveiling the culturable and non-culturable actinobacterial diversity in *Codium tomentosum* and *Chondrus crispus* macroalgae collected from the northern Portuguese coast

The content of this chapter is published in the Q1 journal **Environmental Microbiology**, in open access format:

<u>Girão M.</u>, Alexandrino D.A.M., Weiwei C., Costa I., Zhongjun J., Carvalho M.F. (2024) Unveiling the culturable and non-culturable actinobacterial diversity in two macroalgae species from the northern Portuguese coast. *Environmental Microbiology*, 26(4), e16620 **DOI: 10.1111/EMI.16620**

ABSTRACT

Macroalgae-associated Actinomycetota remains one of the least explored marine niches. Actinomycetota secondary metabolism, as the major microbial source of biotechnologically relevant compounds, sustains efforts into the study of the distribution, dynamics and metabolome of these microorganisms. In this chapter, we combine classic cultivation and metagenomic analysis to survey Actinomycetota diversity in two native macroalgae from the Portuguese coast - Chondrus crispus and Codium tomentosum. A collection of 380 strains was obtained and taxonomically identified, being distributed across 12 orders, 15 families and 25 genera affiliated to the Actinomycetia class, composed by around 60% of Streptomyces. Metagenomic results showed that Actinomycetota is present in both C. crispus and C. tomentosum datasets, with 11 and 2% of relative abundance, respectively. This approach identified 12 orders, 16 families and 17 genera affiliated to Actinomycetota, with little overlapping with the cultivation results. Acidimicrobiales was identified as the dominant actinobacterial order in both macroalgae, but no strain affiliated to this taxonomic group was successfully isolated. Our findings suggest that macroalgae represents a hotspot of Actinomycetota. The synergistic use of both culture dependent and independent approaches proved to be beneficial, enabling the identification and recovery of not only abundant but also rare taxonomic members.

Keywords: Actinomycetota; *Codium tomentosum; Chondrus crispus*; Diversity; Metagenomics

2.1. INTRODUCTION

Actinomycetota represents one of the major Bacteria phyla, both in number and diversity [119]. Members of this phylum can be found in sundry environments, including marine ecosystems where they can establish symbiotic interactions with other organisms, as macroalgae [79]. One of the most recognizable traits of these microorganisms is their unrivaled ability to synthetize biotechnologically-relevant NP [26, 39], making the exploration of their metabolism for chemical novelty the driven force of many research programs. This biosynthetic capability is especially noteworthy for a more restrict group of Actinomycetota members, usually designated as actinomycetes. Yet, one major bottleneck in NP research is the limited accessibility to novel sources for exploration [4], which highlights the importance of retrieving novel marine microbes and explore the extensive pool of underexplored assets that their metabolism encodes [120]. Macroalgae, also referred as seaweeds, represent a diverse group of ecological, biotechnological and industrially-significant organisms that can be found in several marine habitats, from intertidal zones to deeper oceanic regions [121, 122]. They play a major role in nutrient cycling, oxygen production, carbon fixation and coastal protection, with many living beings relying on them as a primary food source, habitat and shelter, stressing their importance in maintaining marine systems health, resilience and biodiversity [123]. Apart from their ecological role, macroalgae represent a billion dollar sized market [124]: these organisms are used in human and animal diets [49, 125], applied in agriculture as fertilizers [126], represent a potential source of renewable biofuels and bioenergy [127] and are able to synthesize a wide range of biotechnologically-relevant bioactive compounds [50, 128-131]. Macroalgae host and provide habitat for a wide range of microorganisms, from fungi to bacteria. These microbes form complex and dynamic communities that contribute to the overall health and functioning of the macroalgae, as well as to their interactions with the surrounding environment [46]. Previous studies have described Actinomycetota associated with species belonging to the phyla Chlorophyta and Rhodophyta and the class Phaeophyceae (green, red and brown, respectively), mostly distributed across Atlantic, Pacific and Baltic Sea Coasts [63, 64, 79, 90, 132, 133], Asia-Pacific [66-68, 70, 80-82, 88, 134, 135] and Antarctica [59] regions, with many of them exhibiting remarkable bioactivities.

In the Atlantic Ocean, the rugged northern Portuguese coastline features diverse intertidal zones with rocky outcrops and tidal pools that provide habitats for numerous species of macroalgae [136]. *C. crispus* and *C. tomentosum* represent two native and

abundant species from the intertidal Portuguese coast, belonging to the phyla Rhodophyta and Chlorophyta (red and green macroalgae, respectively). Both species can be found attached to rocks and other substrates, thriving in highly dynamic habitats with fluctuating environmental and biological conditions: intertidal rocky areas are subject to various stressing factors as desiccation, temperature fluctuations, exposure to UV radiation, salinity and osmotic changes, competition for space and resources, grazing and anthropogenic pressure [74-77]. Microorganisms able to flourish in association with macroalgae living in such distinctive and challenging ecological niches are expected to possess unique adaptive mechanisms and diversity. Recently, studies using Chlorophyta *Ulva* species have shown that the macroalgae-associated bacterial community, including Actinomycetota, can have beneficial and adverse effects on the host growth and development depending on environmental stress conditions [137, 138]. In the single study harnessing exclusively the diversity and bioactive potential of the Actinomycetota culturable community associated to a kelp from the northern Portuguese shore, a rich reservoir of taxonomically diverse strains producing antimicrobial and anticancer metabolites was uncovered [79]. To our knowledge, the Actinomycetota community living in association with C. crispus and C. tomentosum has never been explored before, though previous studies have described other bacterial phyla associated to C. crispus collected in the same region, namely Planctomycetota [139], with brief mentions to the presence of Actinomycetota [140].

In the present study, we aim to survey the Actinomycetota communities living is association with these macroalgae species. By combining metagenomic sequencing and microbial cultivation techniques, as culture-independent and dependent approaches, we targeted to explore the abundance, diversity and taxonomic distribution of this phylum in this symbiotic niche. The main taxa recovered using both methodologies are described and compared, enriching the understanding of the broader landscape of macroalgae-associated actinobacterial communities.

2.2. MATERIALS AND METHODS

2.2.1. Macroalgae Sampling

One specimen of *Chondrus crispus* and one specimen of *Codium tomentosum* were collected in early January 2020 in the intertidal area of the northern Portuguese rocky shore (41.309298°; -8.742228°). The macroalgae were transported to the laboratory under refrigeration conditions and processed on the same day for the study of Actinomycetota culturable and non-culturable communities.

2.2.2. Actinomycetota Isolation

The collected macroalgae (one specimen per species) were thoroughly washed with sterile seawater, to remove any larger particles attached, and each dissected into two distinct parts: holdfast and blades. Each part was segmented into smaller pieces and macerated until the obtainment of 0.5 g of macerated tissues (in total, each macroalgae yielded two macerated tissue samples, extracted from both its holdfast and blades, totaling four samples altogether). To increase the success of Actinomycetota isolation, by limiting the incidence of non-spore forming microorganisms and potentiating the development of slow growing strains, the four samples of macerated tissues were separately placed in 2 mL tubes containing 1 mL of sterile seawater and incubated in a water bath at 58 °C for 15 min. The resulting samples were ten-fold diluted until 10⁻², using sterile seawater, and 100 µL of each dilution was inoculated in duplicate in four distinct selective culture media for Actinomycetota, to enhance the recovery of strains with different growth requirements and metabolic profiles: Nutrient-poor Sediment Extract agar (NPS), Actinomycete Isolation Agar (AIA), Starch-Casein-Nitrate agar (SCN) and Seaweed Agar (SA) (Table 4). SA was formulated to mimic the natural environment of macroalgae-associated microbial symbionts, being solely composed by the tissues of each macroalgae reduced to powder using liquid nitrogen and seawater. Pieces of the macerated tissues (one 10µL loop) were also directly inoculated, in duplicate, on the four agar media mentioned above. The 98 generated plates were incubated for a period of up to 6 months at room temperature (± 24 °C) and periodically inspected to track bacterial growth. All morphologically distinct colonies were streaked on the respective isolation medium until obtainment of pure cultures and preserved at -80°C in 30% (v/v) glycerol.

Table 4. Formulation of the selective culture media used for the isolation of Actinomycetota.

NPS*		AIA**		SCN**		SA*	
Agar	17 g	Agar	17g	Agar	17 g	Agar	17 g
Marine	100mL	Sodium	4 g	Soluble starch	10 g	Seaweed	10 g
sediment		propionate		Casein	0.3 g	powder	
extract		K ₂ HPO ₄	0.5 g	K ₂ HPO ₄	2 g		
(obtained by		Na ₂ CO ₃	0.2 g	KNO₃	2 g		
washing		FeSO ₄	0.2 g	NaCl	2 g		
beach sand		L-arginin	0.1 g	MgSO ₄ .7H ₂ O	0.05 g		
with 500 mL		MgSO ₄	0.2 g	CaCO ₃	0.02 g		
of seawater)				FeSO ₄ .7H ₂ 0	0.01 g		

^{*}per liter of seawater; **per liter of 60:40 seawater/deionized water; All media were supplemented with cycloheximide (50 mg L⁻¹), nalidixic acid (50 mg L⁻¹) and nystatin (50 mg L⁻¹) (Sigma-Aldrich, MO, United States).

2.2.3. Identification of the Isolates and Phylogenetic Analysis

All isolates were taxonomically identified through 16S rRNA gene sequencing. Biomass for DNA extraction was obtained by growing each isolate at 28 °C, for one week, in the corresponding isolation agar media (Table S1 - Appendix I). Genomic DNA was extracted using the E.Z.N.A. Bacterial DNA Kit (Omega Bio-Tek, GA, United States) according to the manufacturer's instructions. The 16S rRNA gene was amplified by PCR using the universal primers 27F/1492R [141], as described by Girão et al., 2019 [79]. The acquired 16S rRNA gene sequences were analyzed using Geneious Prime 2023.1 software (Biomatters, Auckland, New Zealand). EzTaxon tool from EzBioCloud database [142] was used to establish strains taxonomic affiliation based on consensus sequence similarity with deposited quality-controlled 16S rRNA data. All sequences were deposited in GenBank (NCBI, Bethesda, MD, USA) (Table S1 - Appendix I) under the accession numbers OR215046-OR215420. A phylogenetic study was performed to in-depth understanding of the influence of the isolation origin (C. tomentosum or C. crispus tissues) on the evolutionary relationship between the retrieved Actinomycetota strains. Two phylogenetic trees, one comprising all strains identified as Streptomyces and other all the non-Streptomyces isolates (Figs 3 and 4, respectively) were constructed. The sequences were aligned using MUSCLE [143] from within the Geneious software package and the Maximum Likelihood (ML) method with 1000 bootstraps based on the Tamura-Nei model applied. MEGA-X [144] was used to build the tree and iTOL to perform its final display and annotation [145]. Strains identified as potential novel species were subjected to an individual phylogenetic analysis as well. According to EzTaxon database results, for the taxonomic study of each potential novel species, the fifteen closest related valid species were selected, with no more than a single sequence being selected for the same species, and a phylogenic tree was constructed as described above.

2.2.4. DNA Extraction and Quantification for Metagenomic Analysis

For each macroalgae species, 2 g of tissue were macerated with the aid of liquid nitrogen and placed in a collection tube. Environmental DNA (eDNA) was extracted using DNeasy PowerSoil Pro Kit (QIAGEN, Inc., Germany), according to the manufacturer's instructions. The obtained DNA was quantified using Qubit Fluorometer (Thermo Fisher Scientific – United States).

2.2.5. Metagenomic Sequencing and Analysis

For shotgun metagenomic sequencing, libraries were first generated using Illumina TruSeq Nano DNA LT Library Preparation Kit and index codes were added to attribute sequences to each sample. Briefly, for each sample, DNA was fragmented by sonication to a size of ~400 bp, then fragments were end-polished, A-tailed and ligated with the fulllength adaptor for Illumina® sequencing with further PCR amplification. The PCR amplification aimed to selectively enrich DNA fragments that had been ligated with the AATGATACGGCGACCACCGAGATCTACAC, full-length adaptor (R1: R2: TAGAGCATACGGCAGAAGACGAAC). Finally, PCR products were purified (AMPure XP system) and libraries were analyzed for size distribution by Agilent2100 Bioanalyzer and quantified using real-time PCR. Paired-end reads were generated in an Illumina NovaSeq platform (Illumina, USA) with PE150 platform. Metagenomic sequencing data generated in this study were deposited in the European Nucleotide Archive (EMBL-EBI) database and are available under the accession numbers ERR12332060 and ERR12332061. All taxonomical inferences produced from these metagenomic datasets were performed in KBase [146]. For this, paired-end libraries from each sample were first merged and low-quality reads (< 36 bp, < Q15 within 4-base windows) were subtracted from the datasets using Trimmomatic [147]. Then, read hygiene analysis of the post-trimmed libraries was performed using the FastQC function [148] to confirm the quality of these libraries for the downstream annotations. To trace the profiles of prokaryotic taxonomy for each macroalgae, unassembled high-quality metagenomic reads were taxonomically annotated using the Kaiju taxonomic classifier v1.9.0 [149] using the RefSeq Genome database (not including eukaryotes) as reference. Database searches were performed for all taxonomic ranks in the Maximum Exact Matches mode, with no sub-sampling and considering a relative abundance threshold of 0.1%.

2.3. RESULTS AND DISCUSSION

2.3.1. Isolation, Diversity and Phylogeny of Culturable Macroalgae-associated Actinomycetota

In order to investigate the diversity of culturable Actinomycetota associated to the macroalgae *C. tomentosum* and *C. crispus*, specimens of these organisms were collected in the intertidal northern Portuguese rocky shore and processed for bacterial isolation. From the two collected macroalgae, a total of 380 Actinomycetota strains were isolated into pure cultures (210 from *C. tomentosum* tissues and 170 from *C. crispus*), and taxonomically identified. A diverse array of typically morphological and physiological traits associated to this phylum was observed within the collection, with strains encompassing a wide range of sizes, shapes and colors, production of mycelial networks, spores and pigments, synthesis of volatile compounds translated in a distinctive earthy odor and overall slow growth (Fig. 2). To our knowledge, these 380 strains represent the largest published collection of macroalgae-associated Actinomycetota to date.



Figure 2. Examples of the morphological diversity of Actinomycetota strains isolated from *C. crispus* and *C. tomentosum* macroalgae.

To better explore if any particular region of the macroalgae was more prolific for Actinomycetota isolation, the collected specimens were segmented into two parts: holdfast and blades. Several strains were recovered from both regions, with a higher number of isolates being retrieved from holdfasts in both specimens. These finding are consistent with previous results for the kelp Laminaria ochroleuca [79], emphasizing the prevalence of this taxa in this part of the thallus, likely due to the micro-environments established by distinct morphological niches in the host [150]. Four different culture media - distinctive in nutrients composition - were used in this work to isolate the target microorganisms, with more strains being obtained with the medium AIA (Fig. 3A, Table S1 - Appendix I). Former studies have also used this medium to successfully retrieve Actinomycetota from diverse origins, including marine sources [151-153]. The oligotrophic medium, NPS, was used to replicate the nutrient-poor conditions typically found in the marine environment, while the tailor-made medium, SA, was employed to simulate the conditions that the macroalgae under investigation offer to their symbiotic partners. By granting limited and selective nutritional sources, these media can support the growth of bacteria more adapted to marine environments and, more specifically, of those living in symbiotic relationships with macroalgae. Conversely, AIA and SCN, richer in carbon and nitrogen sources, suit better strains that require higher nutritional standards to thrive. The fact that all culture media were effective in the isolation of the target taxa, pinpoints dissimilar metabolic profiles and requirements among the obtained bacteria. This is interesting not only from a diversity angle, but also from a biotechnological perspective: metabolic plasticity is greatly relevant concerning the synthesis of unique bioactive secondary metabolites, a distinctive and remarkable actinobacterial trait. In fact, likewise SA developed in this work, it has been shown that supplementing culture media with the host macroalgae might benefit the growth of Actinomycetota and the production of valuable molecules as antibiotics [154].

To confirm Actinomycetota affiliation and determine taxonomic identity, all the 380 isolates were identified through 16S rRNA gene sequencing. According to the genomic data, these strains are distributed across 12 orders, 15 families and 25 genera affiliated to the Actinomycetia class (Figs. 3B, 3C). The genus *Streptomyces* emerged as the prevailing taxonomic group, with 231 strains successfully isolated, representing near 61% of all collection, followed by the genera *Rhodococcus*, *Nocardiopsis* and *Micromonospora* with 36, 25 and 22 isolates, respectively. This distribution was observed in both macroalgae, with 131 *Streptomyces* retrieved from *C. tomentosum* and 100 from the tissues of *C. crispus*, followed by the higher abundance of *Rhodococcus*,

Nocardiopsis and Micromonospora strains (Fig. 3C). The predominance of Streptomyces is not unexpected, since they represent the most abundant culturable Actinomycetota, and are well adapted to the marine environment [155]. In a previous study harnessing kelp-associated Actinomycetota from the same environment, the over-representation of this particular taxon was also observed [79]. Given its high occurrence on the studied macroalgae, we can hypothesize on its significance to the host-interaction and surrounding environment. Streptomyces are the major microbial source of bioactive secondary metabolites with a broad range of properties [156], and several isolates belonging to this genus have been isolated from macroalgae and explored for the production of such entities [157]. Given their proven ability to produce antimicrobial, antifungal, anti-inflammatory and antifouling compounds, it is reasonable that this wide chemical arsenal might benefit the host, providing a defense to ensure its survival and competitiveness in the environment [78]. Nonetheless, it is important to mention that non-Streptomyces Actinomycetota have also proven their value as producers of bioactive metabolites [35]. While most of the genera were found in both macroalgae, some were obtained only from one of the species: strains affiliated to Actinoalloteichus, Actinomadura, Citricoccus, Krasilnikoviella, Saccharomonospora, Stackebrandtia and Verrucosispora were solely isolated from C. crispus and strains associated to Glycomyces, Kocuria, Nocardioides and Spiractinospora were only recovered from C. tomentosum. Actinomycetota strains were isolated both from the holdfast and blades of the macroalgae. While some genera were obtained from both regions, others were solely retrieved from a specific section of the hosts: Brachybacterium, Brevibacterium, Citricoccus, Glycomyces, Kocuria, Krasilnikoviella, Mycolicibacterium, Stackebrandtia and Verrucosispora strains were exclusively isolated from the blades of the macroalgae and Actinomadura, Nocardioides, Saccharomonospora and Spiractinospora from the holdfasts. Interestingly, though a higher number of isolates were obtained from the holdfast of the two macroalgae species, the blades proved to be a better area for Actinomycetota diversity (Fig. 3C). Linking the isolation culture media with strains diversity, the selective medium AIA was the one associated to a more diverse range of culturable Actinomycetota, enabling the recovery of 17 genera, followed by NPS, SP and NPS media, with 14, 11 and 10 genera recovered, respectively (Fig. 3B). The richest media, AIA and SCN, enabled the retrieval of unique genera as Citricoccus, Glycomyces, Kocuria, Mycolicibacterium, Nocardioides, Saccharomonospora, Spiractinospora and Verrucosispora, which were not recovered in any of the other media. Interestingly, the most oligotrophic media, NPS and SP, allowed the growth of particular taxonomic groups that were not recovered using AIA and SCN media, namely strains affiliated to the genera

Actinomadura, Krasilnikoviella, Micrococcus and Stackebrandtia (Fig. 3B). Nevertheless, strains affiliated to these genera have been cultivated in highly nourishing media - as ISP2, nutrient agar, NZ-amine starch, raffinose—histidine, Sabouraud dextrose and yeast extract agars [158-162] — attesting their compliance to a broad range of culture compositions. Apart from other methods, the use of innovative culture media can boost the isolation of new and diverse Actinomycetota. In our study, the source samples (macroalgae) were used to formulate a culture medium that enabled the exclusive isolation of the rare Krasilnikoviella genus [161]. The success of this strategy has been previously demonstrated in studies that used sediments and sponges extracts to improve Actinomycetota isolation [151, 163].

To better understand the influence of the isolation source – C. tomentosum or C. crispus - on Actinomycetota diversity, two phylogenetic trees - one comprising all Streptomyces strains (Fig. 4) and the other all the non-Streptomyces isolates (Fig. 5) were constructed with the 376 16S rRNA gene sequences generated in this study (sequences shorter than 900 bp were not considered to the analysis). Results from both trees seem to indicate that the macroalgae species do not have a clear influence on the recovered diversity: closest related strains self-group independently of the macroalgae of origin. This can be exemplified by strains CT-F89 and CC-F41, both identified as Brachybacterium paraconglomeratum, with a minimal phylogenetic distance, that were isolated from C. tomentosum and C. crispus, respectively. These results suggest that the overall ecosystem and culture conditions might play a more significant role in shaping Actinomycetota diversity than the macroalgae species of origin itself. The complex interactions between the bacterial community and the environment – specifically in such a dynamic area as the Atlantic intertidal zone, with exposure to desiccation, temperature and salinity fluctuations, UV radiation and grazing pressure - could strongly influence the composition and abundance of Actinomycetota, highlighting the need to consider the broader ecological context when studying their diversity on living macroalgae.

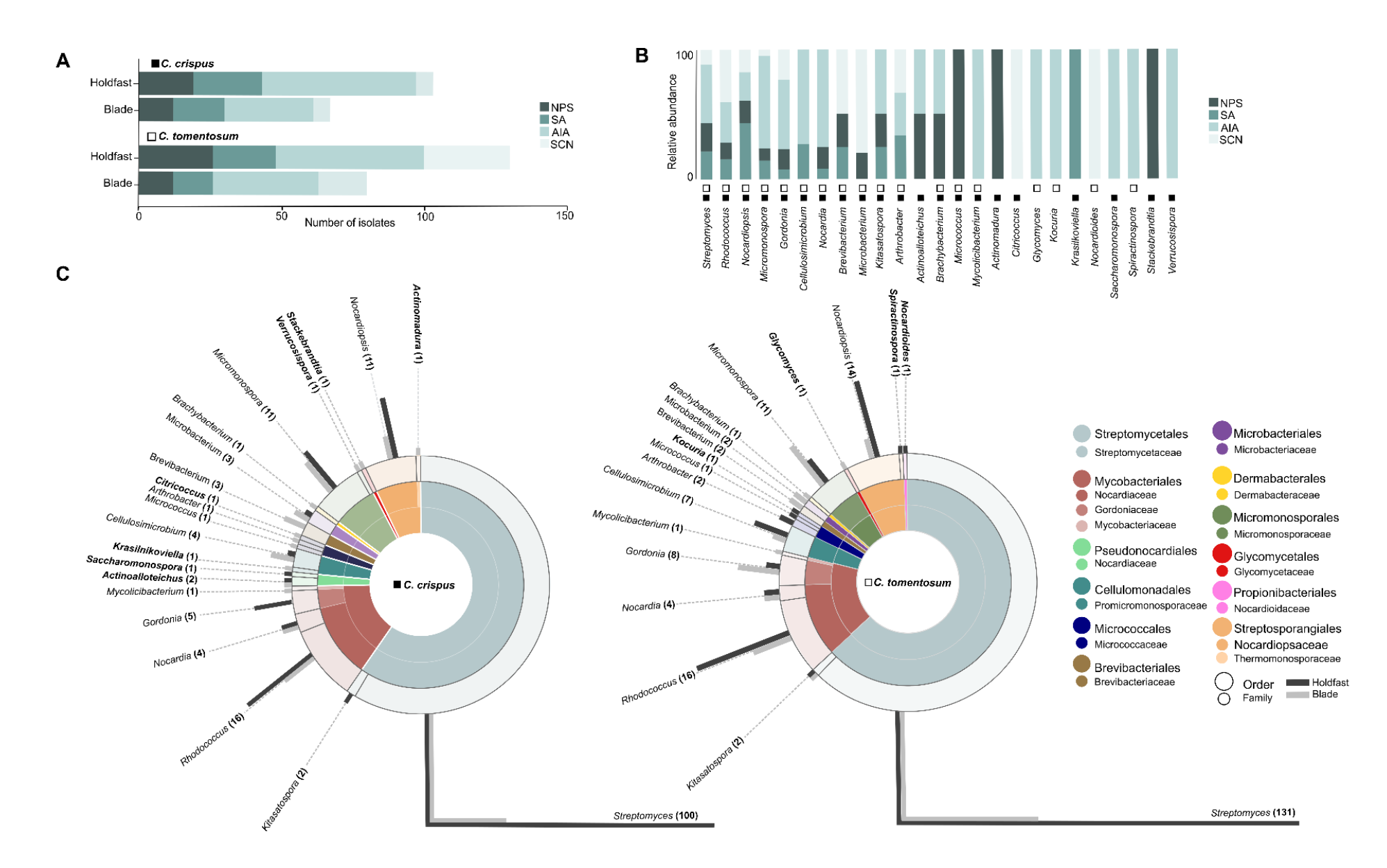


Figure 3. Actinomycetota recovered from *C. crispus* (■) and *C. tomentosum* (□). The number of isolates recovered from the holdfast and blade of each macroalgae species, and the respective isolation media (NPS: Nutrient-poor Sediment Extract agar; AIA: Actinomycete Isolation Agar; SCN: Starch-Casein-Nitrate agar; SA: Seaweed Agar), are presented (A) as well as the distribution of the genera recovered (B). The taxonomic distribution of the strains – order, family, and genus, from the inside to the outside of the circle, respectively – is presented according to the part of the macroalgae from which they were isolated. Numbers in brackets indicate the number of isolates retrieved from each genus. Genera exclusively obtained from a macroalgae species are highlighted in bold (C).

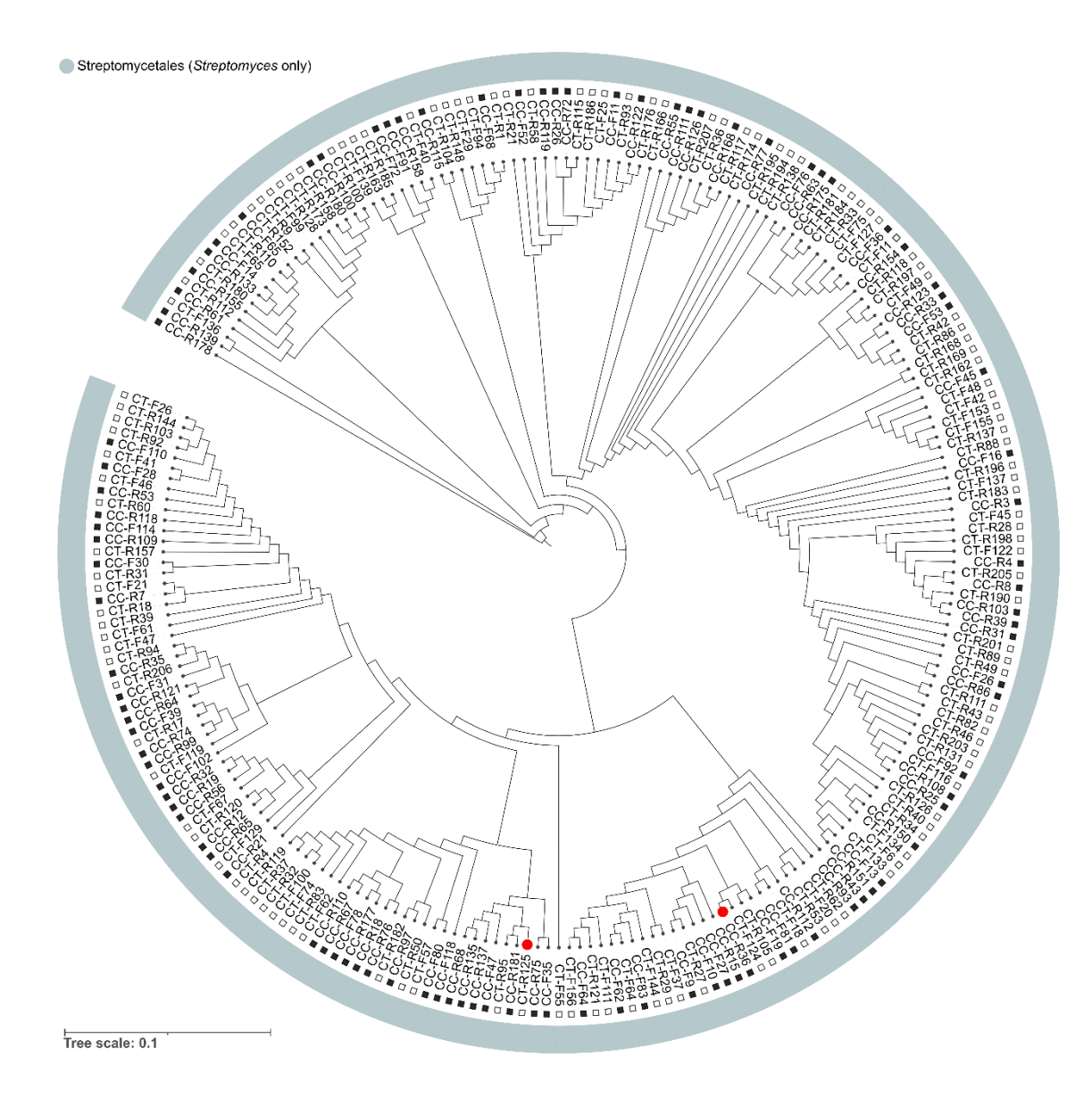


Figure 4. Phylogenetic tree based on the 16S rRNA gene, obtained by Maximum Likelihood analysis of Actinomycetota isolates recovered from *C. crispus* (■) and *C. tomentosum* (□) affiliated to the genus *Streptomyces*. Genomic data from strains CT-R87 and CT-F145 were not considered due to the small size of their consensus sequences. The tree was generated using an alignment of 1522 bp and 1000 bootstraps. The order-level affiliation of the strains is coloured indicated as described in the picture caption. Strains representing potential novel taxa (●) are pointed out as well.

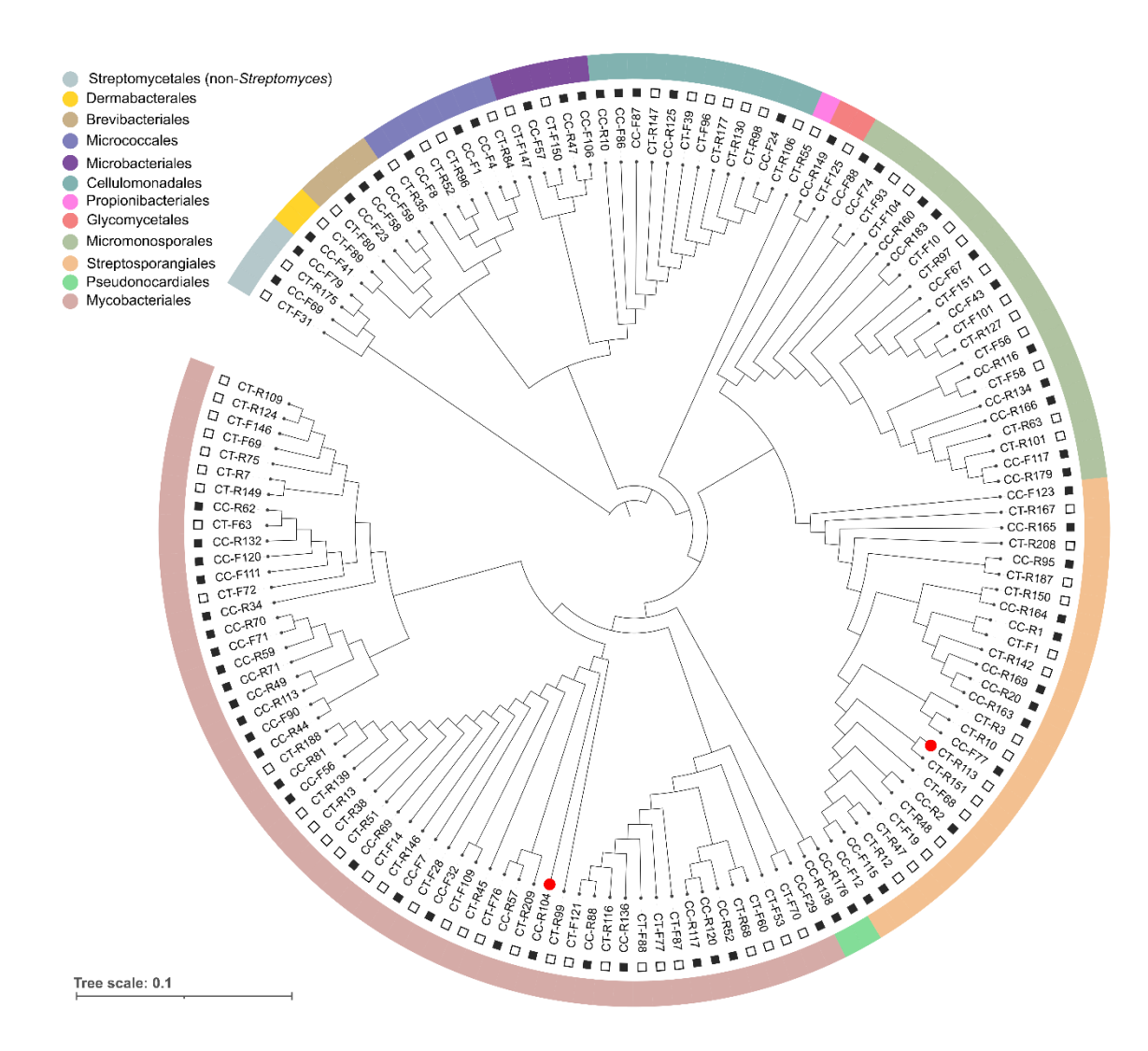


Figure 5. Phylogenetic tree based on the 16S rRNA gene, obtained by Maximum Likelihood analysis of Actinomycetota isolates recovered from *C. crispus* (■) and *C. tomentosum* (□) affiliated to non-*Streptomyces* genera. Genomic data from strains CC-F55 and CT-R135 were not considered due to the small size of their consensus sequences. The tree was generated using an alignment of 1345 bp and 1000 bootstraps. The order-level affiliation of the strains is coloured indicated as described in the picture caption. Strains representing potential novel taxa (●) are pointed out as well.

When analyzing the 16S rRNA gene sequences of our collection, potential novel species were identified. According to the 98.65% 16S rRNA gene sequence similarity cut-off to define a new bacterial species [164], strains CT-R125, CC-R36, CT-R113 and CC-R104 were selected to further phylogenetic analysis based on their prone taxonomic novelty (Fig. 6). CT-R125 and CC-R36, isolated from *C. tomentosum* and *C. crispus*, respectively, represent two potential new species affiliated to the *Streptomyces* genus. The 16S rRNA gene sequence of the first strain has 98.55% similarity with *Streptomyces lusitanus*^T, while the second strain presents a similarity of 97.26% with *Streptomyces*

badius^T. Strains CT-R113 and CC-R104, isolated from C. tomentosum and C. crispus, represent two potential new species affiliated to the Nocardiopsis and Rhodococcus genera, respectively. CT-R113 16S rRNA gene holds a 98.65% similarity with Nocardiopsis umidischolae^T and CC-R104 has a similarity of 98.24% with Rhodococcus pyridinivorans^T, making these two strains potential novel species integrating the Nocardiaceae and Nocardiopsaceae families, correspondingly. All the mentioned taxonomic groups are recognised as prolific producers of bioactive secondary metabolites, especially Streptomyces [165-167], making the discovery of novel bacterial species, and the exploration of their metabolomic chemical diversity, a crucial step in compounds discovery, optimization, and design. Additionally, it is important to notice that the resolution of the 16S rRNA gene might not sufficient for Streptomyces species identification, and likely a deeper phylogenetic analysis might reveal a higher number of potential novel species from these macroalgae [168]. The confirmation of the taxonomic novelty of these isolates will require the complete sequencing of their genomes and comparison with the closest type strains. An average nucleotide identity (ANI) analysis of the genomes, rather than solely a comparison based on the 16S rRNA gene, would be necessary, as well as a set of morphological, physiological and biochemical analysis [164].

Overall, this culturomics approach yielded 380 actinobacterial strains – highly diverse on metabolic requirements and taxonomy –, constituting the largest collection of macroalgae-associated Actinomycetota reported to date. This collection in dominated by *Streptomyces*, reflecting the adaptability this species to marine environments and likely significance in host interactions. Potential new taxa was also identified.

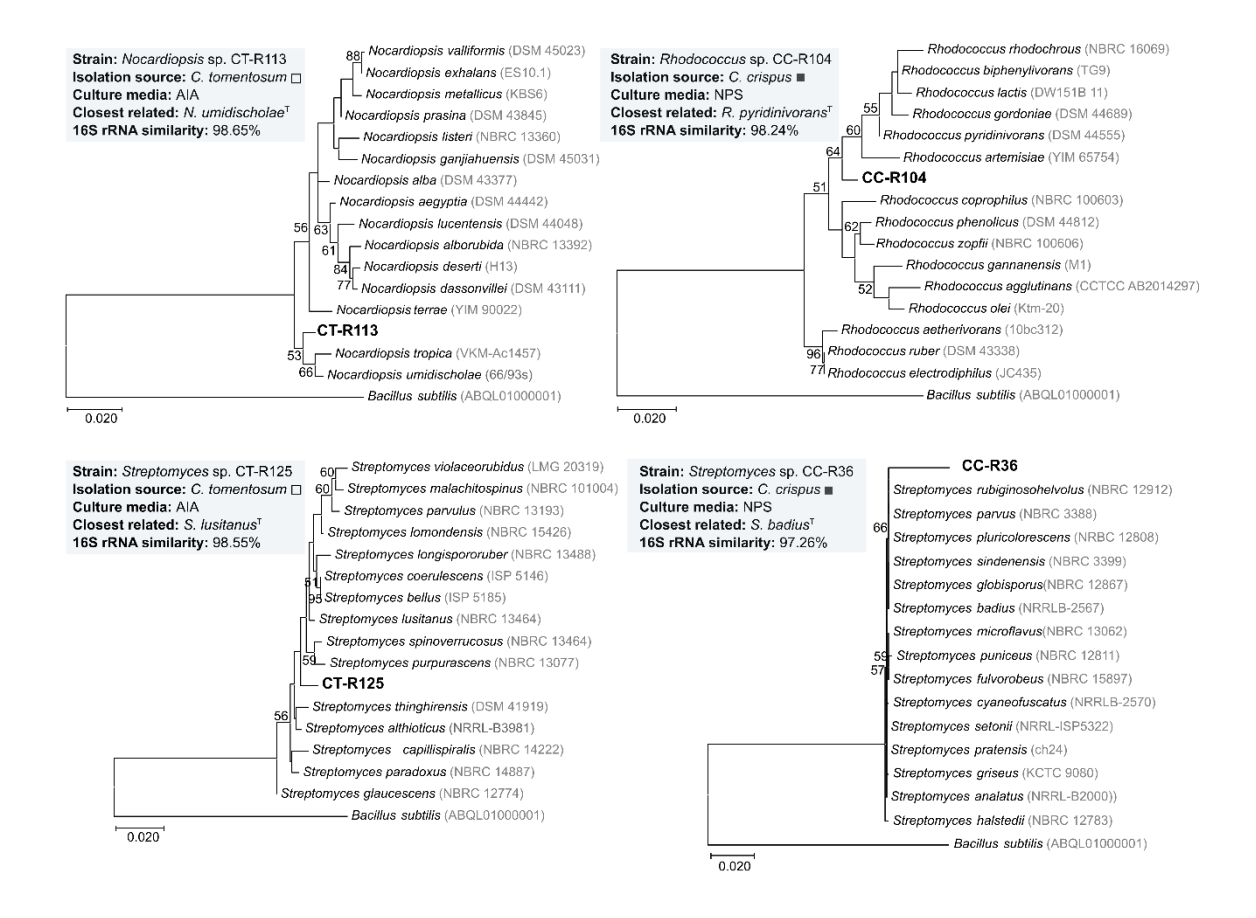


Figure 6. Phylogenetic trees for strains CT-R113, CC-R104, CT-R125 and CT-R113, representing potential novel Actinomycetota species recovered from *C. crispus* (■) and *C. tomentosum* (□). The trees were obtained by Maximum Likelihood analysis of the 16S rRNA gene sequences of the 15 closest related type strains associated to each of the potential novel species. The phylogeny test used was the bootstrap method with 1000 replications. *Bacillus subtilis* ABQL01000001 was used as outgroup. Numbers at nodes represent bootstrap values when higher than 50%. Accession numbers are indicated in brackets.

2.3.2. Macroalgae-associated Actinomycetota Community Accessed by Metagenomic Sequencing

Shotgun metagenomic was used as a culture-independent approach to unravel the Actinomycetota abundance and diversity living in association with *C. crispus* and *C. tomentosum*. A shotgun metagenomic protocol was prioritized instead of an ampliconbased approach, to mitigate potential biases often observed with metabarcoding pipelines. A dataset of almost 140 million reads was generated and classified. Over 50% of prokaryotic relative abundance was attributed to Pseudomonadota taxa, in both macroalgae. Other phyla – Bacteroidota, Cyanobacteria, Planctomycetes, Firmicutes, Verrucomicrobia and Actinomycetota – were also identified. Actinomycetota phylum was particularly abundant in *C. crispus*, ranking as the third most dominant and representing

11.22% of all prokaryotic diversity, while in C. tomentosum this value was considerably lower at only 1.73% (Fig. 7A, Table S2 - Appendix I). Interestingly, this difference was not noticed in the cultivation pipeline, with a higher number of Actinomycetota isolates being retrieved from C. tomentosum tissues. In total, 12 Actinomycetota orders, 16 families and 17 genera were identified using shotgun metagenomic (considering only results of relative abundance above the defined threshold of 0.1%, Figs. 7B and 7C, Table S2 - Appendix I). When comparing shotgun metagenomic diversity results with the isolates retrieved from the macroalgae, it is possible to see that the overlapping between taxonomic groups is limited: 33% at order level (Micrococcales, Streptomycetales, Propionibacteriales, Pseudonocardiales, Micromonosporares and Streptosporangiales) and 20% at genus level (Streptomyces, Nocardioides, Mycolicibacterium, Rhodococcus, Nocardia and Gordonia). Previous studies on marine microbial diversity have demonstrated the same pattern where the complementarity of culture-dependent and independent approaches is represented by only a fraction of taxa detected concomitantly [169, 170]. A deeper look into the Actinomycetota community revealed by metagenomic sequencing showed that the order Acidimicrobiales (Fig. 7B), and the affiliated genus Ilumatobacter, (Fig. 7C) were the most abundant in both samples. No strain classified withing these taxonomic groups was cultured in our work. Other studies on the holobiont of green macroalgae have shown the significant presence of Acidimicrobiia as well [171]. In contrast to other members of Acidimicrobiales, which are obligate acidophiles, *llumatobacter* species grow under neutral or slightly alkaline conditions [172], being in concordance with the conditions from where the two macroalgae under study were collected. In fact, only three *llumatobacter* species – *l. nonamiense*, *l. coccineum* and *l.* fluminis, all retrieved from marine sediments - are reported to date, being this genus described as recalcitrant to cultivation and composed of extremely fastidious strains [173, 174]. Previous studies based on 16S rRNA gene sequencing have also shown that these three species are closely related to some uncultured Actinomycetota, including marine sponge symbionts [175]. Tailor-made optimizations on Actinomycetota isolation procedures from macroalgae, including adjustments in media composition, might lead to the discovery of novel and unique species affiliated to *llumatobacter*, since their presence in the community of both *C. crispus* and *C. tomentosum* is considerably high. Actually, the abundance of *Ilumatobacter* in metagenomic sequencing dataset was more than three-fold higher than the most isolated genus, Streptomyces. Apart from Ilumatobacter, also the genera Aquihabitans, Actinomarinicola and Iamia presented a higher or similar relative abundance in C. crispus metagenomic dataset (1.25, 1.07 and 0.58%, respectively), when compared with the genus Streptomyces (Fig. 7C). Although

their occurrence in the marine environment [176-178], to our knowledge no species affiliated to these taxonomic groups have been so far isolated from macroalgae. As our findings highlight, prior knowledge about the overall community present in a specific sample can empower the development of tailored cultivation pipelines, enabling the recovery of rare or previously uncultivable Actinomycetota.

Though the analysis of host-specificity of the bacterial community associated with the studied macroalgal species was not the focus of this study, shotgun metagenomic analysis revealed substantial differences in microbial diversity associated with C. crispus and C. tomentosum. Pseudomonadota the predominant phylum associated with both macroalgae, comprising over 50% of the prokaryotic relative abundance. However, Actinomycetota was particularly abundant and diverse on C. crispus, with the order Acidimicrobiales and the affiliated genus Ilumatobacter being the most abundant actinobacterial taxa in both macroalgae. Interestingly, these groups were not isolated through cultivation efforts. While previous studies on macroalgae microbiome have reported that both Gram-negative and Gram-positive communities exhibit host-specificity [179-181], they have also highlighted that the structure of bacterial communities is more likely associated with functional genes rather than taxonomy [150, 182]. Though we have detected a higher abundance of Actinomycetota in C. crispus (Fig. 6), the most representative groups within this phylum where the same in both macroalgae. However, a broad comparative study, contemplating more specimens on a higher temporal and biogeographic scale, is necessary to identify the core bacterial community associated to C. crispus and C. tomentosum and determine the driving factors of such associations.

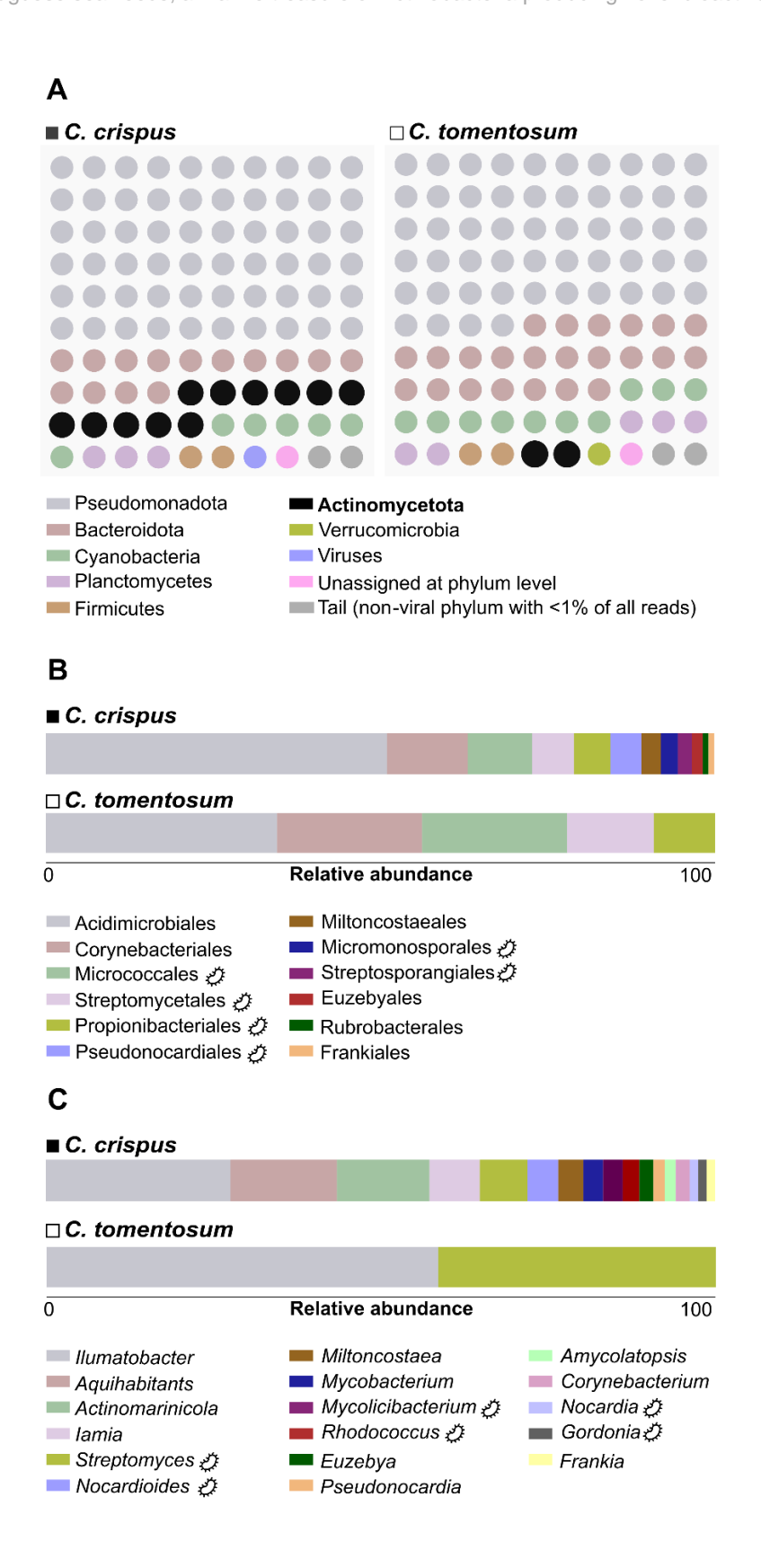


Figure 7. Relative distribution of classified reads from *C. crispus* (■) and *C. tomentosum* (□) shotgun metagenomic dataset at (**A**) phylum-level, with each circle corresponding to 1%, (**B**) actinobacterial order-level and (**C**) actinobacterial genus-level. Taxonomic groups retrieved from cultivation are indicated with a bacteria symbol.

2.4. CONCLUSION

This is the first portrayal of the Actinomycetota community – both culturable and nonculturable – associated to the macroalgae C. crispus and C. tomentosum. The work here presented not only contributes to enlarge the meagre knowledge available on Actinomycetota communities associated with macroalgae, but also provides a collection of 380 unique strains holding great potential for exploration, considering the unmatched biosynthetic machinery encoded by this taxon. Our study highlights the significance of mining untapped marine niches for Actinomycetota discovery. Despite their wellestablished presence in marine habitats, macroalgae have not been in the spotlight for the isolation and exploration of these bacteria compared to other sources such as sediments, sponges, or corals. Yet, our findings unveil macroalgae as excellent hosts for Actinomycetota, both in number and diversity, paving the way for further studies on their diversity, chemical ecological role and likely biotechnological application. It is important to consider that conclusions drawn from this study are based on a single sampling campaign, providing a snapshot of the microbial community present in the macroalgae at one specific moment. Since microbial communities can vary over time, further investigations must be performed to capture the overall dynamics of the Actinomycetota communities living in macroalgae from the Portuguese coast.

3

Nocardiopsis codii sp. nov., and Rhodococcus algaerubra sp. nov., two novel actinomycetes species isolated from macroalgae collected in the northern Portuguese coast

The content of this chapter is under review for publication in the Q1 journal International Journal Of Systematic And Evolutionary Microbiology:

<u>Girão M.</u>, Lequint Z., Rego A., Costa I., Proença D.N., Morais P.V., Carvalho M.F. (2024) *Nocardiopsis codii* sp. nov. and *Rhodococcus algaerubra* sp. nov., two novel actinomycetes species isolated from macroalgae collected in the northern Portuguese coast.

ABSTRACT

In this chapter we describe two novel actinobacterial strains, CT-R113^T and CC-R104^T, isolated from the macroalgae Codium tomentosum and Chondrus crispus, respectively (Chapter 2). Phylogenetic analyses based on the 16S rRNA gene showed that strain CT-R113^T belongs to the genus *Nocardiopsis*, being closest related to *Nocardiopsis* umidischolae 66/93^T and Nocardiopsis tropica VKM Ac-1457^T, with 98.65 and 98.39% sequence similarity, respectively. The clade formed between the three type strains was confirmed by phylogenomic analysis. The genome of strain CT-R113^T was 7.27 Mb in size with a high G+C content of 71.3 mol%, with ANI value of 89.59% and 90.14% with strains 66/93^T and VKM Ac-1457^T strains, respectively. Growth was observed at pH 6.0– 10.0 (optimum, pH 7.0), 12-28 °C (optimum, 28 °C) and 0-10% (w/v) NaCl (optimum, 0-5%). The major cellular fatty acids were identified as $C_{18:1}$ $\omega 9c$, iso- $C_{16:0}$ and anteiso- $C_{17:0}$. Menaquinone 10 (MK-10) was the major respiratory quinone of CT-R113^T and whole-cell hydrolysates contained meso-diaminopimelic acid as the cell-wall diamino acid. Comparative analysis of 16S rRNA gene sequences showed that strain CC-R104^T belongs to the genus Rhodococcus, being closest related to Rhodococcus pyridinivorans DSM 44555^T, with 98.24% sequence similarity. However, phylogenomic analysis revealed that strain CC-R104^T establishes a clade with Rhodococcus artemisae DSM 45380^T, being more distant from *Rhodococcus pyridinivorans* DSM 44555^T. The genome of strain CC-R104^T was 5.34 Mb in size with a high G+C content of 67.01 mol%. ANI value between strains CC-R104^T and DSM 45380^T was 81.2% and between strains CC-R104^T and DSM 44555^T was 81.5%. Growth was observed at pH 6.0–10.0 (optimum, pH 7.0), at 4-37 °C (optimum, 28 °C) and with 0-15% (w/v) NaCl (optimum, 0-5%). The major cellular fatty acids were identified as $C_{18:1}$ $\omega 9c$, $C_{16:0}$ and summed feature 3. Menaguinone 8 (MK-8) was the only respiratory guinone and whole-cell hydrolysates contained meso-diaminopimelic acid as the cell-wall diamino acid. On the basis of phenotypic, molecular and chemotaxonomic characteristics, strains CT-R113^T and CC-R104^T are considered to represent novel species, for which the names Nocardiopsis codii sp. nov. (type strain CT-R113^T=LMG 33234^T=UCCCB 172^T) and Rhodococcus algaerubrum sp. nov. (type strain CC-R104^T=LMG 33233^T=UCCCB 171^T) are proposed.

Keywords: Actinomycetota; *Codium tomentosum; Chondrus crispus*; New taxa; *Nocardiopsis codii, Rhodococus algaerubrum*

3.1. INTRODUCTION

The northern Portuguese coastline features numerous intertidal zones with rocky outcrops and tidal pools, providing habitat for various marine organisms, including macroalgae [136]. These can harbor diverse and abundant bacterial communities, including Actinomycetota taxa yet to be discovered. The discovery of novel species enriches the understanding of biodiversity, providing insights into ecological roles and evolutionary relationships. Additionally, it offers opportunities for biotechnological innovation by tapping into previously unknown biochemical pathways and metabolic capabilities.

The genus *Nocardiopsis*, proposed in 1976 [183], belongs to the family *Nocardiopsaceae* [184], order *Streptosporangiales* and class *Actinomycetia* [185], and currently comprises 47 type species (https://lpsn.dsmz.de/genus/nocardiopsis). Members affiliated to this genus are described as Gram-positive, aerobic, chemoorganotrophic, non-acid-fast, non-motile filamentous actinomycetes, with a well-developed substrate mycelium and densely branched hyphae. Aerial mycelium can be sparse to abundant, fragmenting into spores of various lengths [186]. This genus is widely distributed in the environment, from deserts [187] to cold soils [188], deep ocean [189] and coastal wetlands [190], hypersaline to alkali soils [191]. An additional distinctive trait of *Nocardiopsis* is their ability to produce bioactive secondary metabolites with application in several fields, including the pharmaceutical industry [192]. To date, 24 genomes of type strains of the genus *Nocardiopsis* have been sequenced with genome size ranging from 5.2 Mb (*Nocardiopsis alkaliphila* YIM 80379 [193]) to 7.89 Mb (*Nocardiopsis umidischolae* 66/93 [194]), and *in silico* G+C content between 67.5 (*Nocardiopsis alkaliphila* YIM 80379 [193]) to 75.2 mol% (*Nocardiopsis trehalosi* [195]).

The genus *Rhodococcus*, redefined in 1977 by Goodfellow and Alderson [196], belongs to the family *Nocardiaceae*, order *Corynebacteriales* and class *Actinomycetia*, and currently comprises 55 type species (https://lpsn.dsmz.de/genus/rhodococcus). *Rhodococcus* species are metabolically fit to adapt and thrive in different ecological niches, booming in many environments as the ocean [37], terrestrial soil [197] and industrial and polluted sites [198, 199], living also in association with animals [200] and plants [201], with some species being depicted as human pathogens [202]. One distinctive trait of members affiliated to the genus *Rhodococcus* is their remarkable metabolic diversity, especially noteworthy in the biodegradation of several compounds, acting as catalysts for an array of biotransformations [203-205], in the production of biosurfactants [206] and as source of bioflocculants [207]. Apart from these industrial

and ecological high value properties, relevant antibiotics and anticancer compounds have also been uncovered from *Rhodococcus* secondary metabolism [208, 209], highlighting their pharmaceutical potential. To the moment, 31 genomes of type strains of the genus *Rhodococcus* have been sequenced, with genome size ranging from 3.98 Mb (*Rhodococcus corynebacterioides* NBRC 14404^T) to 10.31 Mb (*Rhodococcus koreensis* DSM 44498^T), and in silico G+C content between 61.7 mol% (*Rhodococcus globerulus* NBRC 14531^T) to 70.7 mol% (*Rhodococcus ruber* NBRC 15591^T).

In this study, we describe two novel actinobacterial strains, designated CT-R113^T and CC-R104^T. These strains were isolated from the tissues of macroalgae collected in the intertidal area of Mindelo beach, Portugal (Chapter 2). According to a polyphasic approach based on chemotaxonomic, phenotypic and phylogenetic data, strain CT-R113^T represents a novel species within the genus *Nocardiopsis* and strain CC-R104^T represents a novel species within the genus *Rhodococcus*.

3.2. MATERIALS AND METHODS

3.2.1. Bacterial Isolation

Strains CT-R113^T and CC-R104^T were isolated from the macroalgae specimens collected in the intertidal rocky area of Mindelo beach (Chapter 2, section 2.2.2.). Strain CT-R113^T was isolated from the holdfast tissues of *C. tomentosum* and strain CC-R104^T from the blade tissues of *C. crispus*, respectively. Strain CT-R113^T was purified from plates of Actinomycete Isolation Agar (AIA) and strain CC-R104^T from plates of Nutrient-Poor Sediment extract agar (NPS). Stock cultures from both strains were maintained with 30% (v/v) glycerol, at -80 °C, using biomass from cultures grown aerobically at 28 °C for two weeks.

3.2.2. Phylogenetic and Phylogenomic Analysis

Phylogenetic relationships of CT-R113^T and CC-R104^T with their respective closest related type strains were inferred based on the 16S rRNA gene. Each strain was grown on solid media and the extraction of genomic DNA, PCR amplification, and sequencing of 16S rRNA gene were carried out as previously described [62]. Pairwise similarity between each strain and its closely related type strains was carried out using the EzBiocloud database [210]. For each strain, CT-R113^T and CC-R104^T, two phylogenetic trees, one based on Maximum-likelihood (ML) and other on Neighbor Joining (NJ) methods, were constructed with their 16S rRNA gene sequence and the top 15 closest related type strains according to Ezbiocloud database. Multiple sequences alignment was carried out using MUSCLE from within the Geneious software package, and 1.000 bootstraps applied. MEGA-X was used to build the trees and iTOL to perform its final display and annotation. Strains CT-R113^T and CC-R104^T 16S rRNA gene sequences were deposited in NCBI with the accession numbers OR578920 and OR578921, respectively. The taxonomic evaluation of both strains was complemented with a phylogenomic study. Phylogenomic trees were computed using PhyloPhlAn 3.0 [211], based on 400 universal marker genes using each strain genome and the available genomes of the closest related type species. MAFFT V.7 [212] was used to perform the multiple sequence alignment (MSA). ML trees using LG substitution model were obtained. NJ trees were computed using MAFFT. Phylogenomic trees were imported and further edited using iTOL. FastANI [213] was used to calculate Average Nucleotide Identity (ANI) between genomes.

3.2.3. Genome Mining

DNA extraction for whole genome sequencing of strains CT-R113^T and CC-R104^T was performed using the E.Z.N.A. Bacterial DNA Kit (Omega Bio-Tek, GA, United States) according to the manufacturer's instructions. Genomic DNA was sequenced using Illumina 2x250bp paired-end technology and raw data were submitted to a bioinformatics pipeline (microbesNG, UK). Briefly, identification of the closest reference genomes for reading mapping was done using Kraken 2 [214], reads quality check was performed using BWA-MEM [215], and de novo assembly was performed using SPAdes [216]. The genomes were annotated using the NCBI Prokaryotic Genome Annotation Pipeline and deposited at GenBank under the accession number JAUZMY00000000 and JAUZMZ000000000, respectively. The closest related type strains of both CT-R113^T and CC-R104^T were purchased, and their genome sequenced and annotated, since their genomes were not previously available. Strains Nocardiopsis umidischolae 66/93^T and Nocardiopsis tropica VKM Ac-1457^T were acquired from the Japan Collection of Microorganisms (JCM; JCM 11758 and JCM 10877, respectively) (GenBank accession numbers JAUUCC000000000 and JAUUCB00000000, respectively). Rhodococcus artemisae DSM 45380^T was acquired from the German Collection of Microorganisms Cell Cultures (DSMZ; DSM45380) (GenBank and accession number: JAUTXY000000000). AntiSMASH 7.0 [217] was used for the automated analysis of the genomes, as well as its closest related type strains, in order to identify, annotate and compare gene clusters responsible for the biosynthesis of secondary metabolites.

3.2.4. Physiology and Chemotaxonomy

Biomass for microscopic, physiological, and chemotaxonomic studies of strains CT-R113^T and CC-R104^T was obtained by cultivation at 28 °C, for two weeks, on Tryptic Soy agar/broth (TSA/TSB). Cultural characteristics were observed in a set of culture media: ISP2-ISP7 [218], Marine agar (MA; MilliporeSigma USA), Potato-dextrose agar (PDA; HiMedia, Germany), Czapek-dox agar (CZA; MilliporeSigma USA), Tryptic Soy agar (TSA; MilliporeSigma USA) and Glycerol Yeast Malt extract agar (GYM) [219]. The concentration of NaCl was adjusted to 1.5% NaCl (w/v) in all culture media, with the exception of MA to which no additional salts were added. General morphological characteristics of the colonies were observed using a binocular magnifier. Physiological traits – temperature and pH range and tolerance to NaCl – were tested using TSA modified with 1.5% NaCl (except in NaCl tolerance test), pH 7 (except in pH range test)

at 28 °C (except in temperature range test), for 2 weeks. Growth was tested at 4, 12, 20, 28, 37, 45 and 50 °C. A range of pH between 5.0 and 10.0 was tested, at intervals of 1.0 pH unit, using the following buffer system: acetate buffer (pH 5.0), phosphate buffer (pH 6.0-8.0), and Tris buffer (pH 9.0-10.0). Tolerance to NaCl concentrations was examined at 0, 1, 2, 3, 5, 10, 15 and 20% (w/v). Sucrose, D-fructose, myo-inositol, D-Raffinose, Dmannitol, L-Rhamnose and α-Cellulose were tested at 1% (w/v) for carbon source utilization, as described [218]. L-alanine, L-arginine, L-asparagine, Glycine, L-proline, L-serine, L-threonine and L-tyrosine were tested at 0.1% (w/v) for nitrogen source utilization, as described [220]. Enzymatic activity was tested using the API® ZYM system (bioMérieux, Linda-a-Velha, Portugal). Catalase activity was determined by using 3% H₂O₂ (v/v), and gas production was identified as a positive reaction. Oxidase activity was evaluated using oxidase discs (Sigma-Aldrich, USA) and blue coloration was identified as a positive reaction. For the analysis of lipoquinones, strains CT-R113^T (and the closest related VKM Ac-1457^T and 66/93^T) and CC-R104^T (and the closest related DSM 45380^T) were cultured on TSB for 48 h at 28 °C, harvested and lyophilized. Lipoquinones were extracted from freeze-dried cells, purified by thin-layer chromatography (TLC) and separated by high-performance liquid chromatography (HPLC) to identify the type present on the three strains [221]. Cells for fatty acid analysis were grown in TSB broth, at 28 °C in Erlenmeyer flasks, for 48 h, at 150 rpm [222], and the fatty acids profiles were determined. Fatty acid methyl esters (FAMEs) were obtained from the fresh wet biomass and were separated, identified and quantified using the standard MIS Library Generation Software (Sherlock Microbial ID System, RTSBA 6 database, version 6.5) as previously described [223]. Analysis of isomers of 2,6-diaminopimelic acid (Dpm) and 2,6-diamino-3-hydroxypimelic acid were carried out by DSMZ Services, Leibniz-Institute DSMZ -Deutsche Sammlung von Mikroorganismen und Zellkulturen GmbH, Braunschweig, Germany – as described before [224].

3.3. RESULTS AND DISCUSSION

3.3.1. Phylogenetic and Phylogenomic Identification

According to Ezbiocloud database results, the highest 16S rRNA gene sequence similarity of strain CT-R113^T was found with *Nocardiopsis umidischolae* 66/93^T (98.65%) [194], followed by *Nocardiopsis tropica* VKM Ac-1457^T (98.39%) [195]). Strain CT-R113^T formed an independent clade with these two type strains, confirmed by both ML and NJ phylogenetic trees (Fig. 8, Fig. S1 - Appendix II). The other closest hits were the strains Nocardiopsis exhalans ES10.1^T (98.31%), Nocardiopsis valliformis DSM 45023^T (98.22%), Nocardiopsis metallicus KBS6^T (98.14%), Nocardiopsis prasina DSM 43845^T (98.05%), Nocardiopsis alba DSM 43377[™] (97.88%), Nocardiopsis aegyptia DSM 44442[™] (97.80%), Nocardiopsis lucentensis DSM 44048^T (97.72%), Nocardiopsis terrae YIM 90022^T (97.72%), Nocardiopsis dassonvillei subsp. dassonvillei DSM 43111^T (97.63%), Nocardiopsis deserti H13^T (97.55%), Nocardiopsis listeri NBRC 13360^T (97.46%), Nocardiopsis alborubida NBRC 13392^T (97.46%) and Nocardiopsis ganjiahuensis DSM 45031^T (97.46%). Interestingly, only N. valliformis, N. aegyptia, N. lucentensis, N. terrae and N. ganjiahuensis were retrieved from marine/saline environments, all from sediment samples [193, 225-228]. In line with the phylogenetic analysis, both phylogenomic trees proved the closest relation of CT-R113^T with N. umidischolae 66/93^T (ANI: 90.6%) and N. tropica VKM Ac-1457^T (ANI: 89.9%) (Fig. 9, Fig. S2 - Appendix II). ANI values of strain CT-R113^T and type strains included in the analysis were in the range of 90.6 – 82.4% (Table S3 - Appendix II), below the 95% boundary that defines a new bacterial species [213]. Phylogenomic data showed that strain CT-R113^T formed an independent branch within the genus Nocardiopsis.

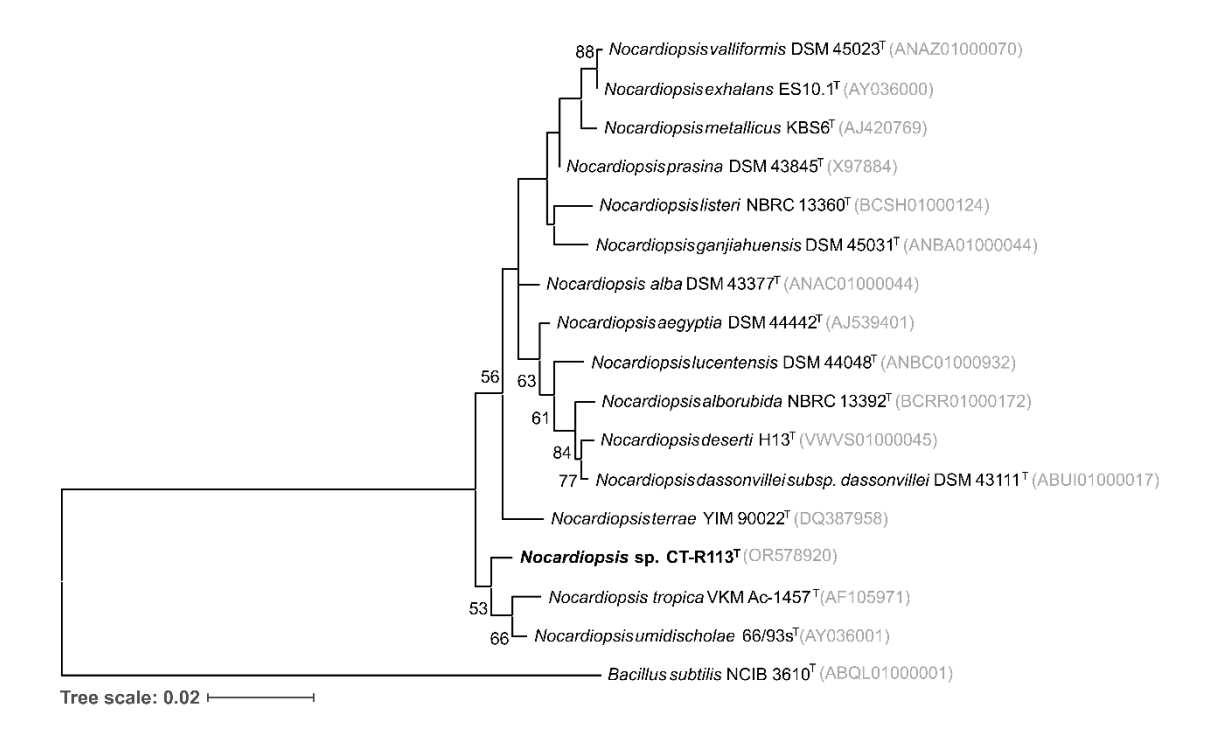


Figure 8. ML phylogenetic tree based on 16S rRNA gene sequences (1,302 nt), showing the relationship between strain CT-R113^T and the closest related type strains within the genus *Nocardiopsis*. Accession numbers are indicated in brackets. Values at the nodes indicate bootstrap values of 50% and above, obtained based on 1000 resampling events. *Bacillus subtilis* NCIB 3610^T was used as outgroup. Scale bar, 2 inferred nucleotide substitution per 100 nucleotides.

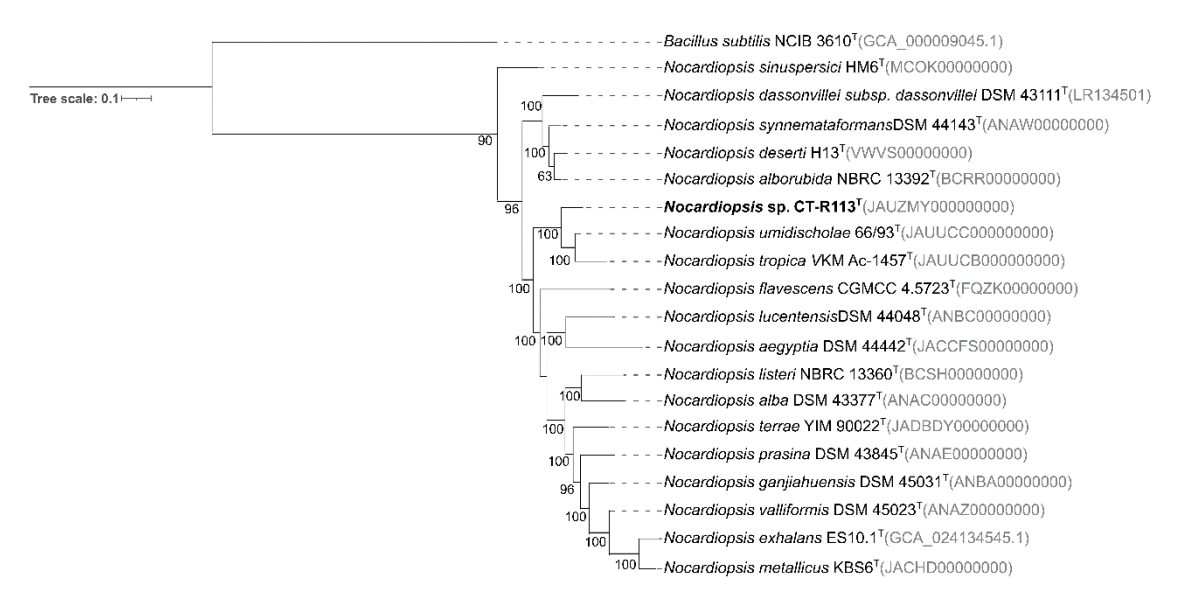


Figure 9. ML phylogenomic tree based on 400 universal marker genes, showing the relationship between strain CT-R113^T and the closest related type strains within the genus *Nocardiopsis*. Accession numbers are indicated in brackets. Values at the nodes indicate bootstrap values of 50% and above obtained based on 1000 resampling events. *Bacillus subtilis* NCIB 3610^T was used as outgroup. Scale bar, 10 inferred nucleotide substitution per 100 nucleotides.

Regarding strain CC-R104^T, the highest 16S rRNA gene sequence similarity was found with Rhodococcus pyridinivorans DSM 44555^T (98.24%) [229], followed by Rhodococcus zopfii NBRC 100606^T (98.00%) [230]. However, results from both ML and NJ phylogenetic trees showed a closest relation between strain CC-R104^T and Rhodococcus artemisae DSM 45380^T (Fig. 10, Fig. S3 - Appendix II), for which the 16S gene similarity was 97.68%. The other closest hits were the strains Rhodococcus rhodochrous NBRC 16069^T (97.92%), Rhodococcus biphenylivorans TG9^T (97.85%), Rhodococcus coprophilus NBRC 100603^T (97.77%), Rhodococcus phenolicus DSM 44812^T (97.77%), Rhodococcus yananensis FBM22-1^T (97.76%), Rhodococcus artemisiae YIM 65754^T (97.68%), Rhodococcus ruber DSM 43338^T (97.53%), Rhodococcus gordoniae DSM 44689^T (97.53%), Rhodococcus electrodiphilus JC435^T (97.53%), Rhodococcus aetherivorans 10bc312^T (97.36%), Rhodococcus lactis DW151B^T (97.36%), Rhodococcus olei Ktm-20^T (97.29%), and Rhodococcus gannanensis M1^T (97.19%). Remarkably, only R. electrodiphilus was retrieved from the marine environment [231]. Confirming the results based on the 16S gene sequences, both phylogenomic trees revealed a higher proximity between strain CC-R104^T and R. artemisae DSM 45380^T [232] (Fig. 11, Fig. S4 - Appendix II). ANI values of strain CC-R104^T and type strains included in the analysis were in the range of 81.7 – 77.9% (Table S4 - Appendix II), all below the mentioned threshold. Even if according to ANI values the closest strain related to CC-R104^T is *Rhodococcus rhodochrous* NBRC 16069^T (ANI 81.7%), phylogenomic trees showed that strain CC-R104^T formed an independent branch with R. artemisae DSM 45380^T (ANI 81.2%).

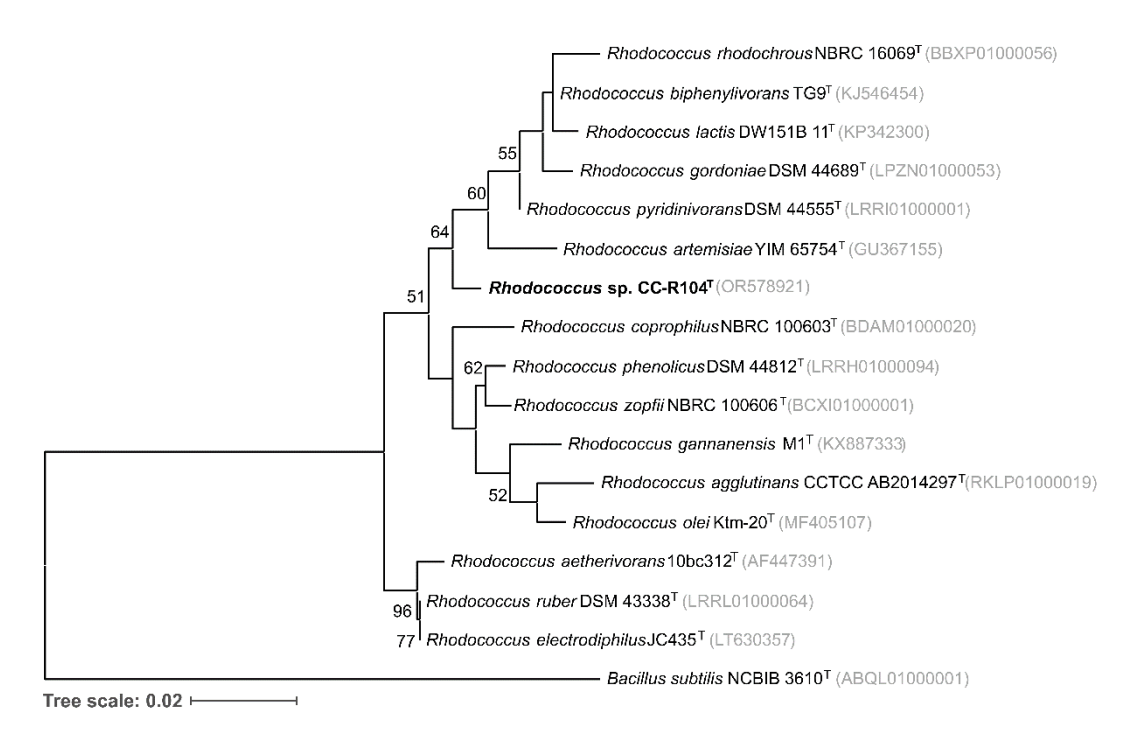


Figure 10. ML phylogenetic tree based on 16S rRNA gene sequences (1,283 nt), showing the relationship between strain CC-R104^T and the closest related type strains within the genus *Rhodococcus*. Accession numbers are indicated in brackets. Values at the nodes indicate bootstrap values of 50% and above, obtained based on 1,000 resampling events. *Bacillus subtilis* NCIB 3610^T was used as outgroup. Scale bar, 2 inferred nucleotide substitution per 100 nucleotides.



Figure 11. ML phylogenomic tree based on 400 universal marker genes, showing the relationship between strain CC-R104^T and the closest related type strains within the genus *Rhodococcus*. Accession numbers are indicated in brackets. Values at the nodes indicate bootstrap values of 50% and above, obtained based on 1,000 resampling events. *Bacillus subtilis* NCIB 3610^T was used as outgroup. Scale bar, 10 inferred nucleotide substitution per 100 nucleotides.

3.3.2. Genomic Features and Biosynthetic Potential

The genome of strain CT-R113^T was assembled into one contig with a length of 7 272 268 bp. DFAST [233] results of completeness and contamination were 97.47 and 0.6%, respectively. The in silico G+C content of strain CT-R113^T was 71.3 mol%, in line with the range for the genus *Nocardiopsis*. Annotation of the strain CT-R113^T genome revealed the presence of 6518 coding sequences (CDS), 77 tRNA and 3 rRNA genes. According to antiSMASH results, strain CT-R113^T (and the closest type strains 66/93^T and VKM Ac-1457^T), encode a different number and nature of BGCs in their genomes, with strain 66/93^T being overall richer, closely followed by CT-R113^T. BGCs in strain VKM Ac-1457 were distinctively less (Fig. 12). Detailed in silico analysis of the genome of strain CT-R113^T revealed that most of the detected BGCs do not blast with known metabolites, or present low similarity values (< 40%), highlighting the opportunity to uncover chemistry novelty. The few hits recorded above the mentioned threshold were siderophore desferrioxamine E (100% similarity, MiBiG accession BGC0001478), the non-ribosomal peptide metallophore coelibactin (90% similarity, MiBiG accession BGC0000324), the terpene isorenieratene (87% similarity, MiBiG accession BGC0001456) and the ribosomally synthesized and post-translationally modified peptide (RiPP) huimycin (70% similarity, MiBIG accession BGC0002354). In comparison, only isorenieratene was confirmed in the genome of N. umidischolae 66/93^T, showcasing the biosynthetic differences between the two species (Table S5 - Appendix II). The genome of CC-R104^T was assembled into one contig of 5 341 903 bp with 93.28% of completeness and 1.15% of contamination, according to DFAST [233] analysis. The in silico G+C content of strain CC-R104^T was 67.01 mol%, in accordance with the typical values associated to the genus *Rhodococcus*. Annotation of CC-R104^T genome revealed the presence of 4731 CDS) 56 tRNA and 3 rRNA genes. For this strain (and the closest type strain DSM 45380^T), it was possible to see that the nature and number of the detected BGCs in each genome was not the same, with CC-R104^T appearing to be particularly richer on non-ribosomal peptide synthetases (NRPSs) genes. Detailed in silico comparative analysis revealed that most of the detected BGCs, both in CC-R104^T and DSM 45380^T genomes, do not blast with known metabolites, or present low similarity scores (< 40%). The only exceptions recorded above the defined threshold for strain CC-R104^T were the terpenes 5-dimethylallylindole-3-acetonitrile from Streptomyces coelicolor A3(2) (55% similarity, MiBiG accession BGC0002128) and isorenieratene from Streptomyces griseus subsp. griseus NBRC 13350 (42% similarity, MiBiG accession BGC0000664). These results highlight the great opportunity for the discovery of novel chemical entities. In comparison, only isorenieratene was found in the genome of DSM 45380^T, together with the NAPAA (non-alpha poly-amino acids like e-Polylysi) ε-Poly-L-lysine biosynthetic gene cluster from the fungi *Epichloe festucae* (100% similarity, MiBiG accession BGC0002174), showcasing the biosynthetic differences between the two species (Table S6 - Appendix II).

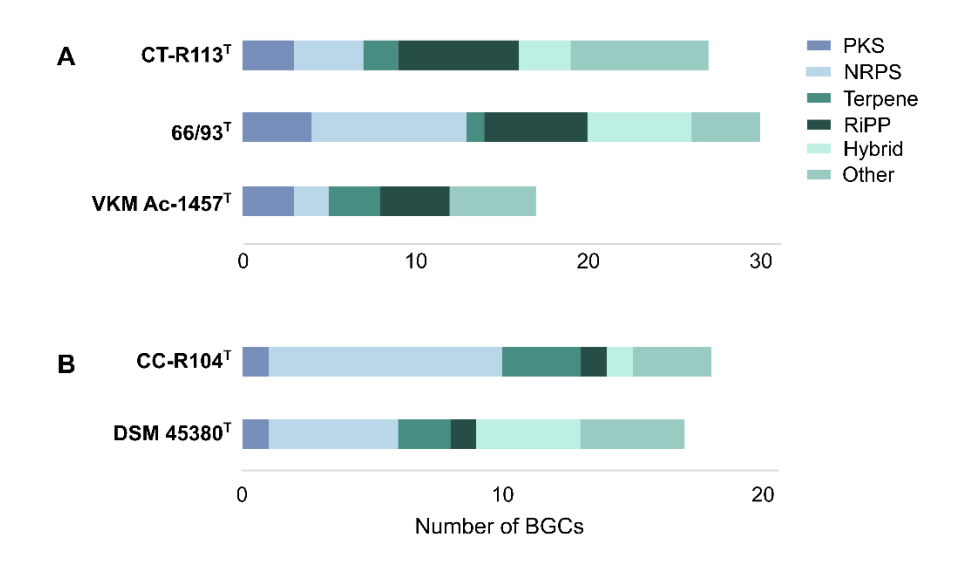


Figure 12. Distribution, number, and type of BGCs detected in (**A**) strain CT-R113^T and the two closest related type strains, 66/93^T and VKM Ac-1457^T, and (**B**) strain CC-R104^T and the closest related type strain DSM 45380^T, as predicted by antiSMASH.

3.3.3. Physiology and Chemotaxonomy

Strain CT-R113^T grew well on ISP7, GYM, MA and TSA, and weakly on ISP5 and CZA. No growth was observed on ISP2, ISP3, ISP4 and PDA. Colonies on TSA, modified with 1.5% NaCl, are small, opaque, circular with regular edges with a light-yellow coloration. In all the proliferative culture media, a dense mycelium with white spores is produced (Fig. 13). Growth was observed at 12–28 °C, pH 6.0–10.0 and NaCl 0-10% (w/v) on TSA, reaching its optimum at 28 °C, pH 7 and 0–5% NaCl. Strain CT-R113^T was catalase positive and oxidase negative. This strain was found to grow on sucrose, myoinositol, L-rhamnose and α -cellulose, with no visible growth on D-fructose, D-raffinose and D-mannitol. Regarding nitrogen sources, strain CT-R113^T was able to grow better on L-alanine, L-arginine, Glycine and L-serine, with a weak growth on L-asparagine, L-proline, L-threonine and L-tyrosine. The enzymatic profiling showed a positive reaction for alkaline phosphatase, esterase, leucine arylamidase and naphtol-AS-Bl-phosphohydrolase and weakly activity for esterase, lipase, α -glucosidase, β -glucosidase

and α -fucosidase. Menaquinone 10 (MK-10) was the respiratory quinone of strain CT-R113^T, as well as of its closest relatives *N. tropica* VKM Ac-1457^T and *N. umidischolae* 66/93^T. The major fatty acids of strain CT-R113^T were C_{18:1} ω 9c, anteiso-C_{17:0} and iso-C_{16:0}, which accounted for 67.9% of the total fatty acids (Table 5). The major three fatty acids of *N. tropica* VKM Ac-1457^T were also shared with strain CT-R113^T but with different relative percentages, which accounted for 57.2% of the total fatty acids. Conversely, the third major fatty acid of *N. umidischolae* 66/93^T was anteiso-C_{15:0}, instead of iso-C_{16:0}. The fatty acids anteiso-C_{11:0}, C_{17:0} 3-OH and anteiso-C_{17:1} ω 9c were not detected in strain CT-R113^T. Whole-cell hydrolysates contained *meso*-Dpm as the cell-wall diamino acid in strain CT-R113^T, similar to strains 66/93^T and VKM Ac-1457^T. Comparative phenotypic, chemotaxonomic and genomic characteristics of strain CT-R113^T and of the two closest related type strains are presented in Table 6.

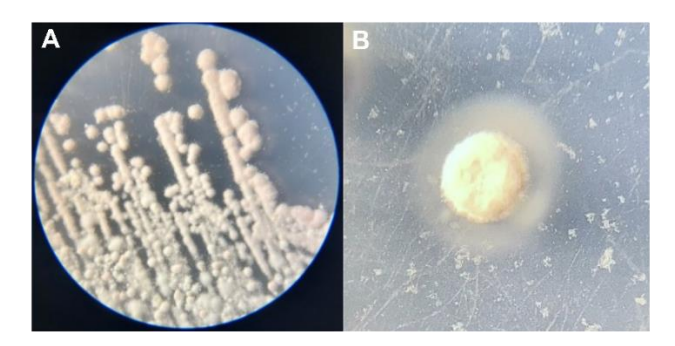


Figure 13. Morphology of strain CT-R113^T colonies in TSA medium, observed using a binocular magnifier (Leica ZOOM 2000) with magnifications of (**A**) 10x and (**B**) 30x.

Table 5. Fatty acids composition of strains CT-R113^T, *Nocardiopsis tropica* VKM Ac-1457^T and *Nocardiopsis umidischolae* 66/93^T. Strains: 1, CT-R113^T; 2, *Nocardiopsis tropica* VKM Ac-1457^T, 3, *Nocardiopsis umidischolae* 66/93^T. All data is from this study. The major cellular fatty acids are in bold. TR, trace amount (fatty acids amounting to < 1%).

Fatty acid	1	2	3
C _{8:0} 3-OH	2.9±0.03	2.3±0.29	2.3±0.68
iso-C _{10:0}	TR	TR	TR
anteiso-C _{11:0}	-	-	TR
C _{12:0}	1.1±0.01	TR	TR
anteiso-C _{13:0}	TR	TR	TR
C _{14:0}	TR	TR	TR
iso-C _{14:0}	1.5±0	2.4±0.13	2.8±0.34
iso-C _{15:0}	1±0.01	1.9±0.14	2.3±0.35
anteiso-C _{15:0}	4.7±0.01	11.1±0.44	12.7±1.28
C _{16:0}	1.9±0.04	2.2±0.11	2.1±0.29
iso-C _{16:0}	21.3±0.3	21.2±0.43	19.7±0.58
C _{17:0}	TR	1.5±0.13	1.2±0.18
iso-C _{17:0}	3.3±0.04	3.8±0.12	3.9±0.12
anteiso-C _{17:0}	22.8±0.17	22.7±0.31	21.1±0.64
C _{17:0} 3-OH	-	TR	TR
C _{17:1} ω8c	2.3±0.02	2.4±0.09	1.8±0.09
anteiso-C _{17:1} ω9c	-	-	TR
C _{18:0}	3.9±0.15	4.9±0.3	5.6±0.81
C _{18:0} 10-methyl	1.0±0.04	TR	1.3±0.1
iso-C _{18:0}	4.0±0.09	2.7±0.14	2.2±0.29
C _{18:1} ω9c	23.8±0.1	13.3±0.1	12.5±0.16
anteiso-C _{19:0}	TR	TR	TR
Summed feature 3 [†]	1.5±0.05	2±0.16	2.3±0.28

 $^{^\}dagger$ Summed features are fatty acids that cannot be resolved reliably from another fatty acid using the chromatographic conditions chosen. The MIDI system groups these fatty acids as one feature with a single percentage of the total. Summed feature 3 contains $C_{16:1}$ $\omega 7c$ and/or $C_{16:1}$ $\omega 6c$.

^{-,} not detected or values lower than 0.45%

Table 6. Differentiating phenotypic, chemotaxonomic and genomic characteristics of strain CT-R113^T and the closest related type strains *Nocardiopsis tropica* VKM Ac-1457^T and *Nocardiopsis umidischolae* 66/93^T; Strains: 1, CT-R113^T; 2, *Nocardiopsis tropica* VKM Ac-1457^T, 3, *Nocardiopsis umidischolae* 66/93^T.

	1	2	3
Isolation Source	Seaweed <i>Codium tomentosum</i> , Portugal	Rhizosphere of Casuarina sp., Seychelles	Indoor dust of a water-damaged school, Finland
Growth			
Temperature (°C)	12 – 28	28 – 37 *	10 – 37 [†]
рН	6.0 - 10.0	ND *	ND [†]
NaCl (% w/v)	0 – 10	0 – 5 *	0 – 7.5 †
Predominant menaquinones	MK-10	MK-10	MK-10
Major fatty acids	$C_{18:1}$ $\omega 9c$, anteiso- $C_{17:0}$ and iso- $C_{16:0}$	$C_{18:1}$ $\omega 9c$, anteiso- $C_{17:0}$ and iso- $C_{16:0}$	$C_{18:1}$ $\omega 9c$, anteiso- $C_{17:0}$ and anteiso- $C_{15:0}$
Cell-wall diamino acid	<i>meso</i> -Dpm	meso-Dpm *	meso-Dpm †
Genome size (bp)	7,272,268	6,210,722	7,893,508
DNA G+C content (mol%)	71.3	72.3	72.7
BGC's (number and type)	27 (PKS, NRPS, Terpene, RiPP, Hybrid)	17 (PKS, NRPS, Terpene, RiPP)	30 (PKS, NRPS, Terpene, RiPP, Hybrid)

^{*} Data from [195]

[†] Data from [194]

ND - not determined

Strain CC-R104^T grew well on MA, GYM and TSA, and weakly on ISP2-ISP7 and CZA. No growth was observed on PDA. A small, opaque, smooth and circular with regular edges dark yellow/orange colony, with no spores or vegetative mycelium, was observed in the most proliferative culture media TSA (Fig. 14). Growth was observed at 4–37 °C, pH 6.0–10.0 and NaCl 0-15% (w/v), reaching its optimum at 28 °C, pH 7 and 0-5% NaCl. Strain CC-R104^T was catalase positive and oxidase negative. This strain was able to use sucrose, myo-inositol, L-rhamnose, α-cellulose, D-fructose and Draffinose as growth carbon sources, with no visible growth with D-mannitol. Regarding nitrogen sources, strain CC-R104^T was able to grow better on L-alanine, L-arginine, Glycine, L-serine, L-asparagine and L-proline, with a weak growth on L-threonine and Ltyrosine. The enzymatic profiling showed a positive reaction for esterase, esterase lipase, leucine arylamidase and naphtol-AS-BI-phosphohydrolase, with weak activity for lipase, valine arylamidase and α-glucosidase. Menaguinone 8 (MK-8) was the only respiratory quinone of strain CC-R104^T, in contrast with its closest relative, R. artemisiae DSM 45380^T, for which MK-8 was not the exclusive quinone. The major fatty acids of strain CC-R104^T were C18:1 ω 9c, C16:0 and summed feature 3, which accounted for 78.1% of the total fatty acids (Table 7). The major three fatty acids of R. artemisiae DSM 45380^T were also shared with strain CC-R104^T but with different relative percentages, which accounted for 85.8% of the total fatty acids. The fatty acids summed feature 9 were detected in R. artemisiae DSM 45380^T but not in strain CC-R104^T. Only strain CC-R104^T possessed C15:1 ω 6c, C17:0, C17:1 ω 8c and summed features 6. Whole-cell hydrolysates contained meso-Dpm as the cell-wall diamino acid in strain CC-R104^T, similar to strain DSM 45380^T. Comparative phenotypic, chemotaxonomic and genomic characteristics of strain CC-R104^T and its closest related type strain DSM 45380^T are presented in Table 8.

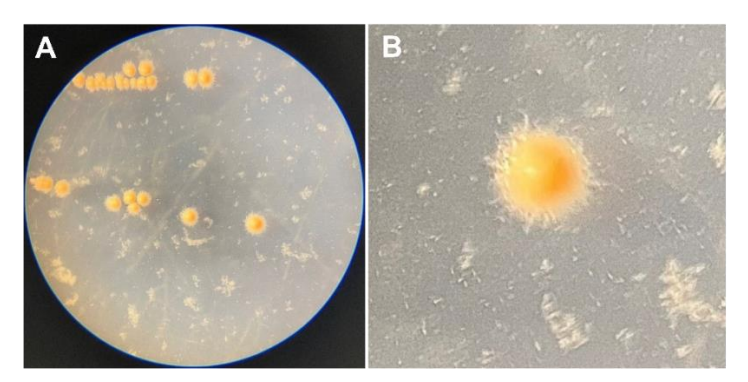


Figure 14. Morphology of colonies of strain CC-R104^T on TSA medium, observed using a binocular magnifier (Leica ZOOM 2000) with magnifications of (**A**) 10x and (**B**) 30x.

Table 7. Fatty acids composition of strain CC-R104^T and *Rhodococcus artemisiae* DSM 45380^T. Strains: 1, CC-R104^T; 2, DSM 45380^T. All data is from this study. The major cellular fatty acids are in bold. TR, trace amount (fatty acids amounting to < 1%).

Fatty acid	1	2
C _{14:0}	2.3±0.2	2.7±0.1
C _{15:1} ω6c	TR	-
C _{16:0}	22.7±0.8	32.6±0.4
C _{17:0}	3.6±0.3	-
C _{17:1} ω8c	7.8±0.9	-
C _{18:0}	3.5±0.4	2.2±0.1
C _{18:0} 10-methyl	TR	6.6±0.3
C _{18:1} ω9c	33.0±3.6	21.5±0.5
Summed features [†]		
3	22.4±1.7	31.7±0.3
6	TR	-
9	-	1.4±0.1

[†] Summed features are fatty acids that cannot be resolved reliably from another fatty acid using the chromatographic conditions chosen. The MIDI system groups these fatty acids as one feature with a single percentage of the total. Summed feature 3 contains $C_{16:1}$ $\omega 7c$ and/or $C_{16:1}$ $\omega 6c$. Summed feature 6 contains $C_{19:1}$ $\omega 9c$ and/or $C_{19:1}$ $\omega 11c$. Summed feature 9 contains $C_{16:0}$ 10-methyl and/or iso- $C_{17:1}$ $\omega 9c$.

^{-,} not detected or values lower than 0.45%

Table 8. Differentiating phenotypic, chemotaxonomic and genomic characteristics of strain CC-R104^T and its closest related type strain DSM 45380^T; Strains: 1, CC-R104^T; 2, DSM 45380^T.

	1	2	
Isolation Source	Seaweed Chondrus crispus, Portugal	Plant Artemisia annua L., China	
Growth (range)			
Temperature (°C)	4 – 37	10 – 40 *	
рН	6.0 – 10.0	6.0 – 9.0 *	
NaCl (% w/v)	0 – 15	0 – 7 *	
Predominant menaquinones	MK-8(H ₂)	MK-8(H ₂)	
•••	$C_{16:0}$ (22.7%), $C_{18:1}$ $\omega 9c$ (33.0%), $C_{16:1}$ $\omega 7c$ and/or $C_{16:1}$	$C_{16:0}$ (31.6%), $C_{18:1}$ ω 9 c (21.5%), $C_{16:1}$ ω 7 c and/or $C_{16:1}$ ω 6 c	
Major fatty acids	ω6c. (22.4%)	(31.7%)	
Cell-wall diamino acid	<i>meso</i> -Dpm	meso-Dpm *	
Genome size (bp)	5,341,903	7,088,132	
DNA G+C content (mol%)	67.01	66.2	
BGC's (number and type)	18 - PKS, NRPS, Terpene, RiPP, Hybrid	17 - PKS, NRPS, Terpene, RiPP, Hybrid	

^{*} Data from [232].

3.4. CONCLUSION

Nocardiopsis codii [(co'di.i. N.L. gen. n. codii, of the algal genus Codium) CT-R113^T is a Gram-positive, aerobic, halotolerant, spore-forming, catalase positive and oxidase negative Actinomycetota. Colonies on TSA, modified with 1.5% NaCl, are small, opaque, circular with regular edges with a light-yellow coloration. In all the proliferative culture media (ISP7, ISP5, CZA, GYM, TSA and MA, all supplemented with 1.5% NaCl, except MA), a dense mycelium with white spores is produced. No growth is observed on ISP2-ISP4 and PDA. Growth occurs at pH 6.0–10.0 (optimum, pH 7.0), at 12–28 °C (optimum, 28 °C) and with 0–10% (w/v) NaCl (optimum, 0–5%). Sucrose, myo-inositol, L-rhamnose and α-cellulose can be used as sole carbon sources, but not D-fructose, D-raffinose and D-mannitol. L-alanine, L-arginine, Glycine and L-serine can be used as sole nitrogen sources, but the growth is weaker when using L-asparagine, L-proline, L-threonine and L-tyrosine. Menaquinone 10 (MK-10) is the only respiratory quinone. The major fatty acids are C_{18:1} ω9c, anteiso-C_{17:0} and iso-C_{16:0}. Whole-cell hydrolysates contain meso-Dpm as the cell-wall diamino acid. The genome size of strain CT-R113^T is 7 272 268 bp and the G+C content of the genomic DNA is 71.3 mol%. The NCBI GenBank accession number for the genome assembly is JAUZMY00000000 and the accession number of the 16S rRNA gene sequence is OR578920. The type species is Nocardiopsis codii CT-R113^T (=LMG 33234^T =UCCCB 172^T) and was isolated from the tissues of the seaweed C. tomentosum collected in the northern Portuguese coast.

Rhodococcus algaerubra [a. I. gae. ru'bra. N.L. fem. adj. algaerubra pertaining to the red algae used as source of isolation for this microorganism (from Latin alga, algae, and ruber, red)]. CC-R104^T is an aerobic, halotolerant, non-spore forming Actinomycetota. Colonies on TSA, modified with 1.5% NaCl, are small, opaque, smooth and circular with regular edges presenting a dark yellow/orange coloration which intensity increases over time. No spores or vegetative mycelium are formed. Cells grow well on MA and GYM culture media and weakly on ISP2-ISP7 and CZA, all modified with 1.5% NaCl expect MA. Growth occurs at pH 6.0–10.0 (optimum, pH 7.0), at 4–37 °C (optimum, 28 °C) and with 0–15% (w/v) NaCl (optimum, 0–5%). Test for catalase activity was positive and for oxidase activity was negative. Sucrose, myo-inositol, L-rhamnose, α-cellulose, D-fructose and D-raffinose can be used as sole carbon sources, but not D-mannitol. L-alanine, L-arginine, Glycine, L-serine, L-asparagine and L-proline can be used as sole nitrogen sources, but the growth is weaker when using L-threonine and L-tyrosine. Menaquinone 8 (MK-8) is the only respiratory quinone. The major fatty acids are C18:1 ω 9c, C16:0 and summed feature 3. Whole-cell hydrolysates contained *meso*-Dpm as the

cell-wall diamino acid. The genome size of strain CC-R104^T is 5 341 903 bp and the G+C content of the genomic DNA is 67.01 mol%. The NCBI GenBank accession number for the genome assembly is JAUZMZ000000000 and the accession number of the 16S rRNA gene sequence is OR578921. The type species is *Rhodococcus algaerubra* CC-R104^T (=LMG 33233^T =UCCCB 171^T) and was isolated from the tissues of the red seaweed *C. crispus* collected in the northern Portuguese coast.

The discovery, description and validation of two novel Actinomycetota species isolated from macroalgae, proves the relevance of this ecological niche of source of new biodiversity, offering access for promising future research on their ecological role and biotechnological application.

4

Bioactive potential of macroalgae-associated Actinomycetota revealed through culturedependent and -independent approaches

The content of this chapter is submitted for publication in the Q1 journal **Microbial Biotechnology**:

<u>Girão, M.</u>, Rego, A., Fonseca A.C., Weiwei C., Zhongjun J., Urbatzka, R., Leão, P. N. & Carvalho, M. F. (2024) Bioactive potential of macroalgae-associated Actinomycetota revealed through culture-dependent and -independent approaches.

ABSTRACT

Actinomycetota are unrivalled producers of bioactive natural products, with strains living in association with macroalgae representing a prolific – yet largely unexplored – source of specialized chemicals. In this work, we have investigated the bioactive potential of macroalgae-associated Actinomycetota through culture-dependent and -independent approaches. In this chapter, a bioprospecting pipeline was applied to a collection of 380 actinobacterial trains, recovered from two macroalgae species collected in the Portuguese northern shore - Codium tomentosum and Chondrus crispus -, in order to explore their ability to produce antibacterial, antifungal, anticancer and lipid-reducing compounds. Around 43% of the crude extracts showed activity in at least one of the screenings performed: 111 presented antimicrobial activity at 1 mg mL⁻¹, 83 significantly decreased cancer cells viability at 15 µg mL⁻¹ and 5 reduced lipid content in zebrafish > 60% at 15 ug mL-1. Dereplication of active extracts unveiled the presence of compounds that could explain most of the recorded results, but also unknown molecules in the metabolome of several strains, highlighting the opportunity for discovery. The bioactive potential of the actinobacterial community associated to the same macroalgae specimens, which served as the source for the aforementioned Actinomycetota collection, was also explored through metagenomics analysis, allowing to obtain a broader picture of its functional diversity and novelty. From the 130 biosynthetic gene clusters and 10 metagenome-assembled genomes recovered, 91 gene cluster families of biosynthetic gene clusters were identified, 83 of which showing less than 30% of similarity to database entries. Our findings provided by culture-dependent and independent approaches underscore the potential held by actinomycetes associated with macroalgae as reservoirs for novel bioactive natural products.

Keywords: Actinomycetota; Antimicrobial; Anticancer; Anti-obesity; Bioactivity; Dereplication; Macroalgae; Metagenomics

4.1. INTRODUCTION

The quest for novel solutions to address pressing global challenges -the rising antibiotic resistance crisis, scarcity of materials, need for industrial innovation and hurried environmental degradation – is triggering the bioprospecting of untapped sources, such as the marine environment, for chemical novelty [234]. Macroalgae, also referred as seaweeds, inhabit the oceans for more than 2 billion years, outlasting several mass extinction events and representing one of the most resilient and notable marine living resources [235]. These organisms and associated by-products have been extensively explored due to their biotechnological applications, especially in food, cosmetic, pharmaceutical, energy and farming industries [124]. Macroalgae can be found in many locations worldwide, being highly dominant in the North-Atlantic rocky coast flora [236]. These organisms host unique microbial communities [47], including members of the most prolific bacterial source of drug-lead chemicals, the Actinomycetota phylum [39]. In fact, life in the ocean is full of remarkable symbiotic and highly refined relationships among life forms, shaped by selective pressures in which one organism (e.g. a bacterium) generates evolutionarily-optimized small molecules that can not only impact the host (and other symbionts), but also be used for other biotechnological endings due to their unique features [44]. Marine Actinomycetota have demonstrated their value in the field of NP by encoding BGCs that translate into unique chemical scaffolds and biosynthetic pathways, yielding secondary metabolites with a broad range of applications [39, 237, 238]. The association between Actinomycetota and macroalgae has been shown before, with these microorganisms exhibiting diverse biological features, from antibiotic, antiinflammatory, anti-tuberculosis and anticancer to heavy metal sorption capability [157]. Further studies had led to the discovery of novel NP from macroalgae-associated Actinomycetota, such as the antibiotic kocumarin, a benzoic acid derivative isolated from Kocuria marina CMG S2, retrieved from the tissues of the brown macroalgae Pelvetia canaliculata collected in a rocky beach in Pakistan [66], or the potent inhibitor of glioblastoma neaumycin B, a novel macrolide isolated from the secondary metabolism of Micromonospora sp. CNY-010, retrieved from the brown macroalgae Stypopodium zonale surface, collected in the Bahamas Islands [64]. Even with proven evidence that a synergistic environment fosters NP production [239], when looking into the overall landscape of marine Actinomycetota symbionts on drug discovery lineups, the metabolomes of macroalgae-associated strains have been little targeted when compared to those of other hosts, like sponges or corals. In a previous study, we unveiled how a kelp from the northern Portuguese coast was accommodating a highly diverse

and bioactive community of Actinomycetota with evidence of novel NP production [79]. However, no study to date has been employed on the biosynthetic potential of macroalgae-associated Actinomycetota from native Chlorophyta and Rhodophyta specimens from the same region. In this study we aim to unveil the biosynthetic potential and chemical novelty encoded on macroalgae-associated Actinomycetota secondary metabolism. We applied a comprehensive and multidisciplinary approach, combining culture-dependent and independent approaches. In vitro and in vivo bioactivity screenings, mass spectrometry-based dereplication and a molecular networking pipeline was used to explore a collection of 380 Actinomycetota strains isolated from two macroalgae collected in the northern Portuguese coast, C. tomentosum and C. crispus [240], both species targeted for the first time for this purpose. We have directed our research efforts towards antimicrobial, anticancer, and lipid-reducing chemicals to tackle urgent global health challenges such as the rising incidence of antibiotic-resistant pathogens and the scarcity of effective therapeutic options for cancer pathologies and metabolic diseases [241-243]. Metagenomics was used to deeper explore the novelty of BGCs encoded by the macroalgae-associated Actinomycetota community, studying at the same time their abundance and diversity. Our results show that the collection of Actinomycetota strains isolated from C. tomentosum and C. crispus represents a hub of diverse and potentially novel bioactive compounds to be fully explored for biotechnological applications. In particular, the Actinomycetota community associated to C. crispus stood out as a rich resource of untapped metabolites worth of further exploration, as revealed by the metagenomics studies. Altogether, our findings highlight the value of macroalgae-associated Actinomycetota in NP discovery.

4.2. MATERIALS AND METHODS

4.2.1. Samples Analyzed in this Study

In this study, we have analyzed the bioactive properties and biosynthetic potential of the actinobacterial community associated with two macroalgae collected from the northern Portuguese coast – *C. tomentosum* and *C. crispus*. From the tissues of both macroalgae, a collection of 380 actinobacterial strains was isolated (Chapter 2, section 2.2.2.) and screened for the production of bioactive compounds. The eDNA from the same tissues was extracted and sequenced (Chapter 2, section 2.2.5.) for metagenomic analysis.

4.2.2. Preparation of the Crude Extract's Library

In order to assess the bioactive properties of the isolated Actinomycetota strains, a library composed by a crude extract of each isolate was created, following the fermentation and organic extraction procedures described in Girão *et al.*, 2019 [79]. Briefly, each strain was cultured at 28 °C, in their corresponding isolation media, except for strains retrieved using NPS (nutrient-poor sediment extract agar) and SA (seaweed agar), which were grown using MB (marine broth, Condalab, Spain) for better yield, in the presence of Amberlite XAD16N resin (Sigma-Aldrich, MO, United States). Organic extraction of both biomass and resin obtained from 7-day cultures was performed using a mixture of 1:1 acetone and methanol. Dimethyl sulfoxide (99.9%, DMSO; Sigma-Aldrich, MO, United States) was used to dissolve the crude extracts for later use in the bioactivity assays.

4.2.3. Antimicrobial Assay

The antimicrobial activity of the crude extract library was tested against five human health-relevant reference microorganisms – *Escherichia coli* ATCC 25922, *Salmonella enterica* ATCC 25241, *Bacillus subtilis* ATCC 6633, *Staphylococcus aureus* ATCC 29213, and *Candida albicans* ATCC 10231 – using the agar-based disk diffusion method as described in Girão et al. 2019 [79]. Using the same method, with minor changes, the activity of the extracts was also tested against three aquaculture-relevant fish pathogenic strains – *Edwardsiella tarda* DSM30052, *Aeromonas hydrophila* DSM3018 and *Pseudomonas anguilliseptica* DSM12111. *E. tarda, A. hydrophila* and *P. anguilliseptica* were grown in TSA (Tryptic Soy agar) (Sigma-Aldrich, MO, United States) and when preparing the suspension for the assay, their turbidity was adjusted to the higher limit of

the 0.5 McFarland standard ($OD_{625} = 0.13$). All extracts were tested at 1 mg mL⁻¹. Antimicrobial activity was determined by measuring the diameter of the inhibition halo formed around each disk after 24 h of incubation at 37 °C for the five human pathogenic strains, and after 48 h of incubation at 28 °C for the fish pathogenic strains. Positive control consisted in Enrofloxacin (1 mg mL⁻¹) for all bacterial strains and Nystatin (1 mg mL⁻¹) for *C. albicans*. DMSO was used as negative control for all the tested microorganisms. One replica of each extract was tested in two independent experiments.

4.2.4. Anticancer Assay

The anticancer activity of the crude extract library was tested in monolayer cell cultures of two cancer lines – T47D (breast ductal carcinoma) and HCT116 (colorectal carcinoma) - and on the non-cancer line hCMEC/D3 (human brain capillary endothelial cells) using the MTT [3-(4,5-dimethylthiazol-2-yl)-2,5-diphenyltetrazolium bromide] assay. T47D and hCMEC/D3 cells were grown in DMEM (Dulbecco's Modified Eagle Medium, Gibco, Thermo Fischer Scientific, Waltham, MA, United States) and HCT116 cells in McCoy's 5 A medium (Gibco, Massachusetts, USA), all supplemented with 10% (v/v) fetal bovine serum (Biochrom, Berlin, Germany), 1% (v/v) antibiotics (100 mg L⁻¹ streptomycin), 100 IU mL ⁻¹ penicillin (Biochrom, Berlin, Germany) and 0.1% (v/v) amphotericin (GE Healthcare, Little Chalfont, United Kingdom), at 37 °C in an incubator with 5% carbon dioxide. Cells were seeded at 6.6x104 cells mL-1, allowed to adhere overnight and exposed to the extracts (final concentration: 15 µg mL⁻¹) for 48 h. The apoptotic agent staurosporine (Sigma-Aldrich, MO, United States) was used as positive control, at 2 µM, and 0.5% DMSO was used as solvent control. After the exposure time, MTT was added per well at the final concentration of 0.2 mg mL⁻¹ (Sigma-Aldrich, MO, United States) and the plates incubated for an additional period of 4 h. The culture medium was then removed from all wells and 100 µL of DMSO added. The absorbance at 570 nm was determined using BioTek Cytation 5 Cell Imaging Multimode Reader (Agilent Technologies, CA, United States). Two independent experiments were performed, each in triplicate. Cellular viability was expressed as a percentage relative to the solvent control.

4.2.5. Lipid-reducing Assay

The lipid-reducing activity of the crude extract library was analyzed using the zebrafish larvae Nile Red fat metabolism assay, as previously described [244]. No permission for

animal experiments was required following the EC Directive 86/609/EEC, since the selected procedures involved non-autonomous feeding stages. Wildtype zebrafish embryos (AB strain) were raised from one DPF (days post-fertilization) in E3 medium (NaCl 10mM, KCl 360 μM, CaCl₂·2H₂O 660 μM, MgCl₂·6H₂O 802 μM), 1% Methylene Blue, and 200 μM 1-phenyl-2-thiourea (PTU; VWR) to inhibit pigmentation. At three DPF, zebrafish larvae morphology was inspected, to remove any individuals with malformations, and exposed to the crude extracts (final concentration: 15 µg mL⁻¹). The experiments were conducted using 96 well plates, with 3 larvae per well. Resveratrol (REV; Sigma-Aldrich, MO, United States) was used as positive control (PC; final concentration: 50 µM) and 0.1% DMSO was used as solvent control. The plates were incubated at 28 °C for 30 h. After this period, neutral lipids were stained overnight with Nile Red (final concentration: 10 ng mL⁻¹). For imaging, the larvae were anesthetized for 5 minutes using Tricaine Methanesulfonate (0.03%; Sigma-Aldrich, MO, United States) and fluorescence analyzed by BioTek Cytation 5 Cell Imaging Multimode Reader. Fluorescence intensity was quantified in individual zebrafish larvae by ImageJ [245]. One independent experiment was performed for each crude extract, with three larvae being exposed to each extract. A second experiment was done to confirm the activity of the previous positive hits. Lipid-reducing activity was expressed as mean fluorescence intensity (MFI) compared to the solvent control (SC).

4.2.6. Statistics

Data from anticancer and lipid-reducing assays (a total of six technical replicates) was tested for significant differences compared to the solvent control, and the significance level was set for all tests at p < 0.05. The Kolmogorov Smirnov test was used to check for normality distribution of data after removing outliers. For parametric data, one-Way ANOVA was applied followed by Dunnett's post hoc test. If statistical test assumptions were not met, data were either square root transformed and re-tested by ANOVA, or the non-parametric Kruskal-Wallis test was applied, followed by Dunn's multiple comparison test.

4.2.7. Evolutionary Relationship of the Bioactive Strains

A phylogenetic tree comprising the 16S rRNA gene consensus sequence of all strains responsible for the extracts considered active was constructed to infer their evolutionary relationship. The sequences were aligned using MUSCLE from within the Geneious software package and the Maximum Likelihood method with 1000 bootstraps based on

the Tamura-Nei model was applied. MEGA-X was used to build the tree and iTOL to perform its final display and annotation.

4.2.8. Dereplication and Metabolic Profiling of Active Extracts

All the extracts considered as active in at least one of the bioactivity tests performed (i.e. presence of an inhibition halo in the antimicrobial screening, and significant in one-way ANOVA analysis in the anticancer and lipid-reducing assays) were selected for metabolic profiling. A liquid chromatography high resolution rlectrospray ionization mass spectrometry coupled to tandem mass spectrometry (LC-HRESIMS/MS) analysis was conducted for each sample (final concentration: 2 mg mL⁻¹ in methanol) using a system composed of a Dionex Ulimate 3000 HPLC coupled to a qExactive Focus Mass spectrometer controlled by XCalibur 4.1 software (Thermo Fisher Scientific, MA, United States). Five microliters of each sample were injected into an ACE UltraCore 2.5 Super C18 column (Advanced Chromatography Technologies, Aberdeen, United Kingdom) The separation, UV reading and data acquisition were carried out as previously described [79]. Converted mzML files from each extract were used in the dereplication tools from the GNPS (Global Natural Products Social Molecular Networking) platform: In silico Peptidic Natural Product Dereplicator [246, 247], Dereplicator + [248] and Dereplicator VarQuest. In all analyses, ion mass tolerance precursor was set to 0.005 Da and fragment ion mass tolerance to 0.01 Da, to account for high resolution data. Extracts with no hits in any of the dereplicators - i.e., no correlation with known actinobacterial secondary metabolites that could explain the recorded bioactivity - were used to generate a molecular network using the GNPS workflow [249]. The network output was visualized with Cytoscape v3.6.1 [250] and searched for clusters of m/z data associated with a single extract. The identified putative compound masses were used for an additional dereplication step by searching the predicted accurate mass (± 5ppm) against the Dictionary of Natural Products (DNP; dnp.chemnetbase.com) and Natural Products Atlas 2.0 (NPA) [251] databases.

4.2.9. Recovery and Mining of Actinobacterial Contigs and MAGs

Shotgun metagenomic sequencing was performed as previously described [240] for the two samples of eDNA extracted from the tissues of the macroalgae under study: *C. tomentosum* and *C. crispus*. The same tissues from where the 380 actinobacterial strains were isolated were used for this analysis. Holdfast and blade of each macroalgae were

poled together in the same sample. The bioinformatic analysis started with quality trimming of paired-end reads using the following parameters: quality trimming at Q20 and sequences shorter than 45 bp removed using BBDuk tool from BBMap (https://sourceforge.net/projects/bbmap/). Paired-end reads were assembled using MEGAHIT v.1.2.9 [252] and taxonomy was assigned to generated contigs using kaiju v.1.9.2 [149]. For the recovery of metagenome assembled genomes (MAGs), mapping was performed using Bowtie2 v.2.5.1 [253, 254] and samtools v.1.13 [255], on the previously assembled reads and the following steps were preformed using Anvi'o v.7.1 tutorial [256] following the "Metagenomic workflow" (http://merenlab.org/2016/06/22/anvio-tutorial-v2/). Briefly, a contigs database was created using "anvi-gen-contigs-database", open reading frames were identified using Prodigal [257] and HMMER [258] was used to identify genes in our contigs matching to bacterial single-copy core genes. For functional annotation of genes in the contigs database "anvi-run-ncbi-cogs" was used. Profiling was performed using "anvi-profile". Binning was performed using the standalone tool CONCOCT v.1.1.0 [259] and the generated bins were imported to Anvi'o using "anvi-import-collection". Bins were manually refined using "anvi-refine". The final taxonomy was assigned to the refined bins using GTDB-Tk v2.1.1 [260]. Quality of the recovered MAGs was determined using Anvi'o "anvi-estimate-genome-completeness" and checkM v.1.2.2 [261]. Refined bins were considered MAGS of high-quality if they had > 90% completeness and < 5% contamination and medium quality with >50% completeness and < 10% of contamination. For identification and recovery of BGCs, the obtained actinobacterial contigs and MAGs were run in a locally installed version of antiSMASH. A network analysis of recovered BGCs was performed using the BiG-SCAPE [262] algorithm. The program was run in the default global mode, the networks were computed using the 'mix' and 'MIBiG' options. The option 'include singletons' was also used, to allow visualizing singleton BGCs in the network. Networks were computed using multiple raw distance cutoff values (from 0.1 to 1.0) and the networks computed sing 0.7 cutoff were chosen. The resulting sequence similarity matrices were then visualized in Cytoscape v.3.9.1 [250] and a column with the assignment of each BGC to the category MIBiG, MAG, or contigs was included to differentiate between the distinct sets of BGCs. A maximumlikelihood phylogenomic tree of the recovered MAGs, was computed using PhyloPhIAn 3.0 [211], imported and edited using iTOL. Metagenomic sequencing data used in this study are deposited in the European Nucleotide Archive (EMBL-EBI) database and are available under the accession numbers ERR12332060 and ERR12332061.

4.3. RESULTS AND DISCUSSION

4.3.1. Bioactivity Screening

4.3.1.1. Antimicrobial Activity

NP have been historically effective against pathogenic bacteria, but the rise of antibiotic-resistant infections emphasizes the necessity for discovering new antibiotics, vital not only for human health but also for other sectors like aquaculture [242, 263]. In this work, we have mined a collection of macroalgae-associated Actinomycetota strains to search for antimicrobials effective against a panel of human health and aquaculturerelevant microbes. From the 380 actinobacterial crude extracts tested for antimicrobial activity, around 30% (n=111) were able to inhibit the growth of at least one reference microorganism tested (Fig. 15, Table S7 - Appendix III). Of these, 72 extracts were active against the growth of the yeast C. albicans and the two Gram-positive bacteria S. aureus and B. subtilis, with inhibition halos ranging between 8 to 27 mm in diameter. C. albicans proved to be the most susceptible microorganism to the actinobacterial extracts (n=47). No activity was detected towards the Gram-negative bacteria E. coli and S. enterica. Conversely, when tested against the aquaculture-relevant Gram-negative species P. anguilliseptica and A. hydrophyla, 47 extracts were active, with inhibition halos between 8 to 25 mm of diameter and a higher number of extracts affecting the first microorganism (n=37) (Fig. 15A). No activity was detected towards E. tarda. Interestingly, only extracts from eight strains – CC-R47, CC-R112, CC-R116, CC-R176, CC-F69, CC-F123, CT-F55 and CT-F61 -, showed activity in both human and aquaculture-relevant pathogens (highlighted in bold in Fig. 15A). From the 111 strains responsible for the active extracts, 41% (n=46) were isolated from C. crispus (CC) and 59% (n=65) from C. tomentosum (CT) tissues. These isolates were recovered from both parts of the macroalgae – holdfast and blade –, with a relative higher yield of strains producing antimicrobials being obtained from the blades of C. tomentosum (39%) (Fig. 15B). Remarkably, more than a half (52.3%; n=58) were cultured using the liquid version of the medium AIA (Actinomycete Isolation Agar), followed by MB (Marine Broth; 33.3%; n=37) and SCN (Starch-Casein-Nitrate broth; 14.4%; n =16) (Fig. 1C). Both AIA and SCN were supplemented with 1.5% NaCl. The 111 active extracts are distributed across 19 Actinomycetota genera, with 51% of them being affiliated to Streptomyces (Fig. 15D). From the 19 genera, only eight recovered from both macroalgae species: Gordonia, Kitasatospora, Microbacterium, Micromonospora, Nocardia. Nocardiopsis. Rhodococcus

Streptomyces. It is interesting to note that from the 14 active genera associated to C. tomentosum, crude extracts of 11 of them were exclusively active towards the aquaculture-relevant pathogens. The same was not observed for C. crispus, with only four genera presenting this bioactivity profile. Marine Actinomycetota, in particular but not exclusively Streptomyces species, are recognized as excellent producers of antibiotics effective against several pathogens, including drug-resistant strains. Examples include abyssomycin C, a polycyclic polyethylene produced by a with antibacterial activity Verrucosispora strain against methicillin-resistant Staphylococcus aureus (MRSA) and Mycobacterium tuberculosis [264, 265], or tirandamycin C, a dienoyl tetramic acid produced by a Streptomyces with activity against vancomycin-resistant Enterococcus faecalis (VRE) [266]. From macroalgae-associated actinomycetes, some NP with similar properties have also been isolated, as exemplified by the macrolide desertomycin G and the indolizinium alkaloid streptopertusacin A, both retrieved from Chlorophyta-associated Streptomyces and active against several clinical pathogens [90, 91]. When compared to other screening studies on the antimicrobial properties of macroalgae-associated Actinomycetota, particularly from Chlorophyta and Rhodophyta hosts, our work unveiled a significant universe of bioactive strains, both in number and taxonomic diversity. Based on available literature, no more than 27 active strains, from a universe of 51 isolates, have been retrieved from a single macroalgae [63, 89, 132, 267], a fairly lower number compared to our results. Although our current study yielded a greater number of strains exhibiting antimicrobial activity, their relative percentage compared to the total collection screened (around 30%) was lower than that reported in the highlighted study (53%). In line with our data, the majority of the strains reported in these studies were identified as Streptomyces. The affiliation of the remaining strains was attributed to other genera, with five of them - Aeromicrobium, Agrococcus, Janibacter, Pseudonocardia and Salinibacterium – being not retrieved in our study. The strains described in the mentioned works displayed activity towards reference Grampositive and Gram-negative pathogenic bacteria and yeasts, but no aquaculture-relevant pathogen was targeted in any of them. In our previous work exploring the bioactive properties of the actinobacterial community associated to the kelp Laminaria ochroleuca [79], collected in the same area as C. tomentosum and C. crispus specimens, 45 isolates producing antimicrobials were retrieved from a collection of 90 strains (45% of the all screened strains, a higher percentage when compared to this study), once again headed by Streptomyces.

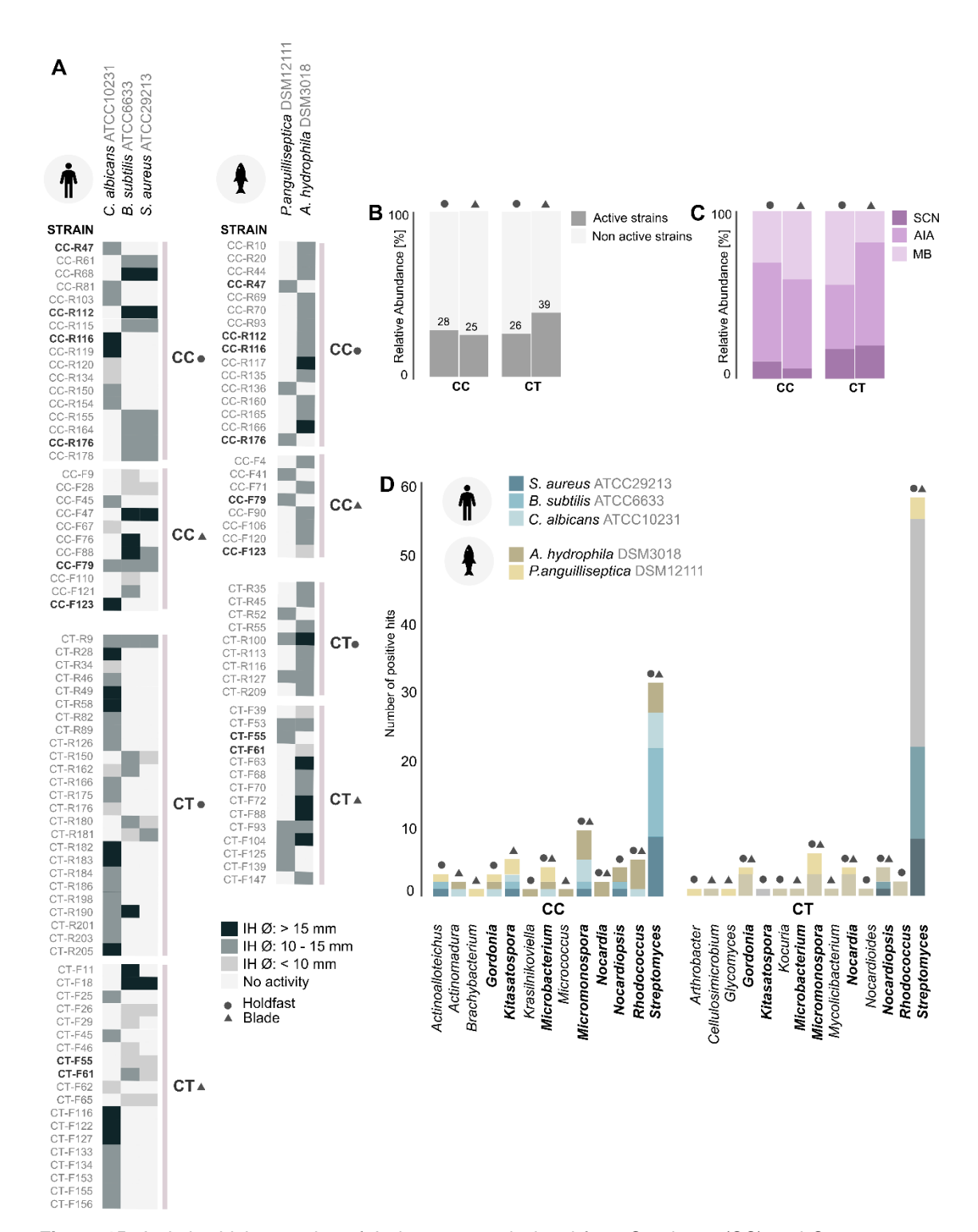


Figure 15. Antimicrobial screening of Actinomycetota isolated from C. crispus (CC) and C. tomentosum (CT). (A) Strains with bioactivity in the antimicrobial assay. Only strains active towards at least one reference microorganism are presented. Data displayed as average measurement (mm) of the inhibition halos (IH) diameter from two independent experiments. Strains highlighted in bold presented inhibitory effect toward the growth of at least one human and fish health-relevant reference microorganism. (B) Distribution of active and non-active strains retrieved from CC and CT. (C) Distribution of active strains according to their fermentation medium. (D) Genus-level taxonomic distribution of active strains. Taxonomic groups

highlighted in bold were found in both macroalgae. The source of isolation, holdfast (\bullet) or blade (Δ) , is indicated in all graphs.

4.3.1.2. Anticancer Activity

Cancer is a major public health problem worldwide, representing one of the main causes of human death [243]. The pursuit of novel NP exhibiting anticancer activities, and/or that may be more effective while causing scarcer damaging effects on healthy cells, is one of the major focuses of current scientific research. In this regard, the 380 actinobacterial crude extracts were tested for anticancer activity in the human cancer cell lines HCT116 and T47D. Around 22% (n=83) of the extracts caused a statistically significant decrease in the cellular viability of at least one tested cell lines after 48 h of exposure, when compared to the solvent control. HCT116 cells proved to be more susceptible to the actinobacterial crude extracts, when compared to T47D cells (70 and 41 extracts active against each cell line, respectively – Fig. 16, Table S7 - Appendix III). Statistical analysis unveiled higher potency in 44 extracts (reduction of viability > 40%; p. value < 0.001), with 55% of them affecting cancer cells only: 24 displayed a specific action towards the proliferation of HCT116 cells, with 3 of them - from strains CT-R49, CC-F27 and CT-F61 – exhibiting targeted toxicity towards the T47D cell line as well (Fig. 16A1). In-depth look into the most potent extracts -i.e. the ones able to reduce the cancer cells viability to < 25% after 48 h of exposure – showed that some are as efficient or more as the apoptotic drug Staurosporine: CT-R9 and CT-F144 were able to decrease the viability of HCT116 cancer cells more than 90% and CT-F37 and CT-R29 decreased the viability of T47D cancer cells more than 95%. However, all extracts responsible for cancer cellular survival rates as low as 5-10%, proved to affect at the same level the viability of healthy cells. Still, the extract obtained from strain CC-R26 was able to significantly decrease the cellular viability of HCT116 line (reduction of > 85%), with no negative effect on the non-carcinogenic cells (Fig. 16A2). Nevertheless, this general cytotoxicity might be overcome to still allow benefit on the therapeutic properties of the encoded active compounds by using targeted drug delivery methodologies, combination therapy, compound structure optimization, gene silencing and/or immunotherapeutic approaches [268-270]. From the 83 strains with anticancer activity, 39% (n=32) were isolated from C. crispus (CC) and 61% (n=51) from C. tomentosum (CT) tissues. These isolates were recovered from both parts of the macroalgae - holdfast and blade -, with a relative higher yield of strains producing anticancer compounds being obtained from the blades of C. tomentosum (39%) (Fig. 16B). The majority of active strains was cultured in MB (48%; n=40), followed by AIA (34%; n=28) and SCN (18%; n=15) (Fig. 16C).

Streptomyces was identified as the dominant genus (61%; n=68) but active strains were identified as belonging to 9 other actinobacterial genera. The 24 extracts with selective anticancer activity are distributed across three genera, Streptomyces, Actinomadura and Rhodococcus, strongly represented by the first genus (92%; n=22) (Fig. 16D). Marine Actinomycetota are prolific producers of secondary metabolites with anticancer and antitumor properties, with the most representative example being salinosporamide A, a rare bicyclic γ-lactam-β-lactone isolated from a marine-sourced Salinispora tropica with a highly cytotoxic proteasome inhibitor, now in clinical trials to treat patients with multiple myeloma, solid tumors and lymphoma [44, 271]. The bioprospecting of macroalgaeassociated Actinomycetota has also led to the uncover of NP with anticancer properties. as exemplified by the polyketide-derived macrolide neaumycin B, a potent inhibitor of glioblastoma, isolated from a Phaeophyta-associated Micromonospora strain [64]. Similar to what we observed regarding the antimicrobial data, in comparison to other studies on the anticancer properties of macroalgae-associated screening Actinomycetota, in particular from green and red algae [91, 132], our results stand out both in number of active strains and in their diversity. While in the reported studies the strains encoding anticancer properties are solely affiliated with the Streptomyces genus, our results show that other actinobacterial genera recovered from macroalgae tissues display the same bioactivity.

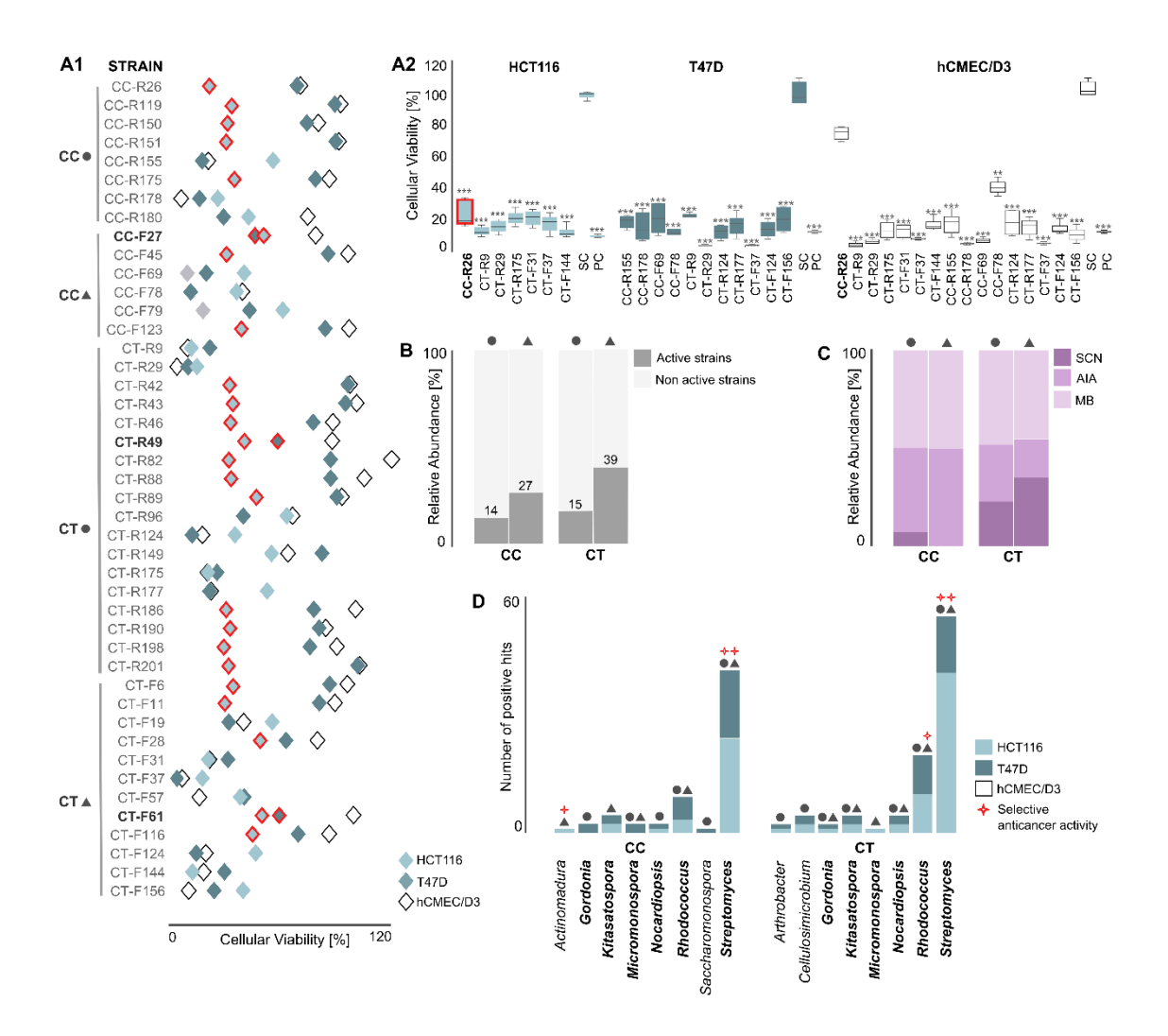


Figure 16. Anticancer screening of Actinomycetota isolated from *C. crispus* (CC) and *C. tomentosum* (CT). (A1) Strains with bioactivity in the MTT assay (15 μg mL⁻¹). Only the most active strains (p value < 0.001) are presented. Data displayed as mean of cellular viability (%) from two independent experiments (n = 6) and significant differences compared to the SC (solvent control: 0.5% DMSO), after 48 h of exposure. Results for the two cancer cell lines (HCT116 and T47D) and the non-cancer cell line (hCMEC/D3) are presented. Extracts with selective activity in cancer cells are red-bordered, with the ones highlighted in bold presenting cytotoxicity towards both cancer cell lines tested. (A2) Most active extracts in each cancer cell line compared to SC and PC (positive control: 15 μg mL⁻¹ Staurosporine). Extracts with selective activity in cancer cells are red-bordered. *** p value < 0.001. (B) Distribution of active and non-active strains retrieved from CC and CT. (C) Distribution of active strains according to their fermentation medium. (D) Genus-level taxonomic distribution of active strains. Taxonomic groups highlighted in bold were found in both macroalgae. The source of isolation, holdfast (•) or blade (Δ), is indicated in all graphs.

4.3.1.3. Lipid-reducing Activity

The escalating obesity epidemic, predisposing individuals to several chronic illnesses such as metabolic syndrome, diabetes, cardiovascular diseases and cancer, presents a significant public health issue. Existing drugs targeting weight loss have a long history of

negative secondary effects, highlighting the lack of safe and efficient drugs to treat obesity and related metabolic complications [241]. To search for new chemicals with potential to address this problematic, the 380 actinobacterial crude extracts were tested for lipid-reducing properties, using the zebrafish larvae Nile Red fat metabolism assay. Around 1.5% (n=5) caused a statistically significant decrease in lipid accumulation in vivo, when compared to the SC (Fig. 17A, Table S7 - Appendix III). The MFI reduced between 30 to 60%, while the positive control REV reduced 72% of neutral lipids. Resveratrol is a polyphenolic compound, part of the stilbene class, that has been identified for its ability to constrain neuropeptide Y and agouti-related protein, two hypothalamic neuropeptides that play a crucial role in regulating food intake [272]. From the 5 active strains, 80% (n=4) were isolated from C. crispus (CC) and 20% (n=1) from C. tomentosum (CT) tissues, exclusively from the holdfast region in both macroalgae (Fig. 17B). The majority of active strains were cultured in AIA (60%; n=3), followed by MB (20%; n=1) and SCN (20%; n=1) (Fig. 17C). The lipid reducing crude extracts were mostly derived from strains affiliated to the genus Streptomyces (80%, all retrieved from C. crispus holdfast), but one extract was obtained from a Nocardiopsis strain, isolated from C. tomentosum tissues (Fig. 17D). Actinobacterial NP with relevant anti-obesity properties have been described to date, as well as their potential as candidates for drug development. A illustrative example is lipstatin, a lipase inhibitor isolated from the secondary metabolism of Streptomyces toxytricini [273], that aids in weight management and has served as the foundation for the development of the pharmaceutical drug Orlistat, widely utilized in the treatment of obesity [274]. Some marine algae primary metabolites, such as astaxanthin, fucoidan and alginates, are already used to address this problematic, with proved results in clinical human trials [275], however to date no secondary metabolite of a macroalgae-associated microbe has been described with antiobesity properties. In fact, to our knowledge, the present study is the first reported screening of macroalgae-associated Actinomycetota for lipid-reducing activity.

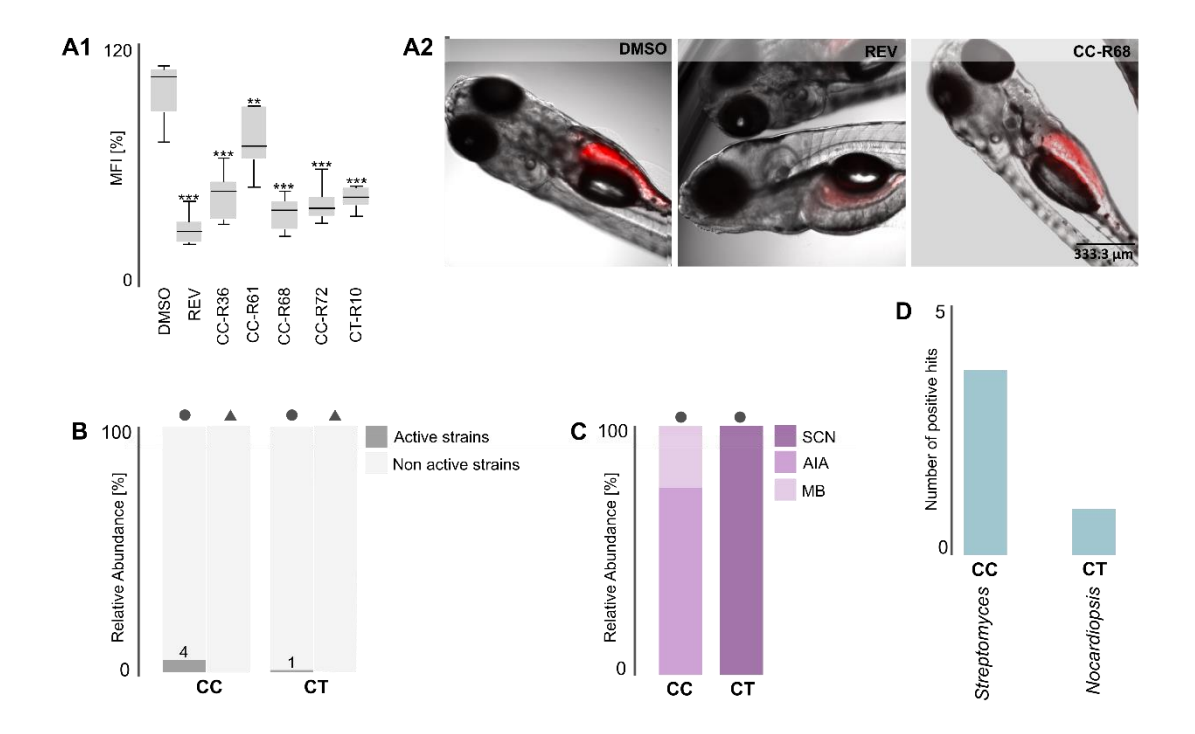


Figure 17. Anti-obesity screening of Actinomycetota isolated from *C. crispus* (CC) and *C. tomentosum* (CT). (A1) Strains with bioactivity in the Nile Red fat metabolism assay. Data displayed as mean fluorescence intensity (MFI) relative to DMSO (dimethylsulfoxide 0.1%, solvent control) from two independent experiments (n = 6). Statistical differences are shown as asterisks, ** p value < 0.01 and *** p value < 0.001. (A2) Representative images of zebrafish larvae (overlay of brightfield picture and red fluorescence channel), showing individuals exposed to DMSO, REV (positive control; 50 μM) and the crude extract of strain CC-F68. (B) Distribution of active and non-active strains retrieved from CC and CT. (C) Distribution of active strains according to their fermentation medium. (D) Genus-level taxonomic distribution of active strains. The source of isolation, holdfast (•) or blade (Δ), is indicated.

4.3.2. Dereplication, Metabolic and Taxonomic Profiling of Active Extracts

In total, 165 strains were considered active in at least one of the bioactivity screenings performed. These are distributed across 20 actinobacterial genera, headed by *Streptomyces* (56%; n=92) (Fig. 18). Driven by the pursuit of novel biologically active NP, the crude extract of each of the mentioned 165 strains was analyzed by LC-HRESIMS/MS to dereplicate for any known bioactive actinobacterial compound and pinpoint the presence of putative novel mass features. The dereplication analysis was performed using GNPS tools and unveiled the presence of several known bioactive NP in most of the crude extracts (Table S8 - Appendix III). Interestingly, the non-ribosomal cyclic peptides surugamides, described as anticancer and antifungal agents [276, 277], were the most frequently detected metabolites, being present in near 35% of all the bioactive crude extracts. Other compounds, including champacyclin, roseofungin,

strevertenes, valinomycin and antimycins, that have been described as displaying antimicrobial, antiviral, anticancer, insecticidal, piscicidal and immunosuppressive activities [278-282], were also commonly detected in our samples, alongside with several other NP (Table S8 - Appendix III). Based on this analysis, we found 22 extracts for which no hit was recorded in none of the three GNPS dereplication tools used, that resulted from strains affiliated to Brachybacterium, Cellulosimicrobium, Krasilnikoviella, Micromonospora, Mycolicibacterium, Nocardiopsis, Rhodococcus and Streptomyces genera. These extracts were obtained from strains isolated from both macroalgae: 55% (n=12) from C. tomentosum (CT) and 45% (n=10) from C. crispus (CC) tissues. Around 68% (n=15) were obtained from strains fermented in AIA medium. The bioactivity profiling of these 22 extracts proved to be fairly dissimilar: extracts CT-F28, CT-R88, CC-F65, CT-F19, CT-R149 and CT-R177 presented anticancer activity; extracts CC-F41, CC-R10, CC-R70, CC-R166, CT-F39, CT-F70 and CT-F93 proved to be effective against the growth of aquaculture-relevant pathogens; extracts CC-F76, CT-F65 and CT-R205 inhibited the growth of human-health relevant strains; extract CT-F62 displayed antifungal activity; extract CC-R72 demonstrated lipid-reducing activity in zebra-fish larvae; only four extracts, CC-F88, CC-R61, CC-R116 and CT-F61, were effective in more than one bioactivity screening, exhibiting a larger spectrum of biological activities (Fig. 18). Regarding the results on lipid-reducing activity, it is noteworthy to mention that known actinobacterial-sourced NP were detected in four of the five active crude extracts (Table S8 - Appendix III). However, to our knowledge, none of these metabolites are described for this bioactivity. Nevertheless, we have excluded these four extracts from the subsequent phase of our analysis in order to specifically focus on strains that exclusively produce unknown NP. LC-HRESIMS/MS data for the 22 extracts with no hits for known bioactive NP was used to construct a molecular network in GNPS (Fig. S5 -Appendix III), allowing the identification and dereplication of mass features of interest present in strain-specific clusters. A total of five clusters under this criterium were identified and analyzed, from strains affiliated to Streptomyces, Micromonospora, Krasilnikoviella and Cellulosimicrobium genera (Table 10). We inferred the likely m/z of the main compound from the corresponding LC-HRESIMS/MS data and used that accurate mass as query in a search against NP databases. None of the clusters presented a match with a known actinobacterial compound in either of the databases used (DNP and NPA). Therefore, these mass features might represent novel NP worthy of further investigation. In addition, it is highly feasible that many of the strains in which we detected the presence of known bioactive metabolites in the corresponding crude extracts, and therefore deprioritized in our workflow, might be able to synthetize new NP

as well. For instance, a single *Streptomyces* genome is described as being able to contain up to 70 BGCs [283], making it reasonable to assume that even with the detection of known compounds, many others can still be uncovered.

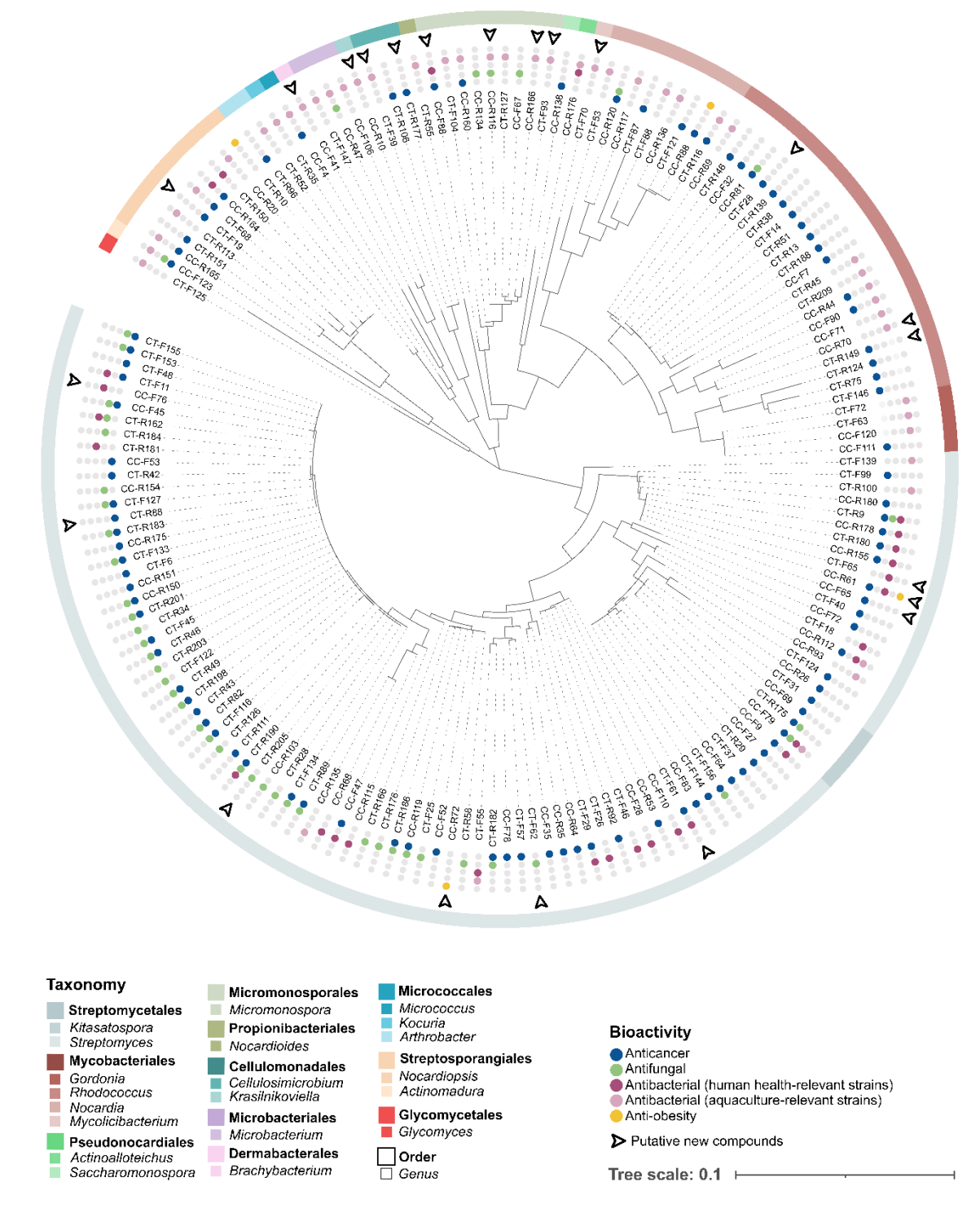


Figure 18. ML phylogenetic tree based on 16S rRNA gene sequences (1,311 nt), showing the evolutionary relationship between all 165 bioactive strains. The results of the bioactivity screenings are provided for every strain. Strains encoding putative new compounds are indicated as well.

Table 9. Single-strain clusters retrieved from the GNPS molecular networking built with MS/MS data from crude extracts without any hit in the GNPS dereplication tools. Manual dereplication for major peaks detected in each cluster (green-colored nodes) was performed using DNP and NPA databases. The value indicated in each node corresponds to the precursor ion.

Strain		Cluster	Base peak [M+H] ⁺	Retention Time (min)	Searched <i>m/z</i> in DNP and NPA (± 5 ppm)	Intensity (NL)
Streptomyces xiamenensis CC-F65	Α	(685.449) 713.4B	699.46497	10.35	698.45713	6.77E6
<i>Micromonospora</i> sp. CC-F88	В	(1316.09) (1316.09) (1316.09) (1288.00) (1286.07) (1202.09) (1202.09)	1290.06763	15.43	1289.05979	7.26E6
Krasilnikoviella muralis CC-R10	С	(780.553) (496.34)	782.56908	13.01	781.56124	6.11E7
Cellulosimicrobium funkei CT-R177	D	(404.055) (891.341) (386.044)	522.10718	3.70	521.09934	3.17E6
Streptomyces sp. CT-R205	E	293.098) (307.116) (294.101) (335.14) (247.095)	335.14447	3.45	334.13663	3.20E6

4.3.3. Actinobacterial Biosynthetic Potential Assessed Through Metagenomes

To gain insights into the biosynthetic potential and NP diversity of the actinobacterial community associated with C. crispus and C. tomentosum, we have recovered contigs and MAGs from shotgun metagenomic sequencing data from both macroalgae, identified the present BGCs, and conducted a network analysis. In total, from the actinobacterial microbiome associated to both C. crispus and C. tomentosum, 88 BGCs from contigs and 10 MAGs of medium/high-quality (encoding 45 BGCs) were identified and recovered. From all of these, only two BGCs were recovered from C. tomentosum, with the Actinomycetota community associated to C. crispus proving to be more abundant and biosynthetically richer. However, these findings do not align with the bioactivity results obtained with the collection of Actinomycetota derived from these two macroalgae, as no differences between the overall bioactive performance of the isolates retrieved from both macroalgae specimens, nor the diversity of secondary metabolites annotated by GNPS tools in their metabolomes were observed. Of the actinobacterial contigs obtained from the C. crispus sample, a total of 86 BGCs, distributed by seven classes and with a mean length of 8100 bps, were identified: NRPS (n=26), PKS types II and III (n=22), RiPPs (n=22), metabolites of other biosynthetic origins (n=8), PKS type I (n=5), Terpene (n=2) and PKS-NRPS Hybrids (n=1) (Table S9 - Appendix III). From the recovered BGCs, only one is predicted to be complete since it is not located at contig edge. Based on KnownClusterBlast analysis, only six of the recovered BGCs exhibit similarity to MIBiG database BGCs. This includes: three heterocyst glycolipid synthaselike PKS (hglE-KS), with similarity to BGCs encoding for eicosapentaenoic acid and heterocyst glycolipids; two RiPP BGCs, with similarity to the BGCs codifying for the potent antibacterial lanthipeptide microvionin [284] and to the lassopeptide cochonodin I [285]; one NRPS with similarity to the BGC that encodes for the production of a streptothricin-related antibiotic (BD-12) [286] (Table S9 - Appendix III). None of these compounds were detected in the dereplication data of the bioactive crude extracts, an expected outcome since their similarity with known molecules is low (7-33%) and there is no evidence that their production is linked to one of the cultivated strains. Nonetheless, it is important to notice that the culture conditions used in our study for bioactivity screening might not favour the expression of all genetically encoded BGCs. The taxonomic assignment of the contigs was further explored to understand the affiliation of the recovered BGCs. The Actinomycetota contigs from which BGCs were identified were distributed by two main classes, Acidimicrobiia (n=38) and Actinomycetes (n=37), while

11 remained unassigned at class level. These were distributed across 11 orders (Fig. 19A) and 25 genera, with Ilumatobacter (n=20) being the most prominent one (Fig. 19B). As previously reported [240], these taxa correspond to the most highly represented in the metagenomics data. While Actinomycetes are extensively studied and described as the major microbial source of NP, members of the class Acidimicrobiia do not share the same status, making the recovery of a similar number of BGCs from both taxa an interesting result. There is genetic indication that Acidimicrobiia harbor essential biosynthetic machinery to synthetize NP, as exemplified by acidirhodopsin, a novel rhodopsin clade related to freshwater actinorhodopsins, discovered by genome mining of an Acidimicrobiales strain [287]. Metagenomic studies have unveiled many uncultured species affiliated to Acidimicrobiia class in freshwater and marine samples, however these microbes are extremely recalcitrant to cultivation, with only a few described cultivable species [288]. In our work, we were unable to cultivate any strain affiliated to this group. From the 25 genera to which the BGCs were attributed, strains affiliated to only six of them – Arthrobacter, Brachybacterium, Kitasatospora, Nocardia, Rhodococcus and Streptomyces - were recovered in the cultivation experiments, being derived from C. crispus tissues. Interestingly, crude extracts from these strains, with the exception of Arthrobacter strains, displayed antimicrobial, anticancer and lipid-reducing activities. From C. tomentosum actinobacterial contigs it was only possible to retrieve two NRPS BGCs, assigned to the Streptomyces genus, which did not showed similarity with MIBiG database BGCs (Table S10 - Appendix III). From this point forward, we have focused our work on exploring the richer C. crispus sample.

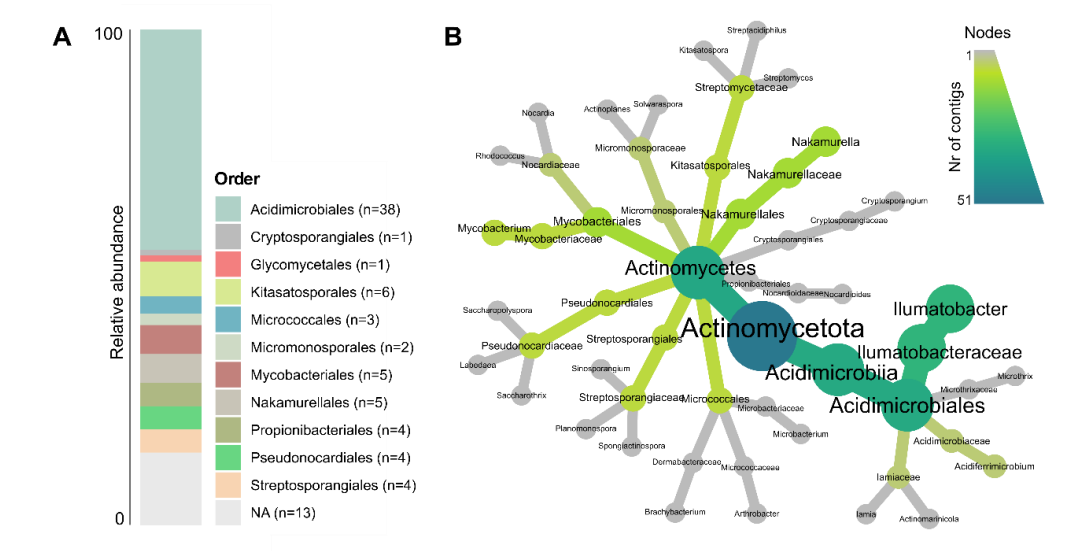


Figure 19. Taxonomic classification of actinobacterial contigs from which BGCs were identified through the antiSMASH analysis. (**A**) Taxonomic classification of actinobacterial contigs at order level. (**B**) Heat tree plot of taxonomic classification of contigs. Only contigs from which it was possible to obtain a taxonomic classification at genus level are depicted (n=51).

As an attempt to increase the number and the completeness of the recovered BGCs, MAGs were obtained from *C. crispus* sample. After refinement, a total of 10 Actinomycetota Bins were recovered: one corresponding to high-quality (>90% competition and <5% contamination) and nine with medium-quality (>50% completion and <10% contamination) MAGs. Nine of the ten MAGs were assigned to the Acidimicrobiales order, whilst one was assigned to the order Miltoncostaeales. The latter belongs to a phylogenetic lineage within the class Thermoleophilia and represents the high-quality MAG (with over 97% of completeness, Bin 8 in Fig. 20).

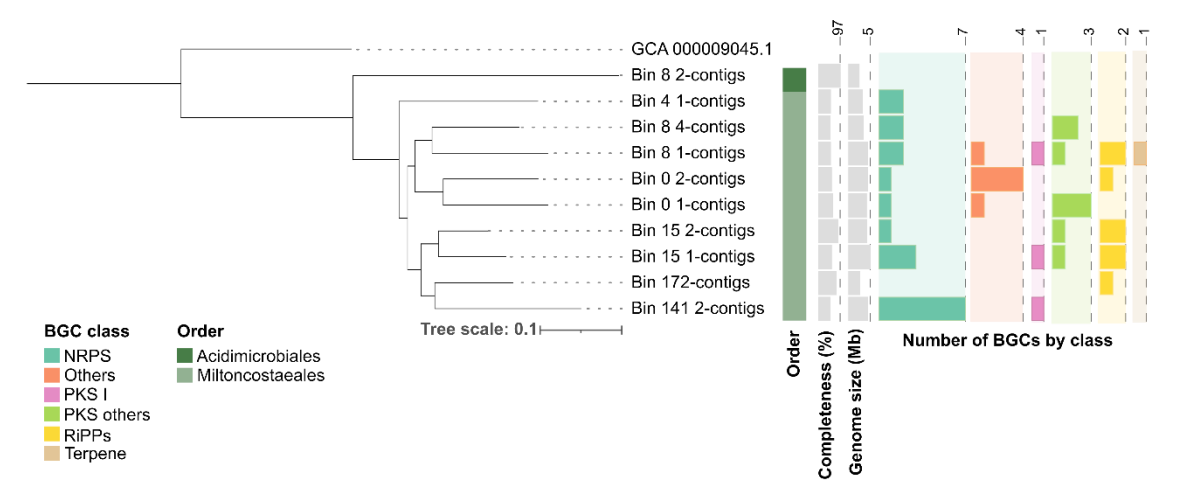


Figure 20. ML phylogenomic tree of the MAGs recovered in this study. Information of completeness (bar represented from 50.7 to 97%), total length (bar represented from 2.4 to 5.1 Mb) and the number of BGCs by class for each MAG is included. *Bacillus subtilis* (GCF_000009045.1) was used as outgroup.

To account for redundancy and fragmentation, BGCs retrieved from both macroalgae samples and assembling strategies (contigs and MAGs) were grouped into gene cluster families (GCFs), which compile BGCs predicted to encode similar natural products and better represent the recovered biosynthetic diversity. At a 0.7 cut-off threshold for similarity, using BiG-SCAPE, the 132 BGCs (88 from contigs and 45 from MAGs) were grouped into 91 GCFs (Fig. 21A), distributed by 6 biosynthetic classes (Fig. 21B). An Upset intersection plot was computed to understand the distribution of GCFs by sample and assembly strategy, which shows that 25 GCFs were singletons, 25 were shared across the distinct samples (and assembling strategies) and 8 were shared with MIBiG BGCs (Fig. 21C). This underlines that the majority of BGCs recovered from the contigs were also recovered from the MAGs, and that 83 of the 91 recovered GCFs share less than 30% of similarity to database BGCs. These results highlight the biosynthetic potential to codify for new NP from the targeted Actinomycetota, in line with the results from the bioprospecting of the macroalgae-derived strains where we identified several

crude extracts encoding putative novel bioactive molecules. While both approaches indicate a clear opportunity for biodiscovery, it is important to note that based solely on this study, we cannot determine which of the recovered BGCs are present in the genome of the cultivated strains. From the sequence similarity network (SSN) computed together with MIBiG BGCs, it is possible to distinguish several GCFs composed exclusively of BGCs recovered from this study. Overall, the followed metagenomics approach allowed for the identification of numerous BGCs from the Actinomycetota associated with the two macroalgae targeted in this study distantly related to database BGCs, likely to be involved in the production of novel NP. To our knowledge, this metagenomic-driven approach has never been employed before to investigate the bioactive potential of the actinobacterial community associated to any macroalgae.

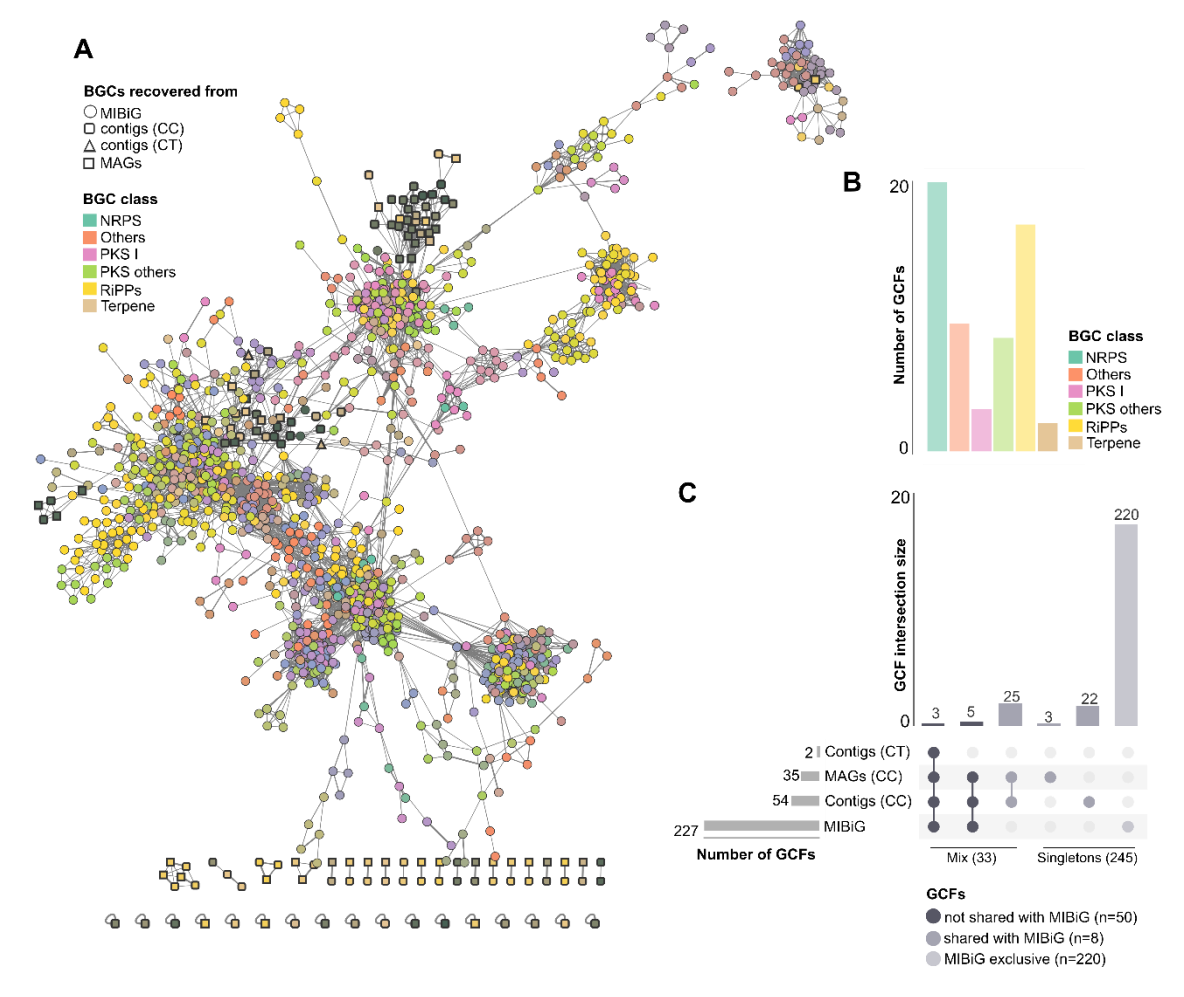


Figure 21. Actinobacterial GCFs associated with *C. crispus* (CC) and *C. tomentosum* (CT). (**A**) SSN of all BGC classes recovered from MIBiG. The different colours correspond to distinct GCFs identified by BiG-SCAPE. BGCs recovered from MAGs are represented by a rectangle, from contigs associated to CT sample by a triangle, from contigs associated to CC sample by a round rectangle, and MIBiG BGCs are represented by a circle. (**B**) Total number of GCFs by BGC class. (**C**) Upset intersection plot for the GCFs by sample type (contigs CT sample, contigs CC sample, MAGs) and the GCFs for MIBiG BGCs.

4.4. CONCLUSION

Macroalgae offer a favorable habitat for several epiphytic and endophytic microorganisms. Although Actinomycetota have been proven to be a valuable source of bioactive compounds, their presence and diversity in macroalgae and their biotechnological potential is largely unknown. In this work, we explored for the first time the bioactive properties of a collection of 380 macroalgae-associated Actinomycetota strains, retrieved from the Rhodophyta C. crispus and the Chlorophyta C. tomentosum, collected in the intertidal northern Portuguese coast. A total of 165 strains with bioactivity, spanning 20 actinobacterial genera, were identified, with Streptomyces exhibiting a notably high representation. These strains proved to be a prolific source of antibacterial, antifungal and anticancer metabolites, with a smaller fraction being capable of synthesizing lipid-reducing compounds, translating in a potential anti-obesity asset. To date there is no reference to secondary metabolites from macroalgae-associated bacteria exhibiting lipid-reducing characteristics, highlighting the novelty and relevance of our screening results. Dereplication of the active crude extracts led to the identification of 22 encoding putative novel NP, which deserve further exploration. In-depth analysis pinpointed mass features that found no match to known actinobacterial secondary metabolites, thus confirming their likely novelty. The biosynthetic potential encoded by the actinobacterial community living in association with the two macroalgae species targeted in this study was also explored using metagenomics, shedding light on the vast reservoir of biosynthetic potential yet to be uncovered. Several BGCs, recovered from both contigs and MAGs and grouped in 91 GCFs, disclosed to likely code for novel chemical diverse NP, distantly related of those annotated in databases. Our findings unveil macroalgae-associated Actinomycetota as an excellent source of both known and novel bioactive NP, underscoring the importance of continued bioprospecting of this particular ecological niche to harness its full spectrum of biotechnological applications. In-depth studies should be conducted to retrieve these novel metabolites and to better understand the underlying mechanisms involved in macroalgae-Actinomycetota symbiosis as both triggers and modulators for their production.

5

Decylprodigiosin: a new member of the prodigiosin family isolated from a seaweed-associated *Streptomyces*

The content of this chapter is published in the Q1 journal **Frontiers in Pharmacology**, in open access format:

<u>Girão, M.</u>, Freitas, S., Martins, T. P., Urbatzka, R., Carvalho, M. F., & Leão, P. N. (2024). Decylprodigiosin: a new member of the prodigiosin family isolated from a seaweed-associated *Streptomyces*. *Frontiers in Pharmacology*, *15*, 1347485.

DOI: 10.3389/fphar.2024.1347485

ABSTRACT

Bioprospecting actinobacterial secondary metabolism from untapped marine sources may lead to the discovery of biotechnologically-relevant compounds. While studying the diversity and bioactive potential of Actinomycetota associated with *Codium tomentosum*, a green macroalgae collected in the northern Portuguese coast, strain CT-F61, identified as *Streptomyces violaceoruber*, was isolated (Chapter 2). Its extracts displayed a strong anticancer activity on breast carcinoma T47D and colorectal carcinoma HCT116 cells, being effective as well against a panel of human and fish pathogenic bacteria (Chapter 4). In this chapter we describe the bioactivity-guided isolation and chemical characterization of decylprodigiosin (1), a new analogue of the red-pigmented family of the antibiotics prodigiosins. Despite this family of natural products being well-known for a long time, we report a new analogue and the first evidence for prodigiosins being produced by a seaweed-associated actinomycete.

Keywords: Actinomycete; Bioactivity; Decylprodigiosin; *Streptomyces*

5.1. INTRODUCTION

Nature is a wealthy reservoir of biotechnologically-relevant molecules, some of them even labelled as prodigious (i.e., something marvellous), as the family of the blood-red pigmented bacterial alkaloids, prodigiosins. This group of compounds harbours a diverse set of heterocyclic NP, with historical evidence dating back to the beginning of the 19th century [289]. Surveying the broad spectrum of properties that prodigiosin and prodigiosin-related molecules encode, from antimicrobial, antimalarial, anticancer, algicidal, antiparasitic to antiviral and immunosuppressive [290-295], it becomes clear why they have attracted the attention of NP research programs for so many years. Apart from their value in medical industry, they are also used in food, cosmetics and dye markets as an eco-friendlier and cost effective alternative to synthetic pigments [296]. Prodigiosins have been reported to be produced by a wide range of Gram-negative and positive bacteria. Examples include members of the Pseudomonadota phylum as Alteromonas rubra, Achromobacter denitrificans, Beneckea gazogenes, Hahella chejuensis, Janthinobacterium lividum, Rugamonas rubra, Zooshikela rubidus, [297-302], Pseudoalteromonas [303, 304], Serratia [305-309] and Vibrio [310, 311]. Members of the phylum Actinomycetota, considered the most prolific bacterial source of drug-lead chemicals [312], have also been reported to synthetize prodigiosins. From several species of Streptomyces (S. longisporuber, S. griseoviridis and S. coelicolor), Actinomadura (A. madurae and A. pelletieri), and from Streptoverticillium rubrireticuli, undecylprodigiosin, butylcycloheptylprodigiosine, metacycloprodigiosin, nonylprodigiosin, prodigiosin 25-C and prodigiosins R1, R2 and R3 were described, highlighting actinobacterial metabolism richness in the production of these tripyrrole red pigments [313-320]. The widespread occurrence of prodigiosins in phylogenetically distant microbes suggests that these molecules may play a significant, albeit uncertain and yet to be fully defined, physiological role. In recent years, marine-sourced Actinomycetota have proved their value as source of relevant chemistry [39]. Some known prodigiosins and related molecules, exhibiting a wide range of bioactive properties, have been found to be produced by Streptomyces species living in association with sponges [321, 322] and inhabiting deep-sea sediments [323]. Also from a marine Streptomyces, two novel spiroaminals, marineosins A and B, obtained from unknown modifications of prodigiosin-like pigment pathways and exhibiting significant anticancer activity, have been discovered [324]. Streptomyces can be found in many places in the marine ecosystem, including in association with seaweeds [79], but little is known regarding bioactive NP biosynthesis as part of such associations. As prodigiosins display algicidal properties, they are able to inhibit and control the growth of various

microalgae and cyanobacteria [294, 325-327], by disrupting cell membranes, interfering with photosynthesis, and/or inducting oxidative stress, having been considered good candidates for algal bloom management and aquatic ecosystem restoration. In this work, by exploring the secondary metabolism of the macroalgae-associated *Streptomyces violaceoruber* CT-F61 (Chapter 4), isolated from the tissues of *C. tomentosum* (Chapter 2), a new 10-carbon alkyl chain prodigiosin was discovered and chemically characterized. To our knowledge, the presence of bacteria producing prodigiosins living in association with macroalgae has hitherto not been described. We briefly discuss the potential ecological significance of this finding.

5.2. MATERIALS AND METHODS

5.2.1. Sampling and Bacterial Isolation

Strain CT-F61 was isolated from the tissues of the macroalgae *Codium tomentosum*, as described in Chapter 2 (section 2.2.2.).

5.2.2. Taxonomic and Phylogenetic Analysis of *Streptomyces violaceoruber* CT-F61

Strain CT-F61 was taxonomically identified through 16S rRNA gene sequencing, as described in Chapter 2 (section 2.2.3.). The taxonomic identification was established by comparison of its 16S rRNA gene consensus sequence with type strains deposited in the EzBioCloud database [210]. To infer the evolutionary relationship between CT-F61 and its closest related species, a phylogenetic tree was built. The 15 consensus sequences closest to CT-F61 (according to ExTaxon database) were selected and aligned, together with CT-F61 16S rRNA gene sequence and *B. subtilis* NCIB 3610^T as an outgroup, using the MUSCLE tool from the Geneious software package. An alignment of 1366 bp was used to construct the phylogenetic tree, applying the Maximum Likelihood method with 1000 bootstraps based on the Tamura-Nei model. Evolutionary analyses were conducted in MEGA X [144].

5.2.3. Bioactivity Screenings

Strain CT-F61 was cultured in AIA medium and its organic extract obtained, as described in Chapter 4 (section 4.2.2.). The crude extract was tested, following the protocols described in the same chapter, against a panel of human and fish pathogenic microbial strains and for cytotoxic activity in monolayer cell cultures of two cancer and one non-cancer cell lines – T47D cells, HCT116 and hCMEC/D3, respectively – using the MTT assay. The crude extract was tested in triplicate, in two independent experiments. Results are presented as percentage of cellular viability relative to the solvent control, after 48h of exposure. Data from cytotoxic assays (six technical replicates in total per sample) was tested for significant differences compared to the solvent control, and the significance level was set for all tests at p < 0.05. The normality distribution of data was accessed using the Kolmogorov Smirnov test. One-Way ANOVA was applied followed by Dunnett's post hoc test for parametric data, and Kruskal-Wallis test, followed by Dunn's multiple comparison test, used for non-parametric data. The apoptotic

Staurosporine (Sigma-Aldrich, MO, United States) was used as positive control, at the same concentration as the extracts, and 0.5% DMSO was used as solvent control.

5.2.4. Decylprodigiosin Isolation and Structure Elucidation

To obtain sufficient amounts of compounds for a bioactivity-guided isolation, strain CT-F61 was cultivated in a larger scale (24 L) using 5 L Erlenmeyer flasks, each containing 2 L of AIA culture medium. A pre-inoculum of 100 mL was prepared in the same culture medium, using a 250 mL Erlenmeyer flask, to inoculate the bigger flasks. After 7 days of incubation, 30 g of Amberlite XAD16N resin (Sigma-Aldrich, MO, United States) were added to each flask and incubation continued for 7 additional days. The biomass and resin were recovered by centrifugation (2500g, 5 min), lyophilized, and repeatedly extracted using a mixture of acetone/methanol 1:1 (v/v). After confirming the previously observed biological activities, by testing the obtained organic extract in the formerly described sets of assays, a reverse-phase vacuum liquid chromatography (VLC) of the organic extract was performed using a solvent polarity gradient (Table S1) on a glass chromatography column. All resulting fractions were tested for antimicrobial and cytotoxic activities and examined for the presence of unknown molecules using GNPS dereplication tools [249], based on LC-HRESIMS/MS analysis, as described in Chapter 4 (section 4.2.8.). The active VLC fractions with no hits for known compounds in the GNPS-based dereplication were selected and further subjected to a reverse-phase semipreparative high-performance liquid chromatography (HPLC) (flow 3 mL min⁻¹, column ACE 10 C18-AR, 250x10mm; Table S12 - Appendix IV). All resulting fractions (Fig. S6 -Appendix IV) were tested for bioactivity. Manual dereplication of mass features present in the most active fractions against the DNP and NP atlas databases unveiled the presence of an undescribed mass feature m/z 380.2699 [M+H]⁺. Fractions containing this mass were pooled and an additional purification step targeting this putative new compound was performed in a reverse-phase analytical HPLC (flow 0.8 mL min-1, column ACE Excel 3 Super C18 V19-3214 75x4.6 mm; Table S13 - Appendix IV). The chemical structure of this compound was elucidated by comparing its MS/MS data with those of commercial undecylprodigiosin [328] standard (Abcam, Netherlands). LC-HRESIMS/MS analysis of both molecules was performed by direct injection of each (1.0 mg mL⁻¹, flow 0.005 mL min⁻¹) into the spectrometer, with a 35 000 fwhm resolution, using an isolation window of 1 m/z, loop count of 3, AGC target of 5 x 10⁴, and a collision energy of 35 (arbitrary units). The parent mass of each molecule was selected for fragmentation and the resulting MS/MS spectra fragmentation patterns compared.

Additionally, 1 H (600 MHz) nuclear magnetic resonance (NMR) spectroscopy was used to a more comprehensive understanding of the novel compound molecular structure. The NMR data were acquired in methanol- d_4 (CD₃OD) (Fig. S7- Appendix IV).

5.2.5. Streptomyces violaceoruber CT-F61 Genome Sequencing

The previously obtained gDNA of strain CT-F61 was sequenced using Illumina 2x250bp paired-end technology and analysed as described in Chapter 3 (section 3.2.3.). The genome sequence was annotated using the NCBI Prokaryotic Genome Annotation Pipeline and deposited at GenBank under the accession number JAZKXI000000000. AntiSMASH was used for the automated analysis and identification of secondary metabolite BGCs using relaxed detection settings and all extra features selected.

5.3. RESULTS AND DISCUSSION

5.3.1. Streptomyces violaceoruber CT-F61 Isolation and Taxonomic Identification

Our continued efforts in exploring seaweed-associated actinobacterial diversity led to the isolation of Streptomyces violaceoruber CT-F61 from the Chlorophyta C. tomentosum. From the macroalgae frond tissues, using the selective culture medium AIA, formulated with 40% of seawater, a regular, opaque, white spore forming colony, able to change the culture medium colour from yellowish to dark blue, was isolated from the frond tissues of C. tomentosum, purified, and named as strain CT-F61. According to the EzBioCloud 16S database, strain CT-F61 showed the highest 16S rRNA gene sequence similarity to S. violaceoruber NBRC 12826^T, S. anthocyanicus NBRC 14892^T and S. tricolor NBRC 15461^T (all 99.85%), three species that have been recently classified as heterotypic synonyms of S. violaceoruber based on multilocus sequence analysis [168]. Phylogenetic assessment showed that strain CT-F61 clustered with the three type strains mentioned above (Fig. 22). Although 16S rRNA gene is traditionally used in bacterial systematics, its resolution might not be sufficient for species identification, especially for genera integrating a large number of species, like the Streptomyces genus. Genome sequencing of strain CT-F61 showed a closest association to S. anthocyanicus JCM 5058, with 99.36% average nucleotide identity (ANI) between the two strains, based on Genome Taxonomy Database (GTDB) taxonomy assignment. Considering all the mentioned aspects, strain CT-F61 was identified as Streptomyces violaceoruber CT-F61.

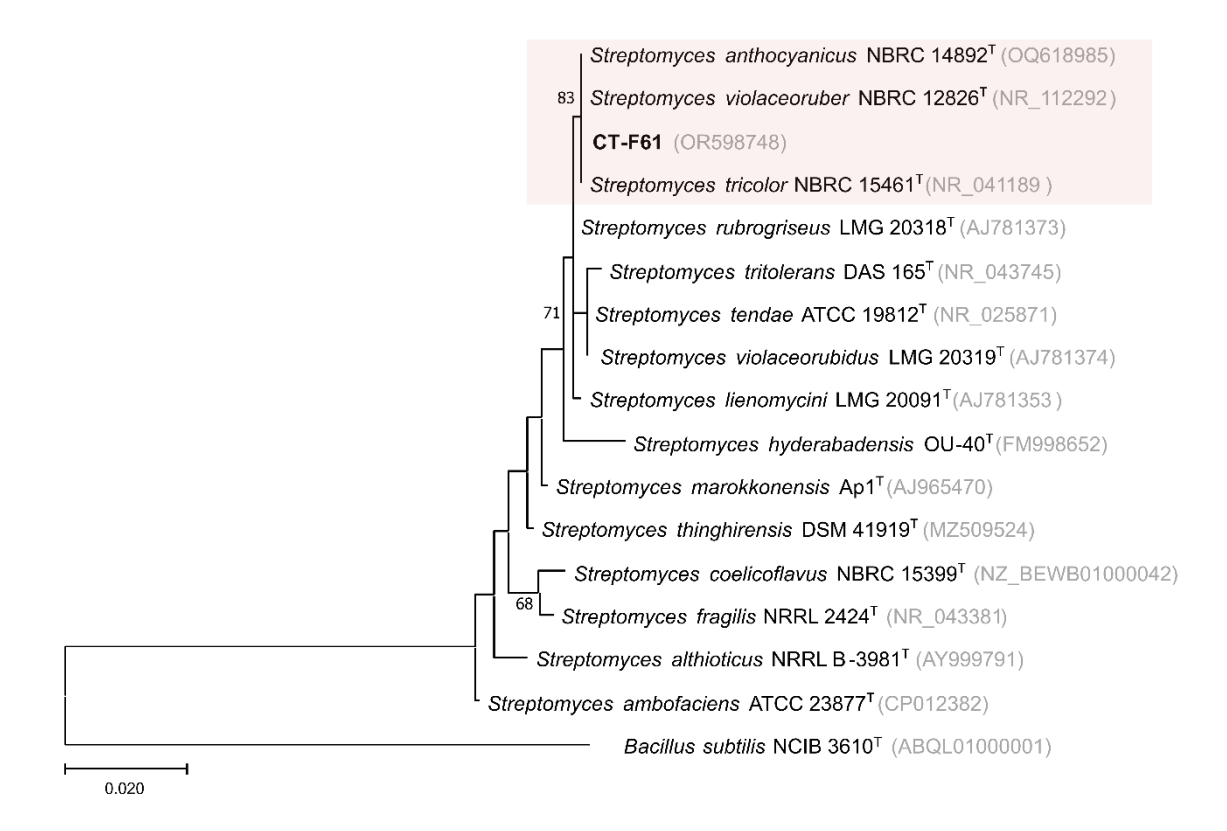


Figure 22. ML phylogenetic tree, based on 16S rRNA gene sequences (1366 nt), showing the relationship between strain CT-F61 and closest related type species. Accession numbers are indicated in brackets. Values at the nodes indicate bootstrap values higher than 50%, obtained from 1000 resampling events. *Bacillus subtilis* NCIB 3610T was used as outgroup.

5.3.2. Bioactivity Screening

In order to assess the bioactive properties of *S. violaceoruber* CT-F61, we cultivated this strain in a small scale (SS; 30 mL) with 0.5 g of resin, and tested an organic (acetone/MeOH, 1:1 - both cells and resin material were extracted together) extract from this culture, dissolved in DMSO, against a panel of pathogenic microbial strains and on different human cancer cell lines, using a test concentration of 15 µg mL-1. The extract from this seaweed-associated actinomycete inhibited the growth of the Gram-positive bacteria *B. subtilis* ATCC 6633 and *S. aureus* ATCC 29213 (Fig. 2A). Exploring new sources of pharmaceutically-relevant compounds is crucial to address major global crisis as antibiotic resistance, responsible for over 700,000 human deaths annually [329], or the pressing and lacking-solution cancer pathologies [330]. Additionally, CT-F61 proved to inhibit the growth of the Gram-negative fish pathogens *T. maritimum* ATCC 43397, *L. anguillarum* ATCC 19264 and *A. hydrophila* ATCC 43397. *T. maritimum* is a bacterial pathogen responsible for tenacibaculosis, an ulcerative disease causing significant mortalities in various marine fish species worldwide, with high economic impact in

aquaculture industry [331]. Similar losses occur due to *L. anguillarum*, agent of vibriosis [332], and *A. hydrophila* that distresses fishes with gastroenteritis and septicemia [333]. Molecules encoded in CT-F61 crude were thus found to have potential to address these diseases, a less-explored biotechnological application of prodigiosins. No inhibitory activity was recorded against the growth of the human pathogens *E.coli* and *S. enterica* and *C. albicans*, and the aquaculture-relevant species *E. tarda*, *P. anguilliseptica* and *Y. ruckeri*. In the cancer cell line assays, the extract reduced the viability of breast carcinoma T47D and colorectal carcinoma HCT116 cell lines by more than 80%, with no deleterious effect on non-cancer cells (Fig. 23A).

5.3.3. Bioactivity-guided Isolation and Structure Elucidation of Decylprodigiosin

Dereplication of the CT-F61 organic extract using GNPS Dereplicator, Dereplicator VarQuest, and Dereplicator+ tools did not lead to the identification of known compounds that could explain the observed biological activity. Thus, we performed large-scale cultivation (LS; 24 L) of the strain, in order to isolate any putative novel bioactive compound from its metabolome. An organic crude extract of 5.7 g, with a similar bioactive profile as the one previously recorded for the SS culture, was obtained (Fig. 23A). A set of sequential chromatographic steps was then used to purify the bioactive compounds of interest. All generated fractions were subjected to high-resolution mass spectrometry (HRMS) dereplication to avoid the isolation of known molecules. The VLC (C18 stationary phase) of the LS crude extract led to 13 fractions (A-M) of decreasing polarity. All fractions were tested for antimicrobial and cytotoxic activities (Fig. 23B). Several fractions proved to be effective in inhibiting the growth of the reference bacterial strains, with fraction K being active against all, except T. maritimum. Fractions K and L presented activity on both cancer cell lines tested (p < 0.001), with no effect on the viability of the non-cancer cell line. From all the results recorded, in this work we decided to follow the strong anticancer activity of fractions K and L towards the human cancer cell lines T47D and HCT116. Fractions K and L were pooled (25.1 mg) and fractionated by C18 semipreparative HPLC. Sixteen fractions were obtained and tested for cytotoxic activity in HCT116 cell line at 15 µg mL⁻¹ and 1.5 µg mL⁻¹ (Fig. 23C). Fractions KL_5 to KL_16 showed strong cytotoxicity when tested at 15 µg mL⁻¹, but at 1.5 µg mL⁻¹ only fractions KL 9 and KL 10 retained strong cytotoxic activity. Despite the initial dereplication step, fractions KL_9 and KL_10 were dereplicated using GNPS tools to investigate if the recorded cytotoxic activity was due to any putative novel compound. From this analysis, two mass features associated to undecylprodigiosin and butylcyclohexylprodigiosin,

known members of the prodigiosins family, were detected. Yet, a more detailed manual search using the DNP and NP atlas databases revealed that the protonated ion [M+H]+ at m/z 380.2699, detected in the same fractions, was not associated to any described prodigiosin, suggesting that this was a new compound (Fig. 24). Is noteworthy to mention that no prodigiosin or related compound was initially detected by GNPS dereplicator tools in the crude extract or VLC fractions, as these were possibly masked by the complex matrix. The presence of undecylprodigiosin and butylcyclohexylprodigiosin could explain the recorded bioactivity, as their anticancer and antibacterial properties are wellrecognized. Nonetheless, we decided to focus on the potentially-new prodigiosin analogue. To our knowledge, prodigiosins or related compounds have not been reported so far from strains affiliated to the species S. violaceoruber, S. anthocyanicus or S. tricolor (heterotypic synonyms of S. violaceoruber). Fractions KL 9 and KL 10 were combined (6.8 mg) and processed in a C18 analytical HPLC to further purify the new molecule. Based on the NMR data it was clear that the compound contained typical prodigiosin signals, (δ_H 7.5-6.20, associated to the pyrrole rings, as well as a large methylene envelope δ_H 1.29-1.25), but was not pure. Due to the low amount of compound isolated we decided to approach its structure elucidation using MS/MS. A standard of undecylprodigiosin was acquired and a MS/MS fragmentation comparative study was performed (Fig. 25A). Using this approach, we could conclude that 1 m/z 380.2699 [M+H]⁺ differs from undecylprodigiosin on the carbon alkyl chain with a loss of a methylene group (-14 atomic mass units), conserving the aromatic moieties (m/z 238.0971). Based on this 10-carbon alkyl chain feature and the absence of ¹H NMR signals pointing towards a terminal isopropyl moiety, this chain is proposed to be linear and the compound was designated as decylprodigiosin (1, Fig. 25B). Reported isopropylcontaining alkyl chains in prodigiosins are odd-numbered [251]. Additional studies must be performed to characterize the bioactive properties of this novel molecule. To confirm that strain CT-F61 contains the genetic information necessary to produce prodigiosins, we sequenced its genome. The genome data was assembled into one contig with a length of 8 599 857 bp, with in silico G+C content of 72.2 mol%. DFAST results of completeness and contamination were 99.92 and 0.08%, respectively. As predicted, using AntiSMASH we identified a genomic region in the genome of strain CT-F61 in which the entire set of genes associated with the production of undecylprodigiosin (biosynthetic gene cluster from Streptomyces coelicolor A3(2) - MIBiG accession: BGC0001063) could be found. The even-numbered chain in 1 could be derived from an odd-numbered starter unit extended by the polyketide synthase machinery involved in the biosynthesis of actinobacterial prodigiosins [334]. The LC-HRESIMS/MS data of the

fraction containing 1 is available in MassIVE (MSV000093436). HRESIMS/MS spectrum for 1 has been added to the GNPS Library under accession CCMSLIB00012176068.

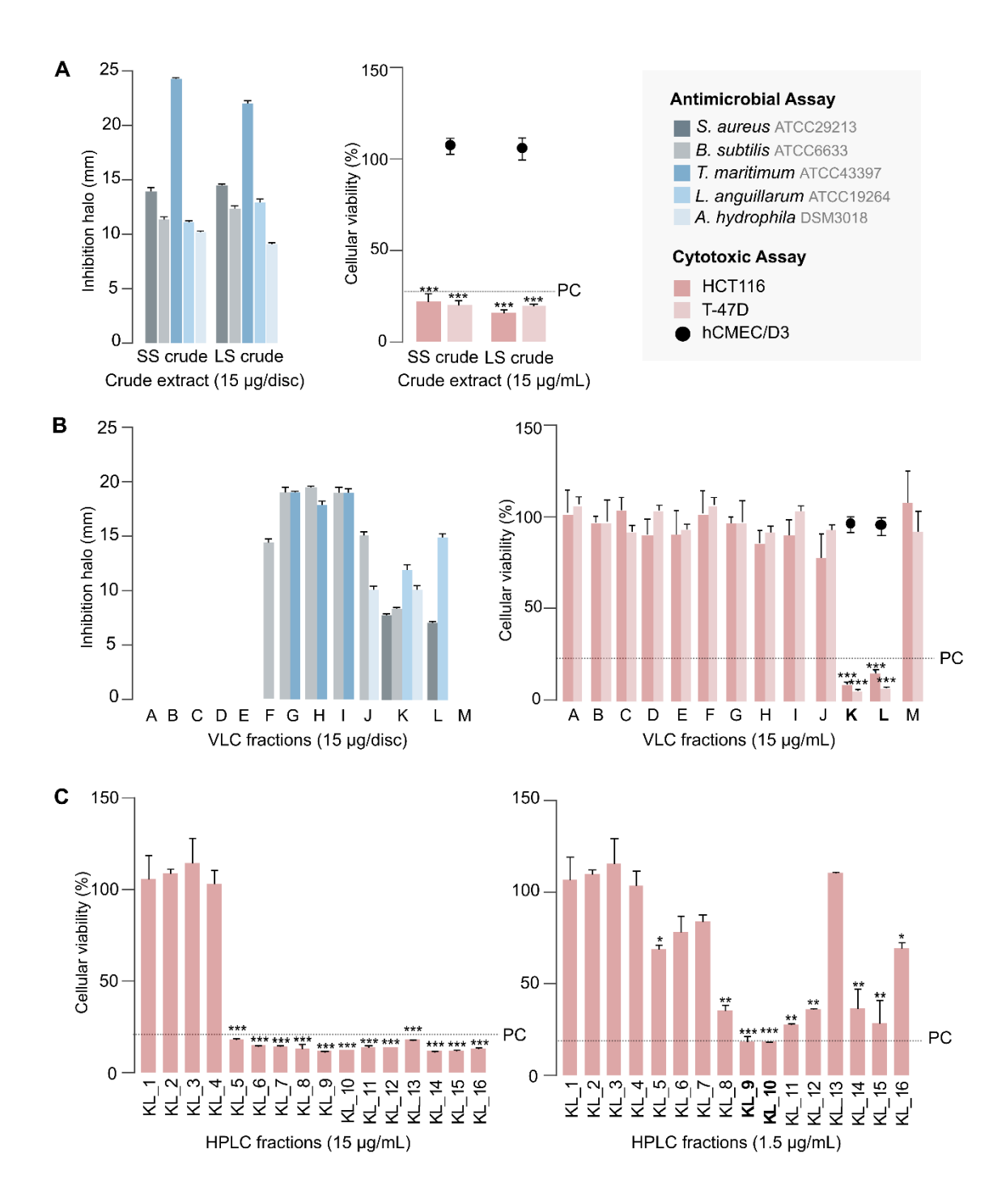


Figure 23. Antimicrobial and cytotoxic activities of CT-F61 crude extract, obtained from the small-scale (SS) and large-scale (LS) cultivation (**A**), C18 VLC fractions of CT-F61 LS crude extract (**B**) and CT-F61 KL C18 HPLC fractions tested at 15 μg mL⁻¹ and 1.5 μg mL⁻¹ in HCT116 cell line (**C**). Antimicrobial results presented as mean of the diameter of the inhibition halos measured from two independent experiments. Only reference strains affected by at least one tested sample are presented. Cytotoxic results presented as percentage of cellular viability after 48h of exposure, measured as mean from two independent MTT experiments,

performed with triplicates to each sample. Significant differences compared to the solvent control (*p < 0.05; **p < 0.01; ***p < 0.001). The percentage of cellular viability for the positive control (PC: Staurporine 15 μ g mL⁻¹) is indicated, as well as the samples activity on the non-carcinogenic cell line hCMEC/D3.

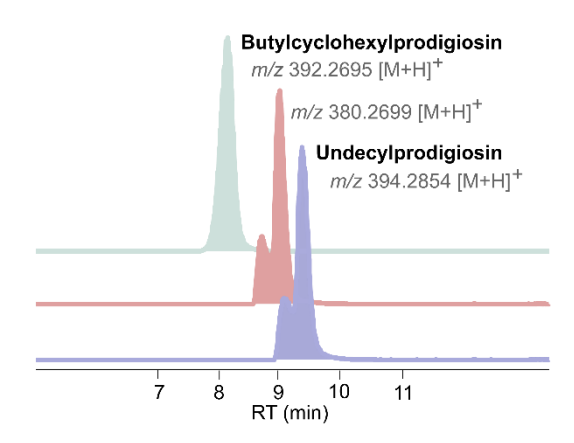


Figure 24. EICs of Undecylprodigiosin and Butylcyclohexylprodigiosin, detected in KL_9 and KL_10 fractions, alongside with the mass feature corresponding to **1**.

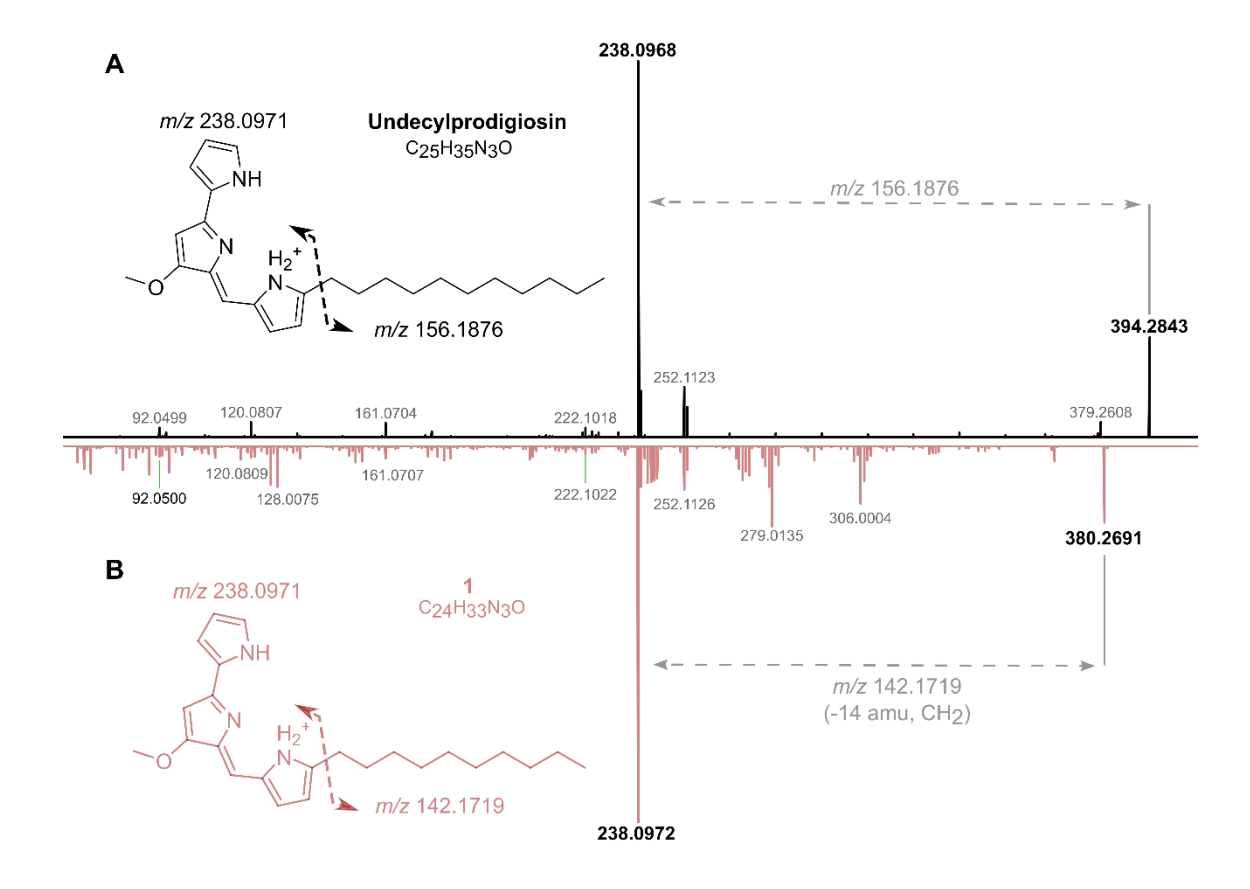


Figure 25. Structure elucidation of **1** by comparison of HRESIMS/MS spectra of undecylprodigiosin (in black) and **1** (in pink) (**A**). Proposed chemical structure of **1** and molecular formula (**B**).

5.3.4. Prodigiosins as Product of Seaweed-associated Actinobacterial Metabolism

The intricate web of symbiotic relationships in nature can shape entire ecosystems. In aquatic environments, symbiosis plays a key role in entire bionetworks, as, for example, in the coral-algae mutualism supporting a quarter of marine life [335]. Seaweeds offer a suitable substratum for bacterial life and provide organic nutrients for multiplication and establishment of biofilms. In return, the host benefits from chemicals synthetized by the bacterial communities that can act as growth-promoting substances, quorum sensing signaling molecules or bioactive compounds responsible for their normal morphogenesis, growth and survival [46, 336]. One distinctive trait of the redpigmented family of the antibiotics prodigiosins is their algicidal activity [294, 325-327]. In this work we show for the first time that a symbiotic Streptomyces strain, isolated from the tissues of a green macroalgae, is able to produce a wide range of bioactive prodigiosins. Prodigiosin and its family derivatives have been widely studied due to their biotechnological applications. In particular, this NP family is efficient across several cancer types with low effects against non-malignant tissues, also offering interesting possibilities for combinatorial applications once they can act synergistically and/or additively with other drugs [293, 337, 338]. Different prodigiosin analogues, with minor modifications on their structures, have shown different modes of action and degrees of cytotoxicity [319]. Therefore, the discovery of a new prodigiosin molecule can provide additional insights into the structure-activity relationships within this natural products family. Even without certainty about the ecological role that these compounds play in this marine niche, we hypothesize that prodigiosins may be involved in protecting the host from algal overgrowth. In this symbiotic relationship, the seaweed provides a hospitable environment for Streptomyces to thrive, while the bacterial partner reciprocates by potentially deploying its potent prodigiosins arsenal. Such a natural defense mechanism could prevent excessive algal colonization that otherwise would compete with the seaweed host for vital resources such as sunlight and nutrients. However, more studies should be conducted to test this possibility.

5.4. CONCLUSION

In this work we have explored the bioactive secondary metabolism of the seaweed-associated *Streptomyces violaceoruber* CT-F61, isolated from the tissues of *C. tomentosum*, a green macroalgae from the northern Portuguese shore. We describe the antimicrobial and anticancer properties of the metabolome of this strain, valuable for both human and animal health. We describe the discovery of 1, a new 10-carbon alkyl chain member of the prodigiosin family. To our knowledge, no prodigiosin or prodigiosin-like molecule has been described before from an actinomycete living is symbiosis with a seaweed, proving the value of this ecological niche as a source of novel NP with biotechnological applications. Additional studies should be performed to allow a better understanding of the bioactivity and ecological role of 1.

6

Cellulamides: a new family of marine-sourced linear peptides from the unexplored *Cellulosimicrobium* genus

The content of this chapter is submitted for publication in the Q1 journal Marine Drugs:

<u>Girão, M.</u>, Murillo-Alba J., Martín J., Pérez-Victoria I., Urbatzka R., Leite, R. B., Leão, P. N., Carvalho, M. F., & Reyes F. (2024) Cellulamides: a new family of marine-sourced linear peptides from the unexplored *Cellulosimicrobium* genus.

ABSTRACT

Bioprospecting the secondary metabolism of underexplored Actinomycetota taxa is a prolific route to uncover novel chemistry. In this Chapter we report the isolation, structure elucidation and bioactivity screening of cellulamides A and B (2 and 3), two novel linear peptides obtained from the culture of the macroalga-associated Cellulosimicrobium funkei CT-R177. The host of this microorganism, the Chlorophyta Codium tomentosum, was collected in the northern Portuguese coast and, in the scope of a bioprospecting study focused on its associated actinobacterial community, strain CT-R177 was isolated, taxonomically identified and screened for the production of antimicrobial and anticancer compounds (Chapters 2 and 4). Dereplication of a crude extract of this strain using LC-HRESIMS/MS analysis unveiled a putative novel natural product, cellulamide A (2), that was isolated following mass spectrometry-guided fractionation. An additional analog, cellulamide B (3) was obtained during the chromatographic process and chemically characterized. The chemical structures of the novel linear peptides, including their absolute configurations, were elucidated using a combination of HRMS, 1D/2D NMR spectroscopy, and Marfey's analysis. Cellulamide A (2) was subjected to a set of bioactivity screenings, but not significant biological activity was observed. The cellulamides represent the first family of natural products reported from the Actinomycetota genus Cellulosimicrobium, showcasing not only the potential of lessexplored taxa but also of host-associated marine strains for novel chemistry discovery.

Keywords: Actinomycetota; *Cellulosimicrobium*; cellulamide; linear peptides; natural products; macroalgae-associated.

6.1. INTRODUCTION

The phylum Actinomycetota, formerly known as Actinobacteria [21], is recognized as the major microbial source of bioactive NP, with the genus *Streptomyces* contributing by itself with nearly 50% of all clinically used antibiotics [156]. However, the discovery of novel actinobacterial secondary metabolites, which have been studied for decades for their useful bioactive properties, has slowed down in part due to the frequent rediscovery of known compounds. This trend however is not consistent with genomic data which estimates that only 3% of the NP potentially encoded in bacterial genomes have been experimentally characterized [35] and highlighting the vast opportunities that still lie ahead for discovery. Examples of profitable strategies to reach chemical novelty rely on mining Actinomycetota from unique habitats, such as the marine environment [36], the development of innovative detection and screening techniques [339] and the bioprospecting of rare (non-*Streptomyces*) taxa [340].

The *Cellulosimicrobium* genus, proposed by Schumann *et al.* [341], belongs to the Micrococcales order and Promicromonosporaceae family, within the phylum Actinomycetota [342]. Currently, only six recognized species with validly published names are affiliated with this genus, described from very dissimilar sources such as soil [341, 343], marine sediments [344], organic-waste compost [345], larvae gut [346] and human blood [347]. Research on *Cellulosimicrobium* was primarily focused on its enzymatic activities, particularly those involved in cellulose and other complex polysaccharides degradation [348-350], and its potential applications in industries such as biofuel production [351] and waste management [352]. Some studies have also investigated their pathogenicity to humans [353-355], highlighting the importance of understanding both their beneficial and potentially harmful roles in various environments. Unlike other actinobacterial taxa, such as *Streptomyces*, the production of NP by this genus has been scarcely explored, representing therefore an untapped reservoir of novel chemistry with potential biotechnological applications.

Marine Actinomycetota have gathered attention due to their ability to synthesize molecules with unique chemical scaffolds, shaped by the exclusive natural pressures of their surroundings [39]. While some exist as free-living entities, others establish symbiotic relationships with several organisms, such as macroalgae; these associations prompt the synthesis of NP with tailored bioactive properties [157]. *Cellulosimicrobium* strains have been retrieved from the marine environment, including as epiphytes of macroalgae [356], and recent studies have shown their antifungal and antioxidant properties [357, 358]. However, to our knowledge, no NP to date has been described from the secondary metabolism of a *Cellulosimicrobium* strain.

During a bioprospecting study focused on exploring the actinobacterial community associated with the green macroalgae *C. tomentosum*, collected in the rocky intertidal northern Portuguese coast, the strain *Cellulosimicrobium funkei* CT-R177 was isolated, taxonomically identified and screened for the production of antimicrobial and anticancer compounds. The analytical LC-HRESIMS/MS profile of the crude extract of this strain revealed the presence of a potentially new secondary metabolite, which prompted a more detailed investigation. Extraction of the culture followed by mass spectrometry-guided fractionation led to the isolation of cellulamides A and B (1 and 2). The structures of the novel linear peptides were elucidated using a combination of 1D/2D NMR spectroscopy and HRMS. Marfey's analysis established the absolute configuration of all the amino acid residues in the cellulamides. Their bioactive properties, biosynthesis and ecological role remain elusive, requiring further studies. This work is the first report of NP from the rare Actinomycetota genus *Cellulosimicrobium*.

6.2. MATERIALS AND METHODS

6.2.1. Sampling and Bacterial Isolation

Strain CT-R177 was isolated from the tissues of the macroalgae *Codium tomentosum*, as described in Chapter 2 (section 2.2.2.).

6.2.2. Taxonomic and Phylogenetic Analysis of *Cellulosimicrobium funkei* CT-R177

Strain CT-R177 was taxonomically identified through 16S rRNA gene sequencing, as described in Chapter 2 (section 2.2.3.). To infer the evolutionary relationship between strain CT-R177 and their closest relatives, a phylogenetic tree using the maximum likelihood method, based on the Tamura-Nei model, was constructed using the 16S rRNA gene sequences of the described type strains closest to strain CT-R177. Multiple sequences alignment was carried out using MUSCLE from within the Geneious software package, and 1,000 bootstraps applied. MEGA-X was used to build the trees. *Bacillus subtilis* NCIB 3610^T was used as outgroup.

6.2.3. Fermentation and Organic Extraction of *Cellulosimicrobium funkei* CT-R177

A cryopreserved (– 80 °C) stock of strain CT-R177 was inoculated in Marine Agar (MA; Sigma-Aldrich, MO, USA) and incubated for 7 days at 28 °C. After confirming the culture purity, one colony of CT-R177 was inoculated in a 100 mL Erlenmeyer flask containing 30 mL of Marine Broth (MB; Sigma-Aldrich, MO, USA). MA and MB were used, instead of the isolation medium (AIA), since they allowed better biomass yield. The flask was incubated in an orbital shaker at 28°C, 100 rpm, in the dark. After 4 days of incubation, 0.5 g of sterilized Amberlite XAD16N resin (Sigma-Aldrich, MO, USA) were added to the flask and incubation continued for three additional days. After this period, both biomass and resin were harvested by centrifugation (2500 g, 5 min), washed twice with deionized water and freeze-dried. A 30 mL 1:1 mixture of C₃H₆O/CH₃OH was added to the lyophilizate of each culture and kept under agitation at 200 rpm for 30 minutes at room temperature. The organic layer was recovered and dried in a rotary evaporator and the extraction procedure repeated one more time. Once the presence of a potential new compound in the crude extract resultant from this culture was confirmed, growth of strain

CT-R177 was scaled-up by repeating this procedure until the obtention of 1.5 L of culture. A final yield of 4.47 g of crude extract from the 1.5 L culture was obtained.

6.2.4. Bioactivity Screening and Dereplication of CT-R177 Crude Extract

The crude extract of CT-R177 culture was tested for antimicrobial and anticancer activity as described in Chapter 4 (sections 4.2.3. and 4.2.4.). The crude extract was tested at 1 mg mL⁻¹ against a panel of Gram-positive and -negative reference bacteria and a yeast, using the disc diffusion assay, and its cytotoxicity assessed at 15 µg mL⁻¹ in monolayer cell cultures of two human cancer lines and one non-cancer cell line – T47D, HCT116 and hCMEC/D3, respectively – using the MTT assay. The crude extract was examined for the presence of known bioactive molecules of actinobacterial origin that could explain the recorded results using GNPS dereplication tools, as described in Chapter 4 (section 4.2.8.). A potentially novel molecule with a protonated adduct [M+H]⁺ at *m/z* 803.3929 (1) was detected using this approach.

6.2.5. Mass Spectrometry Guided Isolation and Structure Elucidation of Cellulamides

A LC/MS guided isolation protocol was performed to isolate the detected molecule with a protonated ion $[M+H]^+$ at m/z 803.3929 (2). The crude extract of strain CT-R177 obtained from the 1.5 L culture was fractionated in a reversed-phase C18 flash chromatography using a 50 min gradient of 5 – 50% H₂O/CH₃CN, followed by 10 min at 100% CH₃CN (CombiFlash NextGen 100, Teledyne Technologies, USA). The column was assembled with 45 g of C18 silica, the flow established at 10 mL/min and UV detection at 210 and 280 nm. From this separation, 40 fractions were generated and analyzed by LC-HRMS to follow the target mass. Fractions containing 2 (17 and 18, 22.6 and 15.5 mg, respectively) were individually subjected to reversed-phase HPLC using a 35 min gradient of 5 - 35% H₂O/CH₃CN. The separation was performed using a X-Bridge[™], XB-C18 5 µm OBD 19×250 mm column (Waters Corporation, Milford, MA, USA), the flow established at 10 mL/min and UV detection at 210 and 280 nm. The same chromatographic method was applied to both fractions, generating 80 new fractions from each that were all analyzed by LC-HRMS. Fractions 17_42 and 17_43 were pooled together yielding 3.6 mg of 2. From fractions 18_42 and 18_43 an additional amount of 2 (3.1 mg) was obtained using the same HPLC conditions. Other fractions containing 2 (17_41, 17_44, 18_41 and 18_44) were pooled together (2.1 mg) and purified by reversed-phase semi-preparative HPLC using a 35 min gradient of 10 - 30%

 H_2O/CH_3CN . The separation was performed using a X-BridgeTM Prep Phenyl 10×150 mm column from Waters, using a flow of 3 mL/min and UV detection at 210 and 280 nm. An additional amount of **2** (1.1 mg) was obtained in this process. Fraction 18_46 contained compound **3** (1.6 mg).

Cellulamide A (**2**): white amorphous solid; $[\alpha]_D^{25}$ – 35.3 (*c* 0.1, MeOH); UV (DAD) λ_{max} no absorption; for ¹H and ¹³C NMR data see Table 10; (+)-ESI-qTOF MS m/z 803.3951 [M+H]⁺ (calcd for $C_{37}H_{55}N_8O_{12}$ ⁺, 803.3934, D 2.1 ppm); 825.3745 [M+Na]⁺ (calcd for $C_{37}H_{54}N_8O_{12}Na$ ⁺, 825.3753, D -1.0 ppm)

Cellulamide B (3): white amorphous solid; $[\alpha]_D^{25}$ – 75.5 (*c* 0.1, MeOH); UV (DAD) λ_{max} no absorption; for ¹H and ¹³C NMR data see Table 10; (+)-ESI-qTOF MS m/z 787.4014 [M+H]⁺ (calcd for $C_{37}H_{55}N_8O_{11}$ ⁺, 787.3985, D 3.7 ppm); 809.3803 [M+Na]⁺ (calcd for $C_{37}H_{54}N_8O_{12}Na$ ⁺, 809.3804, D -0.1 ppm)

6.2.6. Marfey's Analysis of Cellulamide A

A sample of cellulamide A (900 µg) was dissolved in 0.9 mL of 6 N HCl and heated at 110 °C for 16h. The crude hydrolysate was evaporated to dryness under a N₂ stream, and the residue was dissolved in 100 µL of water. To 50 mL and to an aliquot (50 µL) of a 50 mM solution of each amino acid (D and L), 20 µL of 1 M NaHCO₃ solution and a 1% (w/v) solution (100 μL) of D-FDVA (Marfey's reagent, N-(2,4-dinitro-5-fluorophenyl)-Dvalinamide) was added. Derivatization with L-FDVA under the same conditions was additionally performed with the cis and trans L-Hyp standards. The reaction mixture was incubated at 40 °C for 60 min. After this time the reaction was quenched by addition of 10 μL of 1 N HCl, and the crude mixture was diluted with 200 μL of CH₃CN and analyzed by LC/MS on an Agilent 1260 Infinity II single quadrupole LC/MS instrument. Separations were carried out on an Atlantis T3 column (4.6×100 mm, 5 µm) maintained at 40 °C. A mixture of two solvents, A (10% CH₃CN, 90% H₂O) and B (90% CH₃CN, 10% H₂O), both containing 1.3 mM ammonium formate and 1.3 mM trifluoroacetic acid, was used as the mobile phase under a linear gradient elution mode (20-40% B in 20 min, 40-60% B in 5 min, 60-100% B in 0.2 min; isocratic 100% B for 3 min) at a flow rate of 1 mL/min. Retention times (min) for the derivatized (D-FDVA) amino acid standards under the reported conditions were: D-Ser: 6.31, L-Ser: 7.35, D-Pro: 10.24, L-Pro: 13.54, D-Phe: 18.16, L-Phe: 24.33, D-Leu: 18.12, L-Leu: 25.41, trans L-Hyp: 5.15, cis L-Hyp: 6.76. Retention times (min) for the derivatized (L-FDVA) standards of L-Hyp were: trans L-Hyp: 4.89, cis L-Hyp: 5.74. Retention times (min) for the observed peaks in the HPLC

trace of the D-FDVA-derivatized hydrolysis product of cellulamide A were as follows: L-Ser: 7.38, L-Pro: 13.49, L-Phe: 24.32, L-Leu: 25.40, *trans* L-Hyp: 5.12 (Fig. S25; Appendix V).

6.2.7. Cellulosimicrobium funkei CT-R177 Genome Sequencing

C. funkei CT-R177 was cultivated in AIA for 7 days and its genomic DNA extracted using the Dneasy PowerSoil Pro Kit (Qiagen, CA, US). Whole genome sequencing was performed in the Genomics Unit from Instituto Gulbenkian de Ciência aiming a 150x depth coverage of an estimated genome of ~4.5Mb. Briefly, the quantity of DNA was measured using a Qubit 4 Fluorometer using Qubit dsDNA BR assay kit and library was prepared using an in-house protocol based in Nextera XT from Illumina. The resulting library was sequenced on a NextSeq 2000 from Illumina PE 150+150. Final assembly was established using SPAdes [216]. The completeness, contamination and general genome statistics were determined using DFAST [233]. The genome sequence was annotated using the NCBI Prokaryotic Genome Annotation Pipeline and deposited at GenBank under the accession number JBCIVP000000000. AntiSMASH was used for the automated analysis and identification of secondary metabolite BGCs using relaxed detection settings and all extra features selected. Manual search for a putative BGC genes that could be associated to with the biosynthesis of cellulamides was performed using tBlastn from within the Geneious software package.

6.2.8. Bioactivity Screening of Cellulamide A

The biological activity of **1** was tested in all the previously described screenings performed for CT-R177 crude extract. This molecule was additionally screened for antimicrobial activity against *A. baumannii*, methicillin resistant and methicillin sensitive *S. aureus*, *E. faecalis*, and *C. albicans*, using established protocols [359, 360]. Cellulamide A was tested using a two-fold dose response curve starting at 128 mg/mL. Cytotoxicity was additionally determined against the human cancer cell lines A2058 (melanoma), MIA PaCa-2 (pancreas), Hep G2 (liver), MCF-7 (breast) and A549 (lung) at 10 concentrations starting at 50 mM, using a two-fold dose curve, following a reported procedure [361].

6.2.9. General Experimental Procedures

Optical rotations were measured using a Jasco P-2000 polarimeter (JASCO Corporation, Tokyo, Japan). UV spectra were obtained with an Agilent 1260 DAD (Agilent Technologies, Santa Clara, CA, USA). NMR spectra were recorded on a Bruker Avance III spectrometer (500 and 125 MHz for 1 H and 13 C NMR, respectively) equipped with a 1.7 mm TCI MicroCryoProbeTM (Bruker Biospin, Falländen, Switzerland). Chemical shifts were reported in ppm using the signals of the residual solvent as internal reference (δ_H 3.31 ppm and δ_C 49.15 ppm for CD₃OD and CD₃OH). LC-DAD and LC-HRESIMS/MS analysis were performed as described previously [362].

6.3. RESULTS AND DISCUSSION

6.3.1. *Cellulosimicrobium funkei* CT-R177 Isolation and Taxonomic Identification

Strain CT-R177 was isolated from the holdfast tissues of a C. tomentosum macroalgae specimen collected from the intertidal zone of a rocky beach in northern Portugal. This aerobic, non-sporulating strain exhibited colonies with a small-size rodshaped morphology and a bright yellow coloration. A BLASTN search in the Eztaxon database of the PCR-amplified 16S rRNA nucleotide sequence showed that strain CT-R177 is closely related to *Cellulosimicrobium funkei* ATCC BAA-886^T (99.93% similarity) [347], followed by Cellulosimicrobium cellulans LMG 16121^T (99.86% similarity) [341]. A ML phylogenetic tree comprising the type strains closest related to strain CT-R177 was built (Fig. 26), showing its close affiliation to C. funkei, strongly supported by the bootstrap value. Therefore, strain CT-R177 was taxonomically classified as belonging to the species C. funkei. The presented tree incorporates type strains from other genera beyond Cellulosimicrobium, enabling a more comprehensive exploration of its evolutionary relationships among other closely related Actinomycetota taxa. C. funkei, formerly Oerskovia turbata, was firstly isolated from a human blood sample, however strains affiliated with this species have since been isolated from various other settings, including the marine environment [358].

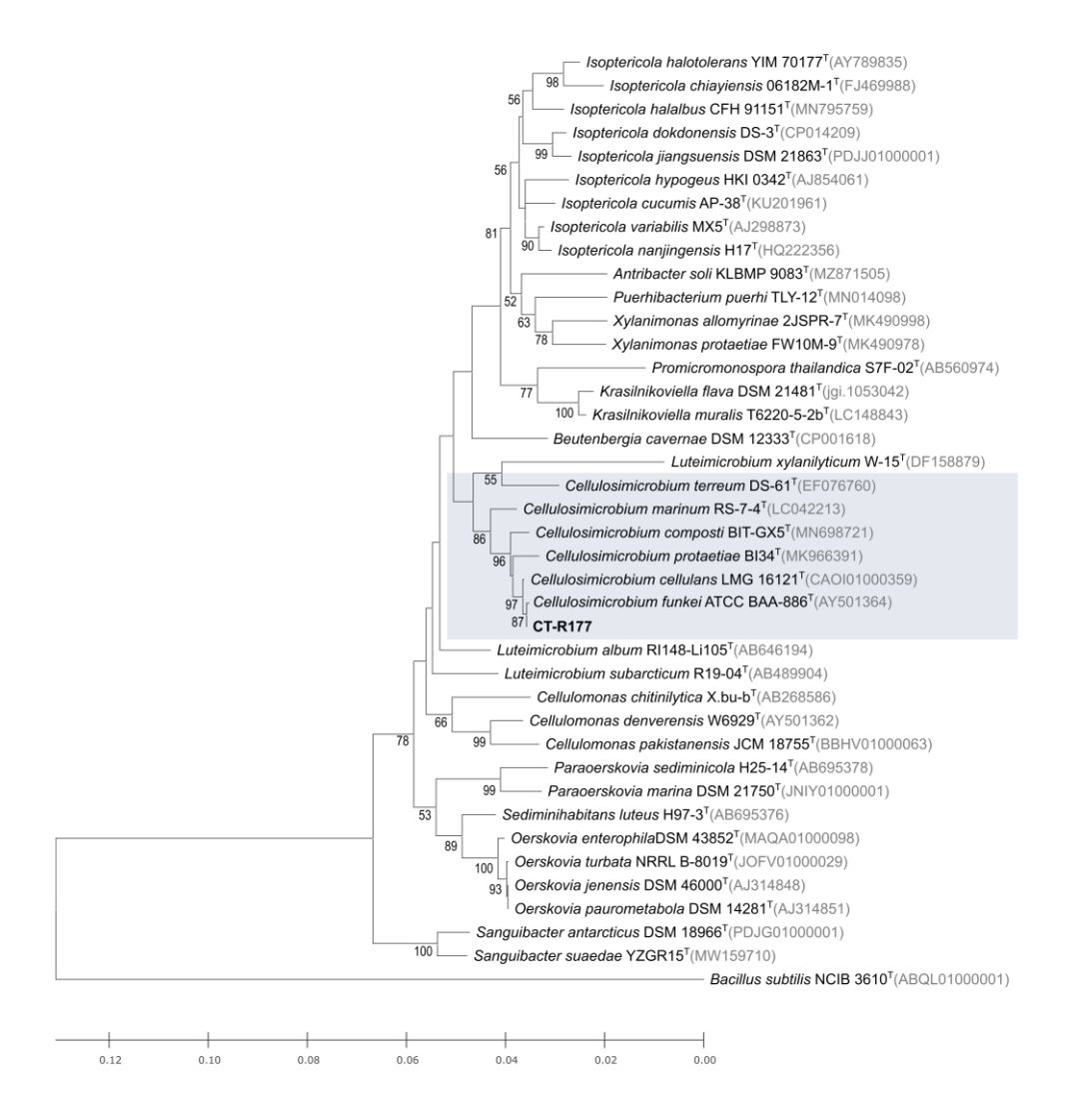


Figure 26. ML phylogenetic tree based on 16S rRNA gene sequences (1,395 nt), showing the relationship between strain CT-R117 and the closest related type strains according to EzBiocloud database. Accession numbers are indicated in brackets. Values at the nodes indicate bootstrap values of 50% and above, obtained based on 1,000 resampling events. *Bacillus subtilis* NCIB 3610^T was used as outgroup. Type strains affiliated to *Cellulosimicrobium* genus are blue shaded.

6.3.2. Bioactivity Screening and Dereplication of *Cellulosimicrobium funkei* CT-R177 Crude Extract

The crude extract of strain CT-R177 was screened for antimicrobial and anticancer metabolites. While no positive result was detected against the growth of the tested microorganisms, the crude extract was able to significantly decrease the viability and proliferation of human breast ductal carcinoma T47D and colorectal carcinoma HCT116 cells (Fig. 27A). However, the same effect was also detected towards the non-cancer cells, indicating general cytotoxicity rather than selectivity against cancer cell lines. In order to understand if the recorded cytotoxicity was due to any known actinobacterial

compound, CT-R177 crude extract was dereplicated using GNPS tools. From this analysis no hit with a known molecule was obtained, indicating the possible presence of a putative novel bioactive molecule in CT-R177 metabolome. Based on this suggestion, a manual dereplication was performed to access any new mass spectrometric features of interest. One particular molecule with a protonated adduct [M+H] $^+$ at m/z 803.3929 was detected, matching no accurate (exact) mass included in the DNP, NPA and Fundación MEDINA in-house database [363] (Fig. 27B). Based on the molecular formula assigned of $C_{37}H_{54}N_8O_{12}$ and its likely novelty, we decided to pursuit a MS-guided isolation and further chemical characterization of this molecule.

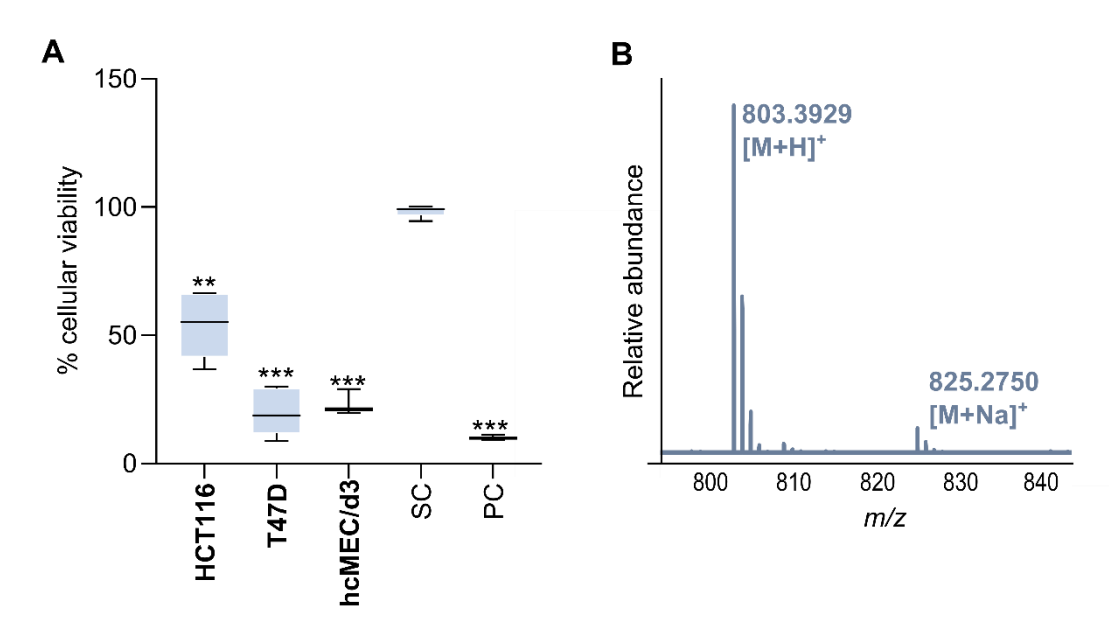


Figure 27. (**A**) Cytotoxic activity of strain CT-R177 crude extract in HCT116, T47D and hcMEC/d3 human cell lines, tested at 15 μg mL⁻¹. Results presented as percentage of cellular viability after 48h of exposure, measured as mean from two independent MTT experiments, each performed in triplicate. Significant differences are compared to the solvent control (**p < 0.01; ***p < 0.001). The percentage of cellular viability for the positive control (PC: Staurosporine 15 μg mL⁻¹) and solvent control (SC: 99.9% DMSO) are indicated as well. (**B**) Zoom of the HRMS spectrum displaying the m/z 803.3929 [M+H]⁺ mass spectrometric feature in strain CT-R177 crude extract.

6.3.3. Mass Spectrometry Guided Isolation and Structural Elucidation of Cellulamides

Applying a chemistry-guided isolation protocol including reversed-phase column chromatography followed by reversed-phase HPLC, cellulamide A (2) and its structurally related congener cellulamide B (3) were isolated from the strain CT-R177 crude extract obtained with a 1:1 mixture of acetone/methanol. A molecular formula of $C_{37}H_{54}N_8O_{12}$ was assigned to cellulamide A based on the presence of a [M+H]⁺ adduct at m/z

803.3951. Inspection of its ¹H and ¹³C NMR spectra evidenced the peptidic nature of the compound, with a significant number of signals in the carbonyl region of the ¹³C NMR spectrum between 170 and 180 ppm combined with signals in the region corresponding to alpha hydrogens of amino acids between 3.9 and 5.0 ppm in its ¹H NMR spectrum (Table 10, Fig. S9; Appendix V). Additionally, signals corresponding to five hydrogens in the aromatic region of this spectrum (d_H 7.24-7.32 ppm) and six carbons in the aromatic region of the ¹³C spectrum (d_C 128.2 CH, 128.9 CH (x2), 131.0 CH (x2), and 138.0 C), (Table 10, Figs. S9 and S10), identified Phe as one of the residues present in the molecule. Correlations observed in the COSY (Figs. 28 and S6) and HSQC (Fig. S11; Appendix V) spectra additionally confirmed the presence in the structure of 2 of the following amino acids: Ser, Pro, two Gly, two g-hydroxyproline (Hyp), and Leu. The molecular formula assigned to the compound evidenced that 2 was a linear peptide. Its sequence was established using a combination of key HMBC correlations (Figs. 28 and S12) together with tandem MS/MS analysis (Fig. 29). The combination of both techniques established the sequence HOOC-Ser-Pro-Gly1-Hyp1-Leu-Gly2-Hyp2-Phe-NH₂ for cellulamide A.

Marfey's analysis was used to determine the absolute configuration of the constituent amino acids of **2** [364]. Hydrolysis of the compound by heating at 110 °C in a sealed vial followed by derivatization with N-(2,4-dinitro-5-fluorophenyl)-D-valinamide (D-FDVA) established an L configuration for the Ser, Pro and Leu residues present in the molecule. In the case of g-hydroxyproline, as only the *cis* and *trans* L amino acid standards were available, a double derivatization strategy using the L and D versions of FDVA was employed. This strategy unequivocally confirmed the presence of *trans* g-L-hydroxyproline as the constituent of the molecule (Figs. S20 to S24 for Marfey's analysis results - Appendix V). The full stereochemistry of the molecule was therefore established as depicted in Figure 28.

Figure 28. (A) Structure of cellulamides A and B (B) Key COSY and HMBC correlations observed in the structure of cellulamide A.

The molecular formula of cellulamide B, accounting for one oxygen atom less than **2**, (**3**) was established as $C_{37}H_{54}N_8O_{11}$ based on the presence of a protonated adduct [M+H]⁺ at m/z 787.4014. Analysis of its NMR spectra evidenced that the most significant structural difference with respect to **2** was the replacement of one of the Hyp residues in **2** by a Pro in the structure of **3**. Such change is in agreement with the difference in molecular formula observed between both compounds. Tandem MS/MS analysis (Fig. 29) unequivocally established that the Hyp/Pro change was in the residue located between Gly-2 and Phe. The existence of a prominent ion at m/z 373.1718 in **2** or 373.1716 in **3**, originated from the breakage of the amide bond between Hyp-1 and Leu in both compounds, additionally supported this structural proposal. Finally, almost identical ¹H and ¹³C NMR chemical shifts (Table 10) and a common biosynthetic origin [365] allowed us to propose the absolute configuration of cellulamide B as depicted in Figure 28.

Table 10. NMR Data of cellulamides A (2) and B (3) in CD₃OD (2) or CD₃OH (3).

		2		3	
Amino Acid	Position	δ _H , m, J (Hz)	δc, type	δ _H , m, J (Hz)	δc, type
Ser	α	4.22, m	58.6, CH	4.23, m	58.5, CH
	β	3.82, m, 2H	64.1, CH ₂	3.82, m, 2H	64.2, CH ₂
	CO		176.5, C		176.5, C
Pro	α	4.46, m	62.3, CH	4.46, m	62.3, CH
	β	2.17, m; 2.09, m	30.5, CH	2.17, m; 2.09, m	30.5, CH
	γ	2.07, m; 1.99, m	25.8, CH ₂	2.07, m; 1.99, m	25.7, CH ₂

	δ	3.67, m; 3.57, m	48.0, CH ₂	3.67, m; 3.57, m	47.9, CH ₂	
	СО		173.9, C		173.9, C	
Gly-1	α	4.13 m; 4.05, m	42.9 CH ₂	4.09 m; 4.02, m	43.0 CH ₂	
	СО		170.0, C		169.7, C	
Hyp-1	α	4.58, m	60.9, CH	4.57, m	60.7, CH	
	β	2.25, m; 2.08, m	38.7, CH ₂	2.23, m; 2.08, m	39.0, CH ₂	
	γ	4.51, m	71.2, CH	4.51, m	71.2, CH	
	δ	3.79, m, 2H	56.8, CH	3.78, m, 2H	56.7, CH	
	СО		174.7, C		174.7, C	
	α	4.80, m	51.2, CH	4.80, m	51.1, CH	
	β	1.62, m, 2H	41.5, CH ₂	1.62, m, 2H	41.6, CH ₂	
Lou	γ	1.69, m	25.8, CH ₂	1.69, m	25.7, CH ₂	
Leu	δ	0.93, m	23.8, CH₃	0.94, m	23.7, CH ₃	
	δ'	0.94, m	22.3, CH ₃	0.95, m	22.3, CH ₃	
	CO		173.4, C		173.2, C	
Gly-2	α	4.13, m, 3.72 m	43.7, CH ₂	4.09, m, 3.74 m	43.7, CH ₂	
	CO		171.6, C		171.5, C	
	α	4.56, m	61.4, CH	4.37, m	62.5, CH	
	β	2.19, m; 2.03, m	39.0, CH ₂	2.18, m; 1.95, m	30.3, CH ₂	
Pro/ Hyp-2	γ	4.41, m	71.2, CH	1.97, m; 1.91, m	26.2, CH ₂	
	δ	3.64, m; 3.24, dd (10.7, 2.9)	56.7, CH ₂	3.64, m; 3.55, m	48.6, CH ₂	
	CO		174.7, C		173.6, C	
	α	3.98, m	55.4, CH	4.02, m	55.3, CH	
Phe		3.05, dd (13.5,		3.10, dd (13.8, 6.4),		
	β	6.4), 2.83, dd,	41.3, CH ₂	2.86, dd, (13.8, 6.9)	41.0, CH ₂	
		(13.5, 6.7)		,, (,,		
	γ		138.0, C		137.7, C	
	δ , δ	7.30, m	131.0, CH	7.30, m	130.9, CH	
	ϵ, ϵ'	7.32, m	129.9, CH	7.32, m	129.8, CH	
	ζ	7.24, m	128.2, CH	7.25, m	128.2, CH	
	CO		174.8, C		173.9, C	

 $\begin{array}{l} \delta-\text{chemical shift}\\ m-\text{multiplicity}\\ J-\text{coupling constant} \end{array}$

700

800

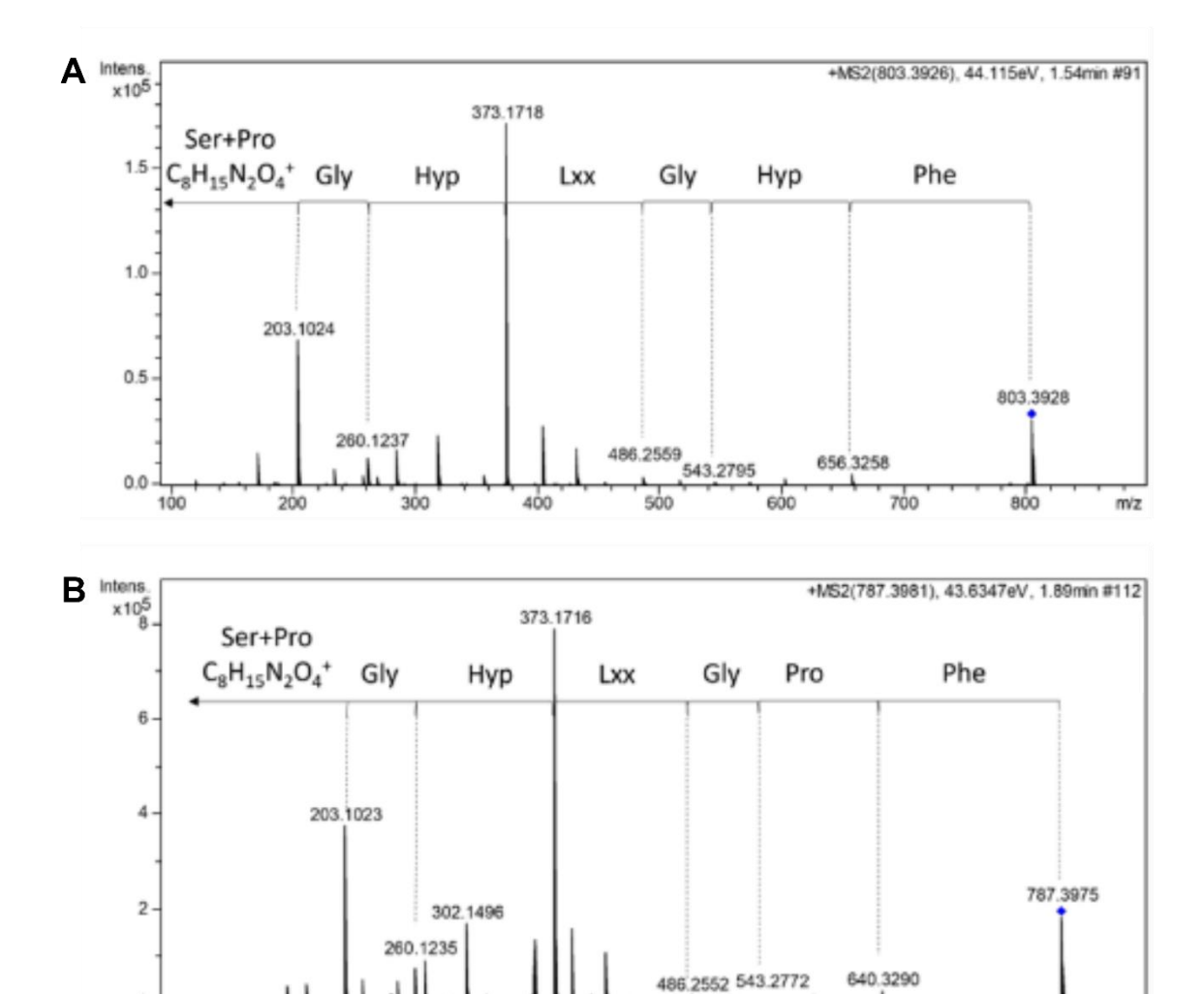


Figure 29. Tandem MS/MS spectra of (A) cellulamide A (2) and (B) cellulamide B (3).

6.3.4. Genomic Analysis

The genome of *C. funkei* CT-R177 was sequenced and explored to better understand the biosynthetic machinery of this strain and unveil any putative BGC behind cellulamides production. The genome data (100% complete genome) was assembled into one contig with a length of 4 424 308 bp and an *in silico* G+C content of 74.6 mol%, in line with values associated to *Cellulosimicrobium* species. Genome Taxonomy Database (GTDB) assignment [260] confirmed the taxonomic identification of strain CT-R177 as *C. funkei*, with an Average Nucleotide Identity (ANI) of 95.98% to the type strain ATCC BAA-886^T. Differently from our prediction, antiSMASH analysis did not allow to clearly assign a BGC to the biosynthesis of the cellulamides. Also, unlike other Actinomycetota taxa that are highly enriched in BGCs, such as *Streptomyces* species that can encode up to 70 BGCs per genome [283], *C. funkei* CT-R177 appears to encode only five BGCs, three of them being assigned to peptide synthesis (Table 11). Because

none of the antiSMASH-detected BGCs matched could be reasonably assigned to the biosynthesis of the cellulamides, we manually explored the genome data. Specifically, we looked for nucleotidic sequences that could translate into the amino acid sequence of **2**, and we searched also for homologs of enzymes that have been shown to be involved in proline hydroxylation a distinctive structural feature of **2**. We further looked into adenylation domains, typical of NRPSs (nonribosomal peptide synthetases - NRPSs), that could activate amino acids found in **2**. These searches did not yield any evidence that could enable us to link the genome data to the cellulamides. Thus, further studies should be conducted in the future to clarify the genetic basis of cellulamide biosynthesis.

Table 11. Secondary metabolite BGCs identified by antiSMASH in the genome of *C. funkei* CT-R177.

Pogion	Type of	Most similar	Similarity	MiBiG	Length (nt)
Region	Compound	known cluster	(%)	accession	
2.1	NI-siderophore/T3PKS	Alkylresorcinol	100	BGC0000282	1 – 23,448
5.1	Terpene	7-deoxypactamycin	n 5	BGC0000119	216,873 – 237,787
7.1	Thioamide-NRP	Enteromycin	12	BGC000249	130,738 – 176,956
12.1	RiPP-like	NH	NH	NH	123,554 – 176,956
16.1	RiPP-like	NH	NH	NH	36,580 - 46,876

T3PKS - Type III polyketide synthase

NRP - non-ribosomal peptide

RiPP - ribosomally synthesized and post-translationally modified peptide

NH – No Hits

6.3.5. Bioactivity Screening of Cellulamide A

The biological activity of cellulamide A was tested in the same antimicrobial and cytotoxic screenings previously performed with the crude extract. The compound was not active, thus proving that it was not the metabolite responsible for the previously detected anticancer activity. Cellulamide A was then tested in an additional panel of microbial human and fish pathogenic strains, including Gram-negative (*Acinetobacter baumannii*) and Gram-positive bacteria (methicillin resistant and methicillin sensitive *Staphylococcus aureus*, and *Enterococcus faecalis*), and a yeast (*Candida albicans*). The compound was not active at the highest concentration tested of 128 mg/mL. Additionally, the compound was not cytotoxic against a panel of five human cancer cell lines when tested at a concentration of 50 mM.

6.4. CONCLUSION

In this study, we have explored a seaweed symbiotic Actinomycetota for novel chemistry discovery, resulting in the isolation and structure elucidation of a new family of linear peptides. Cellulamides constitute the first reported secondary metabolites from the *Cellulosimicrobium* genus, highlighting the so far overlooked value of this taxon for NP discovery. It also draws attention to how symbiotic associations between seaweeds and Actinomycetota might inspire the synthesis of untapped novel molecules. Further investigations should be conducted to clarify the biosynthesis and biological activity of cellulamides, which so far remain elusive. Bacterial marine-derived peptides have proven their value in several fields [366, 367], underscoring the importance of fully exploring the biotechnological potential of cellulamides. Additionally, clarifying the ecological role of these peptides, particularly their interactions with the seaweed host, the surrounding environment, and microbial communities, would provide insights into their broader biological significance and practical applications.

7

Bioactivity-guided isolation of novel chemistry from the secondary metabolism of Streptomyces violaceoruber CT-F61 and Micromonospora sp. CC-F88

ABSTRACT

Actinomycetota living in association with macroalgae are a proved source of novel natural products worthy of in-depth bioprospection. In this chapter, we explore the secondary metabolism of two previously-targeted strains producing putative novel bioactive compounds – *Streptomyces violaceoruber* CT-F61 and *Micromonospora* sp. CC-F88 –, retrieved from the frond tissues of *Codium tomentosum* and *Chondrus crispus*, respectively (Chapter 2). The crude extract of both strains was positively screened for the production of antimicrobial and anticancer compounds, yielding no hits for known actinobacterial metabolites using GNPS dereplication tools (Chapter 4). A tailor-made bioactivity-guided fractionation pipeline was applied to the organic extracts of each strain, coupled with LC-HRESIMS/MS and NMR experiments, leading to the identification and isolation of three putative novel compounds (4-6), one of them with likely antimicrobial properties. Although additional studies are necessary to fully characterize these NP, our findings highlight the richness of unknown chemistry encoded in the metabolome of both *Streptomyces* and non-*Streptomyces* macroalgae-symbiont strains.

Keywords: Bioactivity-guided isolation; Macroalgae; Micromonospora; Streptomyces

7.1. INTRODUCTION

The search for novel NP is a cornerstone in pharmaceutical and biotechnological research. Actinomycetota, renowned for their prolific production of bioactive compounds, stand out as a promising source for discovery [119]. While *Streptomyces* species have been acknowledged for decades as the most productive bacterial taxa, for such specialized chemicals, bioprospecting the metabolome of less targeted groups – the so-called rare actinomycetes – might lead to novel chemistry as well [368]. A successful approach to unveil novel NP has been to look into the secondary metabolism of actinobacterial strains inhabiting unique ecological niches, such as the ones living in symbiosis with marine organisms, including macroalgae [157].

In a previous work, the crude extract of two macroalgae-associated actinomycetes, Streptomyces violaceoruber CT-F61 and Micromonospora sp. CC-F88, caught our attention due to their bioactive properties and the likelihood of encoding novel NP (Chapter 4). Both were effective against the growth of the Gram-positive reference microorganisms Bacillus subtilis ATCC 6633 and Staphylococcus aureus ATCC 29213, decreasing at the same time the cellular viability in more than 50% of human cancer cell lines (with no negative effect on non-carcinogenic cells in the case of CT-F61). A detailed study on the last-mentioned strain CT-F61 also unveiled its ability to inhibit the growth of three Gram-negative aquaculture-relevant pathogens: Tenacibaculum maritimum ATCC 43397, Listonella (Vibrio) anguillarum ATCC 19264 and Aeromonas hydrophila ATCC 43397 (Chapter 5). The dereplication performed using GNPS tools indicated the likely presence of novel NP in the metabolome of both bioactive strains, prompting an in-depth exploration to uncover novel chemistry. The anticancer activity displayed by CT-F61 crude extract was followed in Chapter 5, leading to the discovery and chemical characterization of decylprodigiosin (1), a new member of the red-pigmented antibiotics family prodigiosins. In the present chapter, we solely focused on the bioactivity-guided isolation of the putative novel antimicrobials produced by this macroalgae-associated Streptomyces. Regarding Micromonospora sp. CC-F88, both antibacterial and cytotoxic activity were targeted.

In this work, by employing a bioactivity-guided isolation pipeline on the organic crude extracts of both *S. violaceoruber* CT-F61 and *Micromonospora* sp. CC-F88 strains, three putative novel compounds, one of them with likely antimicrobial properties, were uncovered. Also, the genome mining of both strains revealed a pool of unknown BGCs, showcasing the opportunities for NP discovery.

7.2. MATERIALS AND METHODS

7.2.1. Bacterial Isolation and Taxonomic Identification

Strains CT-F61 and CC-F88 were isolated from the blade tissues of the macroalgae *Codium tomentosum* and Chondrus crispus, respectively, and taxonomically identified through 16S rRNA gene sequencing, as described in Chapter 2 (sections 2.2.2. and 2.2.3.).

7.2.2. Up-scaling and Organic Extraction

To obtain sufficient amounts of compounds for a bioactivity-guided isolation, both CT-F61 and CC-F88 strains were cultivated in a larger scale (24 L) in AIA culture medium, following as described in Chapter 5 (section 5.2.4.). The resulting biomass and resin were recovered by centrifugation (2500g, 5 min), lyophilized, and repeatedly extracted using a mixture of acetone/methanol 1:1 (v/v).

7.2.3. Bioactivity-guided Isolation of NP from *Streptomyces violaceoruber* CT-F61

In a series of previous biological screenings, CT-F61 crude extract displayed both antibacterial and anticancer activities, likely associated with the synthesis of novel NP (Chapter 4). The anticancer properties were attributed to the later-detected prodigiosins (Chapter 5). Here, we focused exclusively in following and isolating the compounds associated with the antibacterial activity against the Gram-positive reference microorganisms B. subtilis ATCC 6633 and S. aureus ATCC 29213. The initial steps testing of both the crude extract resulting from the large-scale fermentation and the reverse-phase vacuum liquid chromatography (C18 VLC) fractions - are described in Chapter 5. All fractions tested positively in the bioactivity assay were examined for the presence of unknown molecules using GNPS dereplication tools, based on LC-HRESIMS/MS analysis, as described in Chapter 4 (section 4.2.8.). This dereplication step was performed between each chromatography. The active VLC fractions with no hits for known compounds in the GNPS-based dereplication were selected, pooled together and further separated in a normal-phase flash-chromatography (FC). A solvent polarity gradient (Table S14 - Appendix VI) was used on a glass fritted chromatography column packed with silica. The column was assembled using 100 g of silica gel 60 (0.015 0.040 mm 40-60µm, 100Å) (Milipore, USA) and 0.5 cm of sand, followed by the dry loading of the sample in 1:1 kieselgel 60 (0.063 0.20 mm) (Merck, USA). The different eluents were sequentially added to the column. The recovered fractions (Table S15 -Appendix VI), established by similarity composition using thin-layer chromatography (TLC), were tested for antimicrobial activity and dereplicated. The active FC fractions with no hits for known compounds were selected and further subjected to a reversephase semi-preparative high-performance liquid chromatography (C18 HPLC) (flow 3 mL min⁻¹; column Jupiter 5 µm C18300 A, 250x10mm; Table S16 - Appendix VI). The recovered fractions (Fig. S26 - Appendix VI; Table S17- Appendix VI) were tested for antimicrobial activity and dereplicated. The purification of each active fraction was performed by a reverse phase analytical HPLC (flow 0.8 mL min⁻¹; column SURF C18 100A µm, 250x4.6mm; isocratic conditions 45:55 H20:MeOH). The recovered fractions (Fig. S27 A-C Appendix VI; Table S18 - Appendix VI) were tested for antimicrobial activity and manually dereplicated against the DNP and NPA databases. Fractions corresponding to single peaks in the HPLC chromatograms were analysed by ¹H (600 MHz) NMR spectroscopy to confirm the compound's purity. The NMR data were acquired in methanol-d₄ (CD₃OD). Pure compounds were subjected to a combination of HRMS and NMR experiments (1H, 13C, HSQC, HMBC and COSY) to elucidate their chemical structures.

7.2.4. Bioactivity-guided Isolation of NP from Micromonospora sp. CC-F88

In the previously-performed bioactivity screenings, CC-F88 crude extract displayed both antibacterial and anticancer activities, seemingly associated with the synthesis of novel NP (Chapter 4). In this work we used a bioactivity-guided approach to follow and isolate these compounds linked with the antibacterial activity against B. subtilis ATCC 6633 and S. aureus ATCC 29213 and cytotoxic effect on the human breast ductal carcinoma cell line T47D. After confirming that the crude extract obtained from the large-scale cultivation upheld the previously detected bioactive properties, it was fractionated in a C18 VLC using a solvent polarity gradient (Table S19 - Appendix VI) on a glass chromatography column. All the generated fractions were tested in the bioactivity assays and the active ones analysed for the presence of unknown molecules using GNPS dereplication tools. This dereplication step was performed between each chromatography. The active VLC fractions with no hits for known compounds in the GNPS-based dereplication were selected, pooled together and further separated in a normal-phase FC. A solvent polarity gradient (Table S20 - Appendix VI) was used on a glass fritted chromatography column packed with silica. The column was assembled using 100 g of silica gel 60 (0.015 0.040 mm 40-60µm, 100Å) and 0.5 cm of sand, followed by the dry loading of the sample in

1:1 kieselgel 60 (0.063 0.20 mm). The different eluents were sequentially added to the column. The recovered fractions were tested for antimicrobial and cytotoxic activity and dereplicated. The active FC fractions with no hits for known compounds were selected and further subjected to a reverse-phase FC using the Pure C-850 FlashPrep (Büchi, UK) in a C18 230-400 mesh 40-63 µm 25 g column (flow 18 mL min⁻¹; Table S21 -Appendix VI). The recovered fractions (Table S22 - Appendix VI) were tested for bioactivity and dereplicated. The active C18 FC fractions with no hits for known compounds were selected and further subjected to a reversed-phase semi-preparative HPLC (flow 2 mL min⁻¹; column Jupiter 5 µm C18300 A, 250x10mm; Table S23 -Appendix VI). The recovered fractions (Fig. S34 - Appendix VI; Table S24 - Appendix VI) followed the usual protocol or bioactivity screening and dereplication. Apart from the screening results, fractions corresponding to single peaks in the HPLC chromatogram were selected to further purification in a reverse-phase analytical HPLC (flow 0.7 mL min-1; column ACE Excel 3 C18 75 x 4.6 mm; Table S25 - Appendix VI). The recovered fractions (Fig. S35 A-C - Appendix VI; Table S26 - Appendix VI) were analysed by ¹H (600 MHz) NMR spectroscopy to confirm the compound's purity. The NMR data were acquired in methanol- d_4 (CD₃OD). Pure compounds were subjected to a combination of HRMS and NMR experiments (1H, 13C, HSQC, HMBC and COSY) to elucidate their chemical structures.

7.2.5. Genome Mining

To better understand the genetically encoded biosynthetic potential of the two strains under study, the genomes of both were sequenced and annotated for the presence, nature and likely novelty of BGCs using antiSMASH, following the procedures described previously (Chapter 3, section 3.2.3.).

7.3. RESULTS AND DISCUSSION

7.3.1. Bioactivity-guided Isolation of NP from *Streptomyces violaceoruber* CT-F61

Dereplication of the CT-F61 organic extract using GNPS tools did not lead to the identification of known compounds that could explain the observed antibacterial activity (Chapter 4). For this reason, we performed large-scale cultivation (24 L) of this strain, in order to isolate any putative novel bioactive compound from its metabolome, yielding an organic crude extract of 5.7 g. A bioactivity-quided isolation protocol was then applied, using a set of sequential chromatographic steps to purify the bioactive compounds of interest. All generated fractions along this process were subjected to HRMS dereplication to avoid the isolation of known molecules, with no hits for any. The VLC (C18 stationary phase) of the crude extract led to 13 fractions (A-M) of decreasing polarity, with a yield of 88.5% (Chapter 5). All fractions were screened for antibacterial activity, with fractions F-L being active against B. subtilis ATCC 6633 and/or S. aureus ATCC 29213 (Fig. 30A). Fractions F-J were pooled (sample FJ: 1888.89 mg) and fractionated by a normal-phase FC using a solvent polarity gradient on a glass fritted chromatography column packed with silica. Fractions K and L were not used in this work and left apart to the isolation of anticancer metabolites (Chapter 5). A total of eleven fractions (FJ_1 - FJ_11) were collected, with a yield of 88.6%, and tested for antibacterial activity. Fractions FJ_2, FJ_9 and FJ 11 were shown to inhibit the growth of B. subtilis ATCC 6633 (Fig. 30B). Based on these results, we decided to select fraction FJ_2 (sample FJ_2; 68.35 mg) to fractionation by C18 semi-preparative HPLC, leading to fourteen fractions (FJ_2_A -FJ 2 N) with a yield of 94.48%. Antibacterial screening revealed fractions FJ 2 G (1.01 mg), FJ_2_H (1.58 mg) and FJ_2_I (3.58 mg) as active (Fig. 30C). Each of the mentioned fractions was individually chromatographed by C18 analytical HPLC, yielding six fractions from FJ 2 G, five from FJ 2 H and seven from FJ 2 I, with yields of 124.75, 117.72 and 105.03%, respectively. All generated fractions were tested against the growth of B. subtilis ATCC 6633, with fraction FJ_2_I_5 displaying a stronger activity. A weaker activity was detected in fractions FJ_2_I_6 and FJ_2_I_7 (Fig. 30D).

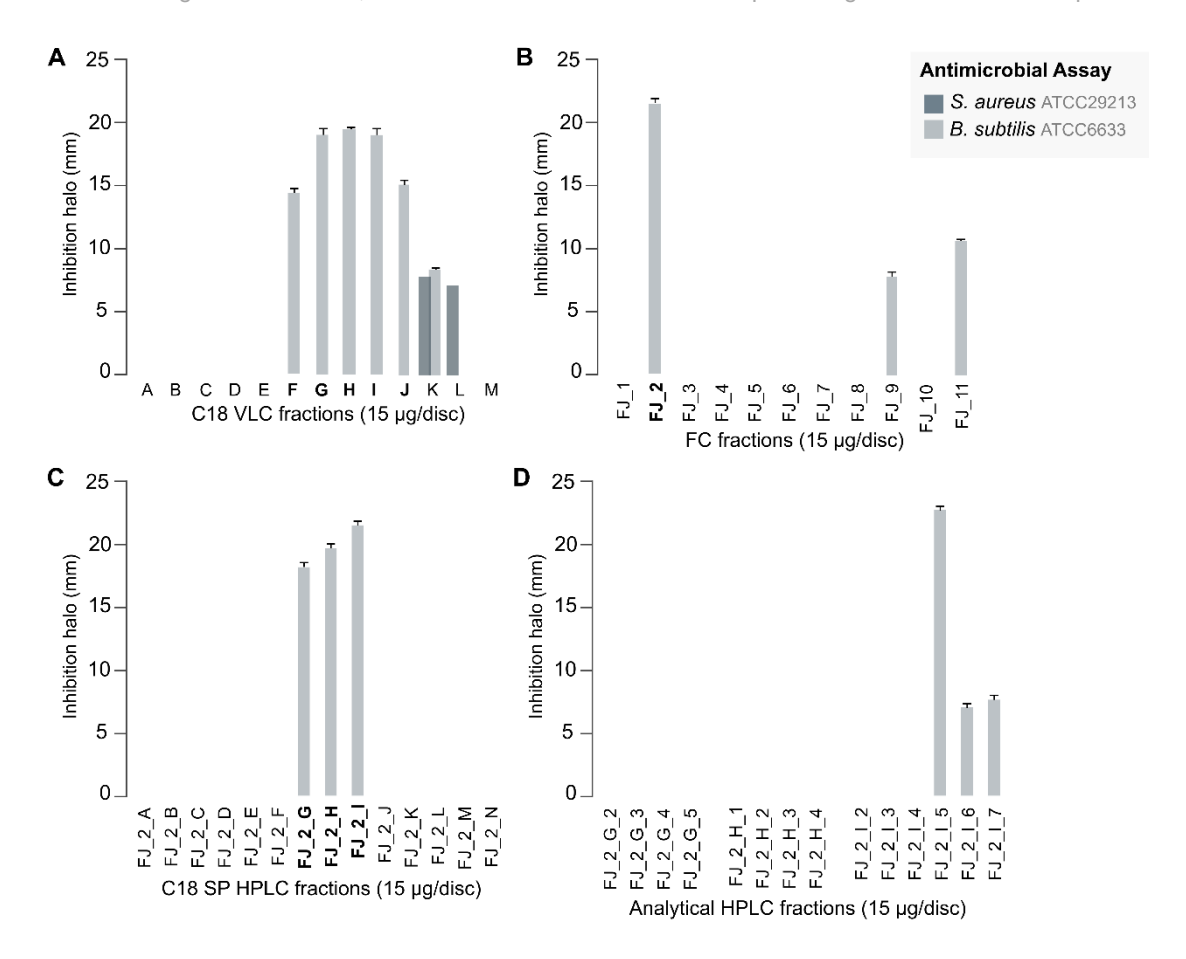


Figure 30. Bioactivity screening of CT-F61 samples. Antimicrobial activity of (**A**) C18 VLC fractions of CT-F61 crude extract, (**B**) FC fractions of CT-F61 FJ sample, (**C**) C18 semi-preparative (SP) HPLC fractions of sample FJ_2 and (**D**) C18 analytical HPLC fractions of samples FJ_2_G, FJ_2_H and FJ_2_I. Antimicrobial results presented as mean of the diameter of the inhibition halos measured from two independent experiments using the agar-based disk diffusion method. Fractions highlighted on bold were selected to the next chromatographic step.

Fraction FJ_2_I_5 was analyzed by ¹H (600 MHz) NMR spectroscopy to conclude about the purity of the existing bioactive compound (Fig. S28 Appendix VI). The presence of several peaks of non-integer integration allowed us to conclude that the molecule was not completely pure. Still, a LC-HRESIMS/MS analysis of this fraction, alongside with all others retrieved from sample FJ_2_I fractionation (except for FJ_2_I_1 that contains more than one peak in the HPLC chromatogram), was performed to infer the putative mass of the active compound, as well as to confirm its novelty by using the NPA and DNP databases. A protonated sodium adduct ion [M+Na]+ at *m*/*z* 539.35605 (**4**) was exclusively detected in the active fraction FJ_2_I_5 (Fig. 31). This compound, with retention time (RT) 7.84 min and calculated chemical formula C₂₇H₄₃O₂N₁₀, was identified as the most abundant metabolite in this fraction. The protonated sodium adduct ion [M+Na]+ at *m*/*z* 539.35605, as well as the protonated ion [M+H]+ at *m*/*z* 517.37372 and

the monoisotopic mass at m/z 316.36592 (\pm 5 ppm) were dereplicated matching with no known actinobacterial-sourced secondary metabolite, confirming therefore the likely novelty of **4**. Based on its solely presence in the bioactive fraction FJ_2_I_5, and being the most abundant compound, we hypothesize that **4** is responsible for the detected activity against the Gram-positive reference strain *B. subtills* ATCC 6633. To confirm both the novelty and biological properties of this metabolite its chemical structure should be elucidated, and the screening repeated with the pure compound. Because of the low amount of sample available (0.21 mg), we were unable to perform these tasks, which are planned to be executed in the future.

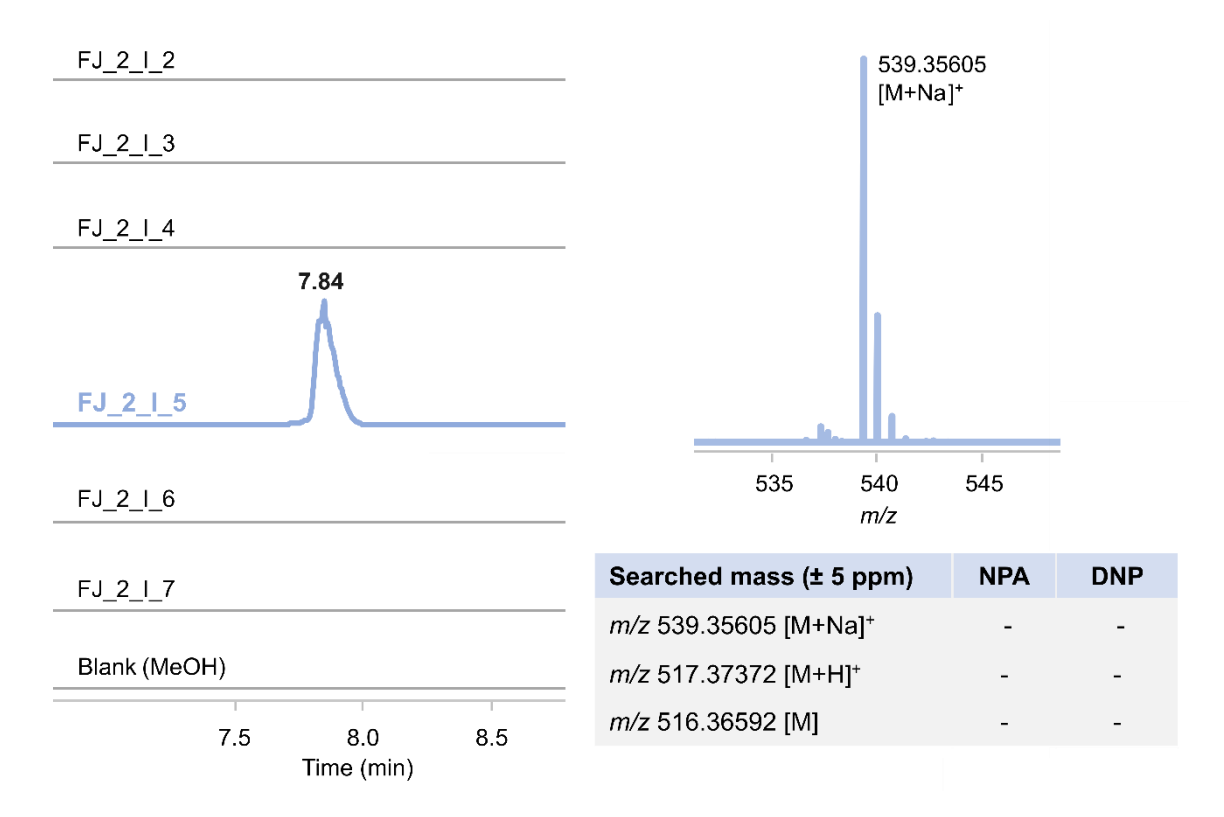


Figure 31. EICs of **4** for fractions generated from sample FJ_2_I. The mass features searched in both NPA and DNP databases are presented, as well as the retrieved results (0 hits).

Even without biological activity detected towards the tested microorganism, all other fractions corresponding to single peaks in the HPLC chromatograms were analyzed by 1 H (600 MHz) NMR spectroscopy to infer on their purity. According to NMR data, fraction FJ_2_I_4 proved to be the only corresponding to a pure compound (Fig. S29 Appendix VI). A protonated ion [M+H]⁺ at m/z 387.18048 (5) was detected in LC-HRESIMS/MS data of this sample, being absent in the blank, with RT 7.76 min and calculated chemical formula $C_{22}H_{27}O_6$ (Fig. 32). The dereplication of 5 using the previously mentioned

databases did not retrieve any match with any known compound, therefore indicating the likely novelty of this molecule as well.

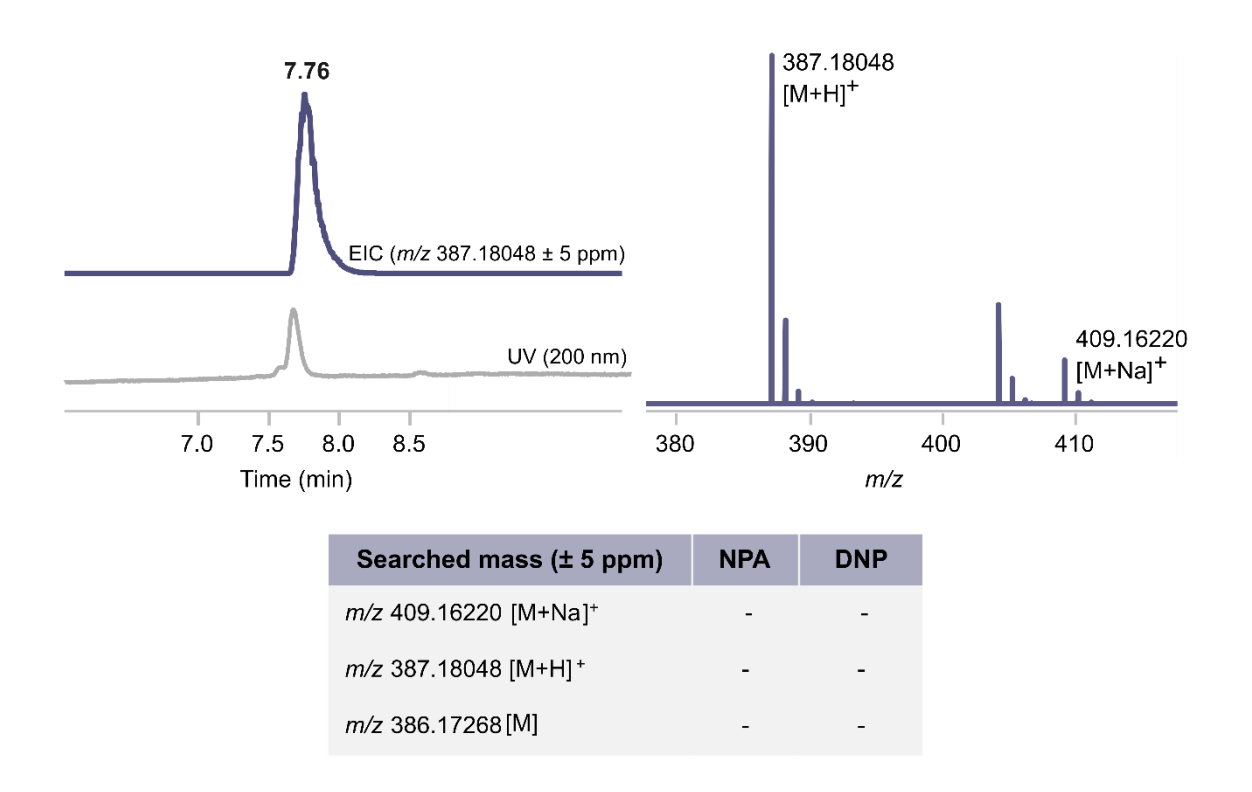


Figure 32. EICs of **5**. The mass features searched in both NPA and DNP databases are presented, as well as the retrieved results (0 hits).

In order to elucidate the chemical structure of **5**, a set of additional one dimensional (1D) and two-dimensional (2D) 600 MHz NMR spectroscopy experiments were performed (Figs. S30-S33 - Appendix VI). However, due to few detected signals, likely related to the low amount of available sample (0.3 mg), we were only able to establish a substructure of **5** (Fig. 33). To fully elucidate the chemical structure of this novel molecule we intend to perform its re-isolation and extend the NMR analysis, namely by acquiring data using other solvents as chloroform-*d* or DMSO-*d6*.

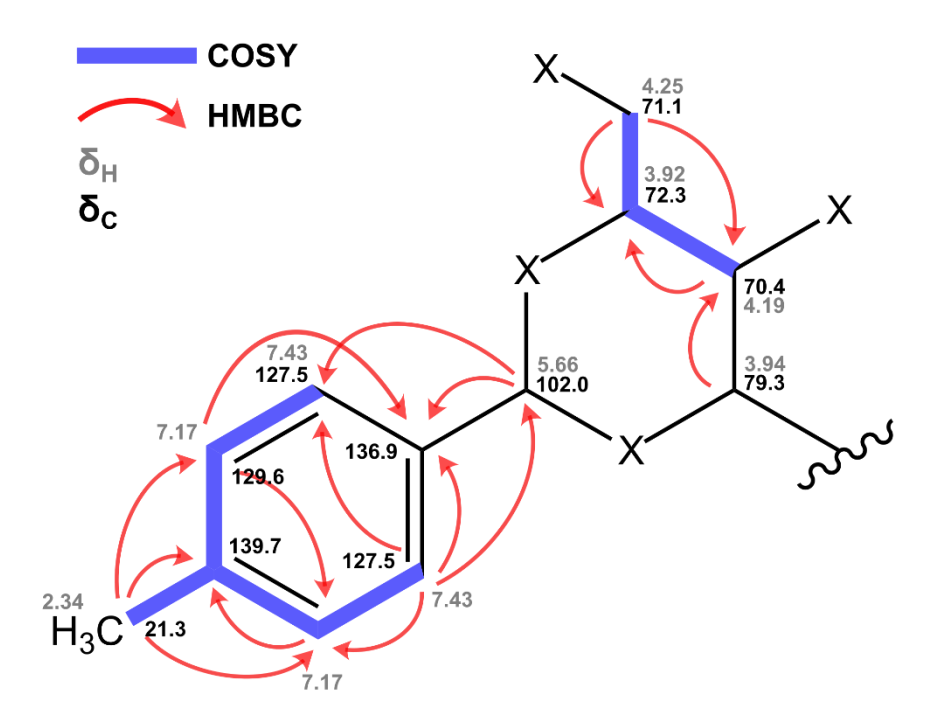


Figure 33. Chemical substructure elucidated of **5** with the indication of key HMBC (arrows) and ${}^{1}H^{-1}H$ COSY (blue lines) correlations, as well as proton (δ_H) and carbon (δ_C) resonance values.

7.3.2. Bioactivity-guided Isolation of NP from Micromonospora sp. CC-F88

Dereplication of the CC-F88 organic extract using GNPS tools did not lead to the identification of known compounds that could explain its antibacterial and cytotoxic properties (Chapter 4). For this reason, we performed large-scale cultivation (24 L) of this strain, in order to isolate any putative novel bioactive compound from its metabolome, yielding an organic crude extract of 6.9 g. A bioactivity-guided isolation protocol was then applied, using a set of sequential chromatographic steps to purify any bioactive compounds of interest. All generated fractions along this process were subjected to HRMS dereplication to avoid the isolation of known molecules, with no hits for any. The VLC (C18 stationary phase) of the crude extract led to 13 fractions (A-L) of decreasing polarity, with a yield of 94.0%. All fractions were screened for bioactivity, with fractions H-L being able to inhibit the growth of B. subtilis ATCC 6633 and/or S. aureus ATCC 29213 (Fig. 34A), and fractions I2 and L displaying significant activity towards the viability of T47D cancer cells (Fig. 34B). Fractions H-L were pooled (sample HL; mass: 1980.07 mg) and fractionated by a normal-phase FC using a solvent polarity gradient on a glass fritted chromatography column packed with silica. A total of twelve fractions (HL_1 - HL_12) were collected, with a yield of 75.0%, and tested for bioactivity in the

antimicrobial and cytotoxic assays. Fractions HL_6 to HL_9 presented activity towards the growth of B. subtilis ATCC 6633 and/or S. aureus ATCC 29213 and together with fraction HL 11 were effective decreasing the viability of the cancer cells (Fig. 34B). Based on this screening results, fractions HL_6 to HL_9 (sample HL_69; mass: 381.21 mg) were pooled and further fractionated by C18 FC, generating fourteen new fractions (HL 69 A - HL 69 N) with a yield of 77%. Bioactivity assays revealed fractions HL_69_H to HL_69_L as the active ones in both assays. These fractions were pooled (sample HL_69_HL; mass: 100.57 mg) and further separated in by C18 semi-preparative HPLC. From this chromatography, with a yield of 111.6%, twelve fractions were generated (HL 69 HL 1 - HL 69 HL 12), as well as an insoluble part of the sample that was kept apart and considered as another fraction (HL_69_HL_13). The results of the bioactivity screening unveiled fraction HL_69_HL_5 as the only one active towards the growth of B. subtilis ATCC 6633, while the previous recorded activity against S. aureus ATCC 29213 was not detected anymore. Also, fractions HL_69_HL_3 to HL_69_HL_7 displayed a significative cytotoxic activity against T47D cells, but not as effective as the fractions from the previous separation. At this point, even with fraction HL 69 HL 5 being the most active, and therefore promising one to the discovery of a novel bioactive NP, due to its high complexity in the HPLC chromatogram, it would be challenging to isolate the bioactive molecule in enough amounts, we decided to redirect our efforts towards exploring other compounds closer to purity, even if they lack a recorded bioactivity in the assays conducted.

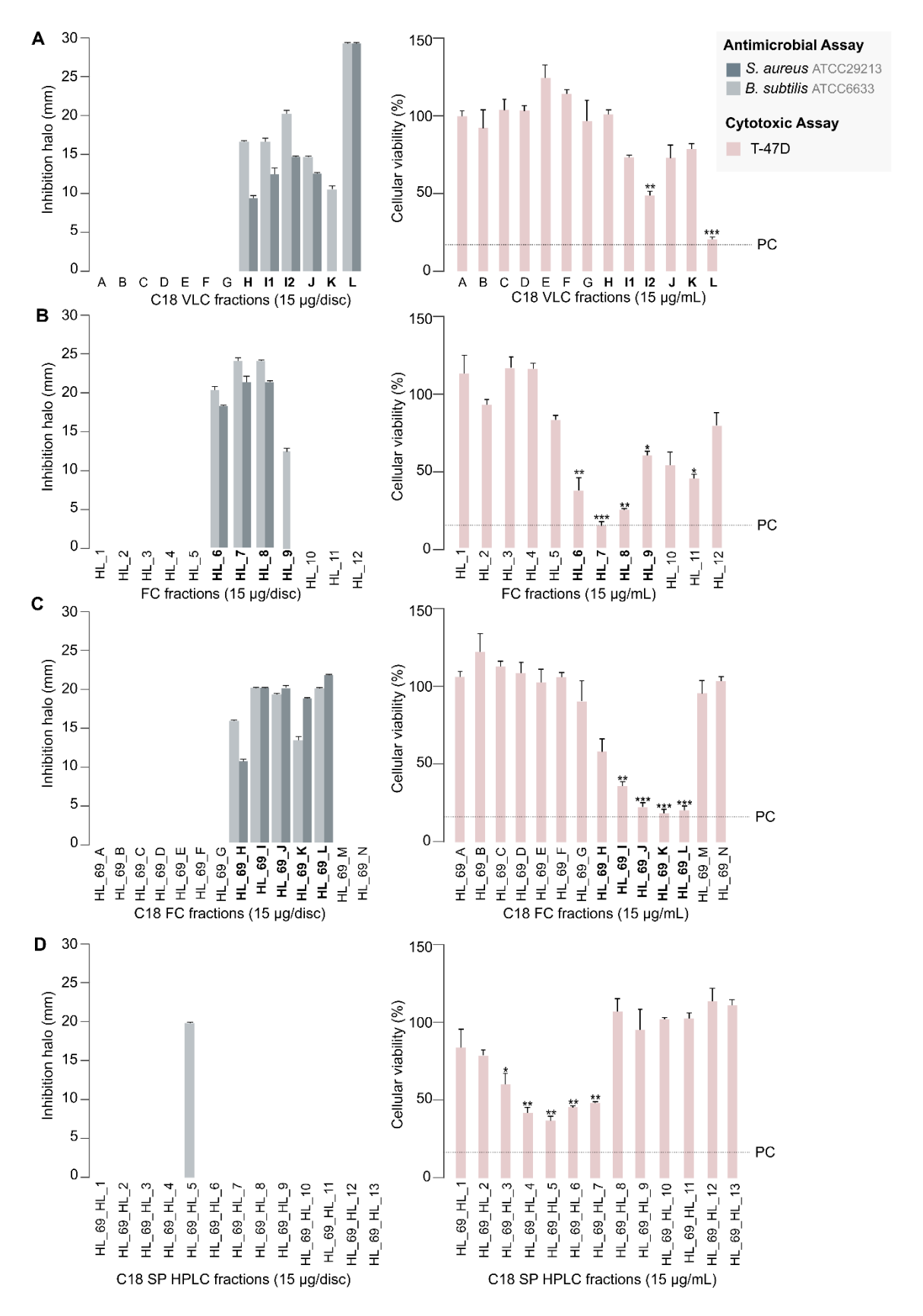


Figure 34. Bioactivity screening fractionation of CC-F88 samples. Antimicrobial and cytotoxic activity of (**A**) C18 VLC fractions of CC-F88 crude extract, (**B**) FC fractions of CC-F88 HL sample, (**C**) C18 FC fractions of sample HL_69 and (**D**) C18 semi-preparative (SP) HPLC fractions of sample HL_69_HL. Antimicrobial results (left pannel) presented as mean of the diameter of the inhibition halos measured from two

independent experiments using the agar-based disk diffusion method. Cytotoxic results (right pannel) presented as percentage of cellular viability after 48h of exposure, measured as mean from two independent MTT experiments, performed with triplicates to each sample. Significant differences compared to the solvent control (*p < 0.05; **p < 0.01; ***p < 0.001). The percentage of cellular viability for the positive control (PC: Staurporine 15 μ g mL⁻¹) is indicated. Fractions highlighted on bold were selected to the next chromatographic step.

The ¹H (600 MHz) ¹H NMR spectroscopy data of fractions HL_6-9_HL_2, HL_6-9_HL_6 and HL_6-9_HL_10 (Fig. S36 A-C - Appendix VI) revealed that they were not yet pure (presence of signals that did not integrate for integers). For that reason, an additional purification step was conducted for each in a C18 analytical HPLC. All generated fractions matching to isolated peaks in the HPLC chromatograms were reanalyzed by ¹H (600 MHz) NMR spectroscopy with the results of this analysis confirming the purity of fraction HL_69_HL_6_B (mass: 0.4 mg; Fig. S37 - Appendix VI). A deprotonated ion [M-H]⁻ at *m/z* 635.41809 (6) was detected in LC-HRESIMS/MS data of this sample, being absent in the blank, with RT 11.69 min and calculated chemical formula C₂₃H₅₇O₁₁N₉ (Fig. 35). The dereplication of 6 using the DNP and NPA databases did not retrieve any match with a known compound, therefore indicating the likely novelty of this molecule.

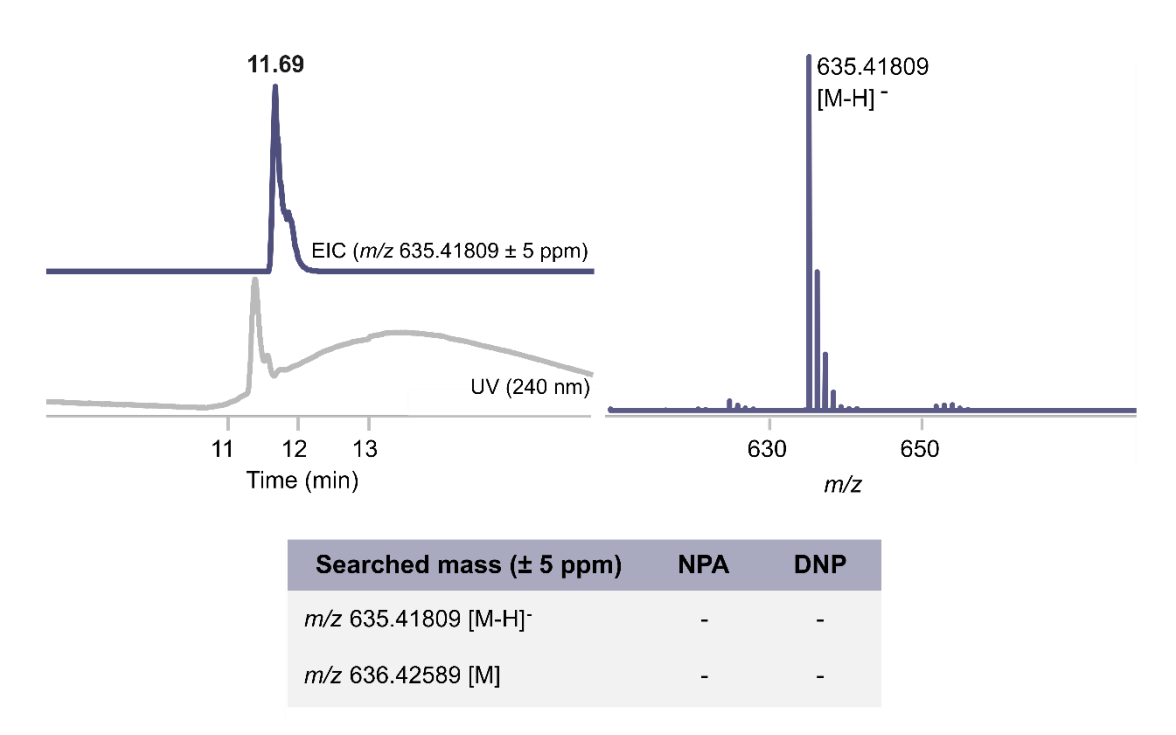


Figure 35. EICs of **6**. The mass features searched in both NPA and DNP databases are presented, as well as the retrieved results (0 hits).

In order to elucidate the chemical structure of **6**, a set of additional 1D/2D 600 MHz NMR spectroscopy experiments were performed (Figs. S38-S41 - Appendix VI). However, due to the high complexity of signals detected, we were only able to stablish two substructures of **6** (Fig. 36). To fully elucidate the chemical structure of this novel molecule we intend to extend the NMR analysis, namely by acquiring data using other solvents as chloroform-*d* or DMSO-*d*6.

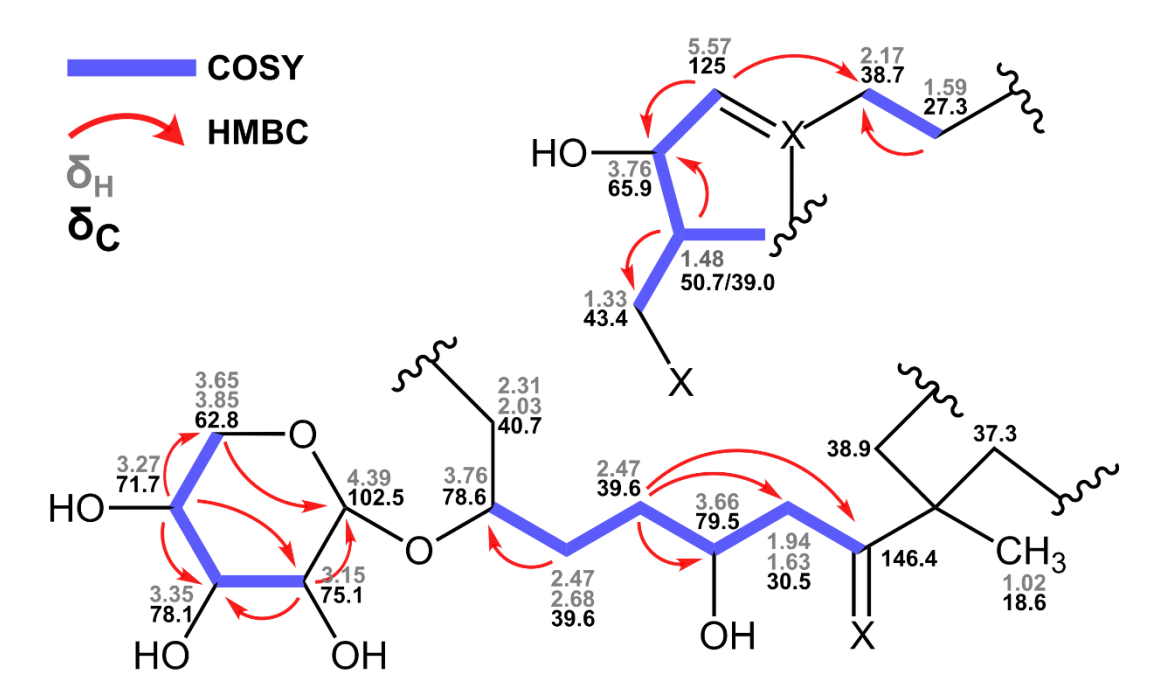


Figure 36. Chemical substructures elucidated of **6** with the indication of key HMBC (arrows) and $^{1}H-^{1}H$ COSY (blue lines) correlations, as well as proton (δ_{H}) and carbon (δ_{C}) resonance values.

7.3.3. Genome Mining

After investigating the production of novel NP by CT-F61 and CC-F88 cultures, a genomic analysis was conducted to evaluate the diversity, abundance, and uniqueness of BGCs present within their genomes. The genome of strain CT-F61 was assembled into one contig with a length of 8 599 857 bp, 99.92% of completeness and *in silico* G+C content of 72.2 mol%, in line with the range for the genus *Streptomyces*. The genome of strain CC-F88 was assembled into one contig with a length of 7 033 835 bp, 95.14% of completeness and *in silico* G+C content of 71.6 mol%, in line with the range for the genus *Micromonospora*. The annotation performed by antiSMASH unveiled the presence of several BGCs encoded in the genomes of both strains, distributed across different classes (Fig. 37). Strain CT-F61 genome exhibited a higher number of detected BGCs,

totaling 30. However, near 70% of these clusters shared more than 60% similarity with those in the MiBIG database, suggesting limited potential for biodiscovery. This finding aligns with Streptomyces' reputation for encoding numerous BGCs [369], but also with the fact that their secondary metabolism is extensively explored [238]. Opposing to these results, 80% of the detected BGCs in strain CC-F88 genome fell below the mentioned similarity threshold, indicating a greater opportunity for uncovering novel NP. This significant percentage of unknown clusters might be related to the fact that, based on the retrieved genomic information, strain CC-F88 represents a potential novel species affiliated to the genus Micromonospora. According to GTDB Taxonomy Assignment, the closest related type strains to CC-F88 are the marine-sourced Micromonospora craniellae LHW63014[™] [370] and Micromonospora craterilacus NA12[™] [371] with 92.7 and 87.3% of ANI, respectively, both values below the 95% boundary that defines a new bacterial species [213]. Even less targeted in drug-discovery screenings, when comparing to Streptomyces, Micromonospora species also represent a group of prolific producers of biotechnologically-relevant metabolites worth of exploration [372]. A more comprehensive analysis, similar to the one described in Chapter 3, will be applied in the future to validate the taxonomy of CC-F88 strain. Additionally, once the chemical structures of all potential novel compounds (4-6) are elucidated, we aim to use the genomic data to uncover their biosynthesis.

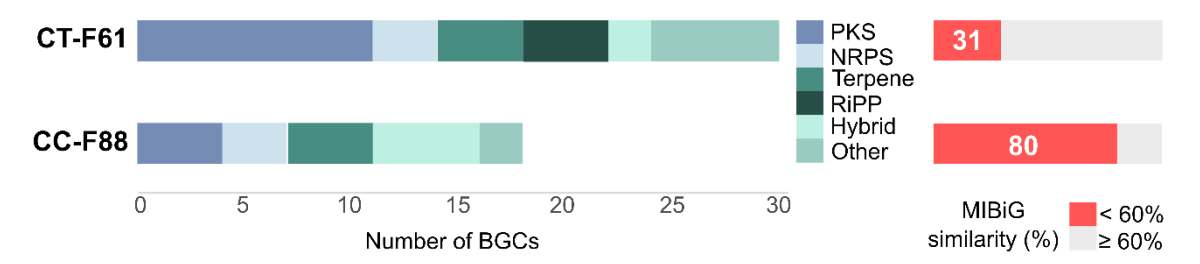


Figure 37. Number of BGCs annotated by antiSMASH in the genome of CT-F61 and CC-F88 strains and their similarity (%) with MIBiG database.

7.4. CONCLUSION

In this work we have used a bioactivity-guided approach to isolate novel NP from the secondary metabolism of two macroalgae-associated actinomycetes – *Streptomyces violaceoruber* CT-F61 and *Micromonospora* sp. CC-F88. We describe three potential novel compounds, two produced by CT-F61 (4-5) and one produced by CC-F88 (6), with 4 displaying antibacterial activity towards the Gram-positive human-health relevant *Bacillus subtilis* ATCC 6633. We further conducted an *in silico* bioprospecting of the biosynthetic machinery encoded in the genomes of both strains, revealing CC-F88 as notably abundant in uncharacterized BGCs. In the future we aim to fully elucidate the chemical structure of the isolated compounds to confirm their novelty. Furthermore, we intend to subject them to a broader array of bioactivity screenings to assess their biotechnological potential. Our results highlight the opportunity for NP discovery from the metabolism of macroalgae actinobacterial holobiont. The exploration of the ecological role of these compounds should also be considered for future studies.

8

General Conclusion and Future Perspectives

8.1. General Discussion and Conclusion

In this final section, a comprehensive discussion of the findings from the preceding chapters is presented, exploring their significance, implications, and potential avenues for future research. Through an analysis of the data obtained and the methodologies employed, a deeper understanding of the broader context in which this research resides, as well as its potential impact on both scientific knowledge and practical applications, is highlighted.

The work undertaken within the framework of this Thesis was motivated by the need to find new NP with biological properties to meet the needs of our society, particularly in tackling health issues impacting human life. The specialized secondary metabolism of Actinomycetota represents the backbone of most currently used drugs, underscoring the importance of in-depth exploration of these microorganisms. However, one of the major bottlenecks in NP chemistry field is the high rate of re-discovery of known compounds, a fact not consistent with genomic data. One key approach to overcome this drawback resides in tapping new ecological niches, and their associated actinobacterial communities, to uncover novel chemistry. The synthesis of such chemicals can be triggered by a wide range of factors, including the symbiotic association between these bacteria and other marine organisms, as macroalgae. Although marine Actinomycetota have proved their high value as producers of biotechnologically relevant metabolites, they have been mostly studied in sediments, corals and sponges, leaving macroalgae as an unexplored opportunity. The work presented in this Thesis aimed to address this gap by bioprospecting macroalgae from the Portuguese coast as a valuable source of Actinomycetota-derived novel bioactive NP using both culture-dependent and independent approaches.

This work started with the sampling of two macroalgae species from the intertidal rocky shore of a northern Portuguese beach – *C. tomentosum* and *C. crispus* – to which a combination of classic cultivation techniques and metagenomic analysis was applied to survey their associated Actinomycetota diversity. While some studies have briefly explored the association of these bacteria with macroalgae, their presence, abundance and taxonomic distribution in these two particular Chlorophyta and Rhodophyta species were explored for the first time in this Thesis. Our findings unveiled the richness of Actinomycetota in both macroalgae, as demonstrated through culture-dependent and independent analysis, providing valuable insights into the thriving actinobacterial communities in this very particular marine ecological niche. As major output of this work, we have curated 380 macroalgae-associated Actinomycetota strains, ready for biotechnological exploration. These isolates represent, to our knowledge, the largest

published collection of macroalgae-associated Actinomycetota to date, and its members are distributed across 12 orders, 15 families and 25 genera affiliated to the Actinomycetia class, composed by around 60% of Streptomyces, being the remaining classified as rare genera, and also comprising novel species. The biosynthesis of NP by the genus Streptomyces is unmatched in the microbial realm, making the recovery of such a high number of strains a promising starting point for biodiscovery. At the same time, rare genera of Actinomycetota represent a much less explored pool of chemicals, which might also lead to the unearthing of new molecules. Interestingly, metagenomic data showed Acidimicrobiales as the dominant actinobacterial order in both macroalgae, but no strain affiliated with this taxonomic group was successfully isolated. Given the high abundance of this highly recalcitrant-to-cultivation taxa in our samples, it would be interesting in the future to develop a tailor-made approach to isolate strains affiliated with it, both to explore their bioactive properties and to study their ecological role in this particular symbiotic environment. In fact, there was little overlapping in the taxonomic results obtained with the culture-dependent and -independent approaches used, a confirmation that the synergistic use of both methods is necessary for a deeper understanding of the whole macroalgae-associated actinobacterial community. Metagenomic data also unveiled a fivefold higher abundancy of Actinomycetota in C. crispus tissues, when comparing to C. tomentosum, a difference not noticed in the isolation protocol.

As a significant outcome of our cultivation experiment, two novel Actinomycetota species – *Nocardiopsis codii* sp. nov., and *Rhodococcus algaerubra* sp. nov. – were isolated and taxonomically described in this Thesis. Apart from expanding the scientific understanding of microbial diversity within macroalgae ecosystems, the description of new species enlarges the pool of organisms available for bioprospecting, potentially uncovering novel biochemical pathways for synthesizing secondary metabolites that might have pharmaceutical or industrial applications. When analyzing the genome of both new species, a notable number of diverse BGCs was detected, with more than 80% of them presenting no hits to any compound already described. Further studies must be conducted to fully explore the biosynthetic potential of these two new actinobacterial species.

Based on the major goal of this Thesis of finding new bioactive NP produced by Actinomycetota, efforts were dedicated to the bioprospecting of the actinobacterial community associated to the two macroalgae species, relying once more in both culture-dependent and -independent approaches. The crude extract of each of the 380 isolates was obtained and tested for antibacterial, antifungal, anticancer and lipid-reducing activities. Remarkably, around 43% of the extracts showed activity in at least one of the screenings performed. The dereplication of the active crude extracts led to the

identification of several known compounds in their composition, likely associated with the observed bioactivity. However, it also pinpointed 22 of the 165 bioactive crude extracts as encoding metabolites non annotated in databases, and therefore likely representing new bioactive NP. Using the eDNA extracted from the tissues of both macroalgae under study, a metagenomic analysis was performed to characterize the biosynthetic genetic potential of the associated actinobacterial communities. In total, 130 BGCs and 10 MAGs were recovered from both samples and grouped in 91 GCFs, 83 of which showing less than 30% of similarity to database entries, once again highlighting the extensive opportunity for NP discovery. From the 130 BGCs, only two were recovered from C. tomentosum, with the Actinomycetota community associated to C. crispus proving to be biosynthetically richer. These findings were not however reflected in the culture-based screening results, as no significant differences were observed in terms of the overall bioactivity displayed by the isolates retrieved from both macroalgae specimens, nor in terms of the diversity of secondary metabolites annotated by GNPS tools in their metabolomes. The recovered BGCs were taxonomically associated to two main classes, Actinomycetes and Acidimicrobiia. While the first is extensively studied and described as the major microbial source of NP, members of the class Acidimicrobiia do not share the same status, making the recovery of a similar number of BGCs from both taxa an interesting result worthy of further exploration. The findings provided by both culturedependent and -independent approaches underscore the large potential held by Actinomycetota associated with macroalgae as reservoirs for novel bioactive NP.

Based on all previous results - phylogenetic assessment and likely production of novel NP -, particular strains of our collection were targeted for up-scaling and bioactivity and/or mass-guided NP isolation, yielding the discovery, structure elucidation and chemical characterization of three novel compounds. These strains contributed to the 22 bioactive crude extracts previously mentioned that potentially encode novel molecules. From the cultivation of Streptomyces violaceoruber CT-F61, a strain isolated from the blade tissues of C. tomentosum, a new analogue of the red-pigmented family of the antibiotics prodigiosins, decylprodigiosin, was uncovered. Based on the strong anticancer activity on breast carcinoma T47D and colorectal carcinoma HCT116 cells of CT-F61 crude extract, effective as well against a panel of human and fish pathogenic bacteria, a bioactivity-guided pipeline was applied leading to the discovery of this new 10-carbon alkyl chain prodigiosin. Despite this family of NP being well-known for a long time, we report a new analogue and the first evidence for prodigiosins being produced by a macroalgae-associated Actinomycetota. From the cultivation of Cellulosimicrobium funkei CT-R177, a strain also isolated from the blade tissues of C. tomentosum, we have discovered a new family of linear peptides, cellulamides A and B. Although the anticancer activity displayed by this strain's crude extract, here we followed a mass-guided approach to isolate a target compound unveiled by mass spectrometry. Cellulamides represent the first family of NP reported from the Actinomycetota genus *Cellulosimicrobium*, showcasing not only the potential of less-explored taxa but also host-associated marine strains for novel chemistry discovery. The bioactive properties and biosynthesis of these peptides remains elusive, requiring further studies. Other new NP were isolated and partially characterized from the secondary metabolism of *Streptomyces violaceoruber* CT-F61 and *Micromonospora* sp. CC-F88, this second one representing a potential new species, but future work is required to fully elucidate their chemical structures and bioactive properties.

It is equally important to acknowledge the limitations encountered during the course of our investigation, as well as opportunities for improvement. While this Thesis represents a significant advancement in the exploration of macroalgae-associated actinobacterial communities for novel bioactive NP discovery, in our vision three main topics merit consideration. Firstly, this project relied on a single sampling campaign, with the collection of only one specimen of each macroalgae – C. crispus and C. tomentosum. To draw better conclusions on macroalgae-Actinomycetota diversity and associated biosynthetic potential, a broader study, contemplating more specimens on a higher temporal and biogeographic scale, should be considered. Secondly, we have not explored alternative fermentation conditions to trigger the expression of more cryptic BGCs, cultivating all our strains in similar conditions. Although we were successful in the discovery of novel NP, our metagenomic data clearly indicate the existence of a larger pool of chemicals to be uncovered. Two likely approaches to access these cryptic BGCs might be through the exploration of dissimilar culture conditions – by employing different media compositions, pH levels, temperature regimes, or co-cultivation strategies –, or through the use of synthetic biology tools, namely heterologous expression. Thirdly, and lastly, it is crucial to reflect on the fermentation up-scaling process, as it can significantly influence metabolite production and subsequent work. We believe that some of the variations in biological activity encountered during our work (and therefore in metabolite production), particularly when testing upscaled cultures, were reflections of slight but still dissimilar culture conditions between small and larger scales. Therefore, gaining a better understanding of how to ensure stable and reproductible culture conditions is an important issue to be further addressed in future work on NP isolation.

8.2. Future Perspectives

The future of NP discovery partially lies in exploring untapped marine ecological niches and developing tailored strategies to explore its associated microbial communities, with the integration of culture-dependent and -independent approaches being crucial for a comprehensive understanding of microbial diversity and biosynthetic potential. The present Thesis brings forward important and new knowledge on Actinomycetota associated with macroalgae specimens inhabiting the intertidal shores of the northern Portuguese coast. For the first time, the symbiotic actinobacterial communities living within the tissues of Chlorophyta and Rhodophyta species from this environment are described and explored for the synthesis of novel bioactive NP. The biggest published collection to date of macroalgae-associated Actinomycetota is presented in this Thesis, as well as the description of three novel NP: one antibiotic, decylprodigiosin, and two linear peptides, cellulamides A and B, which biological properties remain elusive. In the future, it will be central to continue deepening our exploration of this collection of strains, based on the strong indication that much more chemical novelty is yet to be discovered. Additionally, it will be important to fully characterize all the likely novel taxa found in this collection. As macroalgae emerge as a promising hub for diverse and chemically interesting Actinomycetota, efforts to expand our knowledge on these bacteria for NP studies are paramount. With continued exploration and innovation, the potential for discovering new bioactive compounds from macroalgae-associated Actinomycetota is immense.

REFERENCES

- 1. Azman, A.-S., Othman, I., et al., *Antibacterial, anticancer and neuroprotective activities of rare Actinobacteria from mangrove forest soils.* Indian journal of microbiology, 2017. **57**(2): p. 177-187.
- 2. Abdelmohsen, U.R., Bayer, K., et al., *Diversity, abundance and natural products of marine sponge-associated actinomycetes.* Natural product reports, 2014. **31**(3): p. 381-399.
- 3. Koehn, F.E. and Carter, G.T., *The evolving role of natural products in drug discovery.* Nature reviews Drug discovery, 2005. **4**(3): p. 206-220.
- 4. Wright, G.D., *Unlocking the potential of natural products in drug discovery.*Microbial biotechnology, 2019. **12**(1): p. 55-57.
- 5. Baltz, R.H., *Natural product drug discovery in the genomic era: realities, conjectures, misconceptions, and opportunities.* Journal of industrial microbiology & biotechnology, 2019. **46**(3-4): p. 281-299.
- 6. Culp, E.J., Yim, G., et al., *Hidden antibiotics in actinomycetes can be identified by inactivation of gene clusters for common antibiotics.* Nature biotechnology, 2019. **37**(10): p. 1149-1154.
- 7. Bentley, S.D., Chater, K.F., et al., Complete genome sequence of the model actinomycete Streptomyces coelicolor A3 (2). Nature, 2002. **417**(6885): p. 141-147.
- 8. Challis, G.L., Exploitation of the Streptomyces coelicolor A3 (2) genome sequence for discovery of new natural products and biosynthetic pathways.

 Journal of industrial microbiology & biotechnology, 2014. 41(2): p. 219-232.
- 9. Arcamone, F., *Doxorubicin: anticancer antibiotics.* 2012: Elsevier.
- 10. Li, J., Kim, S.G., et al., *Rapamycin: one drug, many effects.* Cell metabolism, 2014. **19**(3): p. 373-379.
- 11. McSorley, F.R., Johnson, J.W., et al., *Natural Products in Antibiotic Discovery*, in *Antimicrobial Resistance in the 21st Century*. 2018, Springer. p. 533-562.
- 12. Newman, D.J. and Cragg, G.M., *Natural products as sources of new drugs over the nearly four decades from 01/1981 to 09/2019.* Journal of Natural Products, 2020. **83**(3): p. 770-803.
- 13. Broggini, M., Marchini, S., et al., Aplidine, a new anticancer agent of marine origin, inhibits vascular endothelial growth factor (VEGF) secretion and blocks VEGF-VEGFR-1 (flt-1) autocrine loop in human leukemia cells MOLT-4. Leukemia, 2003. **17**(1): p. 52-59.

- 14. Liu, Y., Matsumoto, M., et al., *Delamanid: from discovery to its use for pulmonary multidrug-resistant tuberculosis (MDR-TB).* Tuberculosis, 2018. **111**: p. 20-30.
- 15. Barka, E.A., Vatsa, P., et al., *Taxonomy, physiology, and natural products of Actinobacteria*. Microbiol. Mol. Biol. Rev., 2016. **80**(1): p. 1-43.
- 16. Yadav, N. and Yadav, A.N., *Actinobacteria for sustainable agriculture*. Journal of Applied Biotechnology & Bioengineering, 2019. **6**(6).
- 17. Gopikrishnan, V., Radhakrishnan, M., et al., *Antibiofouling potential of quercetin compound from marine-derived actinobacterium, Streptomyces fradiae PE7 and its characterization.* Environmental Science and Pollution Research, 2016. **23**: p. 13832-13842.
- 18. Salwan, R. and Sharma, V., The role of actinobacteria in the production of industrial enzymes, in New and future developments in microbial biotechnology and bioengineering. 2018, Elsevier. p. 165-177.
- 19. Berdy, J., *Bioactive microbial metabolites*. The Journal of antibiotics, 2005. **58**(1): p. 1-26.
- 20. Bhatnagar, I. and Kim, S.-K., *Immense essence of excellence: marine microbial bioactive compounds*. Marine drugs, 2010. **8**(10): p. 2673-2701.
- Oren, A. and Garrity, G.M., Valid publication of the names of forty-two phyla of prokaryotes. International Journal of Systematic and Evolutionary Microbiology, 2021. 71(10): p. 005056.
- 22. Ludwig, W., Euzéby, J., et al., Road map of the phylum Actinobacteria, in Bergey's manual® of systematic bacteriology. 2012, Springer. p. 1-28.
- 23. McDowell, A., Barnard, E., et al., *Proposal to reclassify Propionibacterium acnes type I as Propionibacterium acnes subsp. acnes subsp. nov. and Propionibacterium acnes type II as Propionibacterium acnes subsp. defendens subsp. nov.* International Journal of Systematic and Evolutionary Microbiology, 2016. **66**(12): p. 5358-5365.
- 24. Lacombe-Harvey, M.-È., Brzezinski, R., et al., *Chitinolytic functions in actinobacteria: ecology, enzymes, and evolution.* Applied microbiology and biotechnology, 2018. **102**: p. 7219-7230.
- 25. Větrovský, T., Steffen, K.T., et al., *Potential of cometabolic transformation of polysaccharides and lignin in lignocellulose by soil Actinobacteria.* PloS one, 2014. **9**(2): p. e89108.
- van Bergeijk, D.A., Terlouw, B.R., et al., Ecology and genomics of Actinobacteria: new concepts for natural product discovery. Nature Reviews Microbiology, 2020.
 18(10): p. 546-558.

- 27. Bhatti, A.A., Haq, S., et al., *Actinomycetes benefaction role in soil and plant health*. Microbial pathogenesis, 2017. **111**: p. 458-467.
- 28. Palaniyandi, S.A., Yang, S.H., et al., *Effects of actinobacteria on plant disease suppression and growth promotion.* Applied microbiology and biotechnology, 2013. **97**: p. 9621-9636.
- 29. Kaltenpoth, M., *Actinobacteria as mutualists: general healthcare for insects?*Trends in microbiology, 2009. **17**(12): p. 529-535.
- 30. Koch, A. and Mizrahi, V., *Mycobacterium tuberculosis*. Trends in microbiology, 2018. **26**(6): p. 555-556.
- 31. Jose, P.A., Maharshi, A., et al., *Actinobacteria in natural products research: Progress and prospects.* Microbiological Research, 2021. **246**: p. 126708.
- 32. Waksman, S.A. and Woodruff, H.B., *Bacteriostatic and bactericidal substances* produced by a soil Actinomyces. Proceedings of the society for Experimental Biology and Medicine, 1940. **45**(2): p. 609-614.
- 33. Waksman, S.A. and Woodruff, H.B., Selective antibiotic action of various substances of microbial origin. Journal of bacteriology, 1942. **44**(3): p. 373-384.
- 34. Schatz, A. and Waksman, S.A., Effect of streptomycin and other antibiotic substances upon Mycobacterium tuberculosis and related organisms. Proceedings of the Society for Experimental Biology and Medicine, 1944. **57**(2): p. 244-248.
- 35. Gavriilidou, A., Kautsar, S.A., et al., Compendium of specialized metabolite biosynthetic diversity encoded in bacterial genomes. Nature microbiology, 2022. **7**(5): p. 726-735.
- 36. Jagannathan, S.V., Manemann, E.M., et al., *Marine actinomycetes, new sources of biotechnological products.* Marine Drugs, 2021. **19**(7): p. 365.
- 37. Helmke, E. and Weyland, H., *Rhodococcus marinonascens sp. nov., an actinomycete from the sea.* International Journal of Systematic and Evolutionary Microbiology, 1984. **34**(2): p. 127-138.
- 38. Maldonado, L.A., Fenical, W., et al., Salinispora arenicola gen. nov., sp. nov. and Salinispora tropica sp. nov., obligate marine actinomycetes belonging to the family Micromonosporaceae. International journal of systematic and evolutionary microbiology, 2005. **55**(5): p. 1759-1766.
- 39. Girão, M., Ribeiro, I., et al., *Actinobacteria from marine environments: A unique source of natural products*, in *Natural Products from Actinomycetes: Diversity, Ecology and Drug Discovery.* 2022, Springer. p. 1-45.

- 40. Manivasagan, P., Venkatesan, J., et al., *Pharmaceutically active secondary metabolites of marine actinobacteria.* Microbiological research, 2014. **169**(4): p. 262-278.
- 41. Carroll, A.R., Copp, B.R., et al., *Marine natural products*. Natural Product Reports, 2023. **40**(2): p. 275-325.
- 42. Feling, R.H., Buchanan, G.O., et al., Salinosporamide A: a highly cytotoxic proteasome inhibitor from a novel microbial source, a marine bacterium of the new genus Salinospora. Angewandte Chemie International Edition, 2003. **42**(3): p. 355-357.
- 43. Roth, P., Gorlia, T., et al., *Marizomib for patients with newly diagnosed glioblastoma: a randomized phase 3 trial.* Neuro-oncology, 2024: p. noae053.
- 44. Adnani, N., Rajski, S.R., et al., *Symbiosis-inspired approaches to antibiotic discovery.* Natural product reports, 2017. **34**(7): p. 784-814.
- 45. Pereira, L., *Macroalgae*. Encyclopedia, 2021. **1**(1): p. 177-188.
- 46. Egan, S., Harder, T., et al., *The seaweed holobiont: understanding seaweed-bacteria interactions.* FEMS Microbiology Reviews, 2013. **37**(3): p. 462-476.
- 47. Martin, M., Portetelle, D., et al., *Microorganisms living on macroalgae: diversity, interactions, and biotechnological applications.* Applied microbiology and biotechnology, 2014. **98**: p. 2917-2935.
- 48. Niehs, S.P., Kumpfmüller, J., et al., *Insect-associated bacteria assemble the antifungal butenolide gladiofungin by non-canonical polyketide chain termination.*Angewandte Chemie International Edition, 2020. **59**(51): p. 23122-23126.
- 49. Afonso, N.C., Catarino, M.D., et al., *Brown macroalgae as valuable food ingredients*. Antioxidants, 2019. **8**(9): p. 365.
- 50. Pimentel, F.B., Alves, R.C., et al., *Macroalgae-derived ingredients for cosmetic industry—An update.* Cosmetics, 2017. **5**(1): p. 2.
- 51. Priyanka, K., Rajaram, R., et al., *A critical review on pharmacological properties of marine macroalgae*. Biomass Conversion and Biorefinery, 2022: p. 1-25.
- 52. Seghetta, M., Hou, X., et al., *Life cycle assessment of macroalgal biorefinery for the production of ethanol, proteins and fertilizers—a step towards a regenerative bioeconomy.* Journal of Cleaner production, 2016. **137**: p. 1158-1169.
- 53. Peteiro, C., *Alginate production from marine macroalgae, with emphasis on kelp farming.* Alginates and their biomedical applications, 2018: p. 27-66.
- 54. Sudhakar, K., Mamat, R., et al., *An overview of marine macroalgae as bioresource.* Renewable and Sustainable Energy Reviews, 2018. **91**: p. 165-179.
- 55. Sudek, S., Lopanik, N.B., et al., *Identification of the putative bryostatin polyketide* synthase gene cluster from "Candidatus Endobugula sertula", the uncultivated

- microbial symbiont of the marine bryozoan Bugula neritina. Journal of natural products, 2007. **70**(1): p. 67-74.
- 56. Egan, S., Thomas, T., et al., *Unlocking the diversity and biotechnological potential of marine surface associated microbial communities.* Current opinion in microbiology, 2008. **11**(3): p. 219-225.
- 57. Wood, G., Steinberg, P.D., et al., *Host genetics, phenotype and geography structure the microbiome of a foundational seaweed.* Molecular Ecology, 2022. **31**(7): p. 2189-2206.
- 58. Parrot, D., Blümel, M., et al., *Mapping the surface microbiome and metabolome* of brown seaweed Fucus vesiculosus by amplicon sequencing, integrated metabolomics and imaging techniques. Scientific reports, 2019. **9**(1): p. 1061.
- 59. Alvarado, P., Huang, Y., et al., *Phylogeny and bioactivity of epiphytic Gram- positive bacteria isolated from three co-occurring antarctic macroalgae.* Antonie van Leeuwenhoek, 2018. **111**(9): p. 1543-1555.
- 60. Braña, A.F., Fiedler, H.-P., et al., *Two Streptomyces species producing antibiotic,* antitumor, and anti-inflammatory compounds are widespread among intertidal macroalgae and deep-sea coral reef invertebrates from the central Cantabrian Sea. Microbial ecology, 2015. **69**(3): p. 512-524.
- 61. Cho, J.Y. and Kim, M.S., *Antibacterial benzaldehydes produced by seaweed-derived Streptomyces atrovirens PK288-21.* Fisheries science, 2012. **78**(5): p. 1065-1073.
- 62. Girão, M., Ribeiro, I., et al., *Actinobacteria isolated from Laminaria ochroleuca: a source of new bioactive compounds.* Frontiers in Microbiology, 2019. **10**: p. 683.
- 63. Goecke, F., Labes, A., et al., *Phylogenetic analysis and antibiotic activity of bacteria isolated from the surface of two co-occurring macroalgae from the Baltic Sea*. European journal of phycology, 2013. **48**(1): p. 47-60.
- 64. Kim, M.C., Machado, H., et al., *Integration of genomic data with NMR analysis enables assignment of the full stereostructure of neaumycin B, a potent inhibitor of glioblastoma from a marine-derived Micromonospora*. Journal of the American Chemical Society, 2018. **140**(34): p. 10775-10784.
- 65. Rajivgandhi, G., Vijayan, R., et al., *Molecular characterization and antibacterial* effect of endophytic actinomycetes Nocardiopsis sp. GRG1 (KT235640) from brown algae against MDR strains of uropathogens. Bioactive materials, 2016. **1**(2): p. 140-150.
- 66. Uzair, B., Menaa, F., et al., Isolation, purification, structural elucidation and antimicrobial activities of kocumarin, a novel antibiotic isolated from

- actinobacterium Kocuria marina CMG S2 associated with the brown seaweed Pelvetia canaliculata. Microbiological research, 2018. **206**: p. 186-197.
- 67. Villarreal-Gómez, L.J., Soria-Mercado, I.E., et al., *Antibacterial and anticancer activity of seaweeds and bacteria associated with their surface.* Revista de biología marina y oceanografía, 2010. **45**(2): p. 267-275.
- 68. Wang, M., Chen, L., et al., Screening of alginate lyase-excreting microorganisms from the surface of brown algae. AMB Express, 2017. **7**(1): p. 1-9.
- 69. Wiese, J., Thiel, V., et al., *Diversity of antibiotic-active bacteria associated with the brown alga Laminaria saccharina from the Baltic Sea.* Marine Biotechnology, 2009. **11**(2): p. 287-300.
- Santhi, V.S., Bhagat, A.K., et al., Seaweed (Eucheuma cottonii) associated microorganisms, a versatile enzyme source for the lignocellulosic biomass processing. International Biodeterioration & Biodegradation, 2014. 96: p. 144-151.
- 71. Ulfah, M., Kasanah, N., et al., *Antivibriosis and cytotoxicity of Actinobacteria associated with red seaweed Gelidiella acerosa*. Aquaculture Research, 2021. **52**(12): p. 6786-6794.
- 72. Carroll, A.R., Copp, B.R., et al., *Marine natural products*. Natural product reports, 2019. **36**(1): p. 122-173.
- 73. Park, N.-H., Hong, Y.-K., et al., Screening anti-inflammatory actinomycetes isolated from seaweeds and marine sediments. Korean Journal of Fisheries and Aquatic Sciences, 2006. **39**(4): p. 333-337.
- 74. D'Archino, R. and Piazzi, L., *Macroalgal assemblages as indicators of the ecological status of marine coastal systems: A review.* Ecological Indicators, 2021. **129**: p. 107835.
- 75. Dayton, P.K., Competition, disturbance, and community organization: the provision and subsequent utilization of space in a rocky intertidal community. Ecological Monographs, 1971. **41**(4): p. 351-389.
- 76. Quigley, C.T., Capistrant-Fossa, K.A., et al., *Bacterial communities show algal host (Fucus spp.)/zone differentiation across the stress gradient of the intertidal zone.* Frontiers in microbiology, 2020. **11**: p. 563118.
- 77. Rothäusler, E., Dobretsov, S., et al., Effect of UV-radiation on the physiology of the invasive green seaweed Codium fragile and its associated bacteria. Marine Environmental Research, 2022. **180**: p. 105708.
- 78. Malik, S.A.A., Bedoux, G., et al., *Defence on surface: macroalgae and their surface-associated microbiome*, in *Advances in botanical research*. 2020, Elsevier. p. 327-368.

- 79. Girão, M., Ribeiro, I., et al., *Actinobacteria isolated from Laminaria ochroleuca: a source of new bioactive compounds.* Frontiers in Microbiology, 2019: p. 683.
- 80. Cho, J.Y., Kang, J.Y., et al., *Isolation and structural determination of the antifouling diketopiperazines from marine-derived Streptomyces praecox 291-11.*Bioscience, biotechnology, and biochemistry, 2012. **76**(6): p. 1116-1121.
- 81. Matsuo, Y., Kanoh, K., et al., *Streptobactin, a tricatechol-type siderophore from marine-derived Streptomyces sp. YM5-799.* Journal of natural products, 2011. **74**(11): p. 2371-2376.
- 82. Nguyen, T.N.T., Chataway, T., et al., *Purification and characterization of a novel alginate lyase from a marine Streptomyces species isolated from seaweed.*Marine Drugs, 2021. **19**(11): p. 590.
- 83. Djinni, I., Defant, A., et al., *Antibacterial polyketides from the marine alga-derived endophitic Streptomyces sundarbansensis: a study on hydroxypyrone tautomerism.* Marine Drugs, 2013. **11**(1): p. 124-135.
- 84. Jiang, Z.-D., Jensen, P.R., et al., *Lobophorins A and B, new antiinflammatory macrolides produced by a tropical marine bacterium.* Bioorganic & Medicinal Chemistry Letters, 1999. **9**(14): p. 2003-2006.
- 85. Katif, C., Chilczuk, T., et al., *Isolation and structure elucidation of desferrioxamine* b and the new desferrioxamine b2 antibiotics from a brown marine macroalga carpodesmia tamariscifolia associated streptomyces isolate. Biointerface Res. Appl. Chem, 2022. **12**: p. 5647-5662.
- 86. Hong, Y.-K. and Cho, J.Y., Effect of seaweed epibiotic bacterium Streptomyces violaceoruber SCH-09 on marine fouling organisms. Fisheries Science, 2013. **79**: p. 469-475.
- 87. Kanagasabhapathy, M., Sasaki, H., et al., *Phylogenetic identification of epibiotic bacteria possessing antimicrobial activities isolated from red algal species of Japan.* World Journal of Microbiology and Biotechnology, 2008. **24**(10): p. 2315-2321.
- 88. Ulfah, M., Kasanah, N., et al., *Bioactivity and genetic screening of marine Actinobacteria associated with red algae Gelidiella acerosa.* Indonesian Journal of Biotechnology, 2017. **22**(1): p. 13-21.
- 89. Penesyan, A., Marshall-Jones, Z., et al., *Antimicrobial activity observed among cultured marine epiphytic bacteria reflects their potential as a source of new drugs.* FEMS microbiology ecology, 2009. **69**(1): p. 113-124.
- 90. Braña, A.F., Sarmiento-Vizcaíno, A., et al., *Desertomycin G, a New Antibiotic with Activity against Mycobacterium tuberculosis and Human Breast Tumor Cell Lines*

- Produced by Streptomyces althioticus MSM3, Isolated from the Cantabrian Sea Intertidal Macroalgae Ulva sp. Marine drugs, 2019. **17**(2): p. 114.
- 91. Zhang, X., Chen, L., et al., *A unique indolizinium alkaloid streptopertusacin A and bioactive bafilomycins from marine-derived Streptomyces sp. HZP-2216E.* Phytochemistry, 2017. **144**: p. 119-126.
- 92. Zhang, Z., Chen, L., et al., *Bioactive bafilomycins and a new N-Arylpyrazinone derivative from marine-derived Streptomyces sp. HZP-2216E.* Planta Medica, 2017. **83**(18): p. 1405-1411.
- 93. Chen, Z., Hao, J., et al., New α-glucosidase inhibitors from marine algae-derived Streptomyces sp. OUCMDZ-3434. Scientific reports, 2016. **6**(1): p. 1-9.
- 94. Hertweck, C., *The biosynthetic logic of polyketide diversity*. Angewandte Chemie International Edition, 2009. **48**(26): p. 4688-4716.
- 95. Liu, H., Chen, Z., et al., *Phenolic polyketides from the marine alga-derived Streptomyces sp. OUCMDZ-3434*. Tetrahedron, 2017. **73**(36): p. 5451-5455.
- 96. Seiple, I.B., Zhang, Z., et al., *A platform for the discovery of new macrolide antibiotics*. Nature, 2016. **533**(7603): p. 338-345.
- 97. Hider, R.C. and Kong, X., *Chemistry and biology of siderophores*. Natural product reports, 2010. **27**(5): p. 637-657.
- 98. Ali, S.S. and Vidhale, N., *Bacterial siderophore and their application: a review.* Int J Curr Microbiol App Sci, 2013. **2**(12): p. 303-312.
- 99. P de Carvalho, M. and Abraham, W.-R., *Antimicrobial and biofilm inhibiting diketopiperazines*. Current medicinal chemistry, 2012. **19**(21): p. 3564-3577.
- 100. Jin, H., Tian, L., et al., *Bioinspired marine antifouling coatings: Status, prospects, and future.* Progress in Materials Science, 2022. **124**: p. 100889.
- 101. Kavitha, A., Prabhakar, P., et al., Purification and biological evaluation of the metabolites produced by Streptomyces sp. TK-VL_333. Research in Microbiology, 2010. 161(5): p. 335-345.
- 102. Kim, K.-S., Cui, X., et al., Inhibitory effects of benzaldehyde derivatives from the marine fungus Eurotium sp. SF-5989 on inflammatory mediators via the induction of heme oxygenase-1 in lipopolysaccharide-stimulated RAW264. 7 macrophages. International Journal of Molecular Sciences, 2014. 15(12): p. 23749-23765.
- 103. Wang, S., Li, X.-M., et al., Chaetopyranin, a benzaldehyde derivative, and other related metabolites from Chaetomium globosum, an endophytic fungus derived from the marine red alga Polysiphonia urceolata. Journal of Natural Products, 2006. 69(11): p. 1622-1625.

- 104. Xu, T. and Zhang, X.-H., *Edwardsiella tarda: an intriguing problem in aquaculture*. Aquaculture, 2014. **431**: p. 129-135.
- 105. Yoshida, T., *Streptococcosis in aquaculture*. Gyobyo Kenkyu= Fish Pathology, 2016. **51**(2): p. 44-48.
- 106. AlSalhi, M.S., Elangovan, K., et al., *Synthesis of silver nanoparticles using plant derived 4-N-methyl benzoic acid and evaluation of antimicrobial, antioxidant and antitumor activity.* Saudi Journal of Biological Sciences, 2019. **26**(5): p. 970-978.
- 107. Mao, X., Yang, Q., et al., *Benzoic acid used as food and feed additives can regulate gut functions*. BioMed research international, 2019. **2019**.
- 108. Ye, J. and Chen, X., *Current Promising Strategies against Antibiotic-Resistant Bacterial Infections*. Antibiotics, 2023. **12**(1): p. 67.
- 109. Singh, R., Kumar, M., et al., *Microbial enzymes: industrial progress in 21st century*. 3 Biotech, 2016. **6**: p. 1-15.
- 110. Rab, E., Kekos, D., et al., α-pyrone polyketides from Streptomyces ambofaciens Bl0048, an endophytic actinobacterial strain isolated from the red alga Laurencia glandulifera. Marine Drugs, 2017. **15**(12): p. 389.
- 111. Eliwa, E.M., Abdel-Razek, A.S., et al., New naturally occurring phenolic derivatives from marine Nocardiopsis sp. AS23C: Structural elucidation and in silico computational studies. Vietnam Journal of Chemistry, 2019. **57**(2): p. 164-174.
- 112. Lok, C., Mining the microbial dark matter. Nature, 2015. **522**(7556): p. 270.
- 113. Harvey, A.L., Edrada-Ebel, R., et al., The re-emergence of natural products for drug discovery in the genomics era. Nature reviews drug discovery, 2015. 14(2): p. 111-129.
- 114. Mahapatra, G.P., Raman, S., et al., *Metagenomics approaches in discovery and development of new bioactive compounds from marine actinomycetes.* Current Microbiology, 2020. **77**: p. 645-656.
- 115. Ghai, R., Mizuno, C.M., et al., *Metagenomics uncovers a new group of low GC and ultra-small marine Actinobacteria*. Scientific reports, 2013. **3**(1): p. 2471.
- 116. Piel, J., Hui, D., et al., Antitumor polyketide biosynthesis by an uncultivated bacterial symbiont of the marine sponge Theonella swinhoei. Proceedings of the National Academy of Sciences, 2004. **101**(46): p. 16222-16227.
- 117. Wang, J., Tang, X., et al., *Metagenome-assembled genomes from Pyropia haitanensis microbiome provide insights into the potential metabolic functions to the seaweed.* Frontiers in Microbiology, 2022. **13**: p. 857901.
- 118. Martin, M., Biver, S., et al., *Identification and characterization of a halotolerant,* cold-active marine endo-β-1, 4-glucanase by using functional metagenomics of

- *seaweed-associated microbiota.* Applied and environmental microbiology, 2014. **80**(16): p. 4958-4967.
- 119. Barka, E.A., Vatsa, P., et al., *Taxonomy, physiology, and natural products of Actinobacteria*. Microbiology and molecular biology reviews, 2016. **80**(1): p. 1-43.
- 120. Bull, A.T., Stach, J.E., et al., *Marine actinobacteria: perspectives, challenges, future directions*. Antonie Van Leeuwenhoek, 2005. **87**: p. 65-79.
- 121. Abdel-Kareem, M.S. and ElSaied, A.A., *Global seaweeds diversity*, in *Handbook of Algal Biofuels*. 2022, Elsevier. p. 39-55.
- 122. Ortega, A., Geraldi, N.R., et al., *Important contribution of macroalgae to oceanic carbon sequestration*. Nature Geoscience, 2019. **12**(9): p. 748-754.
- 123. Chan, C.-X., Ho, C.-L., et al., *Trends in seaweed research.* Trends in Plant Science, 2006. **11**(4): p. 165-166.
- 124. Deepika, C., Ravishankar, G.A., et al., *Potential products from macroalgae: An overview.* Sustainable Global Resources Of Seaweeds Volume 1: Bioresources, cultivation, trade and multifarious applications, 2022: p. 17-44.
- 125. García-Vaquero, M. and Hayes, M., Red and green macroalgae for fish and animal feed and human functional food development. Food Reviews International, 2016. **32**(1): p. 15-45.
- 126. Hamed, S.M., Abd El-Rhman, A.A., et al., *Role of marine macroalgae in plant protection & improvement for sustainable agriculture technology.* Beni-Suef University Journal of Basic and Applied Sciences, 2018. **7**(1): p. 104-110.
- 127. Ghadiryanfar, M., Rosentrater, K.A., et al., *A review of macroalgae production, with potential applications in biofuels and bioenergy.* Renewable and Sustainable Energy Reviews, 2016. **54**: p. 473-481.
- 128. Barbosa, M., Valentão, P., et al., *Bioactive compounds from macroalgae in the new millennium: implications for neurodegenerative diseases.* Marine drugs, 2014. **12**(9): p. 4934-4972.
- 129. Cikoš, A.-M., Šubarić, D., et al., *Recent advances on macroalgal pigments and their biological activities (2016–2021).* Algal Research, 2022. **65**: p. 102748.
- 130. Cornish, M.L. and Garbary, D.J., *Antioxidants from macroalgae: potential applications in human health and nutrition.* Algae, 2010. **25**(4): p. 155-171.
- 131. Olasehinde, T.A., Olaniran, A.O., et al., *Macroalgae as a valuable source of naturally occurring bioactive compounds for the treatment of Alzheimer's disease*. Marine drugs, 2019. **17**(11): p. 609.
- 132. Braña, A.F., Fiedler, H.-P., et al., *Two Streptomyces species producing antibiotic,* antitumor, and anti-inflammatory compounds are widespread among intertidal

- macroalgae and deep-sea coral reef invertebrates from the central Cantabrian Sea. Microbial ecology, 2015. **69**: p. 512-524.
- 133. Wiese, J., Thiel, V., et al., *Diversity of antibiotic-active bacteria associated with the brown alga Laminaria saccharina from the Baltic Sea.* Marine Biotechnology, 2009. **11**: p. 287-300.
- 134. Cho, J.Y. and Kim, M.S., *Antibacterial benzaldehydes produced by seaweed-derived Streptomyces atrovirens PK288-21.* Fisheries science, 2012. **78**: p. 1065-1073.
- 135. Kanagasabhapathy, M., Sasaki, H., et al., *Phylogenetic identification of epibiotic bacteria possessing antimicrobial activities isolated from red algal species of Japan.* World Journal of Microbiology and Biotechnology, 2008. **24**: p. 2315-2321.
- 136. Gaspar, R., Pereira, L., et al., *The seaweed resources of Portugal.* Botanica Marina, 2019. **62**(5): p. 499-525.
- 137. Ghaderiardakani, F., Coates, J.C., et al., *Bacteria-induced morphogenesis of Ulva intestinalis and Ulva mutabilis (Chlorophyta): a contribution to the lottery theory.* FEMS Microbiology Ecology, 2017. **93**(8): p. fix094.
- 138. Hmani, I., Ghaderiardakani, F., et al., *High-temperature stress induces bacteria-specific adverse and reversible effects on Ulva (Chlorophyta) growth and its chemosphere in a reductionist model system.* Botanica Marina, 2023(0).
- 139. Bondoso, J., Balague, V., et al., *Community composition of the Planctomycetes associated with different macroalgae.* FEMS microbiology ecology, 2014. **88**(3): p. 445-456.
- 140. Picon, A., Del Olmo, A., et al., *Bacterial diversity in six species of fresh edible seaweeds submitted to high pressure processing and long-term refrigerated storage*. Food Microbiology, 2021. **94**: p. 103646.
- 141. Weisburg, W.G., Barns, S.M., et al., 16S ribosomal DNA amplification for phylogenetic study. Journal of bacteriology, 1991. **173**(2): p. 697-703.
- 142. Chun, J., Lee, J.-H., et al., *EzTaxon: a web-based tool for the identification of prokaryotes based on 16S ribosomal RNA gene sequences.* International journal of systematic and evolutionary microbiology, 2007. **57**(10): p. 2259-2261.
- 143. Edgar, R.C., *MUSCLE: multiple sequence alignment with high accuracy and high throughput.* Nucleic acids research, 2004. **32**(5): p. 1792-1797.
- 144. Kumar, S., Stecher, G., et al., *MEGA X: molecular evolutionary genetics analysis across computing platforms.* Molecular biology and evolution, 2018. **35**(6): p. 1547.

- 145. Letunic, I. and Bork, P., Interactive Tree Of Life (iTOL) v5: an online tool for phylogenetic tree display and annotation. Nucleic acids research, 2021. 49(W1): p. W293-W296.
- 146. Arkin, A.P., Cottingham, R.W., et al., *KBase: the United States department of energy systems biology knowledgebase.* Nature biotechnology, 2018. **36**(7): p. 566-569.
- 147. Bolger, A.M., Lohse, M., et al., *Trimmomatic: a flexible trimmer for Illumina sequence data*. Bioinformatics, 2014. **30**(15): p. 2114-2120.
- Andrews, S., FastQC: a quality control tool for high throughput sequence data.
 Babraham Bioinformatics, Babraham Institute, Cambridge, United Kingdom.
- 149. Menzel, P., Ng, K.L., et al., *Fast and sensitive taxonomic classification for metagenomics with Kaiju*. Nature communications, 2016. **7**(1): p. 11257.
- 150. Morrissey, K.L., Çavaş, L., et al., *Disentangling the influence of environment, host specificity and thallus differentiation on bacterial communities in siphonous green seaweeds.* Frontiers in Microbiology, 2019. **10**: p. 717.
- 151. Abdelmohsen, U.R., Pimentel-Elardo, S.M., et al., *Isolation, phylogenetic* analysis and anti-infective activity screening of marine sponge-associated actinomycetes. Marine drugs, 2010. **8**(3): p. 399-412.
- 152. Valli, S., Suvathi, S.S., et al., *Antimicrobial potential of Actinomycetes species isolated from marine environment.* Asian Pacific Journal of Tropical Biomedicine, 2012. **2**(6): p. 469-473.
- 153. Zainal Abidin, Z.A., Abdul Malek, N., et al., Selective isolation and antagonistic activity of actinomycetes from mangrove forest of Pahang, Malaysia. Frontiers in Life Science, 2016. **9**(1): p. 24-31.
- 154. Okazaki, T., Kitahara, T., et al., Studies on marine microorganisms. IV a new antibiotic SS-228 Y produced by chainia isolated from shallow sea mud. The journal of antibiotics, 1975. **28**(3): p. 176-184.
- 155. Tian, X., Zhang, Z., et al., Comparative genomics analysis of Streptomyces species reveals their adaptation to the marine environment and their diversity at the genomic level. Frontiers in Microbiology, 2016. **7**: p. 998.
- 156. Hutchings, M.I., Truman, A.W., et al., *Antibiotics: past, present and future.*Current opinion in microbiology, 2019. **51**: p. 72-80.
- 157. Xiong, Z., Wang, R., et al., *Natural products and biological activity from actinomycetes associated with marine algae.* Molecules, 2023. **28**(13): p. 5138.

- 158. Eltamany, E.E., Abdelmohsen, U.R., et al., *New antibacterial xanthone from the marine sponge-derived Micrococcus sp. EG45.* Bioorganic & medicinal chemistry letters, 2014. **24**(21): p. 4939-4942.
- 159. Labeda, D. and Kroppenstedt, R., Stackebrandtia nassauensis gen. nov., sp. nov. and emended description of the family Glycomycetaceae. International journal of systematic and evolutionary microbiology, 2005. **55**(4): p. 1687-1691.
- 160. Microbispora, M., *The family Thermomonosporaceae: Actinocorallia, actinomadura, spirillospora and thermomonospora.* A Handbook on the Biology of Bacteria, 2006. **3**: p. 682-724.
- 161. Nishijima, M., Tazato, N., et al., *Krasilnikoviella muralis gen. nov., sp. nov., a member of the family Promicromonosporaceae, isolated from the Takamatsuzuka Tumulus stone chamber interior and reclassification of Promicromonospora flava as Krasilnikoviella flava comb. nov.* International Journal of Systematic and Evolutionary Microbiology, 2017. **67**(2): p. 294-300.
- 162. Wang, Y.-X., Zhi, X.-Y., et al., *Stackebrandtia albiflava sp. nov. and emended description of the genus Stackebrandtia*. International journal of systematic and evolutionary microbiology, 2009. **59**(3): p. 574-577.
- 163. Rego, A., Raio, F., et al., *Actinobacteria and cyanobacteria diversity in terrestrial antarctic microenvironments evaluated by culture-dependent and independent methods.* Frontiers in microbiology, 2019. **10**: p. 1018.
- 164. Kim, M., Oh, H.-S., et al., Towards a taxonomic coherence between average nucleotide identity and 16S rRNA gene sequence similarity for species demarcation of prokaryotes. International journal of systematic and evolutionary microbiology, 2014. 64(Pt_2): p. 346-351.
- 165. Bennur, T., Ravi Kumar, A., et al., *Nocardiopsis species: a potential source of bioactive compounds*. Journal of applied microbiology, 2016. **120**(1): p. 1-16.
- 166. Elsayed, Y., Refaat, J., et al., *The Genus Rhodococcus as a source of novel bioactive substances: A review.* Journal of Pharmacognosy and Phytochemistry, 2017. **6**(3): p. 83-92.
- 167. Hopwood, D.A., *Streptomyces in nature and medicine: the antibiotic makers.* 2007: Oxford University Press.
- 168. Komaki, H., Resolution of housekeeping gene sequences used in MLSA for the genus Streptomyces and reclassification of Streptomyces anthocyanicus and Streptomyces tricolor as heterotypic synonyms of Streptomyces violaceoruber. International Journal of Systematic and Evolutionary Microbiology, 2022. 72(5): p. 005370.

- 169. Singh, P., Raghukumar, C., et al., Fungal diversity in deep-sea sediments revealed by culture-dependent and culture-independent approaches. Fungal Ecology, 2012. **5**(5): p. 543-553.
- 170. Sun, W., Dai, S., et al., Culture-dependent and culture-independent diversity of Actinobacteria associated with the marine sponge Hymeniacidon perleve from the South China Sea. Antonie van leeuwenhoek, 2010. **98**: p. 65-75.
- 171. Califano, G., Kwantes, M., et al., Cultivating the macroalgal holobiont: effects of integrated multi-trophic aquaculture on the microbiome of Ulva rigida (Chlorophyta). Frontiers in Marine Science, 2020. **7**: p. 52.
- 172. Stackebrandt, E., *The family acidimicrobiaceae.* The Prokaryotes: Actinobacteria, 2014: p. 1-1061.
- 173. Matsumoto, A., Kasai, H., et al., *Ilumatobacter fluminis gen. nov., sp. nov., a novel actinobacterium isolated from the sediment of an estuary.* The Journal of general and applied microbiology, 2009. **55**(3): p. 201-205.
- 174. Matsumoto, A., Kasai, H., et al., *Ilumatobacter nonamiense sp. nov. and Ilumatobacter coccineum sp. nov., isolated from seashore sand.* International journal of systematic and evolutionary microbiology, 2013. **63**(Pt_9): p. 3404-3408.
- 175. Montalvo, N.F., Mohamed, N.M., et al., *Novel actinobacteria from marine sponges*. Antonie Van Leeuwenhoek, 2005. **87**: p. 29-36.
- 176. He, Y.-Q., Chen, R.-W., et al., *Actinomarinicola tropica gen. nov. sp. nov., a new marine actinobacterium of the family lamiaceae, isolated from South China Sea sediment environments.* International Journal of Systematic and Evolutionary Microbiology, 2020. **70**(6): p. 3852-3858.
- 177. Jin, L., Huy, H., et al., *Aquihabitans daechungensis gen. nov., sp. nov., an actinobacterium isolated from reservoir water.* International journal of systematic and evolutionary microbiology, 2013. **63**(Pt_8): p. 2970-2974.
- 178. Kurahashi, M., Fukunaga, Y., et al., *lamia majanohamensis gen. nov., sp. nov.,* an actinobacterium isolated from sea cucumber Holothuria edulis, and proposal of lamiaceae fam. nov. International journal of systematic and evolutionary microbiology, 2009. **59**(4): p. 869-873.
- 179. Kuba, G.M., Spalding, H.L., et al., *Microbiota-Macroalgal Relationships at a Hawaiian Intertidal Bench Are Influenced by Macroalgal Phyla and Associated Thallus Complexity*. Msphere, 2021. **6**(5): p. e00665-21.
- 180. Li, H., Li, J.J., et al., *The influence of host specificity and temperature on bacterial communities associated with Sargassum (Phaeophyceae) species.* Journal of Phycology, 2022. **58**(6): p. 815-828.

- 181. Sanders-Smith, R., Segovia, B.T., et al., *Host-specificity and core taxa of seagrass leaf microbiome identified across tissue age and geographical regions.*Frontiers in Ecology and Evolution, 2020. **8**: p. 605304.
- 182. Roth-Schulze, A.J., Pintado, J., et al., Functional biogeography and host specificity of bacterial communities associated with the Marine Green Alga Ulva spp. Molecular ecology, 2018. **27**(8): p. 1952-1965.
- 183. Meyer, J., *Nocardiopsis, a new genus of the order Actinomycetales*. International Journal of Systematic and Evolutionary Microbiology, 1976. **26**(4): p. 487-493.
- 184. Rainey, F.A., Ward-Rainey, N., et al., *The genus Nocardiopsis represents a phylogenetically coherent taxon and a distinct actinomycete lineage: proposal of Nocardiopsaceae fam. nov.* International Journal of Systematic and Evolutionary Microbiology, 1996. **46**(4): p. 1088-1092.
- 185. Salam, N., Jiao, J.-Y., et al., *Update on the classification of higher ranks in the phylum Actinobacteria*. International journal of systematic and evolutionary microbiology, 2020. **70**(2): p. 1331-1355.
- 186. Hozzein, W.N. and Trujillo, M.E., *Nocardiopsis*. Bergey's Manual of Systematics of Archaea and Bacteria, 2015: p. 1-28.
- 187. Kumar, S., Solanki, D.S., et al., *Actinomycetes isolates of arid zone of Indian Thar Desert and efficacy of their bioactive compounds against human pathogenic bacteria.* Biologia Futura, 2021. **72**: p. 431-440.
- 188. Xu, S., Yan, L., et al., Nocardiopsis fildesensis sp. nov., an actinomycete isolated from soil. International journal of systematic and evolutionary microbiology, 2014.
 64(Pt_1): p. 174-179.
- 189. Pinto-Almeida, A., Bauermeister, A., et al., *The diversity, metabolomics profiling,* and the pharmacological potential of actinomycetes isolated from the Estremadura Spur pockmarks (Portugal). Marine drugs, 2021. **20**(1): p. 21.
- 190. Chen, L., Wang, Z., et al., *Antimicrobial activity and functional genes of actinobacteria from coastal wetland.* Current Microbiology, 2021. **78**(8): p. 3058-3067.
- 191. Tatar, D., Isolation, phylogenetic analysis and antimicrobial activity of halophilic actinomycetes from different saline environments located near Çorum province. Biologia, 2021. **76**(2): p. 773-780.
- 192. Shi, T., Wang, Y.-F., et al., *Genus Nocardiopsis: a prolific producer of natural products*. Marine Drugs, 2022. **20**(6): p. 374.
- 193. Hozzein, W.N., Li, W.-J., et al., *Nocardiopsis alkaliphila sp. nov., a novel alkaliphilic actinomycete isolated from desert soil in Egypt.* International journal of systematic and evolutionary microbiology, 2004. **54**(1): p. 247-252.

- 194. Peltola, J.S., Andersson, M.A., et al., *Isolation of toxigenic Nocardiopsis strains* from indoor environments and description of two new Nocardiopsis species, N. exhalans sp. nov. and N. umidischolae sp. nov. Applied and Environmental Microbiology, 2001. **67**(9): p. 4293-4304.
- 195. Evtushenko, L.I., Taran, V.V., et al., *Nocardiopsis tropica sp. nov., Nocardiopsis trehalosi sp. nov., nom. rev. and Nocardiopsis dassonvillei subsp. albirubida subsp. nov., comb. nov.* International journal of systematic and evolutionary microbiology, 2000. **50**(1): p. 73-81.
- 196. Goodfellow, M. and Alderson, G., *The actinomycete-genus Rhodococcus: a home for the 'rhodochrous' complex*. Microbiology, 1977. **100**(1): p. 99-122.
- Matsuyama, H., Yumoto, I., et al., *Rhodococcus tukisamuensis sp. nov., isolated from soil.* International journal of systematic and evolutionary microbiology, 2003.
 53(5): p. 1333-1337.
- 198. Ghosh, A., Paul, D., et al., *Rhodococcus imtechensis sp. nov., a nitrophenol-degrading actinomycete*. International journal of systematic and evolutionary microbiology, 2006. **56**(8): p. 1965-1969.
- 199. Su, X., Liu, Y., et al., *Rhodococcus biphenylivorans sp. nov., a polychlorinated biphenyl-degrading bacterium.* Antonie Van Leeuwenhoek, 2015. **107**: p. 55-63.
- 200. Yassin, A., *Rhodococcus triatomae sp. nov., isolated from a blood-sucking bug.* International journal of systematic and evolutionary microbiology, 2005. **55**(4): p. 1575-1579.
- 201. Vereecke, D., Burssens, S., et al., *The Rhodococcus fascians-plant interaction:* morphological traits and biotechnological applications. Planta, 2000. **210**: p. 241-251.
- 202. Prescott, J.F., *Rhodococcus equi: an animal and human pathogen.* Clinical microbiology reviews, 1991. **4**(1): p. 20-34.
- 203. Larkin, M.J., Kulakov, L.A., et al., *Biodegradation and Rhodococcus–masters of catabolic versatility*. Current opinion in Biotechnology, 2005. **16**(3): p. 282-290.
- 204. Martínková, L., Uhnáková, B., et al., *Biodegradation potential of the genus Rhodococcus*. Environment international, 2009. **35**(1): p. 162-177.
- 205. Zampolli, J., Zeaiter, Z., et al., Genome analysis and-omics approaches provide new insights into the biodegradation potential of Rhodococcus. Applied microbiology and biotechnology, 2019. 103: p. 1069-1080.
- 206. Kuyukina, M.S. and Ivshina, I.B., *Rhodococcus biosurfactants: biosynthesis, properties, and potential applications*, in *Biology of rhodococcus*. 2010, Springer. p. 291-313.

- Chang, W.-N., Liu, C.-W., et al., Hydrophobic cell surface and bioflocculation behavior of Rhodococcus erythropolis. Process Biochemistry, 2009. 44(9): p. 955-962.
- 208. Kitagawa, W. and Tamura, T., *A quinoline antibiotic from Rhodococcus erythropolis JCM 6824*. The Journal of Antibiotics, 2008. **61**(11): p. 680-682.
- 209. Hu, X., Li, D., et al., *Purification, characterization and anticancer activities of exopolysaccharide produced by Rhodococcus erythropolis HX-2.* International journal of biological macromolecules, 2020. **145**: p. 646-654.
- 210. Yoon, S.-H., Ha, S.-M., et al., *Introducing EzBioCloud: a taxonomically united database of 16S rRNA gene sequences and whole-genome assemblies.* International journal of systematic and evolutionary microbiology, 2017. **67**(5): p. 1613.
- 211. Segata, N., Börnigen, D., et al., *PhyloPhlAn is a new method for improved phylogenetic and taxonomic placement of microbes. Nat Commun 4: 2304.* 2013.
- 212. Katoh, K. and Standley, D.M., *MAFFT multiple sequence alignment software version 7: improvements in performance and usability.* Molecular biology and evolution, 2013. **30**(4): p. 772-780.
- 213. Jain, C., Rodriguez-R, L.M., et al., *High throughput ANI analysis of 90K prokaryotic genomes reveals clear species boundaries.* Nature communications, 2018. **9**(1): p. 5114.
- 214. Wood, D.E. and Salzberg, S.L., *Kraken: ultrafast metagenomic sequence classification using exact alignments.* Genome biology, 2014. **15**(3): p. 1-12.
- 215. Li, H., Aligning sequence reads, clone sequences and assembly contigs with BWA-MEM. arXiv preprint arXiv:1303.3997, 2013.
- Bankevich, A., Nurk, S., et al., SPAdes: a new genome assembly algorithm and its applications to single-cell sequencing. Journal of computational biology, 2012.
 19(5): p. 455-477.
- 217. Blin, K., Shaw, S., et al., antiSMASH 7.0: New and improved predictions for detection, regulation, chemical structures and visualisation. Nucleic acids research, 2023: p. gkad344.
- 218. Shirling, E.T. and Gottlieb, D., *Methods for characterization of Streptomyces species*. International journal of systematic bacteriology, 1966. **16**(3): p. 313-340.
- 219. Waksman, S.A., *The Actinomycetes. Vol. II. Classification, identification and descriptions of genera and species.* The Actinomycetes. Vol. II. Classification, identification and descriptions of genera and species., 1961.
- 220. Williams, S., Goodfellow, M., et al., *Numerical classification of Streptomyces and related genera*. Microbiology, 1983. **129**(6): p. 1743-1813.

- 221. Da Costa, M.S., Albuquerque, L., et al., *The extraction and identification of respiratory lipoquinones of prokaryotes and their use in taxonomy*, in *Methods in microbiology*. 2011, Elsevier. p. 197-206.
- 222. Morais, P.V., Francisco, R., et al., Leucobacter chromiireducens sp. nov, and Leucobacter aridicollis sp. nov., two new species isolated from a chromium contaminated environment. Systematic and applied microbiology, 2004. **27**(6): p. 646-652.
- 223. Da Costa, M.S., Albuquerque, L., et al., *The identification of fatty acids in bacteria*, in *Methods in microbiology*. 2011, Elsevier. p. 183-196.
- 224. Schumann, P., *Peptidoglycan structure*, in *Methods in microbiology*. 2011, Elsevier. p. 101-129.
- 225. Chen, Y.-G., Zhang, Y.-Q., et al., *Nocardiopsis terrae sp. nov., a halophilic actinomycete isolated from saline soil.* Antonie van Leeuwenhoek, 2010. **98**: p. 31-38.
- 226. Sabry, S.A., Ghanem, N.B., et al., *Nocardiopsis aegyptia sp. nov., isolated from marine sediment.* International journal of systematic and evolutionary microbiology, 2004. **54**(2): p. 453-456.
- 227. Yang, R., Zhang, L.-P., et al., *Nocardiopsis valliformis sp. nov., an alkaliphilic actinomycete isolated from alkali lake soil in China.* International journal of systematic and evolutionary microbiology, 2008. **58**(7): p. 1542-1546.
- 228. Zhang, X., Zhang, L.-P., et al., *Nocardiopsis ganjiahuensis sp. nov., isolated from a soil from Ganjiahu, China.* International journal of systematic and evolutionary microbiology, 2008. **58**(1): p. 195-199.
- 229. Yoon, J.-H., Kang, S.-S., et al., *Rhodococcus pyridinivorans sp. nov., a pyridine-degrading bacterium.* International journal of systematic and evolutionary microbiology, 2000. **50**(6): p. 2173-2180.
- 230. Stoecker, M.A., Herwig, R.P., et al., *Rhodococcus zopfii sp. nov., a toxicant-degrading bacterium.* International Journal of Systematic and Evolutionary Microbiology, 1994. **44**(1): p. 106-110.
- 231. Ramaprasad, E., Mahidhara, G., et al., Rhodococcus electrodiphilus sp. nov., a marine electro active actinobacterium isolated from coral reef. International Journal of Systematic and Evolutionary Microbiology, 2018. 68(8): p. 2644-2649.
- 232. Zhao, G.-Z., Li, J., et al., Rhodococcus artemisiae sp. nov., an endophytic actinobacterium isolated from the pharmaceutical plant Artemisia annua L. International journal of systematic and evolutionary microbiology, 2012. 62(Pt_4): p. 900-905.

- 233. Tanizawa, Y., Fujisawa, T., et al., *DFAST: a flexible prokaryotic genome annotation pipeline for faster genome publication.* Bioinformatics, 2018. **34**(6): p. 1037-1039.
- 234. Rotter, A., Barbier, M., et al., *The essentials of marine biotechnology.* Frontiers In marine science, 2021. **8**: p. 158.
- 235. Pereira, L., Seaweed flora of the european north atlantic and mediterranean. Springer handbook of marine biotechnology, 2015: p. 65-178.
- 236. Jueterbock, A., Tyberghein, L., et al., Climate change impact on seaweed meadow distribution in the North Atlantic rocky intertidal. Ecology and evolution, 2013. **3**(5): p. 1356-1373.
- 237. Bull, A.T. and Stach, J.E., *Marine actinobacteria: new opportunities for natural product search and discovery.* Trends in microbiology, 2007. **15**(11): p. 491-499.
- 238. Subramani, R. and Sipkema, D., *Marine rare actinomycetes: a promising source of structurally diverse and unique novel natural products.* Marine drugs, 2019. **17**(5): p. 249.
- 239. Gogineni, V., Chen, X., et al., *Role of symbiosis in the discovery of novel antibiotics*. The Journal of Antibiotics, 2020. **73**(8): p. 490-503.
- 240. Girão, M., Alexandrino, D.A.M., et al., *Unveiling the culturable and non-culturable actinobacterial diversity in two macroalgae species from the northern Portuguese coast.* Environ Microbiol, 2024. **26**(4): p. e16620.
- 241. Castro, M., Preto, M., et al., Obesity: The metabolic disease, advances on drug discovery and natural product research. Current topics in medicinal chemistry, 2016. 16(23): p. 2577-2604.
- 242. Rossiter, S.E., Fletcher, M.H., et al., *Natural products as platforms to overcome antibiotic resistance*. Chemical reviews, 2017. **117**(19): p. 12415-12474.
- 243. Siegel, R.L., Miller, K.D., et al., *Cancer statistics, 2023.* Ca Cancer J Clin, 2023. **73**(1): p. 17-48.
- 244. Freitas, S., Silva, N.G., et al., *Chlorophyll derivatives from marine cyanobacteria* with lipid-reducing activities. Marine drugs, 2019. **17**(4): p. 229.
- Schindelin, J., Rueden, C.T., et al., *The ImageJ ecosystem: An open platform for biomedical image analysis*. Molecular reproduction and development, 2015.
 82(7-8): p. 518-529.
- 246. Gurevich, A., Mikheenko, A., et al., *Increased diversity of peptidic natural products revealed by modification-tolerant database search of mass spectra.*Nature microbiology, 2018. **3**(3): p. 319-327.

- 247. Mohimani, H., Gurevich, A., et al., *Dereplication of peptidic natural products through database search of mass spectra*. Nature chemical biology, 2017. **13**(1): p. 30-37.
- 248. Mohimani, H., Gurevich, A., et al., *Dereplication of microbial metabolites through database search of mass spectra*. Nature communications, 2018. **9**(1): p. 4035.
- 249. Wang, M., Carver, J.J., et al., Sharing and community curation of mass spectrometry data with Global Natural Products Social Molecular Networking. Nature biotechnology, 2016. **34**(8): p. 828-837.
- 250. Shannon, P., Markiel, A., et al., *Cytoscape: a software environment for integrated models of biomolecular interaction networks.* Genome research, 2003. **13**(11): p. 2498-2504.
- 251. van Santen, J.A., Poynton, E.F., et al., *The Natural Products Atlas 2.0: A database of microbially-derived natural products.* Nucleic Acids Research, 2022. **50**(D1): p. D1317-D1323.
- 252. Li, D., Luo, R., et al., *MEGAHIT v1. 0:* a fast and scalable metagenome assembler driven by advanced methodologies and community practices. Methods, 2016. **102**: p. 3-11.
- 253. Langmead, B. and Salzberg, S.L., *Fast gapped-read alignment with Bowtie 2.* Nature methods, 2012. **9**(4): p. 357-359.
- 254. Langmead, B., Wilks, C., et al., Scaling read aligners to hundreds of threads on general-purpose processors. Bioinformatics, 2019. **35**(3): p. 421-432.
- 255. Li, H., Handsaker, B., et al., *The sequence alignment/map format and SAMtools.* bioinformatics, 2009. **25**(16): p. 2078-2079.
- 256. Eren, A., Ö C Esen, C Quince, JH Vineis, HG Morrison, ML Sogin, and TO Delmont. Anvi'o: an advanced analysis and visualization platform for'omics data. PeerJ, 2015. **3**: p. e1319.
- 257. Hyatt, D., Chen, G.-L., et al., *Prodigal: prokaryotic gene recognition and translation initiation site identification.* BMC bioinformatics, 2010. **11**: p. 1-11.
- 258. Eddy, S.R., *Accelerated profile HMM searches*. PLoS computational biology, 2011. **7**(10): p. e1002195.
- 259. Alneberg, J., Bjarnason, B.S., et al., *Binning metagenomic contigs by coverage and composition*. Nature methods, 2014. **11**(11): p. 1144-1146.
- 260. Chaumeil, P.-A., Mussig, A.J., et al., *GTDB-Tk: a toolkit to classify genomes with the Genome Taxonomy Database*. 2020, Oxford University Press.
- 261. Parks, D.H., Imelfort, M., et al., *CheckM: assessing the quality of microbial genomes recovered from isolates, single cells, and metagenomes.* Genome research, 2015. **25**(7): p. 1043-1055.

- 262. Navarro-Muñoz, J.C., Selem-Mojica, N., et al., *A computational framework to explore large-scale biosynthetic diversity.* Nature chemical biology, 2020. **16**(1): p. 60-68.
- 263. Bondad-Reantaso, M.G., MacKinnon, B., et al., *Review of alternatives to antibiotic use in aquaculture*. Reviews in Aquaculture, 2023. **15**(4): p. 1421-1451.
- 264. Bister, B., Bischoff, D., et al., *Abyssomicin CA polycyclic antibiotic from a marine Verrucosispora strain as an inhibitor of the p-aminobenzoic acid/tetrahydrofolate biosynthesis pathway.* Angewandte Chemie-International Edition, 2004. **43**(19): p. 2574-2582.
- 265. Freundlich, J.S., Lalgondar, M., et al., *The abyssomicin C family as in vitro inhibitors of Mycobacterium tuberculosis*. Tuberculosis, 2010. **90**(5): p. 298-300.
- 266. Carlson, J.C., Li, S., et al., *Isolation and characterization of tirandamycins from a marine-derived Streptomyces sp.* Journal of natural products, 2009. **72**(11): p. 2076-2079.
- 267. Alvarado, P., Huang, Y., et al., *Phylogeny and bioactivity of epiphytic Gram- positive bacteria isolated from three co-occurring antarctic macroalgae.* Antonie Van Leeuwenhoek, 2018. **111**: p. 1543-1555.
- 268. Manzari, M.T., Shamay, Y., et al., *Targeted drug delivery strategies for precision medicines*. Nature Reviews Materials, 2021. **6**(4): p. 351-370.
- Zhang, M., Kim, J.A., et al., Optimizing tumor microenvironment for cancer immunotherapy: β-glucan-based nanoparticles. Frontiers in immunology, 2018.
 9: p. 341.
- 270. Zhou, Y., Li, X., et al., *Structural optimization and biological evaluation for novel artemisinin derivatives against liver and ovarian cancers.* European Journal of Medicinal Chemistry, 2021. **211**: p. 113000.
- 271. Gulder, T.A. and Moore, B.S., Salinosporamide natural products: Potent 20 S proteasome inhibitors as promising cancer chemotherapeutics. Angewandte Chemie International Edition, 2010. 49(49): p. 9346-9367.
- 272. Cho, A.-S., Jeon, S.-M., et al., *Chlorogenic acid exhibits anti-obesity property and improves lipid metabolism in high-fat diet-induced-obese mice.* Food and chemical toxicology, 2010. **48**(3): p. 937-943.
- 273. Weibel, E., Hadvary, P., et al., Lipstatin, an inhibitor of pancreatic lipase, produced by Streptomyces toxytricini I. Producing organism, fermentation, isolation and biological activity. The Journal of antibiotics, 1987. 40(8): p. 1081-1085.

- 274. Guerciolini, R., *Mode of action of orlistat*. International journal of obesity and related metabolic disorders: journal of the International Association for the Study of Obesity, 1997. **21**: p. S12-23.
- 275. Magwaza, S.t.N. and Islam, M.S., Roles of marine macroalgae or seaweeds and their bioactive compounds in combating overweight, obesity and diabetes: A comprehensive review. Marine Drugs, 2023. **21**(4): p. 258.
- 276. Takada, K., Ninomiya, A., et al., Surugamides a–e, cyclic octapeptides with four d-amino acid residues, from a marine Streptomyces sp.: Lc–ms-aided inspection of partial hydrolysates for the distinction of d-and l-amino acid residues in the sequence. The Journal of Organic Chemistry, 2013. **78**(13): p. 6746-6750.
- 277. Xu, F., Nazari, B., et al., *Discovery of a cryptic antifungal compound from Streptomyces albus J1074 using high-throughput elicitor screens.* Journal of the American Chemical Society, 2017. **139**(27): p. 9203-9212.
- 278. Huang, S., Liu, Y., et al., *The nonribosomal peptide valinomycin: From discovery to bioactivity and biosynthesis.* Microorganisms, 2021. **9**(4): p. 780.
- 279. Jalmakhanbetova, R., Suleimen, Y.M., et al., *Isolation and biological evaluation of roseofungin and its cyclodextrin inclusion complexes.* Вестник Карагандинского университета. Серия: Химия, 2020(4): p. 35-44.
- 280. Liu, J., Zhu, X., et al., *Antimycin-type depsipeptides: discovery, biosynthesis, chemical synthesis, and bioactivities.* Natural product reports, 2016. **33**(10): p. 1146-1165.
- 281. Pesic, A., Baumann, H.I., et al., Champacyclin, a new cyclic octapeptide from Streptomyces strain C42 isolated from the Baltic Sea. Marine Drugs, 2013. 11(12): p. 4834-4857.
- 282. Schlingmann, G., Milne, L., et al., *Strevertenes, antifungal pentaene macrolides produced by Streptoverticillcum LL-30F848.* Tetrahedron, 1999. **55**(19): p. 5977-5990.
- 283. Belknap, K.C., Park, C.J., et al., Genome mining of biosynthetic and chemotherapeutic gene clusters in Streptomyces bacteria. Scientific Reports, 2020. **10**(1): p. 2003.
- 284. Wiebach, V., Mainz, A., et al., *The anti-staphylococcal lipolanthines are ribosomally synthesized lipopeptides*. Nature chemical biology, 2018. **14**(7): p. 652-654.
- 285. Hegemann, J.D., Jeanne Dit Fouque, K., et al., A bifunctional leader peptidase/ABC transporter protein is involved in the maturation of the lasso peptide cochonodin I from Streptococcus suis. Journal of natural products, 2021. 84(10): p. 2683-2691.

- 286. Maruyama, C., Niikura, H., et al., tRNA-dependent aminoacylation of an amino sugar intermediate in the biosynthesis of a streptothricin-related antibiotic.

 Applied and Environmental Microbiology, 2016. **82**(12): p. 3640-3648.
- 287. Mizuno, C.M., Rodriguez-Valera, F., et al., Genomes of planktonic acidimicrobiales: widening horizons for marine actinobacteria by metagenomics. MBio, 2015. **6**(1): p. 10.1128/mbio. 02083-14.
- 288. Hu, D., Cha, G., et al., *A phylogenomic and molecular markers based analysis of the class Acidimicrobiia.* Frontiers in microbiology, 2018. **9**: p. 361535.
- 289. Bennett, J. and Bentley, R., Seeing red: the story of prodigiosin. 2000.
- 290. Castro, A., *Antimalarial activity of prodigiosin.* Nature, 1967. **213**(5079): p. 903-904.
- 291. Ehrenkaufer, G., Li, P., et al., *Identification of anisomycin, prodigiosin and obatoclax as compounds with broad-spectrum anti-parasitic activity.* PLoS neglected tropical diseases, 2020. **14**(3): p. e0008150.
- 292. Lapenda, J., Silva, P., et al., *Antimicrobial activity of prodigiosin isolated from Serratia marcescens UFPEDA 398.* World Journal of Microbiology and Biotechnology, 2015. **31**: p. 399-406.
- 293. Montaner, B. and Prez-Toms, R., *The prodigiosins: a new family of anticancer drugs*. Current cancer drug targets, 2003. **3**(1): p. 57-65.
- 294. Zhang, H., Peng, Y., et al., *Algicidal effects of prodigiosin on the harmful algae Phaeocystis globosa*. Frontiers in microbiology, 2016. **7**: p. 602.
- 295. Zhou, W., Zeng, C., et al., *Antiviral activity and specific modes of action of bacterial prodigiosin against Bombyx mori nucleopolyhedrovirus in vitro.* Applied microbiology and biotechnology, 2016. **100**(9): p. 3979-3988.
- 296. Paul, T., Bandyopadhyay, T.K., et al., *A comprehensive review on recent trends in production, purification, and applications of prodigiosin.* Biomass Conversion and Biorefinery, 2020: p. 1-23.
- 297. Austin, D.A. and Moss, M., *Numerical taxonomy of red-pigmented bacteria isolated from a lowland river, with the description of a new taxon, Rugamonas rubra gen. nov.*, sp. nov. Microbiology, 1986. **132**(7): p. 1899-1909.
- 298. Gerber, N.N. and Gauthier, M., *New prodigiosin-like pigment from Alteromonas rubra*. Applied and environmental microbiology, 1979. **37**(6): p. 1176-1179.
- 299. Harwood, C., Beneckea gazogenes sp. nov., a red, facultatively anaerobic, marine bacterium. Current Microbiology, 1978. **1**(4): p. 233-238.
- 300. Lee, J.S., Kim, Y.-S., et al., Exceptional production of both prodigiosin and cycloprodigiosin as major metabolic constituents by a novel marine bacterium,

- Zooshikella rubidus S1-1. Applied and environmental microbiology, 2011. **77**(14): p. 4967-4973.
- 301. Pradeep, S., Josh, M.S., et al., Achromobacter denitrificans SP1 produces pharmaceutically active 25C prodigiosin upon utilizing hazardous di (2-ethylhexyl) phthalate. Bioresource technology, 2014. **171**: p. 482-486.
- 302. Schloss, P.D., Allen, H.K., et al., *Psychrotrophic strain of Janthinobacterium lividum from a cold Alaskan soil produces prodigiosin.* DNA and cell biology, 2010. **29**(9): p. 533-541.
- 303. Kawauchi, K., Shibutani, K., et al., A Possible Immunosuppressant, Cycloprodigiosin Hydrochloride, Obtained fromPseudoalteromonas denitrificans. Biochemical and biophysical research communications, 1997. 237(3): p. 543-547.
- 304. Klein, A.S., Domröse, A., et al., New prodigiosin derivatives obtained by mutasynthesis in Pseudomonas putida. ACS synthetic biology, 2017. **6**(9): p. 1757-1765.
- 305. Berg, G., *Diversity of antifungal and plant-associated Serratia plymuthica strains.*Journal of Applied Microbiology, 2000. **88**(6): p. 952-960.
- 306. Halder, U., Banerjee, A., et al., *Production of prodigiosin by a drug-resistant Serratia rubidaea HB01 isolated from sewage.* Environmental Sustainability, 2020. **3**(3): p. 279-287.
- 307. Miao, L., Wang, X., et al., Optimization of the culture condition for an antitumor bacterium Serratia proteamacula 657 and identification of the active compounds. World Journal of Microbiology and Biotechnology, 2013. 29(5): p. 855-863.
- 308. Su, C., Xiang, Z., et al., Analysis of the genomic sequences and metabolites of Serratia surfactantfaciens sp. nov. YD25T that simultaneously produces prodigiosin and serrawettin W2. BMC genomics, 2016. **17**(1): p. 1-19.
- 309. Williams, R.P., *Biosynthesis of prodigiosin, a secondary metabolite of Serratia marcescens*. Applied microbiology, 1973. **25**(3): p. 396-402.
- 310. Allen, G.R., Reichelt, J.L., et al., *Influence of environmental factors and medium composition on Vibrio gazogenes growth and prodigiosin production.* Applied and Environmental Microbiology, 1983. **45**(6): p. 1727-1732.
- 311. Vitale, G.A., Sciarretta, M., et al., *Genomics–metabolomics profiling disclosed marine Vibrio spartinae 3.6 as a producer of a new branched side chain prodigiosin.* Journal of Natural Products, 2020. **83**(5): p. 1495-1504.
- 312. Bahrami, Y., Bouk, S., et al., *Natural products from Actinobacteria as a potential source of new therapies against colorectal cancer: A review.* Frontiers in Pharmacology, 2022. **13**.

- 313. Gerber, N.N., *Prodigiosin-like pigments from Actinomadura (Nocardia) pelletieri and Actinomadura madurae.* Applied microbiology, 1969. **18**(1): p. 1-3.
- 314. Gerber, N.N., *A new prodiginine (prodigiosin-like) pigment from streptomyces.*Antimalarial activity of several prodiginines. The Journal of Antibiotics, 1975.

 28(3): p. 194-199.
- 315. Harashima, K., Tsuchida, N., et al., *Prodigiosin-25 C: isolation and the chemical structure.* Agricultural and Biological Chemistry, 1967. **31**(4): p. 481-489.
- 316. Islan, G.A., Rodenak-Kladniew, B., et al., *Prodigiosin: a promising biomolecule with many potential biomedical applications*. Bioengineered, 2022. **13**(6): p. 14227-14258.
- 317. Kawasaki, T., Sakurai, F., et al., *A prodigiosin from the roseophilin producer Streptomyces griseoviridis*. Journal of natural products, 2008. **71**(7): p. 1265-1267.
- 318. Kimata, S., Matsuda, T., et al., *Prodigiosin R3, a new multicyclic prodigiosin formed by prodigiosin cyclization genes in the roseophilin producer.* The Journal of Antibiotics, 2023. **76**(1): p. 14-19.
- 319. Kimata, S., Matsuda, T., et al., *Prodigiosin R2, a new prodigiosin from the roseophilin producer Streptomyces griseoviridis 2464-S5.* The Journal of Antibiotics, 2018. **71**(3): p. 393-396.
- 320. TSAO, S.-W., RUDD, B.A., et al., *Identification of a red pigment from Streptomyces coelicolor A3 (2) as a mixture of prodigiosin derivatives.* The Journal of antibiotics, 1985. **38**(1): p. 128-131.
- 321. Abdelfattah, M.S., Elmallah, M.I., et al., *Prodigiosins from a marine sponge-associated actinomycete attenuate HCl/ethanol-induced gastric lesion via antioxidant and anti-inflammatory mechanisms.* PloS one, 2019. **14**(6): p. e0216737.
- 322. El-Bondkly, A., El-Gendy, M., et al., Overproduction and biological activity of prodigiosin-like pigments from recombinant fusant of endophytic marine Streptomyces species. Antonie Van Leeuwenhoek, 2012. **102**(4): p. 719-734.
- 323. Song, Y., Liu, G., et al., *Cytotoxic and antibacterial angucycline-and prodigiosin-analogues from the deep-sea derived Streptomyces sp. SCSIO 11594.* Marine drugs, 2015. **13**(3): p. 1304-1316.
- 324. Boonlarppradab, C., Kauffman, C.A., et al., *Marineosins A and B, cytotoxic spiroaminals from a marine-derived actinomycete.* Organic letters, 2008. **10**(24): p. 5505-5508.
- 325. Yang, K., Chen, Q., et al., *The algicidal mechanism of prodigiosin from Hahella sp. KA22 against Microcystis aeruginosa.* Scientific reports, 2017. **7**(1): p. 7750.

- 326. Zhang, H., Wang, H., et al., *Toxic effects of prodigiosin secreted by Hahella sp. KA22 on harmful alga Phaeocystis globosa.* Frontiers in Microbiology, 2017. **8**: p. 999.
- 327. Zhang, S., Zheng, W., et al., Physiological response and morphological changes of Heterosigma akashiwo to an algicidal compound prodigiosin. Journal of hazardous materials, 2020. 385: p. 121530.
- 328. Wasserman, H., Rodgers, G., et al., *The structure and synthesis of undecylprodigiosin. A prodigiosin analogue from Streptomyces.* Chemical Communications (London), 1966(22): p. 825-826.
- 329. Church, N.A. and McKillip, J.L., *Antibiotic resistance crisis: challenges and imperatives.* Biologia, 2021. **76**(5): p. 1535-1550.
- 330. Ferlay, J., Colombet, M., et al., *Cancer statistics for the year 2020: An overview.* International journal of cancer, 2021. **149**(4): p. 778-789.
- 331. Mabrok, M., Algammal, A.M., et al., *Tenacibaculosis caused by Tenacibaculum maritimum: Updated knowledge of this marine bacterial fish pathogen.* Frontiers in cellular and infection microbiology, 2023. **12**: p. 1068000.
- 332. Hickey, M.E. and Lee, J.L., *A comprehensive review of Vibrio (Listonella) anguillarum: ecology, pathology and prevention.* Reviews in Aquaculture, 2018. **10**(3): p. 585-610.
- 333. Semwal, A., Kumar, A., et al., *A review on pathogenicity of Aeromonas hydrophila* and their mitigation through medicinal herbs in aquaculture. Heliyon, 2023.
- 334. Hu, D.X., Withall, D.M., et al., *Structure, chemical synthesis, and biosynthesis of prodiginine natural products.* Chemical reviews, 2016. **116**(14): p. 7818-7853.
- 335. Tirichine, L. and Piganeau, G., *Algal symbiotic relationships in freshwater and marine environments*. 2023, Frontiers Media SA. p. 1155759.
- 336. Singh, R.P. and Reddy, C., Seaweed–microbial interactions: key functions of seaweed-associated bacteria. FEMS microbiology ecology, 2014. **88**(2): p. 213-230.
- 337. Anwar, M.M., Albanese, C., et al., *Rise of the natural red pigment 'prodigiosin'as an immunomodulator in cancer.* Cancer Cell International, 2022. **22**(1): p. 419.
- 338. Manderville, R., Synthesis, proton-affinity and anti-cancer properties of the prodigiosin-group natural products. Current Medicinal Chemistry-Anti-Cancer Agents, 2001. **1**(2): p. 195-218.
- 339. Caesar, L.K., Montaser, R., et al., *Metabolomics and genomics in natural products research: complementary tools for targeting new chemical entities.*Natural product reports, 2021. **38**(11): p. 2041-2065.

- 340. Parra, J., Beaton, A., et al., *Antibiotics from rare actinomycetes, beyond the genus Streptomyces*. Current Opinion in Microbiology, 2023. **76**: p. 102385.
- 341. Schumann, P., Weiss, N., et al., Reclassification of Cellulomonas cellulans (Stackebrandt and Keddie 1986) as Cellulosimicrobium cellulans gen. nov., comb. nov. International Journal of Systematic and Evolutionary Microbiology, 2001. **51**(3): p. 1007-1010.
- 342. Schumann, P. and Stackebrandt, E., *Cellulosimicrobium*. Bergey's Manual of Systematics of Archaea and Bacteria, 2015: p. 1-9.
- 343. Yoon, J.-H., Kang, S.-J., et al., *Cellulosimicrobium terreum sp. nov., isolated from soil.* International Journal of Systematic and Evolutionary Microbiology, 2007. **57**(11): p. 2493-2497.
- 344. Hamada, M., Shibata, C., et al., *Cellulosimicrobium marinum sp. nov., an actinobacterium isolated from sea sediment.* Archives of Microbiology, 2016. **198**: p. 439-444.
- 345. Hu, L., Xia, M., et al., *Cellulosimicrobium composti sp. nov., a thermophilic bacterium isolated from compost.* International Journal of Systematic and Evolutionary Microbiology, 2021. **71**(7): p. 004905.
- 346. Le Han, H., Nguyen, T.T., et al., *Cellulosimicrobium protaetiae sp. nov., isolated from the gut of the larva of Protaetia brevitarsis seulensis.* International Journal of Systematic and Evolutionary Microbiology, 2022. **72**(3): p. 005296.
- 347. Brown, J.M., Steigerwalt, A.G., et al., *Characterization of clinical isolates* previously identified as Oerskovia turbata: proposal of Cellulosimicrobium funkei sp. nov. and emended description of the genus Cellulosimicrobium. International Journal of Systematic and Evolutionary Microbiology, 2006. **56**(4): p. 801-804.
- 348. Ferrer, P., Revisiting the Cellulosimicrobium cellulans yeast-lytic β-1, 3-glucanases toolbox: A review. Microbial cell factories, 2006. **5**(1): p. 1-8.
- 349. Ham, S.-J., Lee, H.J., et al., Cloning and characterization of a modular GH5 β-1, 4-mannanase with high specific activity from the fibrolytic bacterium Cellulosimicrobium sp. strain HY-13. Bioresource technology, 2011. **102**(19): p. 9185-9192.
- 350. Kim, D.Y., Han, M.K., et al., *Novel GH10 xylanase, with a fibronectin type 3 domain, from Cellulosimicrobium sp. strain HY-13, a bacterium in the gut of Eisenia fetida.* Applied and environmental microbiology, 2009. **75**(22): p. 7275-7279.
- 351. Liu, W., Zhao, C., et al., *Bioflocculant production from untreated corn stover using Cellulosimicrobium cellulans L804 isolate and its application to harvesting microalgae*. Biotechnology for biofuels, 2015. **8**: p. 1-12.

- 352. Bharagava, R.N. and Mishra, S., Hexavalent chromium reduction potential of Cellulosimicrobium sp. isolated from common effluent treatment plant of tannery industries. Ecotoxicology and Environmental Safety, 2018. **147**: p. 102-109.
- 353. Petkar, H., Li, A., et al., Cellulosimicrobium funkei: first report of infection in a nonimmunocompromised patient and useful phenotypic tests for differentiation from Cellulosimicrobium cellulans and Cellulosimicrobium terreum. Journal of clinical microbiology, 2011. **49**(3): p. 1175-1178.
- 354. Rivero, M., Alonso, J., et al., *Infections due to Cellulosimicrobium species: case report and literature review.* BMC Infectious Diseases, 2019. **19**: p. 1-9.
- 355. Sharma, A., Gilbert, J.A., et al., (Meta) genomic insights into the pathogenome of Cellulosimicrobium cellulans. Scientific reports, 2016. **6**(1): p. 25527.
- 356. Kumar, P., Verma, A., et al., *Exploring diversity and polymer degrading potential of epiphytic bacteria isolated from marine macroalgae*. Microorganisms, 2022. **10**(12): p. 2513.
- 357. Mahajan, G., Chauhan, V., et al., Combining in vitro and in silico studies to unravel the antifungal potential of chitinase from a marine bacterial isolate Cellulosimicrobium cellulans RS7. Process Biochemistry, 2023. **134**: p. 88-100.
- 358. Tanveer, F., Shehroz, M., et al., Genome sequence analysis and bioactivity profiling of marine-derived actinobacteria, Brevibacterium luteolum, and Cellulosimicrobium funkei. Archives of Microbiology, 2021. **203**: p. 2491-2500.
- 359. Audoin, C., Bonhomme, D., et al., *Balibalosides, an original family of glucosylated sesterterpenes produced by the Mediterranean sponge Oscarella balibaloi.*Marine drugs, 2013. **11**(5): p. 1477-1489.
- 360. Monteiro, M.C., de la Cruz, M., et al., A new approach to drug discovery: high-throughput screening of microbial natural extracts against Aspergillus fumigatus using resazurin. Journal of biomolecular screening, 2012. **17**(4): p. 542-549.
- 361. Mackenzie, T.A., Reyes, F., et al., Naphthoquinone Derivatives from Angustimassarina populi CF-097565 Display Anti-Tumour Activity in 3D Cultures of Breast Cancer Cells. Molecules, 2024. **29**(2): p. 425.
- 362. Martin, J., Crespo, G., et al., *MDN-0104, an antiplasmodial betaine lipid from Heterospora chenopodii.* Journal of natural products, 2014. **77**(9): p. 2118-2123.
- 363. Pérez-Victoria, I., Martín, J., et al., *Combined LC/UV/MS and NMR strategies for the dereplication of marine natural products.* Planta medica, 2016. **82**(09/10): p. 857-871.
- 364. Marfey, P., Determination of D-amino acids. II. Use of a bifunctional reagent, 1, 5-difluoro-2, 4-dinitrobenzene. Carlsberg Research Communications, 1984. **49**: p. 591-596.

- Pérez-Victoria, I., Co-occurring Congeners Reveal the Position of Enantiomeric Amino Acids in Nonribosomal Peptides. ChemBioChem, 2021. 22(12): p. 2087-2092.
- 366. Bundale, S., Singh, J., et al., *Rare actinobacteria: a potential source of bioactive polyketides and peptides.* World Journal of Microbiology and Biotechnology, 2019. **35**: p. 1-11.
- 367. Zhao, P., Xue, Y., et al., *Actinobacteria–derived peptide antibiotics since 2000.* Peptides, 2018. **103**: p. 48-59.
- 368. Tiwari, K. and Gupta, R.K., *Rare actinomycetes: a potential storehouse for novel antibiotics*. Critical reviews in biotechnology, 2012. **32**(2): p. 108-132.
- 369. Caicedo-Montoya, C., Manzo-Ruiz, M., et al., *Pan-genome of the genus Streptomyces and prioritization of biosynthetic gene clusters with potential to produce antibiotic compounds.* Frontiers in microbiology, 2021. **12**: p. 677558.
- 370. Li, L., Zhu, H.-r., et al., *Micromonospora craniellae sp. nov., isolated from a marine sponge, and reclassification of Jishengella endophytica as Micromonospora endophytica comb. nov.* International Journal of Systematic and Evolutionary Microbiology, 2019. **69**(3): p. 715-720.
- 371. Ay, H., Nouioui, I., et al., *Genome-based classification of Micromonospora craterilacus sp. nov., a novel actinobacterium isolated from Nemrut Lake.* Antonie van Leeuwenhoek, 2020. **113**: p. 791-801.
- 372. Boumehira, A.Z., El-Enshasy, H.A., et al., *Recent progress on the development of antibiotics from the genus Micromonospora.* Biotechnology and Bioprocess Engineering, 2016. **21**: p. 199-223.
- 373. Kumazawa, S., Asami, Y., et al., STRUCTURAL STUDIES OF NEW MACROLIDE ANTIBIOTICS, SHURIMYCINS1 A AND B. The Journal of Antibiotics, 1994. 47(6): p. 688-696.
- 374. Huang, X., Roemer, E., et al., *Lydiamycins A–D: cyclodepsipetides with antimycobacterial properties*. Angewandte Chemie International Edition, 2006. **45**(19): p. 3067-3072.
- 375. Helaly, S.E., Kulik, A., et al., *Langkolide, a 32-membered macrolactone antibiotic produced by Streptomyces sp. acta 3062.* Journal of natural products, 2012. **75**(6): p. 1018-1024.
- 376. Pandey, R.C., RINEHART, K.L., et al., *POLYENE ANTIBIOTICS. VI THE STRUCTURES OF DERMOSTATINS A AND B1.* The Journal of Antibiotics, 1973. **26**(8): p. 475-477.

- 377. MCALPINE, J.B., TUAN, J.S., et al., New antibiotics from genetically engineered actinomycetes I. 2-Norerythromycins, isolation and structural determinations. The Journal of Antibiotics, 1987. **40**(8): p. 1115-1122.
- 378. Salomon, A.R., Voehringer, D.W., et al., *Apoptolidin, a selective cytotoxic agent, is an inhibitor of F0F1-ATPase.* Chemistry & biology, 2001. **8**(1): p. 71-80.
- 379. Muller, C., Nolden, S., et al., Sequencing and analysis of the biosynthetic gene cluster of the lipopeptide antibiotic friulimicin in Actinoplanes friuliensis.

 Antimicrobial agents and chemotherapy, 2007. **51**(3): p. 1028-1037.
- 380. Belova, Z. and Stolpnik, V., *The isolation, purification and some physico-chemical properties of the polypeptide antibiotic 128 (neotelomycin).* Antibiotiki, 1966. **11**(1): p. 21-25.
- 381. Kishi, T., HARADA, S., et al., *STUDIES ON JUVENIMICIN, A NEW ANTIBIOTIC.*II ISOLATION, CHEMICAL CHARACTERIZATION AND STRUCTURES. The
 Journal of Antibiotics, 1976. **29**(11): p. 1171-1181.
- 382. Fu, C., Keller, L., et al., *Biosynthetic studies of telomycin reveal new lipopeptides with enhanced activity.* Journal of the American Chemical Society, 2015. **137**(24): p. 7692-7705.
- 383. Metelev, M., Tietz, J.I., et al., *Structure, bioactivity, and resistance mechanism of streptomonomicin, an unusual lasso peptide from an understudied halophilic actinomycete.* Chemistry & biology, 2015. **22**(2): p. 241-250.
- 384. Uri, J. and Bekesi, I., *Flavofungin, a new crystalline antifungal antibiotic: origin and biological properties.* Nature, 1958. **181**(4613): p. 908-908.
- 385. Lu, L., Zhang, W., et al., *Amphidinolide B: total synthesis, structural investigation, and biological evaluation.* The Journal of organic chemistry, 2013. **78**(6): p. 2213-2247.
- 386. Rateb, M.E., Houssen, W.E., et al., *Diverse metabolic profiles of a Streptomyces strain isolated from a hyper-arid environment.* Journal of natural products, 2011. **74**(9): p. 1965-1971.
- 387. Ye, X., Anjum, K., et al., Antiproliferative cyclodepsipeptides from the marine actinomycete Streptomyces sp. P11-23B downregulating the tumor metabolic enzymes of glycolysis, glutaminolysis, and lipogenesis. Phytochemistry, 2017. 135: p. 151-159.
- 388. Schlegel, R., Thrum, H., et al., *The structure of roflamycoin, a new polyene macrolide antifungal antibiotic.* The Journal of Antibiotics, 1981. **34**(1): p. 122-123.

- 389. Vartak, A., Mutalik, V., et al., *Isolation of a new broad spectrum antifungal polyene from Streptomyces sp. MTCC 5680.* Letters in applied microbiology, 2014. **58**(6): p. 591-596.
- 390. Meyers, E., Pansy, F.E., et al., *The in vitro activity of nonactin and its homologs: monactin, dinactin and trinactin.* The Journal of Antibiotics, Series A, 1965. **18**(3): p. 128-129.
- 391. Yin, X., Chen, Y., et al., *Enduracidin analogues with altered halogenation patterns produced by genetically engineered strains of Streptomyces fungicidicus.* Journal of natural products, 2010. **73**(4): p. 583-589.
- 392. Higashide, E., Hatano, K., et al., *ENDURACIDIN, A NEW ANTIBIOTIC. I STREPTOMYCES FUNGICIDICUS NO. B 5477, AN ENDURACIDIN PRODUCING ORGANISM.* The journal of antibiotics, 1968. **21**(2): p. 126-137.
- 393. Pérez, M., Schleissner, C., et al., *PM100117 and PM100118, new antitumor macrolides produced by a marine Streptomyces caniferus GUA-06-05-006A.* The Journal of antibiotics, 2016. **69**(5): p. 388-394.
- 394. Geng, M., Austin, F., et al., *Covalent structure and bioactivity of the type All lantibiotic salivaricin A2.* Applied and Environmental Microbiology, 2018. **84**(5): p. e02528-17.
- 395. Andersen, F.D., Pedersen, K.D., et al., *Triculamin: an unusual lasso peptide with potent antimycobacterial activity.* Journal of Natural Products, 2022. **85**(6): p. 1514-1521.
- 396. McCafferty, D.G., Cudic, P., et al., *Chemistry and biology of the ramoplanin family of peptide antibiotics*. Peptide Science: Original Research on Biomolecules, 2002. **66**(4): p. 261-284.
- 397. Capstick, D.S., Willey, J.M., et al., SapB and the chaplins: connections between morphogenetic proteins in Streptomyces coelicolor. Molecular microbiology, 2007. **64**(3): p. 602-613.
- 398. Evans, D.A. and Connell, B.T., *Synthesis of the antifungal macrolide antibiotic* (+)-roxaticin. Journal of the American Chemical Society, 2003. **125**(36): p. 10899-10905.
- 399. Łowicki, D. and Huczyński, A., *Structure and antimicrobial properties of monensin A and its derivatives: summary of the achievements.* BioMed Research International, 2013. **2013**.
- 400. Yang, X., Fu, B., et al., *Total synthesis of landomycin A, a potent antitumor angucycline antibiotic.* Journal of the American Chemical Society, 2011. **133**(32): p. 12433-12435.
- 401. Stankovic, N., Senerovic, L., et al., *Properties and applications of undecylprodigiosin and other bacterial prodigiosins.* Applied microbiology and biotechnology, 2014. **98**: p. 3841-3858.
- 402. Suzuki, N., Ohtaguro, N., et al., *A compound inhibits biofilm formation of Staphylococcus aureus from Streptomyces.* Biological and Pharmaceutical Bulletin, 2015. **38**(6): p. 889-892.
- 403. Bartz, Q.R., Ehrlich, J., et al., *Viomycin, a new tuberculostatic antibiotic.* American Review of Tuberculosis, 1951. **63**(1): p. 4-6.
- 404. Borowski, E., Malyshkina, M., et al., *Isolation and Characterization of Levorin A and B, the Heptaene Macrolide Antifungal Antibiotics of 'Aromatic'Subgroup.* Chemotherapy, 1965. **10**(3): p. 176-194.

- 405. Wang, F., Fu, S.-N., et al., *Kitamycin C, a new antimycin-type antibiotic from Streptomyces antibioticus strain 200-09.* Natural Product Research, 2017. **31**(15): p. 1819-1824.
- 406. IMAMURA, N., NISHIJIMA, M., et al., *Novel antimycin antibiotics, urauchimycins A and B, produced by marine actinomycete.* The Journal of antibiotics, 1993. **46**(2): p. 241-246.
- 407. Navarro, G., Cheng, A.T., et al., *Image-based 384-well high-throughput screening method for the discovery of skyllamycins A to C as biofilm inhibitors and inducers of biofilm detachment in Pseudomonas aeruginosa.* Antimicrobial agents and chemotherapy, 2014. **58**(2): p. 1092-1099.
- 408. Sekizawa, R., Momose, I., et al., *Isolation and structural determination of phepropeptins A, B, C, and D, new proteasome inhibitors, produced by Streptomyces sp.* The Journal of Antibiotics, 2001. **54**(11): p. 874-881.
- 409. Messaoudi, O., Sudarman, E., et al., *Kenalactams A–E, polyene macrolactams isolated from Nocardiopsis CG3.* Journal of natural products, 2019. **82**(5): p. 1081-1088.
- 410. Ebata, E., KASAHARA, H., et al., LYSOCELLIN, A NEW POLYETHER ANTIBIOTIC I. ISOLATION, PURIFICATION, PHYSICO-CHEMICAL AND BIOLOGICAL PROPERTIES. The Journal of Antibiotics, 1975. **28**(2): p. 118-121.
- 411. Ohta, T., Arakawa, H., et al., *Bafilomycin A1 induces apoptosis in the human pancreatic cancer cell line Capan-1.* The Journal of Pathology: A Journal of the Pathological Society of Great Britain and Ireland, 1998. **185**(3): p. 324-330.
- Vazquez, D., Macrolide antibiotics Spiramycin, Carbomycin, Angolamycin, Methymycin and Lancamycin, in Mechanism of Action, D. Gottlieb and P.D. Shaw, Editors. 1967, Springer Berlin Heidelberg: Berlin, Heidelberg. p. 366-377.
- 413. Höfer, I., Crüsemann, M., et al., *Insights into the biosynthesis of hormaomycin,* an exceptionally complex bacterial signaling metabolite. Chemistry & biology, 2011. **18**(3): p. 381-391.
- 414. Yu, Z., Vodanovic-Jankovic, S., et al., *New WS9326A congeners from Streptomyces sp. 9078 inhibiting Brugia malayi asparaginyl-tRNA synthetase.*Organic letters, 2012. **14**(18): p. 4946-4949.
- 415. OMURA, S., MAMADA, H., et al., *TAKAOKAMYCIN, A NEW PEPTIDE ANTIBIOTIC PRODUCED BYSTREPTOMYCESSP.* The Journal of Antibiotics, 1984. **37**(7): p. 700-705.
- 416. Hu, Z., Liu, Y., et al., *Isolation and characterization of novel geldanamycin analogues*. The Journal of Antibiotics, 2004. **57**(7): p. 421-428.
- 417. Farver, D.K., Hedge, D.D., et al., *Ramoplanin: a lipoglycodepsipeptide antibiotic.* Annals of Pharmacotherapy, 2005. **39**(5): p. 863-868.
- 418. Bruna, C.D., Ricciardi, M., et al., *Axenomycins, new cestocidal antibiotics*. Antimicrobial Agents and Chemotherapy, 1973. **3**(6): p. 708-710.
- Kong, F. and Carter, G.T., Structure determination of glycinocins A to D, further evidence for the cyclic structure of the amphomycin antibiotics. The Journal of Antibiotics, 2003. 56(6): p. 557-564.
- 420. Gebhardt, K., PUKALL, R., et al., Streptocidins AD, Novel Cyclic Decapeptide Antibiotics Produced by Streptomyces sp. Tü 6071 I. Taxonomy, Fermentation, Isolation and Biological Activities. The Journal of Antibiotics, 2001. **54**(5): p. 428-433.

- 421. TAKESAKO, K. and BEPPU, T., Studies on new antifungal antibiotics, guanidylfungins A and B I. Taxonomy, fermentation, isolation and characterization. The Journal of Antibiotics, 1984. **37**(10): p. 1161-1169.
- 422. Brown, R. and Hazen, E.L., *Present knowledge of nystatin, an antifungal antibiotic*. Transactions NY Acad. Sci., 1957. **19**(5).
- 423. Fukai, T., Kuroda, J., et al., *Structure of new cyclic depsipeptides, Bu-2841-08 and-10.* The Journal of Antibiotics, 1995. **48**(10): p. 1115-1122.
- 424. Heidary, M., Khosravi, A.D., et al., *Daptomycin.* Journal of Antimicrobial Chemotherapy, 2018. **73**(1): p. 1-11.
- 425. Tweit, R.C., Pandey, R.C., et al., *Characterization of the antifungal and antiprotozoal antibiotic partricin and structural studies on partricins A and B.* The Journal of antibiotics, 1982. **35**(8): p. 997-1012.
- 426. Mohan, R., Pianotti, R., et al., *Fungimycin production, isolation, biosynthesis, and in vitro antifungal activity.* Fungimycin production, isolation, biosynthesis, and in vitro antifungal activity., 1964: p. 462-470.
- 427. Hayashi, K.-i. and Nozaki, H., *Kitamycins, new antimycin antibiotics produced by Streptomyces sp.* The Journal of antibiotics, 1999. **52**(3): p. 325-328.
- 428. KINASHI, H., SAKAGUCHI, K., et al., *Structures of concanamycins B and C.* The Journal of Antibiotics, 1982. **35**(11): p. 1618-1620.
- 429. Jain, S.K., Pathania, A.S., et al., *Chrysomycins A–C, antileukemic naphthocoumarins from Streptomyces sporoverrucosus.* RSC advances, 2013. **3**(43): p. 21046-21053.
- 430. Counter, F., Allen, N., et al., *A54145 a new lipopeptide antibiotic complex:* microbiological evaluation. The Journal of Antibiotics, 1990. **43**(6): p. 616-622.
- 431. Torikata, A., Enokita, R., et al., *Mycoplanecins, novel antimycobacterial antibiotics from Actinoplanes awajinensis subsp. mycoplanecinus subsp. nov. I. Taxonomy of producing organism and fermentation.* The Journal of Antibiotics, 1983. **36**(8): p. 957-960.
- 432. Jomon, K., Kuroda, Y., et al., *A new antibiotic, ikarugamycin.* The Journal of antibiotics, 1972. **25**(5): p. 271-280.
- 433. MUKHOPADHYAY, T., Vijayakumar, E., et al., *Mathemycin A, a New Antifungal Macrolactone from Actinomycete sp. HIL Y-8620959 II. Structure Elucidation.* The Journal of Antibiotics, 1998. **51**(6): p. 582-585.
- 434. Strangman, W.K., Kwon, H.C., et al., *Potent inhibitors of pro-inflammatory cytokine production produced by a marine-derived bacterium.* Journal of medicinal chemistry, 2009. **52**(8): p. 2317-2327.
- 435. ROBISON, R.S., ASZALOS, A., et al., *Production of fungichromin by Streptoverticillium cinnamomeum subsp. cinnamomeum NRRL B-1285.* The Journal of Antibiotics, 1971. **24**(4): p. 273-273.
- 436. Kalinovskaya, N.I., Romanenko, L.A., et al., *Marine isolate Citricoccus sp. KMM* 3890 as a source of a cyclic siderophore nocardamine with antitumor activity. Microbiological research, 2011. **166**(8): p. 654-661.
- 437. Sezaki, M., HARA, T., et al., *Studies on a new antibiotic pigment, aquayamycin.* The Journal of Antibiotics, 1968. **21**(2): p. 91-97.
- 438. Pourtier-Manzanedo, A., Boesch, D., et al., *FK-506 (fujimycin) reverses the multidrug resistance of tumor cells in vitro.* Anti-cancer drugs, 1991. **2**(3): p. 279-284.

- 439. Koba, M. and Konopa, J., *Actinomycin D and its mechanisms of action.* Advances in Hygiene and Experimental Medicine, 2005. **59**.
- 440. YAGINUMA, S., MORISHITA, A., et al., *Sporeamicin A, a new macrolide antibiotic I. Taxonomy, fermentation, isolation and characterization.* The Journal of Antibiotics, 1992. **45**(5): p. 599-606.
- 441. Kim, B.S., Moon, S.S., et al., *Isolation, identification, and antifungal activity of a macrolide antibiotic, oligomycin A, produced by Streptomyces libani.* Canadian Journal of Botany, 1999. **77**(6): p. 850-858.
- 442. Griffith, R. and Black, H., *Erythromycin.* Medical Clinics of North America, 1970. **54**(5): p. 1199-1215.
- 443. Okujo, N., Iinuma, H., et al., *Bispolides, novel 20-membered ring macrodiolide antibiotics from Microbispora.* The Journal of Antibiotics, 2007. **60**(3): p. 216-219.
- 444. Qian, Z., Antosch, J., et al., *Structures and biological activities of cycloheptamycins A and B.* Organic & Biomolecular Chemistry, 2019. **17**(27): p. 6595-6600.
- 445. Wang, J., Cong, Z., et al., Soliseptide A, a cyclic hexapeptide possessing piperazic acid groups from Streptomyces solisilvae HNM30702. Organic letters, 2018. **20**(5): p. 1371-1374.
- 446. Gärtner, A., Ohlendorf, B., et al., Levantilides A and B, 20-membered macrolides from a Micromonospora strain isolated from the mediterranean deep sea sediment. Marine drugs, 2011. **9**(1): p. 98-108.
- 447. Ding, Z.-G., Zhao, J.-Y., et al., *Griseusins F and G, spiro-naphthoquinones from a tin mine tailings-derived alkalophilic Nocardiopsis species.* Journal of Natural Products, 2012. **75**(11): p. 1994-1998.
- 448. Borowski, E., Schaffner, C., et al., *Perimycin, a novel type of heptaene antifungal antibiotic.* 1961.
- 449. Arai, T., Kuroda, S., et al., *Copiamycin, a new antifungal antibiotic derived from S. hygroscopicus var. chrystallogenes.* The Journal of Antibiotics, Series A, 1965. **18**(2): p. 63-67.
- 450. Xu, C.-D., Zhang, H.-J., et al., *Pyrimidine nucleosides from Streptomyces sp. SSA28.* Journal of natural products, 2019. **82**(9): p. 2509-2516.
- 451. Wyche, T.P., Hou, Y., et al., *Peptidolipins B–F, antibacterial lipopeptides from an ascidian-derived Nocardia sp.* Journal of natural products, 2012. **75**(4): p. 735-740.
- 452. Bertasso, M., Holzenkaempfer, M., et al., *Ripromycin and Other Polycyclic Macrolactams from Streptomyces sp. Tü 6239 Taxonomy, Fermentation, Isolation and Biological Properties.* The Journal of antibiotics, 2003. **56**(4): p. 364-371.

APPENDIX

APPENDIX I

Table S1. Taxonomic identification of the Actinomycetota isolates recovered from *C. crispus* and *C. tomentosum*, collected in the intertidal area of the northern Portuguese rocky shore. Information regarding culture media and genomic data, including the GenBank accession number, is presented. Potential novel species are indicated as well (**).

Strain	Isolation Media	Closest Related *	16S rRNA gene similarity	Sequence length (bp)	GenBank accession number
CC-F1	SCN	Citricoccus zhacaiensis	98.40	1371	OR215069
CC-F4	SCN	Micrococcus luteus	99.71	1389	OR215097
CC-F7	SA	Rhodococcus rhodochrous	99.93	1386	OR215173
CC-F8	SA	Arthrobacter gandavensis	99.34	1373	OR215048
CC-F9	SA	Streptomyces badius	100.00	1393	OR215279
CC-F10	SA	Streptomyces badius	100	1395	OR215257
CC-F11	SA	Streptomyces gougerotii	99.78	1391	OR215259
CC-F12	SA	Nocardiopsis prasina	99.21	1397	OR215149
CC-F13	SA	Streptomyces hydrogenans	100.00	1394	OR215263
CC-F14	SA	Streptomyces xiamenensis	99.77	1143	OR215405
CC-F16	SA	Streptomyces albidoflavus	99.78	1391	OR215264
CC-F19	SA	Streptomyces atroolivaceus	99.78	1387	OR215265
CC-F23	AIA	Brevibacterium sediminis	99.86	1392	OR215054
CC-F24	AIA	Cellulosimicrobium cellulans	99.71	1384	OR215061
CC-F26	AIA	Streptomyces violascens	99.86	1393	OR215266
CC-F27	AIA	Streptomyces badius	100.00	1341	OR215267
CC-F28	AIA	Streptomyces violaceolatus	100	1383	OR215268
CC-F29	AIA	Mycolicibacterium moriokaense	98.85	1389	OR215120
CC-F30	AIA	Streptomyces coelescens	99.93	1377	OR215269

	AIA	Streptomyces diastaticus subsp.			OR215216
CC-F31		ardesiacus	100.00	1346	
CC-F32	AIA	Rhodococcus rhodochrous	99.71	1383	OR215171
CC-F35	AIA	Streptomyces althioticus	100.00	1340	OR215203
CC-F36	AIA	Streptomyces albidoflavus	99.71	1370	OR215270
CC-F39	AIA	Streptomyces coelicoflavus	99.78	1394	OR215210
CC-F41	AIA	Brachybacterium paraconglomeratum	99.71	1390	OR215051
CC-F43	NPS	Micromonospora chalcea	99.78	1369	OR215103
CC-F45	NPS	Streptomyces albidoflavus	99.78	1390	OR215271
CC-F47	NPS	Streptomyces pseudogriseolus	100.00	1377	OR215251
CC-F52	NPS	Streptomyces gougerotii	99.86	1392	OR215272
CC-F53	NPS	Streptomyces albidoflavus	99.57	1390	OR215273
CC-F55	SCN	Actinoalloteichus hoggarensis	93.93	1007	
CC-F56	SCN	Rhodococcus rhodochrous	99.64	1378	OR215172
CC-F57	SCN	Microbacterium aerolatum	98.92	1387	OR215094
CC-F58	SA	Brevibacterium sediminis	99.86	1390	OR215055
CC-F59	SA	Brevibacterium sediminis	99.86	1388	OR215056
CC-F62	SA	Streptomyces fulvissimus	99.78	1381	OR215274
CC-F64	SA	Streptomyces setonii	100.00	1386	OR215275
CC-F65	SA	Streptomyces xiamenensis	99.64	1397	OR215406
CC-F67	SA	Micromonospora chalcea	99.63	1365	OR215104
CC-F68	NPS	Streptomyces griseoaurantiacus	99.71	1386	OR215222
CC-F69	NPS	Kitasatospora albolonga	99.78	1387	OR215085
CC-F71	NPS	Rhodococcus erythropolis	99.78	1392	OR215158
CC-F72	AIA	Streptomyces radiopugnans	99.48	1378	OR215252
CC-F74	AIA	Micromonospora arida	99.71	1369	OR215116
CC-F76	AIA	Streptomyces albidoflavus	99.71	1378	OR215276

CC-F77	AIA	Nocardiopsis alba	99.63	1350	OR215132
CC-F78	AIA	Streptomyces griseorubens	100	1388	OR215229
CC-F79	AIA	Kitasatospora albolonga	99.85	1386	OR215086
CC-F80	AIA	Streptomyces griseoincarnatus	99.35	1398	OR215277
CC-F81	AIA	Streptomyces niveus	99.55	1335	OR215248
CC-F83	AIA	Streptomyces pratensis	100.00	1376	OR215278
CC-F86	AIA	Cellulosimicrobium funkei	98.99	1386	OR215062
CC-F87	AIA	Cellulosimicrobium funkei	99.28	1387	OR215063
CC-F88	AIA	Micromonospora zingiberis	99.70	1330	OR215117
CC-F90	AIA	Rhodococcus koreensis	97.75	1380	OR215167
CC-F91	AIA	Streptomyces catenulae	98.35	1400	OR215280
CC-F92	AIA	Streptomyces hydrogenans	100	1393	OR215281
CC-F102	SCN	Streptomyces olivaceus	99.57	1387	OR215258
CC-F106	AIA	Microbacterium oxydans	99.93	1378	OR215093
CC-F110	AIA	Streptomyces violaceolatus	99.92	1261	OR215260
CC-F111	SA	Nocardia cyriacigeorgica	100.00	1392	OR215126
CC-F114	SA	Streptomyces coelescens	99.85	1371	OR215261
CC-F115	AIA	Nocardiopsis prasina	99.86	1400	OR215148
CC-F117	NPS	Micromonospora aurantiaca	99.86	1382	OR215098
CC-F118	NPS	Streptomyces griseoincarnatus	99.76	1256	OR215262
CC-F120	NPS	Nocardia carnea	99.78	1376	OR215122
CC-F123	NPS	Actinomadura geliboluensis	99.63	1370	OR215081
CC-R1	SA	Nocardiopsis alba	100.00	1401	OR215133
CC-R2	SA	Nocardiopsis prasina	99.69	1287	OR215150
CC-R3	SA	Streptomyces violascens	99.86	1391	OR215299
CC-R4	SA	Streptomyces hydrogenans	100.00	1392	OR215305
CC-R7	SA	Streptomyces coelescens	99.93	1393	OR215310

CC-R8	SA	Streptomyces violascens	99.85	1340	OR215312
CC-R10	SA	Krasilnikoviella muralis	99.28	1391	OR215090
CC-R12	SA	Streptomyces marokkonensis	99.35	1387	OR215287
CC-R15	SA	Streptomyces badius	100	1342	OR215292
CC-R18	SA	Streptomyces griseorubens	99.93	1393	OR215232
CC-R19	SA	Streptomyces marokkonensis	99.14	1391	OR215296
CC-R20	SA	Nocardiopsis alba	99.92	1286	OR215137
CC-R21	SA	Streptomyces tendae	99.42	1390	OR215401
CC-R25	NPS	Streptomyces hydrogenans	100.00	1388	OR215297
CC-R26	NPS	Streptomyces diastaticus	99.78	1394	OR215298
CC-R31	NPS	Streptomyces violascens	99.86	1390	OR215300
CC-R32	NPS	Streptomyces marokkonensis	99.14	1394	OR215301
CC-R33	NPS	Streptomyces albidoflavus	99.78	1395	OR215302
CC-R34	NPS	Rhodococcus kroppenstedtii	99.11	1367	OR215188
CC-R35	NPS	Streptomyces ardesiacus	100.00	1380	OR215218
CC-R36	NPS	Streptomyces badius	97.26**	1206	OR215303
CC-R39	NPS	Streptomyces violascens	99.86	1392	OR215304
CC-R43	SCN	Streptomyces jiujiangensis	99.33	1335	OR215245
CC-R44	SCN	Rhodococcus jostii	99.85	1379	OR215166
CC-R47	SCN	Microbacterium foliorum	99.64	1383	OR215091
CC-R49	SCN	Rhodococcus qingshengii	99.78	1383	OR215189
CC-R52	AIA	Gordonia paraffinivorans	99.71	1387	OR215077
CC-R53	AIA	Streptomyces violaceolatus	100.00	1336	OR215306
CC-R55	AIA	Streptomyces intermedius	99.41	1370	OR215239
CC-R56	AIA	Streptomyces marokkonensis	99.34	1370	OR215307
CC-R57	AIA	Rhodococcus phenolicus	98.84	1385	OR215168
CC-R59	AIA	Rhodococcus erythropolis	99.78	1388	OR215123

CC-R61	AIA	Streptomyces xiamenensis	99.63	1341	OR215411
CC-R62	AIA	Nocardia nova	99.55	1399	OR215129
CC-R63	AIA	Streptomyces albidoflavus	99.71	1384	OR215308
	AIA	Streptomyces diastaticus subsp.			
CC-R64		ardesiacus	99.40	1335	OR215219
CC-R65	AIA	Streptomyces marokkonensis	99.30	1285	OR215199
CC-R67	AIA	Streptomyces griseorubens	99.78	1338	OR215233
CC-R68	AIA	Streptomyces atrovirens	98	1391	OR215309
CC-R69	AIA	Rhodococcus rhodochrous	99.64	1393	OR215174
CC-R70	AIA	Rhodococcus erythropolis	99.70	1368	OR215124
CC-R71	AIA	Rhodococcus erythropolis	99.78	1382	OR215125
CC-R72	AIA	Streptomyces gougerotii	100	1394	OR215311
CC-R74	AIA	Streptomyces coelicoflavus	100.00	1297	OR215211
CC-R75	AIA	Streptomyces althioticus	100	1394	OR215204
CC-R76	AIA	Streptomyces griseorubens	100.00	1372	OR215234
CC-R77	AIA	Streptomyces intermedius	99.77	1324	OR215240
CC-R81	SCN	Rhodococcus rhodochrous	99.86	1380	OR215175
CC-R86	SA	Streptomyces violascens	99.86	1391	OR215313
CC-R88	SA	Gordonia sputi	99.78	1386	OR215082
CC-R93	SA	Streptomyces aureus	99.71	1393	OR215206
CC-R95	SA	Nocardiopsis alba	99.64	1401	OR215138
CC-R97	SA	Streptomyces griseoflavus	99.78	1378	OR215227
CC-R99	SA	Streptomyces coelicoflavus	100.00	1382	OR215212
CC-R100	SA	Streptomyces xiamenensis	99.57	1395	OR215407
CC-R103	NPS	Streptomyces violascens	99.78	1389	OR215282
CC-R104	NPS	Rhodococcus pyridinivorans	98.34**	1390	OR215186
CC-R108	AIA	Streptomyces violascens	99.85	1305	OR215283

CC-R109	AIA	Streptomyces coelescens	99.78	1391	OR215284
CC-R110	AIA	Streptomyces griseorubens	100	1383	OR215230
CC-R111	AIA	Streptomyces intermedius	99.64	1389	OR215236
CC-R112	AIA	Streptomyces camponoticapitis	99.64	1378	OR215207
CC-R113	AIA	Rhodococcus qingshengii	100	1390	OR215187
CC-R115	AIA	Streptomyces afghaniensis	99.78	1393	OR215197
CC-R116	AIA	Micromonospora maritima	99.78	1375	OR215111
CC-R117	AIA	Gordonia paraffinivorans	99.85	1376	OR215075
CC-R118	AIA	Streptomyces violaceolatus	99.78	1398	OR215285
CC-R119	AIA	Streptomyces diastaticus	100.00	1377	OR215286
CC-R120	AIA	Gordonia paraffinivorans	99.86	1389	OR215076
	AIA	Streptomyces diastaticus subsp.			
CC-R121		ardesiacus	99.47	1347	OR215217
CC-R122	AIA	Streptomyces gougerotii	99.78	1390	OR215288
CC-R123	AIA	Streptomyces albidoflavus	99.78	1394	OR215289
CC-R125	AIA	Cellulosimicrobium funkei	99.78	1385	OR215058
CC-R126	AIA	Streptomyces intermedius	99.92	1287	OR215237
CC-R132	AIA	Nocardia nova	99.56	1382	OR215128
CC-R133	AIA	Streptomyces xiamenensis	99.64	1395	OR215290
CC-R134	AIA	Micromonospora maritima	99.56	1378	OR215112
CC-R135	AIA	Streptomyces atrovirens	99.41	1384	OR215205
CC-R136	AIA	Gordonia aichiensis	99.64	1384	OR215071
CC-R137	AIA	Streptomyces pseudogriseolus	98.91	1196	OR215291
CC-R138	AIA	Saccharomonospora azurea	100.00	1396	OR215190
CC-R139	AIA	Streptomyces mayteni	99.84	1268	OR215246
CC-R149	NPS	Stackebrandtia endophytica	100.00	1375	OR215192
CC-R150	NPS	Streptomyces hydrogenans	100.00	1394	OR215293

CC-R151	NPS	Streptomyces violascens	99.86	1390	OR215215
CC-R154	NPS	Streptomyces albidoflavus	99.78	1389	OR215294
CC-R155	NPS	Streptomyces xiamenensis	99.86	1390	OR215408
CC-R158	SA	Streptomyces xinghaiensis	99.93	1385	OR215419
CC-R160	SA	Micromonospora fluminis	99.64	1378	OR215110
CC-R163	SA	Nocardiopsis alba	99.71	1397	OR215134
CC-R164	SA	Nocardiopsis alba	99.71	1401	OR215135
CC-R165	AIA	Nocardiopsis mangrovei	99.71	1390	OR215147
CC-R166	AIA	Micromonospora aurantiaca	99.78	1386	OR215099
CC-R168	AIA	Streptomyces intermedius	99.50	1393	OR215238
CC-R169	AIA	Nocardiopsis alba	99.93	1397	OR215136
CC-R175	SCN	Streptomyces albidoflavus	99.71	1377	OR215295
CC-R176	AIA	Actinoalloteichus hoggarensis	99.56	1380	OR215046
CC-R177	AIA	Streptomyces griseorubens	100.00	1385	OR215231
CC-R178	AIA	Streptomyces xiamenensis	99.64	1396	OR215409
CC-R179	AIA	Micromonospora aurantiaca	99.93	1373	OR215100
CC-R180	NPS	Streptomyces xiamenensis	99.35	1390	OR215410
CC-R181	NPS	Streptomyces thermocarboxydus	99.71	1380	OR215402
CC-R183	NPS	Micromonospora maritima	99.28	1392	OR215113
CT-F1	NPS	Nocardiopsis alba	99.93	1377	OR215139
CT-F6	NPS	Streptomyces violascens	99.86	1390	OR215341
CT-F10	NPS	Micromonospora aurantiaca	99.26	1377	OR215105
CT-F11	NPS	Streptomyces albidoflavus	99.71	1394	OR215315
CT-F14	SCN	Rhodococcus rhodochrous	99.71	1394	OR215177
CT-F18	SCN	Streptomyces camponoticapitis	99.42	1389	OR215208
CT-F19	SCN	Nocardiopsis prasina	99.78	1374	OR215151
CT-F20	SCN	Streptomyces olivochromogenes	99.86	1392	OR215249

CT-F21	SCN	Streptomyces violaceolatus	99.78	1391	OR215329
CT-F25	SCN	Streptomyces gougerotii	99.78	1389	OR215330
CT-F26	SCN	Streptomyces violaceolatus	99.64	1395	OR215331
CT-F28	SCN	Rhodococcus rhodochrous	99.71	1395	OR215178
CT-F29	SCN	Streptomyces griseoaurantiacus	99.93	1391	OR215223
CT-F31	SA	Kitasatospora albolonga	100.00	1378	OR215087
CT-F37	SA	Streptomyces halstedii	100.00	1391	OR215332
CT-F39	SA	Cellulosimicrobium funkei	99.71	1385	OR215059
CT-F40	SA	Streptomyces chumphonensis	99.78	1392	OR215209
CT-F41	SA	Streptomyces violaceolatus	98.18	1321	OR215333
CT-F42	SA	Streptomyces albidoflavus	99.78	1390	OR215334
CT-F45	AIA	Streptomyces hydrogenans	100	1388	OR215335
CT-F46	AIA	Streptomyces coelescens	99.78	1387	OR215336
CT-F47	AIA	Streptomyces lienomycini	99.71	1393	OR215337
CT-F48	AIA	Streptomyces albidoflavus	99.78	1391	OR215338
CT-F49	AIA	Streptomyces albidoflavus	99.57	1397	OR215339
CT-F53	AIA	Gordonia caeni	99.93	1376	OR215074
CT-F55	AIA	Streptomyces chumphonensis	99.78	1377	OR215404
CT-F56	AIA	Micromonospora maritima	99.78	1370	OR215114
CT-F57	AIA	Streptomyces griseoincarnatus	99.21	1397	OR215340
CT-F58	AIA	Micromonospora marina	99.64	1386	OR215118
CT-F60	AIA	Gordonia paraffinivorans	99.64	1389	OR215078
CT-F61	AIA	Streptomyces coelescens	99.85	1344	OR215342
CT-F62	AIA	Streptomyces griseorubens	98.78	1395	OR215235
CT-F63	AIA	Nocardia nova	99.64	1384	OR215130
CT-F64	AIA	Streptomyces setonii	100.00	1390	OR215343
CT-F65	AIA	Streptomyces violaceolatus	100.00	1393	OR215344

CT-F67	AIA	Streptomyces rubrogriseus	99.50	1392	OR215256
CT-F68	AIA	Nocardiopsis listeri	99.71	1401	OR215146
CT-F69	AIA	Rhodococcus hoagii	100	1390	OR215160
CT-F70	AIA	Mycolicibacterium vaccae	99.42	1369	OR215121
CT-F72	AIA	Nocardia farcinica	99.34	1374	OR215127
CT-F74	AIA	Streptomyces albogriseolus	99.55	1339	OR215345
CT-F75	AIA	Streptomyces albidoflavus	99.50	1395	OR215346
CT-F76	SCN	Rhodococcus phenolicus	98.71	1391	OR215169
CT-F77	SCN	Gordonia alkanivorans	99.78	1385	OR215072
CT-F80	SCN	Brevibacterium anseongense	99.27	1381	OR215053
CT-F87	NPS	Gordonia terrae	97.58	1340	OR215080
CT-F88	NPS	Gordonia bronchialis	100.00	1391	OR215073
CT-F89	NPS	Brachybacterium paraconglomeratum	99.41	1355	OR215052
CT-F93	AIA	Micromonospora matsumotoense	99.05	1369	OR215115
CT-F94	AIA	Streptomyces griseoaurantiacus	99.78	1382	OR215224
CT-F96	AIA	Cellulosimicrobium cellulans	99.86	1393	OR215064
CT-F99	AIA	Streptomyces xiamenensis	99.35	1399	OR215347
CT-F100	AIA	Streptomyces albogriseolus	100	1389	OR215314
CT-F101	AIA	Micromonospora chalcea	99.57	1389	OR215106
CT-F104	AIA	Micromonospora yangpuensis	99.35	1385	OR215119
CT-F109	SA	Rhodococcus rhodochrous	99.64	1393	OR215176
CT-F111	SA	Streptomyces fulvissimus	99.27	1365	OR215316
CT-F116	NPS	Streptomyces hydrogenans	99.64	1379	OR215317
CT-F119	NPS	Streptomyces coelicoflavus	100.00	1393	OR215213
CT-F121	SCN	Gordonia sputi	99.78	1384	OR215083
CT-F122	SCN	Streptomyces hydrogenans	100.00	1392	OR215318
CT-F124	SCN	Streptomyces halstedii	98.46	1362	OR215319

CT-F125	AIA	Glycomyces phytohabitans	99.34	1386	OR215070
CT-F127	AIA	Streptomyces albidoflavus	99.71	1390	OR215320
CT-F129	AIA	Streptomyces marokkonensis	99.27	1377	OR215321
CT-F133	AIA	Streptomyces hydrogenans	100.00	1380	OR215322
CT-F134	AIA	Streptomyces violascens	99.86	1392	OR215323
CT-F136	SA	Streptomyces mayteni	99.85	1375	OR215247
CT-F137	SA	Streptomyces albidoflavus	100.00	1391	OR215324
CT-F139	SA	Streptomyces aculeolatus	98.77	1387	OR215193
CT-F144	SA	Streptomyces pratensis	99.85	1389	OR215325
CT-F145	SA	Streptomyces coelicoflavus	99.70	1088	
CT-F146	SCN	Rhodococcus hoagii	100.00	1377	OR215159
CT-F147	SCN	Microbacterium immunditiarum	99.64	1395	OR215092
CT-F148	NPS	Brevibacterium sediminis	99.83	1383	OR215057
CT-F150	NPS	Microbacterium aerolatum	99.20	1382	OR215095
CT-F151	SA	Micromonospora chalcea	99.57	1386	OR215107
CT-F153	AIA	Streptomyces albidoflavus	100.00	1378	OR215326
CT-F155	AIA	Streptomyces albidoflavus	100.00	1390	OR215327
CT-F156	NPS	Streptomyces pratensis	99.93	1389	OR215328
CT-R1	SCN	Streptomyces griseoaurantiacus	100.00	1328	OR215225
CT-R3	SCN	Nocardiopsis alba	99.86	1395	OR215145
CT-R4	SCN	Streptomyces xylanilyticus	99.49	1381	OR215420
CT-R7	SCN	Rhodococcus hoagii	100.00	1392	OR215164
CT-R9	SCN	Streptomyces xiamenensis	99.33	1352	OR215398
CT-R10	SCN	Nocardiopsis alba	99.78	1396	OR215140
CT-R12	SCN	Nocardiopsis prasina	99.63	1349	OR215152
CT-R13	SCN	Rhodococcus rhodochrous	99.64	1394	OR215179
CT-R17	SCN	Streptomyces coelicoflavus	99.78	1393	OR215214

CT-R18	SCN	Streptomyces coelescens	99.71	1387	OR215366
CT-R21	SCN	Streptomyces diastaticus	99.57	1388	OR215381
CT-R27	SA	Streptomyces badius	100	1393	OR215382
CT-R28	SA	Streptomyces hydrogenans	100.00	1379	OR215383
CT-R29	SA	Streptomyces halstedii	99.86	1386	OR215384
CT-R31	AIA	Streptomyces violaceolatus	99.78	1395	OR215385
CT-R32	AIA	Streptomyces albogriseolus	99.78	1395	OR215201
CT-R33	AIA	Streptomyces albidoflavus	99.71	1387	OR215386
CT-R34	AIA	Streptomyces hydrogenans	99.86	1395	OR215387
CT-R35	AIA	Kocuria rosea	99.86	1395	OR215089
CT-R36	AIA	Streptomyces intermedius	99.50	1393	OR215388
CT-R37	AIA	Streptomyces albogriseolus	100	1396	OR215202
CT-R38	AIA	Rhodococcus rhodochrous	99.86	1381	OR215183
CT-R39	AIA	Streptomyces violaceolatus	99.64	1398	OR215389
CT-R40	AIA	Streptomyces hydrogenans	100	1397	OR215390
CT-R42	NPS	Streptomyces albidoflavus	99.57	1392	OR215391
CT-R43	NPS	Streptomyces violascens	99.86	1389	OR215254
CT-R45	NPS	Rhodococcus pyridinivorans	99.78	1391	OR215170
CT-R46	NPS	Streptomyces violascens	99.86	1389	OR215255
CT-R47	NPS	Nocardiopsis prasina	99.64	1392	OR215153
CT-R48	NPS	Nocardiopsis prasina	99.50	1392	OR215154
CT-R49	NPS	Streptomyces hydrogenans	99.86	1388	OR208769
CT-R50	NPS	Streptomyces griseoflavus	99.49	1366	OR215228
CT-R51	SCN	Rhodococcus rhodochrous	99.78	1395	OR215184
CT-R52	SCN	Arthrobacter luteolus	99.28	1388	OR215050
CT-R53	SCN	Streptomyces olivochromogenes	99.64	1390	OR215250
CT-R55	SCN	Nocardioides cavernae	99.21	1386	OR215131

CT-R58	SCN	Streptomyces gougerotii	99.78	1391	OR208768
CT-R60	SCN	Streptomyces violaceolatus	99.86	1388	OR215392
CT-R62	SCN	Streptomyces adustus	99.86	1393	OR215196
CT-R63	SCN	Micromonospora aurantiaca	100.00	1366	OR215102
CT-R68	SCN	Gordonia paraffinivorans	99.86	1390	OR215079
CT-R75	SCN	Rhodococcus hoagii	99.78	1371	OR215165
CT-R82	NPS	Streptomyces violascens	99.86	1391	OR215393
CT-R83	NPS	Streptomyces albogriseolus	99.78	1394	OR215394
CT-R84	NPS	Micrococcus luteus	99.64	1385	OR215096
CT-R86	NPS	Streptomyces albidoflavus	99.50	1389	OR215395
CT-R87	NPS	Streptomyces violaceus	99.50	838	
CT-R88	NPS	Streptomyces violaceus	99.50	1391	OR215396
CT-R89	NPS	Streptomyces hydrogenans	100.00	1377	OR215397
CT-R92	AIA	Streptomyces violaceolatus	99.78	1390	OR215399
CT-R93	AIA	Streptomyces gougerotii	100.00	1392	OR215400
		Streptomyces diastaticus subsp.			
CT-R94	AIA	ardesiacus	100.00	1395	OR215221
CT-R95	AIA	Streptomyces thermocarboxydus	99.93	1396	OR215403
CT-R96	AIA	Arthrobacter luteolus	98.98	1376	OR215049
CT-R97	AIA	Micromonospora chalcea	99.56	1378	OR215109
CT-R98	AIA	Cellulosimicrobium cellulans	99.71	1371	OR215068
CT-R99	AIA	Rhodococcus ruber	100.00	1383	OR215185
CT-R100	AIA	Streptomyces xiamenensis	98.79	1240	OR215412
CT-R101	AIA	Micromonospora aurantiaca	99.78	1380	OR215101
CT-R103	AIA	Streptomyces violaceolatus	100.00	1393	OR215348
CT-R104	AIA	Streptomyces afghaniensis	99.64	1394	OR215198
CT-R105	AIA	Streptomyces atroolivaceus	99.64	1393	OR215349

CT-R106	AIA	Cellulosimicrobium cellulans	99.93	1395	OR215065
CT-R109	AIA	Rhodococcus hoagii	100.00	1392	OR215161
CT-R110	AIA	Streptomyces xiamenensis	99.71	1400	OR215413
CT-R111	AIA	Streptomyces violascens	99.86	1391	OR215253
CT-R112	AIA	Streptomyces xiamenensis	99.86	1396	OR215414
CT-R113	AIA	Nocardiopsis umidischolae	98.65**	1413	OR215155
CT-R115	AIA	Streptomyces gougerotii	99.78	1392	OR215350
CT-R116	AIA	Gordonia jacobaea	99.78	1384	OR215084
CT-R117	AIA	Streptomyces intermedius	99.28	1394	OR215241
CT-R118	AIA	Streptomyces albidoflavus	99.78	1393	OR215351
CT-R119	AIA	Streptomyces albogriseolus	99.64	1399	OR215200
CT-R120	AIA	Streptomyces marokkonensis	99.35	1380	OR215352
CT-R121	AIA	Streptomyces pratensis	99.93	1389	OR215353
CT-R124	AIA	Rhodococcus hoagii	99.86	1390	OR215162
CT-R125	AIA	Streptomyces lusitanus	98.55**	1384	OR215354
CT-R126	AIA	Streptomyces violascens	99.86	1393	OR215355
CT-R127	AIA	Micromonospora chalcea	99.78	1373	OR215108
CT-R128	SA	Streptomyces xiamenensis	99.57	1396	OR215415
CT-R130	SA	Cellulosimicrobium cellulans	99.93	1372	OR215066
CT-R131	SA	Streptomyces hydrogenans	100.00	1393	OR215356
CT-R135	SA	Nocardia nova	99.07	785	
CT-R137	SA	Streptomyces albidoflavus	100.00	1379	OR215357
CT-R138	SA	Streptomyces albidoflavus	99.64	1388	OR215358
CT-R139	SA	Rhodococcus rhodochrous	99.57	1381	OR215180
CT-R142	SA	Nocardiopsis alba	99.79	1399	OR215141
CT-R144	SA	Streptomyces violaceolatus	100.00	1398	OR215359
CT-R146	SA	Rhodococcus rhodochrous	99.71	1388	OR215181

CT-R147	SA	Cellulosimicrobium funkei	99.57	1385	OR215067
CT-R148	SCN	Streptomyces albidoflavus	99.71	1375	OR215226
CT-R149	SCN	Rhodococcus hoagii	100.00	1368	OR215163
CT-R150	SCN	Nocardiopsis alba	99.93	1397	OR215142
CT-R151	SCN	Nocardiopsis umidischolae	99.00	1396	OR215156
CT-R152	SCN	Streptomyces xiamenensis	99.57	1389	OR215416
CT-R157	SCN	Streptomyces coelescens	99.93	1342	OR215360
CT-R158	SCN	Streptomyces xiamenensis	99.35	1394	OR215417
CT-R162	SCN	Streptomyces albidoflavus	99.78	1390	OR215361
CT-R163	SCN	Streptomyces aculeolatus	99.13	1375	OR215194
CT-R166	AIA	Streptomyces intermedius	99.57	1391	OR215242
CT-R167	AIA	Salinactinospora qingdaonensis	99.28	1398	OR215191
CT-R168	AIA	Streptomyces albidoflavus	99.93	1378	OR215362
CT-R169	AIA	Streptomyces albidoflavus	99.71	1379	OR215363
CT-R173	AIA	Streptomyces xiamenensis	99.35	1394	OR215364
CT-R174	AIA	Streptomyces intermedius	99.78	1391	OR215243
CT-R175	AIA	Kitasatospora albolonga	99.78	1391	OR215088
CT-R176	AIA	Streptomyces diastaticus	100.00	1394	OR215365
CT-R177	AIA	Cellulosimicrobium funkei	99.93	1388	OR215060
CT-R180	AIA	Streptomyces xiamenensis	99.64	1392	OR215418
CT-R181	SA	Streptomyces albidoflavus	99.50	1389	OR215367
CT-R182	SA	Streptomyces griseoflavus	99.78	1376	OR215368
CT-R183	SA	Streptomyces albidoflavus	99.78	1391	OR215369
CT-R184	SA	Streptomyces albidoflavus	99.64	1392	OR215370
CT-R185	NPS	Streptomyces aculeolatus	99.93	1402	OR215195
CT-R186	NPS	Streptomyces diastaticus	100.00	1378	OR215371
CT-R187	NPS	Nocardiopsis alba	99.64	1387	OR215143

CT-R188	NPS	Rhodococcus rhodochrous	99.93	1395	OR215182
CT-R190	NPS	Streptomyces hydrogenans	100.00	1378	OR215372
CT-R194	NPS	Streptomyces violascens	99.57	1391	OR215373
CT-R195	NPS	Streptomyces hydrogenans	99.50	1394	OR215374
CT-R196	NPS	Streptomyces albidoflavus	100.00	1378	OR215375
CT-R197	NPS	Streptomyces albidoflavus	99.57	1391	OR215376
CT-R198	NPS	Streptomyces hydrogenans	100.00	1394	OR215377
CT-R201	NPS	Streptomyces violascens	99.86	1391	OR215378
CT-R203	AIA	Streptomyces daghestanicus	100.00	1378	OR215379
CT-R205	AIA	Streptomyces violascens	99.86	1390	OR215380
CT-R206	SA	Streptomyces ardesiacus	100.00	1392	OR215220
CT-R207	SA	Streptomyces intermedius	99.78	1388	OR215244
CT-R208	SA	Nocardiopsis alba	99.86	1391	OR215144
CT-R209	SA	Rhodococcus coprophilus	99.50	1393	OR215157

^{*}according to EzBioCloud database

Table S2. Prokaryotic taxonomic profiles produced from the metagenomes of *C. tomentosum* and *C. crispus*. The abundance of each taxonomic group, as well as the number of reads, are presented.

Codium tomentosum

Phylum		Abundance (%)	Number of reads
Pseudomonac	lota	54.23	3202739
Bacteroidota		23.10	1363910
Cyanobacteria	ì	10.04	593176
Planctomycete	es	4.64	274035
Firmicutes		2.02	119102
Actinomyceto	ota	1.73	101926
Verrucomicrob	pia	1.11	65801
Viruses		0.08	4979
Unassigned at	t phylum level	1.02	60233
Tail (non-viral	phylum with less than 1% of all reads)	2.03	119617
Actinomy	cetota		
Order	Acidimicrobiales	0.40	23630
	Corynebacteriales	0.25	14738
	Micrococcales	0.25	14633
	Streptomycetales	0.15	9108
	Propionibacteriales	0.11	6360
Class	Actinomycetia	1.07	62897
	Acidimicrobiia	0.40	23630
	Coriobacteriia	0.10	6001
Family	Ilumatobacteraceae	0.20	11701
	lamiaceae	0.18	10631
	Streptomycetaceae	0.15	9108
	Mycobacteriaceae	0.11	6329
Genus	llumatobacter	0.20	11701
	Streptomyces	0.14	8174
Species	Ilumatobacter coccineus	0.20	11701

Chondrus crispus

Phylum		Abundance (%)	Number of reads
Pseudomonad	dota	59.79	6448075
Bacteroidota		14.21	1532126
Actinomyceto	ota	11.22	1209945
Cyanobacteria	a	6.40	690721
Planctomycete	es	2.78	299500
Firmicutes		1.67	179611
Viruses		0.07	7754
Unassigned at phylum level		0.76	82287
Tail (non-viral phylum with less than 1% of all reads)		3.10	334796
Actinomycetota			
Order	Acidimicrobiales	5.32	573333
	Corynebacteriales	1.26	135740
	Micrococcales	0.98	105695
	Streptomycetales	0.65	70445

	Propionibacteriales	0.60	64406
	Pseudonocardiales	0.48	51971
	Miltoncostaeales	0.31	32963
	Micromonosporales	0.25	27115
	Streptosporangiales	0.24	26154
	Euzebyales	0.15	16637
	Rubrobacterales	0.12	12582
	Frankiales	0.10	11138
Class	Acidimicrobiia	5.32	573333
	Actinomycetia	5.09	549096
	Thermoleophilia	0.33	36064
	Nitriliruptoria	0.26	27639
	Rubrobacteria	0.12	12582
Family	lamiaceae	3.03	326423
	Ilumatobacteraceae	2.18	235091
	Streptomycetaceae	0.65	70445
	Mycobacteriaceae	0.58	62263
	Pseudonocardiaceae	0.48	51971
	Nocardioidaceae	0.42	45357
	Nocardiaceae	0.34	36725
	Microbacteriaceae	0.33	35811
	Miltoncostaeaceae	0.33	32963
		0.31	27115
	Micromonosporaceae Micrococcaceae	0.23	20828
		0.19	
	Euzebyaceae	0.15	16637 15479
	Propionibacteriaceae	0.14	
	Corynebacteriaceae		14733
	Gordoniaceae	0.12	12858
0	Frankiaceae	0.10	11138
Genus	llumatobacter	2.18	235091
	Aquihabitans	1.25	134658
	Actinomarinicola	1.07	115152
	lamia	0.58	62988
	Streptomyces	0.58	62136
	Nocardioides	0.35	37336
	Miltoncostaea	0.31	32963
	Mycobacterium	0.24	25655
	Mycolicibacterium	0.23	24939
	Rhodococcus	0.21	22942
	Euzebya	0.15	16637
	Pseudonocardia	0.15	15976
	Amycolatopsis	0.14	14852
	Corynebacterium	0.14	14733
	Nocardia	0.12	13467
	Gordonia	0.10	11150
	Frankia	0.10	11138
Species	llumatobacter coccineus	2.18	235091
	Actinomarinicola tropica	1.07	115152
	Euzebya pacifica	0.15	16637
	Miltoncostaea oceani	0.15	15738
	Miltoncostaea marina	0.11	11997

APPENDIX II

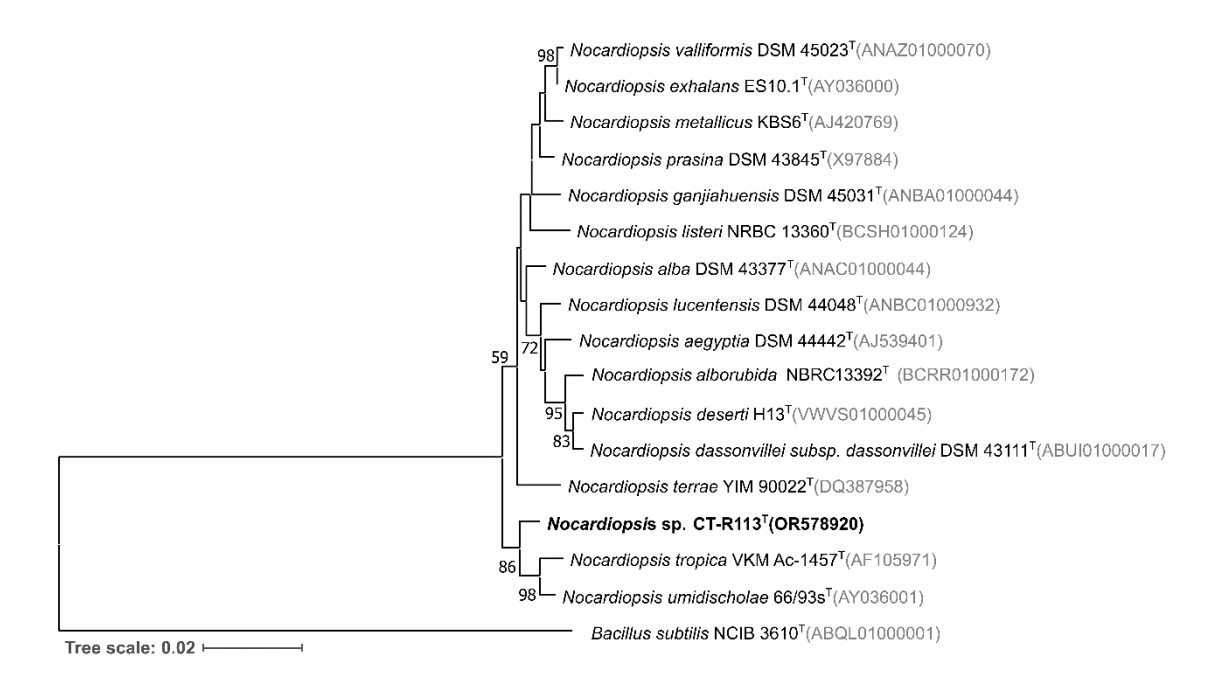


Figure S1. NJ phylogenetic tree based on 16S rRNA gene sequences (1,302 nt), showing the relationship between strain CT-R113^T and the closest related type strains within the genus *Nocardiopsis*. Accession numbers are indicated in brackets. Values at the nodes indicate bootstrap values of 50% and above, obtained based on 1,000 resampling events. *Bacillus subtilis* NCIB 3610^T was used as outgroup. Scale bar, 2 inferred nucleotide substitution per 100 nucleotides.

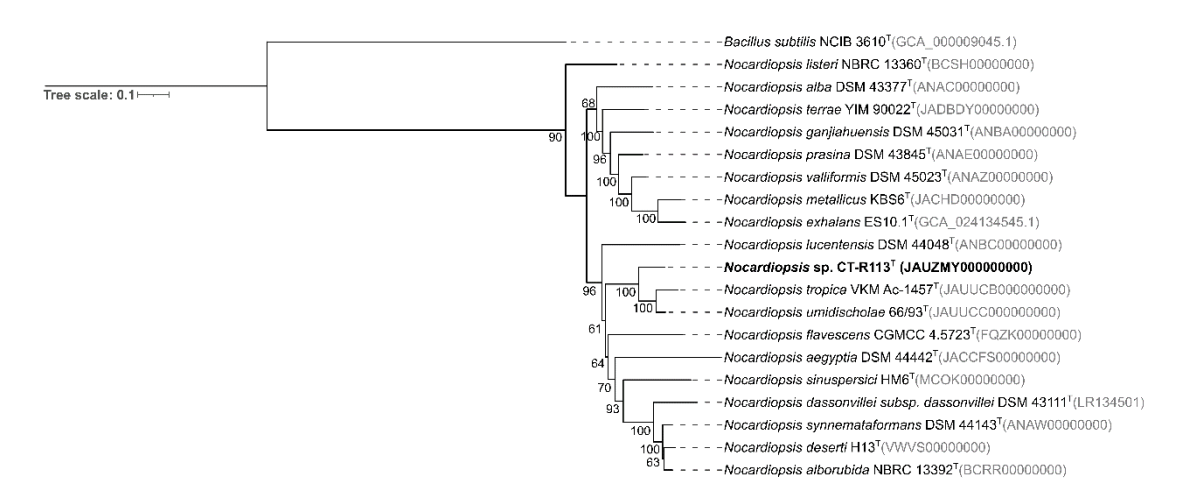


Figure S2. NJ phylogenomic tree based on 400 universal marker genes, showing the relationship between strain CT-R113^T and the closest related type strains within the genus *Nocardiopsis*. Accession numbers are indicated in brackets. Values at the nodes indicate bootstrap values of 50% and above obtained based on 1,000 resampling events. *Bacillus subtilis* NCIB 3610^T was used as outgroup. Scale bar, 10 inferred nucleotide substitution per 100 nucleotides.

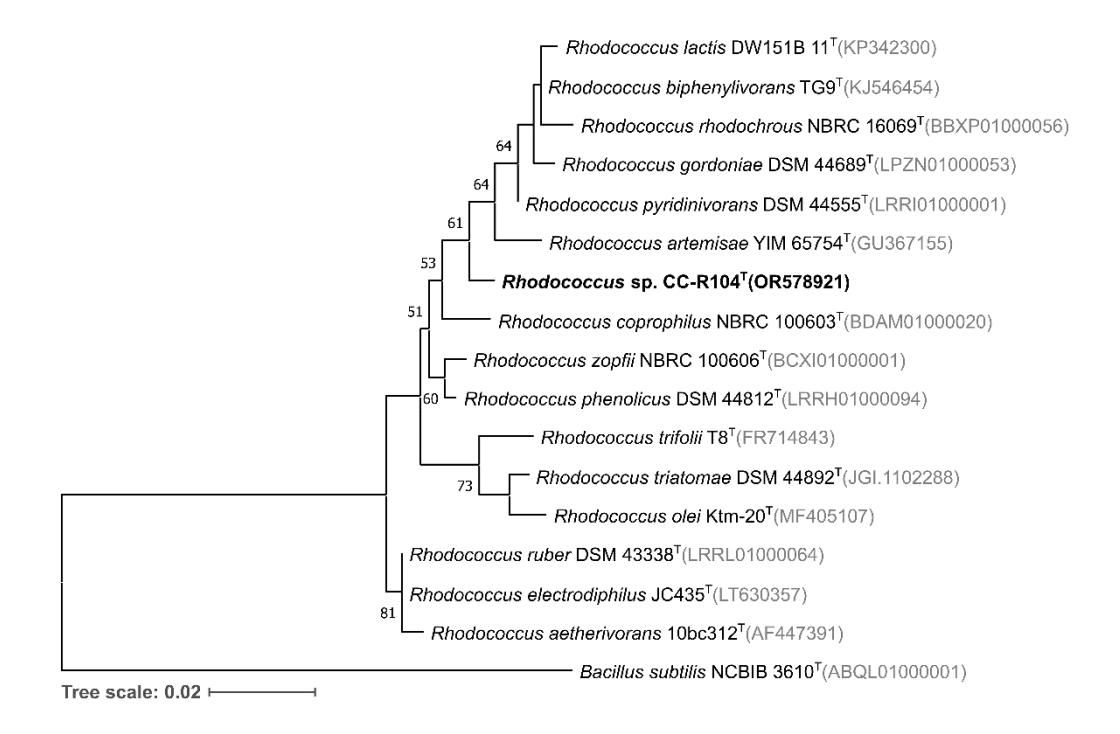


Figure S3. NJ phylogenetic tree based on 16S rRNA gene sequences (1,283 nt), showing the relationship between strain CC-R104^T and the closest related type strains within the genus *Rhodococcus*. Accession numbers are indicated in brackets. Values at the nodes indicate bootstrap values of 50% and above, obtained based on 1,000 resampling events. *Bacillus subtilis* NCIB 3610^T was used as outgroup. Scale bar, 2 inferred nucleotide substitution per 100 nucleotides.

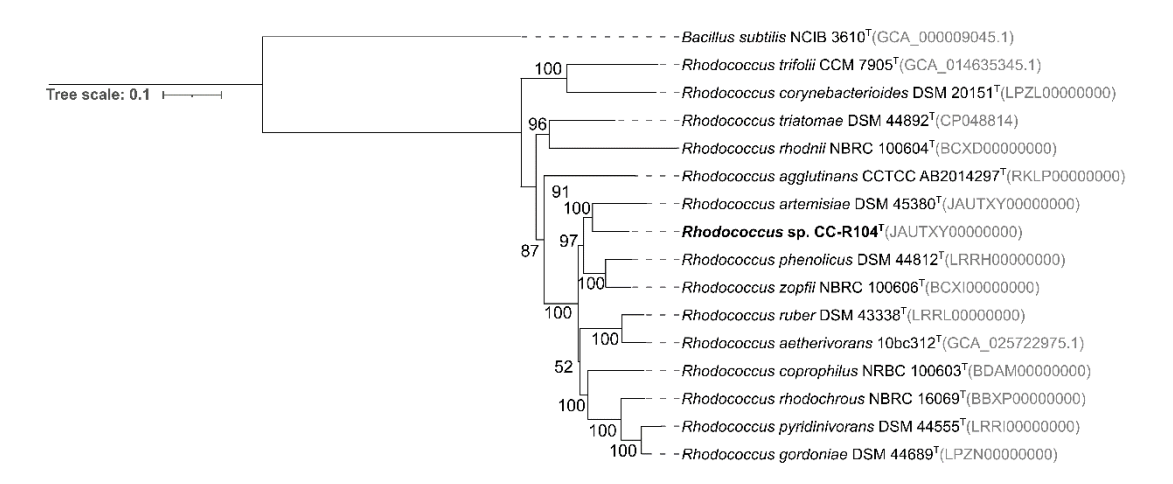


Figure S4. NJ phylogenomic tree based on 400 universal marker genes, showing the relationship between strain CC-R104^T and the closest related type strains within the genus *Rhodococcus*. Accession numbers are indicated in brackets. Values at the nodes indicate bootstrap values of 50% and above obtained based on 1,000 resampling events. *Bacillus subtilis* NCIB 3610^T was used as outgroup. Scale bar, 10 inferred nucleotide substitution per 100 nucleotides.

Table S3. ANI (%) of the genome of strain CT-R113^T and the closest related type strains within the genus *Nocardiopsis*. Query genome: *Nocardiopsis* sp. CT-R113^T (JAUZMY000000000).

Reference Genome	ANI (%)
Nocardiopsis umidischolae 66/93 ^T (JAUUCC000000000)	90.6
Nocardiopsis tropica VKM Ac-1457 ^T (JAUUCB000000000)	89.9
Nocardiopsis synnemataformans DSM 44143 ^T (ANAW00000000)	85.6
Nocardiopsis dassonvillei subsp. dassonvillei DSM 43111 [⊤] (LR134501)	85.5
Nocardiopsis sinuspersici HM6 ^T (MCOK0000000)	85.5
Nocardiopsis deserti H13 ^T (VWVS0000000)	85.5
Nocardiopsis alborubida NBRC 13392 [™] (BCRR00000000)	85.4
Nocardiopsis terrae YIM 90022 [™] (JADBDY00000000)	83.4
Nocardiopsis ganjiahuensis DSM 45031 [⊤] (ANBA00000000)	83.3
Nocardiopsis aegyptia DSM 44442 ^T (JACCFS00000000)	83.3
Nocardiopsis metallicus KBS6 [™] (JACHD00000000)	83.3
Nocardiopsis exhalans ES10.1 ^T (GCA_024134545.1)	83.2
Nocardiopsis flavescens CGMCC 4.5723 ^T (FQZK00000000)	83.2
Nocardiopsis valliformis DSM 45023 ^T (ANAZ00000000)	83.0
Nocardiopsis lucentensis DSM 44048 ^T (ANBC00000000)	83.1
Nocardiopsis alba DSM 43377 ^T (ANAC00000000)	82.5
Nocardiopsis listeri NBRC 13360 ^T (BCSH00000000)	82.4

Table S4. ANI (%) between the genome of strain CC-R104^T and the closest related type strains within the genus *Rhodococcus*. Query genome: *Rhodococcus* sp. CC-R104^T (JAUTXY000000000).

Reference Genome	ANI (%)
Rhodococcus rhodochrous NBRC 16069 ^T (BBXP00000000)	81.7
Rhodococcus gordoniae DSM 44689 ^T (LPZN00000000)	81.6
Rhodococcus pyridinivorans DSM 44555 [™] (LRRI00000000)	81.5
Rhodococcus phenolicus DSM 44812 ^T (LRRH00000000)	81.4
Rhodococcus zopfii NBRC 100606 ^T (BCXI00000000)	81.3
Rhodococcus coprophilus NBRC 100603 [™] (BDAM00000000)	81.2
Rhodococcus artemisiae YIM 65754 ^T (JAUTXY000000000)	81.2
Rhodococcus aetherivorans 10bc312 ^T (GCA_025722975.1)	81.0
Rhodococcus ruber DSM 43338 ^T (LRRL00000000)	80.9
Rhodococcus agglutinans CCTCC AB2014297 ^T (RKLP00000000)	79.6
Rhodococcus triatomae DSM 44892 ^T (CP048814)	78.8
Rhodococcus rhodnii NBRC 100604 ^T (BCXD00000000)	78.6
Rhodococcus corynebacterioides DSM 20151 ^T (LPZL00000000)	78.3
Rhodococcus trifolii T8 ^T (GCA_014635345.1)	77.9

Table S5. BGCs identified by antiSMASH (version 7.1.0) in the genomes of strains CT-R113^T, VKM Ac-1457^T and 66/93^T. Relaxed detection settings and all extra features were selected.

CT-R113^T

Region	Type of compound	Most similar known cluster	Similarity	MiBiG	BGC origin	Length (nt)
J			(%)	accession	J	• ,
1.1	T1PKS	Aldgamycin J	13	BGC0001396	Streptomyces sp. A1(2016)	323,681 – 381,248
2.1	Ectoine	Ectoine	75	BGC0002052	Streptomyces sp.	22,28 - 32,681
2.2	T2PKS	Formicamycins A-M	9	BGC0001590	Streptomyces sp. KY5	350,126 - 422,602
4.1	Butyrolactone	Murayaquinone	3	BGC0001675	Streptomyces griseoruber	7,683 – 18,786
4.2	NI-siderophore	Desferrioxamine E	100	BGC0001478	Streptomyces sp. ID38640	154,004 - 183,926
5.1	Nucleoside	Huimycin	70	BGC0002354	Kutzneria albida DSM 43870	217,701 – 238,063
6.1	Butyrolactone	-	-	-	-	123,541 – 134,584
7.1	NRPS	Incednine	4	BGC0000078	Streptomyces sp. ML694-90F	21,12 - 65,568
8.1	NRPS	Surugamide A	19	BGC0001792	Streptomyces albidoflavus	64,853 – 124,582
11.1	Terpene	Isorenieratene	87	BGC0001456	Streptomyces argillaceus	128,703 – 154,316
15.1	Lassopeptide/T3PKS	-	-	-	-	13,241 – 73,434
15.2	Terpene	Legonindolizidine A6	12	BGC0002666	Streptomyces sp. MA37	73,708 - 95,084
15.3	RiPP-like	-	-	-	-	102,276 -112,572
16.1	Lanthipeptide-class-i	-	-	-	-	93,18 - 118,636
16.2	Guanidinotides	Actagardine	6	BGC0000495	Actinoplanes garbadinensi	159,992 – 173,472
19.1	HR-T2PKS/Butyrolactone	Colabomycin E	13	BGC0000213	Streptomyces aureus	1 – 39,94
19.2	Ectoine	Kosinostatin	4	BGC0001073	Micromonospora sp. TP-A046	143,778 – 149,237
22.1	Lanthipeptide-class-iv	Duramycin	25	BGC0001579	Streptomyces cinnamoneus	61,069 - 83,645
24.1	NRP-metallophore/NRPS/T1PKS	Coelibactin	90	BGC0000324	Streptomyces coelicolor A3(2	41,121 – 120,809
43.1	NI-siderophore	Nonactin	33	BGC0000244	Streptomyces griseus subsp.	21,682 - 45,602
					griseus	

48.1	T3PKS	Feglymycin	26	BGC0001233	Streptomyces sp. DSM 11171	1 – 22,133
57.1	Oligosaccharide/Other,PKS-like	Kosinostatin	6	BGC0001073	Micromonospora sp. TP-A0468	1 – 27,728
61.1	Lanthipeptide-class-iii	-	-	-	-	5,123 – 20,015
65.1	RRE-containing	-	-	-	-	1 – 11,785
67.1	Thiopeptide,LAP	-	-	-	-	1 – 7,838
68.1	NRPS	-	-	-	-	1 – 5,932
75.1	NRPS	-	-	-	-	1 – 2,515

VKM Ac-1457^T

Type of compound	Most similar known sluster	Similarity	MiBiG	PCC origin	Length (nt)	
Type of compound	Most similar known cluster	(%)	accession	BGC origin	Length (III)	
Lassopeptide	Streptomonomicin	40	BGC0001176	Streptomonospora alba	1 – 11,342	
Terpene	Isorenieratene	18	BGC0001227	Streptomyces collinus Tu 365	1 – 10,074	
RiPP-like	Funisamine	7	BGC0001944	Streptosporangium sp.	1 - 9,077	
Lanthipeptide-class-i	-	-	-	-	1 – 7,321	
Terpene	-	-	-	-	1 – 5,673	
Other	Rubradirin	6	BGC0000141	Streptomyces achromogenes	1 – 5,431	
				subsp. rubradiris		
NI-siderophore	Desferrioxamine E	100	BGC0001478	Streptomyces sp. ID38640	1 - 4,767	
RRE-containing	-	-	-	-	1 – 4,316	
Ectoine	Ectoine	75	BGC0002052	Streptomyces sp.	1 - 4,048	
NRPS	-	-	-	-	1 - 3,766	
Butyrolactone	-	-	-	-	1 - 3,562	
T1PKS	Nanchangmycin	30	BGC0000105	Streptomyces nanchangensis	1 – 3,536	
Butyrolactone	-	-	-	-	1 – 3,436	
Terpene	Isorenieratene	37	BGC0001456	Streptomyces argillaceus	1 – 2,956	
	Terpene RiPP-like Lanthipeptide-class-i Terpene Other NI-siderophore RRE-containing Ectoine NRPS Butyrolactone T1PKS Butyrolactone	Lassopeptide Streptomonomicin Terpene Isorenieratene RiPP-like Funisamine Lanthipeptide-class-i - Terpene - Other Rubradirin NI-siderophore Desferrioxamine E RRE-containing - Ectoine Ectoine NRPS - Butyrolactone - T1PKS Nanchangmycin Butyrolactone -	Type of compound Most similar known cluster (%) Lassopeptide Streptomonomicin 40 Terpene Isorenieratene 18 RiPP-like Funisamine 7 Lanthipeptide-class-i Terpene Other Rubradirin 6 NI-siderophore Desferrioxamine E 100 RRE-containing Ectoine Ectoine 75 NRPS Butyrolactone T1PKS Nanchangmycin 30 Butyrolactone	Type of compoundMost similar known cluster (%)(%)accessionLassopeptideStreptomonomicin40BGC0001176TerpeneIsorenieratene18BGC0001227RiPP-likeFunisamine7BGC0001944Lanthipeptide-class-iTerpeneOtherRubradirin6BGC0000141NI-siderophoreDesferrioxamine E100BGC0001478RRE-containingEctoineEctoine75BGC0002052NRPSButyrolactoneT1PKSNanchangmycin30BGC0000105Butyrolactone	Type of compoundMost similar known cluster (%)(%)accessionBGC originLassopeptideStreptomonomicin40BGC0001176Streptomonospora albaTerpeneIsorenieratene18BGC0001227Streptomyces collinus Tu 365RiPP-likeFunisamine7BGC0001944Streptosporangium sp.Lanthipeptide-class-iTerpeneOtherRubradirin6BGC0000141Streptomyces achromogenes subsp. rubradirisNI-siderophoreDesferrioxamine E100BGC0001478Streptomyces sp. ID38640RRE-containingEctoineEctoine75BGC0002052Streptomyces sp.NRPSButyrolactoneT1PKSNanchangmycin30BGC0000105Streptomyces nanchangensisButyrolactone	

712.1	NRPS-like	-	-	-	-	1 - 2,697
844.1	PKS-like	Calicheamicin	2	BGC0000033	Micromonospora echinospora	1 – 2,415
852.1	T1PKS	-	-	-	-	1 – 2,405

66/93^T

Dogion	Type of compound	Most similar known	Similarity	MiBiG	BCC origin	Longth (nt)
Region	Type of compound	cluster	(%)	accession	BGC origin	Length (nt)
1.1	T3PKS	-	-	-	-	27,844 – 68,902
1.2	Terpene/Lassopeptide	Legonindolizidine A6	12	BGC0002666	Streptomyces sp. MA37	132,834 – 175,451
1.3	RiPP-like	-	-	-	-	211,985 – 222,281
2.1	T2PKS/Furan	Accramycin A	10	BGC0002315	Streptomyces sp.	93,728 – 166,205
3.1	NI-siderophore	Petrichorin A	11	BGC0002315	Streptomyces sp.	23,524 - 53,452
3.2	Betalactone	Formicamycins A-M	4	BGC0001590	Streptomyces sp. KY5	55,433 - 86,522
6.1	CDPS	-	-	-	-	72,627 - 93,475
7.1	T1PKS/NRPS-like/NRPS	a201a	10	BGC0001138	Marinactinospora thermotolerans	15,384 – 72,675
10.1	HR-T2PKS/Butyrolactone/Thioamide-	Colabomycin E	13	BGC0000213	Streptomyces aureus	12,864 - 96,777
	NRP					
22.1	NRPS-like	Guanipiperazine A	80	BGC0002582	Streptomyces chrestomyceticus	39,858 - 78,026
24.1	NRPS	Malonomycin	44	BGC0001942	Streptomyces rimosus subsp.	47,621 – 77,767
					paromomycinus	
36.1	Terpene	Isorenieratene	87	BGC0001456	Streptomyces argillaceus	1 – 18,804
38.1	Butyrolactone	SF2575	4	BGC0000269	Streptomyces sp. SF2575	55,38 - 61,42
40.1	Guanidinotides	Mannopeptimycin	7	BGC0000388	Streptomyces hygroscopicus	3,633 - 26,186
54.1	Oligosaccharide/Other/PKS-like	Mycinamicin II	14	BGC0000102	Micromonospora griseorubida	3,909 - 48,935
61.1	NRPS	CDA1b	12	BGC0000315	Streptomyces coelicolor A3(2)	1 – 43,978

65.1	NRPS	Malonomycin	27	BGC0001942	Streptomyces rimosus subsp.	7,602 – 42,375
					paromomycinus	
86.1	Lanthipeptide-class-iii	Auroramycin	2	BGC0001522	Streptomyces filamentosus	7,621 – 29,216
90.1	Butyrolactone	-	-	-	-	19,237 – 30,18
92.1	T1PKS	Aldgamycin J	13	BGC0001396	Streptomyces sp. A1(2016)	1 – 28,851
95.1	NRPS	Coelibactin	45	BGC0000324	Streptomyces coelicolor A3(2)	1 – 26,759
101.1	Ectoine	-	-	-	-	20,351 – 25,868
107.1	T1PKS	Uncialamycin	12	BGC0001377	Streptomyces uncialis	1 – 23,592
112.1	NRP-metallophore,NRPS	Coelibactin	27	BGC0000324	Streptomyces coelicolor A3(2)	1 – 24,314
129.1	Lanthipeptide-class-iv	-	-	-	-	6,791 – 19,571
134.1	RiPP-like	-	-	-	-	12,437 – 18,779
137.1	Lanthipeptide-class-iii	-	-	-	-	1 – 13,356
145.1	NRPS	Incednine	4	BGC0000078	Streptomyces sp. ML694-90F3	1 – 17,092
153.1	NRPS	Acyldepsipeptide 1	15	BGC0001967	Streptomyces hawaiiensis	1 – 14,712
158.1	T1PKS/NRPS/NRPS-like	BE-43547A1	10	BGC0001330	Micromonospora sp. RV43	1 – 14,397
242.1	T1PKS	-	-	-	-	1 – 3,310

T1PKS: Type I polyketide synthase T2PKS: Type 2 polyketide synthase T3PKS: Type 3 polyketide synthase

NRPS: Non-ribosomal peptide synthetase
RiPP-like: Other unspecified ribosomally synthesised and post-translationally modified peptide product
NRPS-like: Non-ribosomal peptide synthetase-like fragment

PKS-like: Polyketide synthase-like fragment

(-) no hits

Table S6. BGCs identified by antiSMASH (version 7.1.0) in the genomes of strains CC-R104^T and DSM 45380^T. Relaxed detection settings and all extra features were selected.

CC-R104^T

Domina	Turns of sommound	Most similar language alvetor	Circilority (0/)	MiBiG	DOC animin	Longth (nt)
Region	Type of compound	Most similar known cluster	Similarity (%)	accession	BGC origin	Length (nt)
2.1	Terpene	5-dimethylallylindole-3-acetonitrile	55	BGC0002128	Streptomyces coelicolor A3(2)	20,325 - 41,314
18.1	Terpene	Isorenieratene	42	BGC0000664	Streptomyces griseus subsp.	8,206,573 - 8,214,963
					griseus NBRC 13350	
25.1	Redox-cofactor	-	-	-	-	15,707 - 38,518
40.1	NRPS	-	-	-	-	1 - 34,048
49.1	Betalactone/NRPS-	Hedamycin	6	BGC0000233	Streptomyces griseoruber	1 - 45,603
	like					
61.1	Terpene	SF2575	4	BGC0000269	Streptomyces sp. SF2575	1 - 53,273
106.1	NAPAA	Rifamorpholine A	3	BGC0001759	Amycolatopsis sp.	1 - 113,830
109.1	RiPP-like	-	-	-	-	5,328 – 16,131
161.1	Ectoine	Ectoine	75	BGC0000853	Streptomyces anulatus	1 – 3,366
162.1	NRPS	-	-	-	-	1 – 10,151
171.1	NRPS	Atratumycin	7	BGC0001975	Streptomyces atratus	1 – 9,747
175.1	NRPS	Tetrocarcin A	4	BGC0000162	Micromonospora chalcea	1 – 9,313
191.1	NRPS-like	-	-	-	-	1 – 8,416
194.1	T1PKS	-	-	-	-	1 – 8,250
207.1	NRPS-like	-	-	-	-	1 – 7,676
230.1	NRPS	-	-	-	-	1 – 5,946
279.1	NRPS	-	-	-	-	1 – 3,860
280.1	NRPS	-	-	-	-	1 - 3,809
308.1	NRPS	-	-	-	-	1 – 2,935

316.1	NRPS	-	-	-	-	1 – 2,724
325.1	NRPS-like	-	-	-	-	1 – 2,405
355.1	NRPS	-	-	-	-	1 – 1,485
363.1	NRPS-like	-	-	-	-	1 – 3,347
366.1	NRPS	-	-	-	-	1 – 3,335

DSM 45380^T

Domina	Turns of someoned	Mast similar known skyster	Circilority (0/)	MiBiG	DCC animin	Lameth (nt)	
Region	Type of compound	Most similar known cluster	Similarity (%)	accession	BGC origin	Length (nt)	
1.1	NRPS	-			-	1 – 24,688	
1.2	Terpene	SF2575	6	BGC0000269	Streptomyces sp. SF2575	216,338 – 237,456	
1.3	Ectoine	Ectoine	75	BGC0000853	Streptomyces anulatus	681,998 – 692,399	
2.1	Butyrolactone	-	-	-	-	655,789 – 666,925	
4.1	T1PKS	-	-	-	-	369.022 - 413.992	
6.1	NAPAA	ε-Poly-L-lysine	100	BGC0002174	Epichloe festucae	1 – 3,894	
7.1	NRPS/NRPS	Amychelin A	33	BGC0002544	Amycolatopsis methanolica	1 – 39,399	
	metallophore						
7.2	RiPP-like	-	-	-	-	295,872 – 306,675	
8.1	Redox-cofactor	-	-	-	-	191,139 – 213,953	
8.2	NRPS	Cinnapeptin	7	BGC0002108	Streptomyces viridosporus	221,462 - 317,220	
					ATCC 14672		
10.1	Terpene	Isorenieratene	37	BGC0000664	Streptomyces griseus subsp.	12,679 - 33,653	
					griseus NBRC 13350		
11.1	NRPS/T1PKS/Betalactone	Scopranone A	5	BGC0002558	Streptomyces sp.	74,137 – 148,225	
12.1	NRPS	-	-	-	-	13,660 - 87,160	
12.2	NRPS	-	-	-	-	139,749 – 198,594	

18.1	NRPS/Betalactone	-	-	-	-	1 – 32,486
23.1	NRPS	Chloramphenicol	17	BGC0000893	Streptomyces venezuelae	35,764 - 72,800
					ATCC 10712	
25.1	NRPS/T1PKS	-	-	-	-	1 – 43,905

NRPS: Non-ribosomal peptide synthetase

NRPS-like: Non-ribosomal peptide synthetase-like fragment NAPAA: Non-alpha poly-amino acids like e-Polylysin

RiPP-like: Other unspecified ribosomally synthesised and post-translationally modified peptide product

T1PKS: Type I polyketide synthase

(-) no hits

APPENDIX III

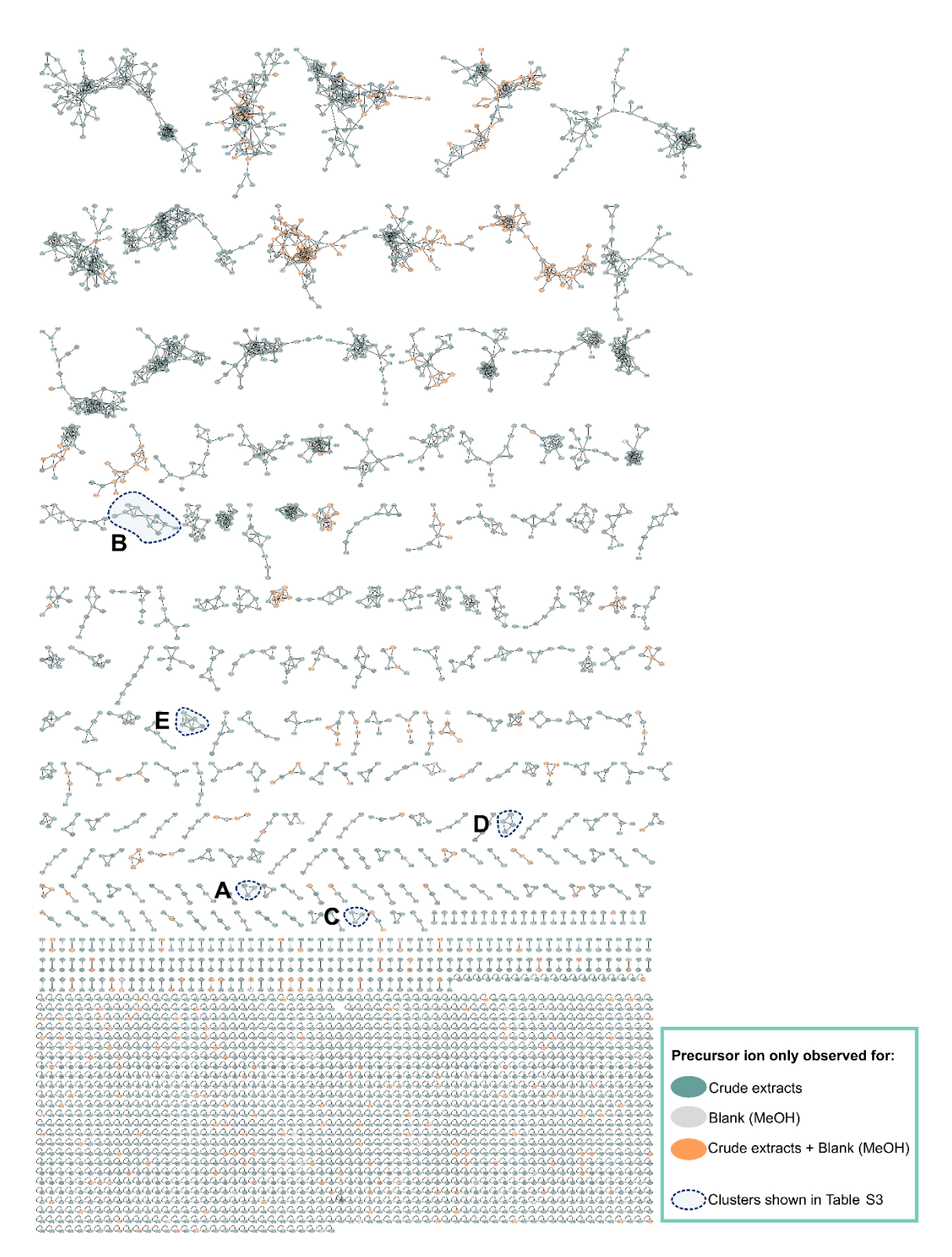


Figure S5. GNPS molecular networking using MS/MS data from the 22 crude extracts without any hit in the GNPS dereplication tools. The value indicated in each node corresponds to the precursor ion. Detailed information regarding each highlighted cluster is presented in Table 9.

Table S7. Bioactivity profiling of all active actinobacterial crude extracts. Information regarding the fermentation medium used for each strain is also presented.

	FERMENTATION MEDIUM	BIOACTIVITY ASSAY									
OTDAIN				ANTIMICR	OBIAL			LIPID REDUCING			
STRAIN			Inhibition halo (mm)					Cellular viability (%)			
		C. albicans	B. subtilis	S. aureus	P. anguilliseptica	A. hydrophila	HCT116	T47D	hCMEC/D3	MFI (%)	
CC-F4	SCN	-	-	-	<u>-</u>	12	-	<u>-</u>	<u>-</u>	-	
CC-F7	MB	-	-	-	-	-	60.55 **	-	75.44	-	
CC-F9	MB	-	9	=	-	-	-	-	-	-	
CC-F27	AIA	-	=	=	-	-	52.61*** †	47.92 *** †	80.83	-	
CC-F28	AIA	-	9	8	-	-	-	-	-	-	
CC-F32	AIA	-	=	=	-	-	61.68 **	66.43 **	89.85	-	
CC-F35	AIA	-	=	=	-	-	67.35 *	-	86.16	-	
CC-F41	AIA	-	=	=	14	-	-	-	-	-	
CC-F45	MB	10	-	-	-	-	32.44 *** †	-	98.35	-	
CC-F47	MB	-	24	15	-	-	-	57.18 **	105.14	-	
CC-F52	MB	-	=	=	-	-	75.36 *	-	102.80	-	
CC-F53	MB	-	-	-	-	-	67.61 *	-	93.19	-	
CC-F64	MB	-	=	=	-	-	52.21 **	-	83.77 *	-	
CC-F65	MB	-	-	-	-	-	56.63 **	-	54.96 **	-	
CC-F67	MB	9	=	=	-	-	-	-	-	-	
CC-F69	MB	-	-	-	-	-	41.89 ***	21.41 ***	11.08 ***	-	
CC-F71	MB	-	-	-	-	13	-	-	-	-	
CC-F72	AIA	-	-	-	-	-	74.38 **	-	92.26	-	
CC-F76	AIA	-	15	-	-	-	-	-	-	-	
CC-F78	AIA	-	-	-	-	-	37.80 ***	12.85 ***	40.93 ***	-	
CC-F79	AIA	11	20	10	13	-	42.85 ***	44.78 ***	19.48 ***	-	
CC-F83	AIA	-	-	-	-	-	-	64.73 *	86.78	-	
CC-F88	AIA	_	25	13	_	-	-	50.03 **	41.44 ***	_	

ICBAS
Portuguese seaweeds, a marine treasure of Actinobacteria producing novel bioactive compounds

CC-F90	AIA	-	-	-	-	11	-	-	-	-
CC-F106	AIA	-	-	-	-	12	-	-	-	-
CC-F110	AIA	-	9	-	-	-	-	-	-	-
CC-F120	MB	-	-	-	-	10	-	-	-	-
CC-F123	MB	26	-	-	-	9	40.2 *** †	-	98.7	-
CC-R10	MB	-	-	-	-	12	-	-	-	-
CC-R20	MB	-	-	-	-	15	-	-	-	-
CC-R26	MB	15	-	-	-	-	23.42 *** †	-	82.86	-
CC-R35	MB	-	-	-	-	-	64.34 *	-	94.14	-
CC-R36	MB	-	-	-	-	-	-	-	-	45.2
CC-R44	SCN	-	-	-	-	11	-	-	-	-
CC-R47	SCN	10	-	-	13	-	-	-	-	-
CC-R53	AIA	-	-	-	-	-	63.76 *	-	97.09	-
CC-R61	AIA	-	14	13	-	-	-	56.01 *	39.59 **	72.9
CC-R64	AIA	-	15	-	-	-	-	-	-	-
CC-R68	AIA	-	20	15	-	-	-	-	-	39.9
CC-R69	AIA	-	-	-	-	14	-	-	-	-
CC-R70	AIA	-	-	-	-	15	-	-	-	-
CC-R72	AIA	-	-	-	-	-	-	-	-	40.3
CC-R81	SCN	12	-	-	-	-	-	-	-	-
CC-R88	MB	-	-	-	-	-	-	58.45 **	91.64	-
CC-R93	MB	-	-	-	-	12	-	-	-	-
CC-R103	MB	11	-	-	-	-	-	-	-	-
CC-R112	AIA	-	20	16	-	10	61.13 *	46.61 *	98.03	-
CC-R115	AIA	-	13	12	-	-	-	-	-	-
CC-R116	AIA	20	-	-	-	14	-	-	-	-
CC-R117	AIA	-	-	-	-	26	-	-	-	-
CC-R119	AIA	18	-	-	-	-	35.26 *** †	-	94.65	-
CC-R120	AIA	10	-	-	-	-	-	-	-	-

ICBAS
Portuguese seaweeds, a marine treasure of Actinobacteria producing novel bioactive compounds

CC-R134	AIA	9	=	-	-	-	-	-	-	-
CC-R135	AIA	-	-	-	-	13	-	-	-	-
CC-R136	AIA	-	-	-	12	-	-	-	-	-
CC-R138	AIA	-	-	-	-	-	-	58.02 *	96.96	-
CC-R150	MB	14	-	-	-	-	33.17 *** †	-	82.45	-
CC-R151	MB	-	-	-	-	-	27.54 *** †	-	93.70	-
CC-R154	MB	12	-	-	-	-	-	-	-	-
CC-R155	MB	-	12	11	-	-	57.90 **	19.43 ***	22.76 ***	-
CC-R160	MB	-	-	-	-	14	-	-	-	-
CC-R164	MB	-	8	12	-	-	-	-	-	-
CC-R165	AIA	-	-	-	-	11	-	-	-	-
CC-R166	AIA	-	-	-	-	22	-	-	-	-
CC-R175	SCN	-	-	-	-	-	36.87 *** †	-	88.32	-
CC-R176	AIA	-	13	14	13	-	-	-	-	-
CC-R178	AIA	-	-	-	-	-	27.81 ***	17.81 ***	7.95 ***	-
CC-R180	MB	-	-	-	-	-	39.91 ***	30.92 ***	66.57 *	-
CT-F6	MB	-	-	-	-	-	30.62 *** †	-	97.11	-
CT-F11	MB	-	17	-	-	-	30.53 *** †	-	90.31	-
CT-F14	SCN	-	-	-	-	-	56.77 **	65.88 *	74.93 *	-
CT-F18	SCN	-	25	25	-	-	-	-	-	-
CT-F19	SCN	-	-	-	-	-	56.22 **	32.65 ***	40.76 **	-
CT-F25	SCN	14	-	-	-	-	-	-	-	-
CT-F26	SCN	-	9	8	-	-	-	-	-	-
CT-F28	SCN	-	-	-	-	-	49.66 *** †	63.65 **	80.75	-
CT-F29	SCN	-	8	-	-	-	52.18 *	-	60.01 *	-
CT-F31	MB	-	-	-	-	-	21.51 ***	32.12 ***	22.13 ***	-
CT-F37	MB	-	=	-	-	-	18.16 ***	4.80 ***	7.25 ***	-
CT-F39	MB	-	-	-	-	9	-	-	-	-
CT-F40	MB	-	=	-	-	-	61.39 *	63.35 *	57.56 **	-

ICBAS
Portuguese seaweeds, a marine treasure of Actinobacteria producing novel bioactive compounds

CT-F45	AIA	10	-	-	-	-	-	=	-	-
CT-F46	AIA	-	9	-	-	-	-	-	-	-
CT-F48	AIA	-	-	-	-	-	59.48 **	-	97.86	-
CT-F53	AIA	-	-	-	12	14	-	-	-	-
CT-F55	AIA	-	9	9	14	-	-	-	-	-
CT-F57	AIA	-	-	-	-	-	38.71 ***	40.85 ***	16.48 ***	-
CT-F61	AIA	-	10	9	-	13	45.4 *** †	52.78 *** †	100.02	-
CT-F62	AIA	9	-	-	-	-	-	-	-	-
CT-F63	AIA	-	-	-	-	19	-	-	-	-
CT-F65	AIA	-	8	9	-	-	-	=	-	=
CT-F68	AIA	-	-	-	-	11	-	-	-	-
CT-F70	AIA	-	-	-	-	14	-	-	-	-
CT-F72	AIA	-	-	-	-	20	-	=	-	=
CT-F87	MB	-	-	-	-	-	69.91 *	-	96.92	-
CT-F88	MB	-	-	-	-	25	-	=	-	-
CT-F93	AIA	-	-	-	13	11	-	=	-	=
CT-F99	AIA	-	-	-	-	-	60.51 **	-	88.19	-
CT-F104	AIA	-	-	-	14	18	-	=	-	-
CT-F116	MB	15	-	-	-	-	45.37 *** †	-	86.99	-
CT-F121	SCN	-	-	-	-	-	59.31 *	=	92.25	-
CT-F122	SCN	18	-	-	-	-	-	-	-	-
CT-F124	SCN	-	-	-	-	-	46.97 ***	14.80 ***	19.91 ***	-
CT-F125	AIA	-	-	-	11	-	-	=	-	=
CT-F127	AIA	16	-	-	-	-	-	=	-	-
CT-F133	AIA	14	-	-	-	-	-	=	-	-
CT-F134	AIA	14	-	-	-	-	-	=	-	=
CT-F139	MB	-	-	-	12	-	-	-	-	-
CT-F144	MB	-	-	-	-	-	12.61 ***	29.98 ***	18.74 ***	-
CT-F146	SCN	-	-	-	-	-	60.36 *	65.87 *	59.24 *	-

ICBAS
Portuguese seaweeds, a marine treasure of Actinobacteria producing novel bioactive compounds

CT-F147	SCN	-	-	-	-	13	-	-	-	-
CT-F153	AIA	14	=	-	-	-	-	-	-	-
CT-F155	AIA	14	=	-	-	-	-	-	-	-
CT-F156	MB	11	=	-	-	-	-	24.39 ***	10.55 ***	-
CT-R9	SCN	13	11	10	-	-	13.11 ***	23.19 ***	4.56 ***	-
CT-R10	SCN	-	=	-	-	-	-	=	-	43.9
CT-R13	SCN	-	=	-	-	-	-	60.73 *	90.01	-
CT-R28	MB	27	-	-	-	-	-	-	-	-
CT-R29	MB	-	=	-	-	-	16.10 ***	4.72 ***	5.59 ***	-
CT-R34	AIA	9	-	-	-	-	-	-	-	-
CT-R35	AIA	-	8	-	-	14	-	-	-	-
CT-R38	AIA	-	-	-	-	-	-	62.99 *	62.84 *	-
CT-R42	MB	-	-	-	-	-	29.10 *** †	-	99.17	-
CT-R43	MB	-	-	-	-	-	30.99 *** †	-	102.71	-
CT-R45	MB	-	-	-	-	11	-	-	-	-
CT-R46	MB	14	-	-	-	-	34.15 *** †	-	89.80	-
CT-R49	MB	16	-	-	-	-	41.70 *** †	49.75 *** †	89.36	-
CT-R51	SCN	-	-	-	-	-	-	62.13 *	88.68-	-
CT-R52	SCN	-	-	-	13	-	-	-		-
CT-R55	SCN	-	-	-	-	12	-	-	-	-
CT-R58	SCN	16	-	-	-	-	-	-	-	-
CT-R75	SCN	-	-	-	-	-	60.17 *	58.22 *	65.67 *	-
CT-R82	MB	10	-	-	-	-	28.40 *** †	-	109.90	-
CT-R88	MB	-	-	-	-	-	34.42 *** †	-	106.63	-
CT-R89	MB	11	-	-	-	-	48.11 *** [†]	-	94.48	-
CT-R96	AIA	-	9	-	-	-	-	40.93 ***	67.68 **	-
CT-R100	AIA	-	-	-	10	23	-	-	-	-
CT-R106	AIA	-	-	-	-	-	61.9 *	54.02 **	53.66 **	-
CT-R111	AIA	-	-	-	-	-	57.58 *	-	58.61 *	-

ICBAS
Portuguese seaweeds, a marine treasure of Actinobacteria producing novel bioactive compounds

CT-R113	AIA	-	-	-	-	14	-	-	-	=
CT-R116	AIA	-	-	-	-	12	54.81 **	-	63.20 *	=
CT-R124	AIA	-	-	-	-	-	36.41 ***	13.11 ***	18.77 ***	-
CT-R126	AIA	12	-	-	-	-	-	-	-	-
CT-R127	AIA	-	-	-	10	13	-	-	-	-
CT-R139	MB	-	-	-	-	-	54.44 **	-	53.75 **	-
CT-R146	MB	-	-	-	-	-	50.31 **	-	67.73 *	-
CT-R149	SCN	-	-	-	-	-	56.16 **	-	65.08 *	-
CT-R150	SCN	-	12	11	-	-	55.87 **	-	72.42 *	-
CT-R151	SCN	-	-	-	-	-	53.43 **	62.70 *	63.58 *	-
CT-R162	SCN	10	25	-	-	-	-	-	-	-
CT-R166	AIA	11	-	-	-	-	-	-	-	-
CT-R175	AIA	13	-	-	-	-	21.57 ***	26.53 ***	21.37 ***	-
CT-R176	AIA	9	-	-	-	-	-	-	-	-
CT-R177	AIA	-	-	-	-	-	53.77 **	22.45 ***	23.33 ***	-
CT-R180	AIA	-	14	10	-	-	66.20 *	52.82 **	45.97 ***	-
CT-R181	MB	-	9	11	-	-	-	-	-	-
CT-R182	MB	16	-	-	-	-	-	-	-	-
CT-R183	MB	22	-	-	-	-	-	-	-	-
CT-R184	MB	12	-	-	-	-	-	-	-	-
CT-R186	MB	12	-	-	-	-	31.39 ***†	-	101.68	-
CT-R190	MB	15	17	-	-	-	33.51 ***†	-	85.52	-
CT-R198	MB	10	-	-	-	-	25.03 ***†	-	91.44	-
CT-R201	MB	10	-	-	-	-	32.61 ***†	-	103.79	_
CT-R203	AIA	12	-	-	-	-	-	-	-	_
CT-R205	AIA	15	-	-	-	-	-	-	-	-
CT-R209	MB	-	-	-	-	14	-	-	-	-

^(†) Anticancer activity (i.e., no statistically significant cytotoxic activity on non-cancer cells). $^*=p<0.1;\ ^{**}=p<0.01;\ ^{***}p<0.001$ (-) no activity

Table S8. Actinomycetota-sourced compounds identified in the active crude extracts using GNPS dereplication tools. Data presented only for hits with score >10 and for compounds of actinobacterial origin with described bioactive properties, which are indicated in the Table. crude extracts with no hit in any of the dereplication tools are highlighted (bold and grey shaded).

			LC-HRESIMS/MS DE	EREPLICATION - GNPS		
STRAIN	Der	replicator	Derep	olicator +	Dereplicat	or VarQuest
	Compound	Described bioactivity	Compound	Described bioactivity	Compound	Described bioactivity
			Shurimycin A	Antimicrobial [373]		
CC-F4	NH	NH	Lipiarmycin A	Antimycobacterial [374]	NH	NH
			Langkolide	Antimicrobial,		
				Antiproliferative [375]		
CC-F7	Companyidas A. C.	Autinoman Autifum and [070]	Cumuramidae A. C	Antinoppe Antifum	Surugamides A, C	Anticancer, Antifungal
CC-F7	Surugamides A, C	Anticancer, Antifungal [276]	Surugamides A, C	Anticancer, Antifungal	Champacyclin	Antimicrobial [281]
	NH	NH	Roseofungin	Antifungal, Antiviral [279]		
CC-F9			Dermostatin B	Antimicrobial [376]	NH	NH
			Norerythromycin A	Antimicrobial [377]		
CC-F27	NH	NH	Strevertene D	Antifungal [282]	NH	NH
CC-F21			Apoptolidin A	Cytotoxic [378]	INΠ	INΠ
CC-F28	NH	NH	NH	NH	Friulimicin A	Antibacterial [379]
CC-F32	Surugamides A, C	Anticancer, Antifungal	Surugamides A, C	Anticancer, Antifungal	Surugamides A, C	Anticancer, Antifungal
00-1 32	Surugarnides A, C	Anticancer, Antilungar	Surugamides A, C	Anticancer, Antirungar	Champacyclin	Antimicrobial
CC-F35	Surugamides A, C	Anticancer, Antifungal	Surugamides A, C	Anticancer, Antifungal	Surugamides A, C	Anticancer, Antifungal
00133	odrugamides A, o	Antibancor, Antirungar	ourugamides A, O	Anticancer, Antirungar	Champacyclin	Antimicrobial
CC-F41	NH	NH	NH	NH	NH	NH
			Surugamides A, D	Anticancer, Antifungal	Champacyclin	Antimicrobial
CC-F45	Surugamides A, C	Anticancer, Antifungal	Champacyclin	Antimicrobial	Surugamides A,C	Anticancer, Antifungal
			Lydiamycin A	Antimycobacterial [374]	Neotelomycin	Antimicrobial [380]

CC-F47	NH	NH	Juvenimicin B	Antimicrobial [381]	Telomycin	Antimicrobial [382]
			00.00	7	Streptomonomicin	Antimicrobial [383]
CC-F52	Surugamides A, B	Anticancer, Antifungal	Surugamides A, B	Anticancer, Antifungal	Surugamide A	Anticancer, Antifungal
00-1 32	Surugamides A, D	Anticancer, Antilungal	Surugariides A, B	Anticancer, Antinungar	Champacyclin	Antimicrobial
CC-F53	Surugamides A, B	Anticancer, Antifungal	Surugamides A, B	Anticancer, Antifungal	Surugamide A	Anticancer, Antifungal
00 1 33	Ourugamides A, D	Anticancer, Antirungar	Ourugamides A, B	Anticaricer, Antirungar	Champacyclin	Antimicrobial
			Flavofungin	Antifungal [384]		
CC-F64	NH	NH	Amphidinolide B	Anticancer [385]	NH	NH
			Chaxalactin B	Antimicrobial [386]		
CC-F65	NH	NH	NH	NH	NH	NH
CC-F67	NH	NH	NH	NH	Friulimicin A	Antibacterial
CC-F69 CC-F71	Valinomycin NH	Anticancer, Antimicrobial Insecticidal, Antiviral [278]	Valinomycin Roseofungin Streptodepsipeptide P11A Roflamycoin E'PN00053 Nonactin Shurimycin A Lipiarmycin A	Anticancer, Antimicrobial Insecticidal, Antiviral Antifungal, Antiviral Antitumor [387] Antifungal [388] Antifungal [389] Antimicrobial [390] Antimicrobial Antimycobacterial	Valinomycin Dideschloroenduracidin B Enduracidin D Dideschloroenduracidin A	Anticancer, Antimicrobial Insecticidal, Antiviral Antibacterial [391] Antimicrobial [392] Antibacterial
CC-F72	Surugamides A, C	Anticancer, Antifungal	Langkolide Surugamides A, C	Antimicrobial, Antiproliferative Anticancer, Antifungal	Surugamides A, C	Anticancer, Antifungal
	,		•	. •	Champacyclin	Antimicrobial
CC-F76	NH	NH	NH	NH	NH	NH
CC-F78	Valinomycin	Anticancer, Antimicrobial Insecticidal, Antiviral	Valinomycin	Anticancer, Antimicrobial Insecticidal, Antiviral	Valinomycin Strevertene B PM100118	Anticancer, Antimicrobial Insecticidal, Antiviral Antifungal [282] Antitumor [393]

ICBAS
Portuguese seaweeds, a marine treasure of Actinobacteria producing novel bioactive compounds

CC-F79	Valinomycin Salivaricin A2	Anticancer, Antimicrobial Insecticidal, Antiviral Antibacterial [394]	Valinomycin	Anticancer, Antimicrobial Insecticidal, Antiviral	Valinomycin Triculamin Ramoplanin Dideschloroenduracidin B	Anticancer, Antimicrobial Insecticidal, Antiviral Antimycobacterial [395] Antibacterial [396] Antibacterial
CC-F83	Surugamides A, C	Anticancer, Antifungal	Surugamides A, C	Anticancer, Antifungal	Surugamides A, C Champacyclin	Anticancer, Antifungal Antimicrobial
CC-F88	NH	NH	NH	NH	NH	NH
CC-F90	NH	NH	Shurimycin A Lipiarmycin A	Antimicrobial Antimycobacterial	NH	NH
CC-F106	NH	NH	NH	NH	Skyllamycin A	Biofilm inhibitor
CC-F110	NH	NH	SapB Roxaticin Monensin Landomycin A Undecylprodigiosin Streptorubin B Viomycin	Antimicrobial, Biosurfactant [397] Antifungal [398] Antimicrobial [399] Antitumor [400] Anticancer, Antimalarial Antimicrobial [401] Antibacterial [402] AntiNHtuberculosis [403]	NH	NH
CC-F120	NH	NH	Norerythromycin A	Antimicrobial	NH	NH

CC-F123	Surugamides A-D Champacyclin	Anticancer, Antifungal Antimicrobial	Surugamides A-D, G Strevertene D Apoptolidin A Levorin A0, A2, A3 Antimycins Kitamycin A Urauchimycin A	Anticancer, Antifungal Antifungal [282] Cytotoxic [378] Antifungal [404] Antifungal, Insecticidal, Nematocidal Piscicidal, Antiviral, Anticancer, Immunosuppressive [280] Antifungal [405] Antifungal [406]	Surugamides A-D Champacyclin Telomycin Skyllamycin A	Anticancer, Antifungal Antimicrobial Antimicrobial Biofilm inhibitor [407]
CC-R10	NH	NH	NH	NH	NH	NH
CC-R20	NH	NH	Phepropeptin A Kenalactam A Lysocellin	Proteosome inhibitor [408] Anticancer [409] Antimicrobial [410]	NH	NH
CC-R26	Surugamides A, B Champacyclin	Anticancer, Antifungal Antimicrobial	Surugamides A, D Streverten	Anticancer, Antifungal Antifungal	Surugamides ANHC	Anticancer, Antifungal
CC-R35	Surugamides A, C	Anticancer, Antifungal	Surugamides A, C	Anticancer, Antifungal	Surugamides A, C Champacyclin	Anticancer, Antifungal Antimicrobial
CC-R36	NH	NH	Amphidinolide B Copiamycin	Anticancer Antifungal	NH	NH
CC-R44	NH	NH	Shurimycin A Lipiarmycin A	Antimicrobial Antimycobacterial	NH	NH
CC-R47	NH	NH	Roseofungin Bafilomycin A Strevertene D Methymycin	Antifungal, Antiviral Anticancer [411] Antifungal Antibacterial [412]	Skyllamycin B	Biofilm inhibitor
CC-R53	Surugamides A, C	Anticancer, Antifungal	Surugamides A, C	Anticancer, Antifungal	Surugamides A, C Champacyclin NH	Anticancer, Antifungal Antimicrobial NH

ICBAS
Portuguese seaweeds, a marine treasure of Actinobacteria producing novel bioactive compounds

CC-R64	NH	NH	Roseofungin Roxaticin Streptorubin B	Antifungal, Antiviral Antifungal Antibacterial	NH	NH
CC-R68	Hormaomycin WS9326A	Antibacterial [413] Antiparasitic [414]	WS9326A Hormaomycin Takaokamycin Geldanamycinate	Antiparasitic Antibacterial Antibacterial [415] Cytotoxic [416]	Hormaomycin WS9326A, WS9326C Enduracidin A-C Friulimicin A Ramoplanin	Antibacterial Antiparasitic Antibacterial Antibacterial Antibacterial [417]
CC-R69	NH	NH	Shurimycin A	Antimicrobial	NH	NH
CC-R70 CC-R72	NH NH	NH NH	NH NH	NH NH	NH NH	NH NH
CC-R81	NH	NH	Axenomycin	Antiparasitic [418]	Glycinocin B Skyllamycin B	Antibacterial [419] Biofilm inhibitor
CC-R88	Surugamides A, C	Anticancer, Antifungal	Surugamides A, C	Anticancer, Antifungal	Surugamides A, C Champacyclin	Anticancer, Antifungal Antimicrobial
CC-R93	NH	NH	Copiamycin Sporeamicin A	Antifungal Antibacterial	NH	NH
CC-R103	Surugamide B, D Champacyclin	Anticancer, Antifungal Antimicrobial	NH	NH	Surugamide B, C, D Streptocidin A	Anticancer, Antifungal Antibacterial [420]
CC-R112	NH	NH	Dermostatin B PM100118 Methymycin Monensin	Antimicrobial Antitumor Antibacterial Antimicrobial	NH	NH
CC-R115	NH	NH	Monensin	Antimicrobial	NH	NH
CC-R116 CC-R117	NH NH	NH NH	NH Guanidylfungin B	NH Antimicrobial [421]	NH	NH

CC-R119	Surugamide A. B	Anticancer, Antifungal	Surugamide A. B	Anticancer, Antifungal	Champacyclin Glycinocin D Surugamide B Triculamin Telomycin	Antimicrobial Antibacterial Antimicrobial Antimycobacterial Antimicrobial
CC-R120	NH	NH	Levorin A0 Monensin Strevertenes	Antifungal Antimicrobial Antifungal	Friulimicin A, D	Antibacterial
CC-R134	NH	NH	Strevertene F PM100118	Antifungal Antitumor	NH	NH
CC-R135	NH	NH	Amphidinolide B Copiamycin Sporeamicin A	Anticancer Antifungal Antibacterial	NH	NH
CC-R136	NH	NH	Norerythromycin A Sporeamicin A Concanamycin A	Antimicrobial Antibacterial Anticancer	NH	NH
CC-R138	NH	NH	Surugamide A. B	Anticancer, Antifungal	NH	NH
CC-R150	Surugamide A Champacyclin	Anticancer, Antifungal Antimicrobial	Nystatin Levorin A0, A3 Surugamides A, D Champacyclin Partricin A Fungimycin Lipiarmycin A Antimycin A	Antifungal [422] Antifungal, Insecticidal, Nematocidal Anticancer, Antifungal Antimicrobial Antifungal, Antiprotozoal [425] Antifungal [426] Antimycobacterial Nematocidal Piscicidal, Antiviral, Anticancer,	Bu_2841NH08 Surugamides A, C, D Glycinocin D Champacyclin Telomycin Daptomycin	Antimicrobial [423] Anticancer, Antifungal Antibacterial Antimicrobial Antimicrobial Antibacterial [424]

Immunosuppressive

				minanocappioceivo		
CC-R151	Surugamides A, B Champacyclin	Anticancer, Antifungal Antimicrobial	Surugamides A, D Strevertenes Kitamycin A	Anticancer, Antifungal Antifungal Plant growth inhibition [427]	Surugamides ANHC	Anticancer, Antifungal
CC-R154	NH	NH	Concanamycin A Surugamide A	Anticancer [428] Anticancer, Antifungal	NH	NH
CC-R155	NH	NH	Chrysomycin B	Anticancer [429]	Daptomycin Neotelomycin	Antibacterial Antimicrobial
CC-R160	NH	NH	Norerythromycin A	Antimicrobial	NH	NH
CC-R164	NH	NH	NH	NH	Telomycin A_54145 Triculamin Skyllamycins A, B	Antimicrobial Antibacterial [430] Antimycobacterial Biofilm inhibitor
CC-R165	NH	NH	Norerythromycin A	Antimicrobial	NH	NH
CC-R166	NH	NH	NH	NH	NH	NH
CC-R175	NH	NH	Champacyclin Surugamide A	Antimicrobial Anticancer, Antifungal	Champacyclin Surugamide D	Antimicrobial Anticancer, Antifungal
CC-R176	NH	NH	Apoptolidin A Strevertenes B, D	Antimicrobial, Antiproliferative Cytotoxic Antifungal	Skyllamycin B Telomycin	Biofilm inhibitor Antimicrobial
			Mycoplanecin A Lipiarmycin A Ikarugamycin	Antimycobacterial [431] Antimycobacterial Antiprotozoal [432]		
			Valinomycin	Anticancer, Antimicrobial	Valinomycin	Anticancer, Antimicrobial
		Anticancer. Antimicrobial		Insecticidal, Antiviral		Insecticidal, Antiviral
CC-R178	Valinomycin	Valinomycin Anticancer, Antimicrobial Insecticidal, Antiviral	Mathemycin A	Antifungal [433]	Telomycin	Antimicrobial
			Langkolide	Antimicrobial, Antiproliferative	Skyllamycin B	Biofilm inhibitor

CC-R180	NH	NH	Langkolide Levorin A3 Valinomycin	Antimicrobial, Antiproliferative Antifungal, Insecticidal, Nematocidal Anticancer, Antimicrobial Insecticidal, Antiviral	Dideschloroenduracidin A, B	Antibacterial
CT-F6	Surugamide A Champacyclin	Anticancer, Antifungal Antimicrobial	Surugamides A, D	Anticancer, Antifungal	Surugamides A, C Champacyclin	Anticancer, Antifungal Antimicrobial
CT-F11	NH	NH	Splenocin J	AntiNHinflammatory [434]	Champacyclin Glycinocin D Surugamide C	Antimicrobial Antibacterial Anticancer, Antifungal
CT-F14	NH	NH	Flavofungin	Antifungal	NH	NH
CT-F18	NH	NH	Dermostatins A, B Fungichromin Roseofungin Concanamycin A Streptorubin B Norerythromycin A Undecylprodigiosin Marineosin A	Antimicrobial Antifungal [435] Antifungal, Antiviral Anticancer Antibacterial Antimicrobial Anticancer, Antimalarial Antimicrobial Cytotoxic [324]	NH	NH
CT-F19	NH	NH	NH	NH	NH	NH
CT-F25	NH	NH	Roseofungin Antimycin A	Antifungal Nematocidal Piscicidal, Antiviral, Anticancer, Immunosuppressive	NH	NH
CT-F26	NH	NH	Undecylprodigiosin	Anticancer, Antimalarial Antimicrobial	NH	NH

			Nocardamine Aquayamycin	Antitumor [436] Antibacterial, Anticancer [437]		
CT-F28	NH	NH	NH	NH	NH	NH
CT-F29	NH	NH	Dermostatins A, B Roseofungin Undecylprodigiosin Streptorubin B Marineosin A Lipiarmycin A	Antimicrobial Antifungal, Antiviral Anticancer, Antimalarial Antimicrobial Antibacterial Cytotoxic Antimycobacterial	NH	NH
CT-F31	Valinomycin	Anticancer, Antimicrobial Insecticidal, Antiviral	Fujimycin Valinomycin Dehydroxynocardamine	Anticancer [438] Anticancer, Antimicrobial Insecticidal, Antiviral Antitumor	Valinomycin	Anticancer, Antimicrobial Insecticidal, Antiviral
CT-F37	NH	NH	Langkolide Roxaticin Actinomycin	Antimicrobial, Antiproliferative Antifungal Antibacterial, Antitumor [439]	Streptomonomicin Glycinocin C	Antimicrobial Antibacterial
CT-F39	NH	NH	NH	NH	NH	NH
CT-F40	Surugamides A, B	Anticancer, Antifungal	Surugamides A, B Methymycin	Anticancer, Antifungal Antibacterial	Surugamides A, B Triculamin	Anticancer, Antifungal Antimycobacterial
CT-F45	Surugamides A, B	Anticancer, Antifungal	Surugamides A, B Methymycin	Anticancer, Antifungal Antibacterial	Surugamides A, B Triculamin Streptomonomicin	Anticancer, Antifungal Antimycobacterial Antimicrobial
CT-F46	NH	NH	Roseofungin Roxaticin Streptorubin B	Antifungal, Antiviral Antifungal Antibacterial	NH	NH

ICBAS
Portuguese seaweeds, a marine treasure of Actinobacteria producing novel bioactive compounds

CT-F48	Curumomidae A. D.	Anticoncer Antifungal	Surugamides A, B	Anticancer, Antifungal	Surugamides A, B	Anticancer, Antifungal	
C1-F46	Surugamides A, B	Anticancer, Antifungal	Methymycin	Antibacterial	Triculamin	Antimycobacterial	
			Norerythromycin A	Antimicrobial			
CT-F53	NH	NH	Sporeamicin A	Antibacterial [440]	NH	NH	
			Concanamycin A	Anticancer			
CT-F55	NH	NH	Roseofungin	Antifungal, Antiviral	NH	NH	
01133	INIT	1401	Strevertene F	Antifungal			
CT-F57	NH	NH	Strevertene D	Antifungal	NH	NH	
01-137	INII	INIT	Apoptolidin A	Cytotoxic	INII	INH	
CT-F61	NH	NH	NH	NH	NH	NH	
CT-F62	NH	NH	NH	NH	NH	NH	
CT-F63	NH	NH	Norerythromycin A	Antimicrobial	NH	NH	
CT-F65	NH	NH	NH	NH	NH	NH	
			Phepropeptin A	Proteosome inhibitor			
CT-F68	NH	NH	Kenalactam A	Anticancer	NH	NH	
			Lysocellin	Antimicrobial			
CT-F70	NH	NH	NH	NH	NH	NH	
CT-F72	NH	NH	Norerythromycin A	Antimicrobial	NH	NH	
CT-F87	Surugamides A, B	Anticancer, Antifungal	Surugamides A, B	Anticancer, Antifungal	Surugamides A, B	Anticancer, Antifungal	
CT-F88	NH	NH	Guanidylfungin B	Antimicrobial	NH	NH	
CT-F93	NH	NH	NH	NH	NH	NH	
			Strevertene D	Antifungal			
CT-F99	NH	NH	Oligomycin A	Antifungal [441]	NH	NH	
			Lipiarmycin A	Antimycobacterial			
CT-F104	NH	NH	Norerythromycin A	Antimicrobial	NH	NH	

CT-F116	Surugamides A, B, D Champacyclin	Anticancer, Antifungal Antimicrobial	Surugamides A, B, D, E, G Levorin A3 Strevertene D Antimycin A	Anticancer, Antifungal Antifungal, Insecticidal, Nematocidal Antifungal Nematocidal Piscicidal, Antiviral, Anticancer, Immunosuppressive	Surugamides ANHD Champacyclin Telomycin Dideschloroenduracidin A Triculamin	Anticancer, Antifungal Antimicrobial Antimicrobial Antibacterial Antimycobacterial
CT-F121	Surugamides A, B	Anticancer, Antifungal	Surugamides A, B	Anticancer, Antifungal	Surugamides A, B	Anticancer, Antifungal
CT-F122	Surugamide A	Anticancer, Antifungal	NH	NH	Surugamide C	Anticancer, Antifungal
CT-F124	NH	NH	Monensin Surugamide A	Antimicrobial Anticancer, Antifungal	NH	NH
CT-F125	NH	NH	Langkolide Erythromycin Bispolide A Cycloheptamycin	Antimicrobial, Antiproliferative Antimicrobial [442] Antibacterial [443] Antibacterial [444]	Skyllamycin A	Biofilm inhibitor
CT-F127	NH	NH	Champacyclin Soliseptide A	Antimicrobial Antibacterial, Antiviral [445]	Champacyclin	Antimicrobial
CT-F133	Surugamide C Champacyclin	Anticancer, Antifungal Antimicrobial	Dermostatin B Fungimycin Surugamides D, E Antimycin Kitamycin A Lipiarmycin A Urauchimycin A Levantilide A	Antimicrobial Antifungal Anticancer, Antifungal Nematocidal, Piscicidal, Antiviral, Anticancer, Immunosuppressive Plant growth inhibition Antimycobacterial Antifungal Antitumor [446]	Surugamide A	Anticancer, Antifungal

CT-F134	NH	NH	Antimycin A Surugamide A	Nematocidal Piscicidal, Antiviral, Anticancer, Immunosuppressive Anticancer, Antifungal	NH	NH
CT-F139	NH	NH	Guanidylfungin B	Antimicrobial	NH	NH
CT-F144	NH	NH	Strevertenes	Antifungal	NH	NH
CT-F146	Surugamides A, D	Anticancer, Antifungal	Surugamides A, D	Anticancer, Antifungal	Surugamides A, D Champacyclin	Anticancer, Antifungal Antimicrobial
CT-F147	NH	NH	NH	NH	Skyllamycin A	Biofilm inhibitor
CT-F153	Curumomido A	Anticoncer Antifungal	Surugamide A	Anticancer, Antifungal	Surugamide A	Anticancer, Antifungal
C1-F103	Surugamide A	Anticancer, Antifungal	Urauchimycin A	Antifungal	Champacyclin	Antimicrobial
CT-F155	NH	NH	Langkolide Levorin A0 Landomycin A Antimycin A	Antimicrobial, Antiproliferative Antifungal, Insecticidal, Nematocidal Antitumor Nematocidal, Piscicidal, Antiviral, Anticancer, Immunosuppressive	NH	NH
CT-F156	Valinomycin	Anticancer, Antimicrobial Insecticidal, Antiviral	Valinomycin Griseusin F Perimycin A	Anticancer, Antimicrobial Insecticidal, Antiviral Antibacterial, Cytotoxic [447] Antifungal [448]	Dideschloroenduracidin B Valinomycin Streptomonomicin Triculamin	Antibacterial Anticancer, Antimicrobial Insecticidal, Antiviral Antimicrobial Antimycobacterial
CT-R9	Valinomycin	Anticancer, Antimicrobial Insecticidal, Antiviral	Valinomycin	Anticancer, Antimicrobial Insecticidal, Antiviral	Valinomycin	Anticancer, Antimicrobial Insecticidal, Antiviral

ICBAS
Portuguese seaweeds, a marine treasure of Actinobacteria producing novel bioactive compounds

			Dehydroxynocardamine	Antitumor	Streptomonomicin Glycinocin C	Antimicrobial Antibacterial
CT-R10	NH	NH	Amphidinolide B Copiamycin	Anticancer Antifungal [449]	NH	NH
CT-R13	Surugamides A, C	Anticancer, Antifungal [276]	Surugamides A, C	Anticancer, Antifungal	Surugamides A, C Champacyclin	Anticancer, Antifungal Antimicrobial
CT-R28	Surugamides A, B, D	Anticancer, Antifungal	Surugamides A, D, E	Anticancer, Antifungal	Surugamides A, B, D	Anticancer, Antifungal
CT-R29	NH	NH	Urauchimycin A Flavofungin Lipiarmycin A Cytosaminomycin E	Antifungal Antifungal Antimycobacterial Cytotoxic [450]	Champacyclin	Antimicrobial
CT-R34	Surugamides A, B, D	Anticancer, Antifungal	Surugamides A, D Roseofungin Monensin Methymycin Strevertene D	Anticancer, Antifungal Antifungal, Antiviral Antimicrobial Antibacterial Antifungal	Surugamides A, B Champacyclin	Anticancer, Antifungal Antimicrobial
CT-R35	Surugamide A	Anticancer, Antifungal	Surugamide A	Anticancer, Antifungal	Surugamides A, B	Anticancer, Antifungal
CT-R38	Surugamide A	Anticancer, Antifungal	Surugamide A	Anticancer, Antifungal	Surugamides A, B Champacyclin	Anticancer, Antifungal Antimicrobial
CT-R42	NH	NH	Strevertene D	Antifungal	NH	NH
CT-R43	Surugamide A	Anticancer, Antifungal	Strevertene B, F Surugamide A PM100118	Antifungal Anticancer, Antifungal Antitumor	Surugamide A, C	Anticancer, Antifungal
CT-R45	NH	NH	Shurimycin A Lipiarmycin A	Antimicrobial Antimycobacterial	NH	NH
CT-R46	Surugamide A	Anticancer, Antifungal	Surugamide A	Anticancer, Antifungal	Surugamides A, B Champacyclin	Anticancer, Antifungal Antimicrobial
CT-R49	Surugamides A, D Champacyclin	Anticancer, Antifungal Antimicrobial	Surugamides A, D, G Nystatin	Anticancer, Antifungal Antifungal	Surugamides ANHD Champacyclin	Anticancer, Antifungal Antimicrobial

			Partricin A Fungimycin Strevertenes Antimycin Urauchimycin A	Antifungal, Antiprotozoal Antifungal Antifungal Nematocidal Piscicidal, Antiviral, Anticancer, Immunosuppressive Antifungal	Ramoplanin Telomycin Enduracidin A	Antibacterial Antimicrobial Antimicrobial
CT-R51	Surugamide A	Anticancer, Antifungal	Surugamide A	Anticancer, Antifungal	Surugamides A, B Champacyclin	Anticancer, Antifungal Antimicrobial
CT-R52	Surugamides A, B	Anticancer, Antifungal	Surugamides ANHD	Anticancer, Antifungal	Surugamides A, B	Anticancer, Antifungal
CT-R55	NH	NH	Erythromycin	Antimicrobial	Peptidolipin F	Antibacterial [451]
CT-R58	Surugamides A, B, D	Anticancer, Antifungal	Surugamides A, D, E Urauchimycin A	Anticancer, Antifungal Antifungal	Surugamides A, B, D Champacyclin	Anticancer, Antifungal Antimicrobial
CT-R75	Surugamides A, B, D	Anticancer, Antifungal	Surugamides A, D, E	Anticancer, Antifungal	Surugamides A, B, D	Anticancer, Antifungal
CT-R82	NH	NH	Urauchimycin A Surugamide A Strevertenes	Antifungal Anticancer, Antifungal Antifungal	Champacyclin	Antimicrobial
CT-R88	NH	NH	NH	NH	NH	NH
CT-R89	Surugamide A, B Champacyclin	Anticancer, Antifungal Antimicrobial	Surugamides A, D, E, G Champacyclin Fungimycin	Anticancer, Antifungal Antimicrobial Antifungal	Surugamides A, B, C Champacyclin Glycinocin D Neotelomycin	Anticancer, Antifungal Antimicrobial Antibacterial Antimicrobial
CT-R96	NH	NH	Strevertene B Norerythromycin A Juvenimicin B Lipiarmycin A	Antifungal Antimicrobial Antimicrobial Antimycobacterial	Glycinocins A, D	Antibacterial
CT-R100	NH	NH	Amphidinolide B Copiamycin	Anticancer Antifungal	NH	NH

			Sporeamicin A	Antibacterial		
			•		Ouronaudida A. D. D.	A = C = = = = = A = Cf = = = = 1
CT-R106	Surugamides A, B, D	Anticancer, Antifungal	Surugamides A, D, E	Anticancer, Antifungal	Surugamides A, B, D	Anticancer, Antifungal
			Urauchimycin A	Antifungal	Champacyclin	Antimicrobial
CT-R111	Surugamides A, B, D	3, D Anticancer, Antifungal	Surugamides A, D, E	Anticancer, Antifungal	Surugamides A, B, D	Anticancer, Antifungal
S	3 , ,	, 0	Urauchimycin A	Antifungal	Champacyclin	Antimicrobial
			Phepropeptin A	Proteosome inhibitor		
CT-R113	NH	NH	Kenalactam A	Anticancer	NH	NH
			Lysocellin	Antimicrobial		
			Landomycin A	Antitumor		
CT-R116	NH	NH	Dermostatin A	Antimicrobial	NH	NH
			Norerythromycin A	Antimicrobial		
CT-R124	NH	NH	Langkolide	Antimicrobial,	NH	NH
			Norerythromycin A	Antiproliferative		
				Antimicrobial		
CT-R126	NH	NH	Norerythromycin A	Antimicrobial	NH	NH
CT-R127	NH	NH	Norerythromycin A	Antimicrobial	NH	NH
CT-R139	Compressides A. D.	Austinanaan Austis waxal	Compressides A. D.	Austinauman Austifumanal	Surugamides A, B, D	Anticancer, Antifungal
C1-K139	Surugamides A, D	Anticancer, Antifungal	Surugamides A, D	Anticancer, Antifungal	Champacyclin	Antimicrobial
CT-R146	NH	NH	Flavofungin	Antifungal	Skyllamycin A	Biofilm inhibitor
CT-R149	NH	NH	NH	NH	NH	NH
			Langkolide	Antimicrobial,		
CT-R150	NH	NH		Antiproliferative	Telomycin	Antimicrobial
			Norerythromycin A	Antimicrobial		
OT D454	Companidas A. D.	Antinopon Antifus	Compressides A. D.	Antinonnan Antibur	Surugamides A, B, D	Anticancer, Antifungal
CT-R151	Surugamides A, D	Anticancer, Antifungal	Surugamides A, D	Anticancer, Antifungal	Champacyclin	Antimicrobial
CT-R162	Surugamide A	Anticancer, Antifungal	Surugamide A	Anticancer, Antifungal	Surugamide A	Anticancer, Antifungal
			Levorin A0	Antifungal, Insecticidal,		
CT-R166	NH	NH		Nematocidal	NH	NH
			Norerythromycin A	Antimicrobial		

			Antimycin A	Nematocidal, Piscicidal, Antiviral, Anticancer, Immunosuppressive		
		Anticancer, Antimicrobial	Urauchimycin A	Antifungal Anticancer, Antimicrobial		Anticancer, Antimicrobial
CT-R175	Valinomycin	Insecticidal, Antiviral	Valinomycin	Insecticidal, Antiviral	Valinomycin	Insecticidal, Antiviral
CT-R176	NH	NH	Roseofungin	Antifungal, Antiviral	NH	NH
CT-R177	NH	NH	NH	NH	NH	NH
CT-R180	NH	NH	Ripromycin	Antibacterial, Cytotoxic [452]	Triculamin	Antimycobacterial
CT-R181	Surugamide A	Anticancer, Antifungal	Surugamide A	Anticancer, Antifungal	Surugamide A	Anticancer, Antifungal
CT-R182	NH	NH	Langkolide Roseofungin Lipiarmycin A	Antimicrobial, Antiproliferative Antifungal, Antiviral Antimycobacterial	NH	NH
CT-R183	Surugamides A, C	Anticancer, Antifungal	Surugamides A, C	Anticancer, Antifungal	Surugamides A, C	Anticancer, Antifungal
CT-R184	Surugamides A, C	Anticancer, Antifungal	Surugamides A, C	Anticancer, Antifungal	Surugamides A, C Champacyclin	Anticancer, Antifungal Antimicrobial
CT-R186	Surugamide A	Anticancer, Antifungal	Surugamide A	Anticancer, Antifungal	Surugamide A	Anticancer, Antifungal
CT-R190	NH	NH	Surugamide A	Anticancer, Antifungal	Surugamide B Champacyclin Skyllamycin A, B Daptomycin	Anticancer, Antifungal Antimicrobial Biofilm inhibitor Antibacterial
CT-R198	Surugamide A Champacyclin	Anticancer, Antifungal Antimicrobial	Surugamides A, D Fungimycin Strevertenes	Anticancer, Antifungal Antifungal Antifungal	Surugamides A, D	Anticancer, Antifungal
CT-R201	Surugamides A, C	Anticancer, Antifungal	Strevertenes	Antifungal	Surugamide A	Anticancer, Antifungal

			Champacyclin Monensin	Antimicrobial Antimicrobial		
CT-R203	Surugamide A	Anticancer, Antifungal	Surugamide A	Anticancer, Antifungal	Surugamide A	Anticancer, Antifungal
CT-R205	NH	NH	NH	NH	NH	NH
CT-R209	NH	NH	Shurimycin A Lipiarmycin A Langkolide	Antimicrobial Antimycobacterial Antimicrobial, Antiproliferative	NH	NH

NH – No Hits

Table S9. List of BGCs recovered from *C. crispus* sample.

Contig	BGC length (bp)) Contig edge	BCG class	KnownClusterBlast	Taxonomic assignment
Contig	BGC leligtii (bp)	Confing edge	DOG Class	Kilowii Ciustei Biast	(genus-level)
c_000000096938	3513	Yes	NRPS	NH	llumatobacter
c_000000455524	12520	Yes	RiPPs	NH	llumatobacter
c_000000078416	4725	Yes	Terpene	NH	llumatobacter
c_000001341924	8772	Yes	RiPPs	NH	Microbacterium
c_000000728292	15298	Yes	RiPPs	NH	NA
c_000001570871	2893	Yes	PKS other	NH	llumatobacter
c_000000573023	9588	Yes	RiPPs	cochonodin I (30%) NH BGC0002575	Spongiactinospora
c_000000105397	11831	Yes	PKS other	NH	llumatobacter
c_000001348584	6553	Yes	PKS other	NH	llumatobacter
c_000000052331	2141	Yes	PKS other	NH	llumatobacter

c_000000743684	15565	Yes	RiPPs	NH	NA
c_000001532302	11356	Yes	Others	NH	NA
c_000000914231	12660	Yes	PKS other	NH	NA
c_000000025183	7665	Yes	PKS other	eicosapentaenoic (22%) NH BGC0000862	llumatobacter
c_000000634999	10019	Yes	NRPS	NH	Microthrix
c_000000295094	3728	Yes	NRPS	NH	Arthrobacter
c_000001558399	1700	Yes	NRPS	NH	Saccharothrix
c_000000603792	7880	Yes	RiPPs	NH	NA
c_000000245412	21962	No	RiPPs	microvionin (8%) NH BGC0001669	NA
c_000000026426	14925	Yes	NRPS	NH	llumatobacter
c_000000793019	5207	Yes	NRPS	NH	NA
c_000000393636	30204	Yes	PKS-NRP Hybrids	NH	NA
c_000000071034	4023	Yes	PKSI	NH	llumatobacter
c_000001380690	15354	Yes	NRPS	NH	NA
c_000001156790	3164	Yes	PKS other	NH	Mycobacterium
c_000001136276	13735	Yes	RiPPs	NH	NA
c_000001175850	4785	Yes	NRPS	NH	NA
c_000000661740	10618	Yes	NRPS	NH	NA
c_000000727491	10064	Yes	PKS other	eicosapentaenoic acid (33%) NH BGC0000861	llumatobacter
c_000000396789	21597	Yes	RiPPs	NH	NA
c_000000516599	17178	Yes	Others	BDNH12 (7%) NH BGC0001379	NA

c_000001011979 2059 Yes RiPPs NH Nocardia c_000000559834 1514 Yes PKS other NH Ilumatobacter c_00000002479 1103 Yes PKS other NH Ilumatobacter c_0000000278341 2697 Yes NRPS NH Streptaclidiphilus c_000001541725 1725 Yes RiPPs NH Saccharopolyspora c_00000168826 1624 Yes PKS other NH Actinoplanes c_0000018854 2346 Yes PKS other NH Nakamurella c_000000592422 2848 Yes NRPS NH Rhodococcus c_00000169251 18261 Yes RiPPs NH Ilumatobacter c_00000162115 2816 Yes RiPPs NH Cryptosporangium c_00000176035 1153 Yes PKS other NH Ilumatobacter c_00000076035 1153 Yes RiPPs NH Acidiferimicrobium	c_000000427121	8821	Yes	NRPS	NH	NA
c_000000892224 1886 Yes NRPS NH Solwaraspora c_00000002479 1103 Yes PKS other NH Ilumatobacter c_000000278341 2697 Yes NRPS NH Streptacidiphilus c_000001541725 1725 Yes RiPPs NH Saccharopolyspora c_00000068826 1624 Yes PKS other NH Actinoplanes c_00000108854 2346 Yes PKS other NH NAckamurella c_000000592422 2848 Yes NRPS NH Rhodococcus c_000000467235 5505 Yes Terpene NH Ilumatobacter c_000001460551 18261 Yes RiPPs NH NA c_00000162115 2816 Yes Others NH Ilumatobacter c_00000072035 1153 Yes PKS other NH Acidiferrimicrobium c_000000721337 3679 Yes PKS other NH NH NH <	c_000001011979	2059	Yes	RiPPs	NH	Nocardia
C_00000002479 1103 Yes PKS other NH Illumatobacter c_000000278341 2697 Yes NRPS NH Streptacidiphilus c_000001541725 1725 Yes RiPPs NH Saccharopolyspora c_000000688826 1624 Yes PKSI NH Actinoplanes c_00000108854 2346 Yes PKS other NH Nh Rhodococcus c_00000467235 5505 Yes Terpene NH Illumatobacter c_000001460551 18261 Yes RiPPs NH Cryptosporangium c_00000162115 2816 Yes PKS other NH Illumatobacter c_00000706035 1153 Yes PKS other NH Acidiferrimicrobium c_000000721337 3679 Yes PKS other NH NH NA c_000001422367 2082 Yes PKS other NH Mycobacterium c_000001553214 13484 Yes RiPPs NH	c_000000559834	1514	Yes	PKS other	NH	llumatobacter
c_000000278341 2697 Yes NRPS NH Streptacidiphillus c_000001541725 1725 Yes RiPPs NH Saccharopolyspora c_000000688826 1624 Yes PKSI NH Actinoplanes c_00000108854 2346 Yes PKS other NH NH Nakamurella c_00000592422 2848 Yes NRPS NH Rhodococcus c_00000467235 5505 Yes Terpene NH Ilumatobacter c_000001460551 18261 Yes RiPPs NH NA c_000001162115 2816 Yes Others NH Ilumatobacter c_000000706035 1153 Yes PKS other NH Acidiferrimicrobium c_000000721337 3679 Yes RiPPs NH NA c_000000558373 14612 Yes PKS other NH Mycobacterium c_00000153214 13484 Yes RiPPs NH Ilumatobacter	c_000000892224	1886	Yes	NRPS	NH	Solwaraspora
C_000001541725 1725 Yes RiPPs NH Saccharopolysporal C_000000688826 1624 Yes PKSI NH Actinoplanes C_00000108854 2346 Yes PKS other NH NAkamurella C_00000592422 2848 Yes NRPS NH Rhodococcus C_00000467235 5505 Yes Terpene NH Ilumatobacter C_000001460551 18261 Yes RiPPs NH NA C_00000162115 2816 Yes Others NH Cryptosporangium C_00000706035 1153 Yes PKS other NH Acidiferrimicrobium C_000001582133 1455 Yes RiPPs NH Ilumatobacter C_000000721337 3679 Yes PKS other NH NA C_000001422367 2082 Yes PKS other NH Mycobacterium C_000001553214 13484 Yes RiPPs NH Ilumatobacter C_0000	c_000000002479	1103	Yes	PKS other	NH	llumatobacter
c_000000688826 1624 Yes PKSI NH Actinoplanes c_000000108854 2346 Yes PKS other NH NAkamurella c_000000592422 2848 Yes NRPS NH Rhodococcus c_000000467235 5505 Yes Terpene NH Ilumatobacter c_000001460551 18261 Yes RiPPs NH NA c_000001162115 2816 Yes Others NH Cryptosporangium c_000000706035 1153 Yes PKS other NH Acidiferrimicrobium c_000001582133 1455 Yes RiPPs NH Acidiferrimicrobium c_000000721337 3679 Yes PKS other NH NH NA c_00000056155 14612 Yes RiPPs NH NA Mycobacterium c_000001553214 13484 Yes RiPPs NH Ilumatobacter c_000001553214 13484 Yes RiPPs NH Kitasatospora	c_000000278341	2697	Yes	NRPS	NH	Streptacidiphilus
c_000000108854 2346 Yes PKS other NH Nakamurella c_000000592422 2848 Yes NRPS NH Rhodococcus c_000000467235 5505 Yes Terpene NH Ilumatobacter c_000001460551 18261 Yes RiPPs NH NA c_000001162115 2816 Yes Others NH Cryptosporangium c_000000706035 1153 Yes PKS other NH Acidiferrimicrobium c_000001582133 1455 Yes RiPPs NH Alumatobacter c_000000721337 3679 Yes PKS other NH NH NA c_00000056155 14612 Yes RiPPs NH Mycobacterium c_000001422367 2082 Yes PKS other NH Ilumatobacter c_000001553214 13484 Yes RiPPs NH Ilumatobacter c_000001430076 2544 Yes NRPS NH Kitasatospora <td>c_000001541725</td> <td>1725</td> <td>Yes</td> <td>RiPPs</td> <td>NH</td> <td>Saccharopolyspora</td>	c_000001541725	1725	Yes	RiPPs	NH	Saccharopolyspora
C_000000592422 2848 Yes NRPS NH Rhodococcus C_000000467235 5505 Yes Terpene NH Ilumatobacter C_000001460551 18261 Yes RiPPs NH NA C_000001162115 2816 Yes Others NH Cryptosporangium C_000000706035 1153 Yes PKS other NH Ilumatobacter C_000001582133 1455 Yes RiPPs NH Acidiferrimicrobium C_000000721337 3679 Yes PKS other NH Ilumatobacter C_0000001422367 2082 Yes PKS other NH Mycobacterium C_000000558373 14639 Yes PKS other NH Ilumatobacter C_000001553214 13484 Yes RiPPs NH Ilumatobacter C_000001430076 2544 Yes NRPS NH Kitasatospora	c_000000688826	1624	Yes	PKSI	NH	Actinoplanes
C_000000467235 5505 Yes Terpene NH Ilumatobacter C_000001460551 18261 Yes RiPPs NH NA C_000001162115 2816 Yes Others NH Cryptosporangium C_000000706035 1153 Yes PKS other NH Ilumatobacter C_000001582133 1455 Yes RiPPs NH Acidiferrimicrobium C_000000721337 3679 Yes PKS other NH Ilumatobacter C_00000056155 14612 Yes RiPPs NH Mycobacterium C_0000001422367 2082 Yes PKS other NH Ilumatobacter C_000000558373 14639 Yes PKS other NH Ilumatobacter C_000001553214 13484 Yes RiPPs NH Ilumatobacter C_000001430076 2544 Yes NRPS NH Kitasatospora	c_000000108854	2346	Yes	PKS other	NH	Nakamurella
c_000001460551 18261 Yes RiPPs NH NA c_000001162115 2816 Yes Others NH Cryptosporangium c_000000706035 1153 Yes PKS other NH Ilumatobacter c_000001582133 1455 Yes RiPPs NH Acidiferrimicrobium c_000000721337 3679 Yes PKS other NH NH NA c_00000056155 14612 Yes RiPPs NH NA NA c_000001422367 2082 Yes PKS other NH Mycobacterium c_000000558373 14639 Yes PKS other NH Ilumatobacter c_000001553214 13484 Yes RiPPs NH Ilumatobacter c_000001430076 2544 Yes NRPS NH Kitasatospora	c_000000592422	2848	Yes	NRPS	NH	Rhodococcus
c_000001162115 2816 Yes Others NH Cryptosporangium c_000000706035 1153 Yes PKS other NH Ilumatobacter c_000001582133 1455 Yes RiPPs NH Acidiferrimicrobium c_000000721337 3679 Yes PKS other NH Ilumatobacter c_00000056155 14612 Yes RiPPs NH Mycobacterium c_000001422367 2082 Yes PKS other NH Mycobacterium c_000000558373 14639 Yes PKS other NH Ilumatobacter c_000001553214 13484 Yes RiPPs NH Ilumatobacter c_000001430076 2544 Yes NRPS NH Kitasatospora	c_000000467235	5505	Yes	Terpene	NH	llumatobacter
c_000000706035 1153 Yes PKS other NH Ilumatobacter c_000001582133 1455 Yes RiPPs NH Acidiferrimicrobium c_000000721337 3679 Yes PKS other NH Ilumatobacter c_00000056155 14612 Yes RiPPs NH NA c_000001422367 2082 Yes PKS other NH Mycobacterium c_000000558373 14639 Yes PKS other NH Ilumatobacter c_000001553214 13484 Yes RiPPs NH Ilumatobacter c_000001430076 2544 Yes NRPS NH Kitasatospora	c_000001460551	18261	Yes	RiPPs	NH	NA
c_000001582133 1455 Yes RiPPs NH Acidiferrimicrobium c_000000721337 3679 Yes PKS other NH Ilumatobacter c_000000056155 14612 Yes RiPPs NH NA c_000001422367 2082 Yes PKS other NH Mycobacterium c_000000558373 14639 Yes PKS other NH Ilumatobacter c_000001553214 13484 Yes RiPPs NH Ilumatobacter c_000001430076 2544 Yes NRPS NH Kitasatospora	c_000001162115	2816	Yes	Others	NH	Cryptosporangium
C_000000721337 3679 Yes PKS other NH Ilumatobacter C_000000056155 14612 Yes RiPPs NH NA C_000001422367 2082 Yes PKS other NH Mycobacterium C_000000558373 14639 Yes PKS other NH Ilumatobacter C_000001553214 13484 Yes RiPPs NH Ilumatobacter C_000001430076 2544 Yes NRPS NH Kitasatospora	c_000000706035	1153	Yes	PKS other	NH	llumatobacter
c_000000056155 14612 Yes RiPPs NH NA c_000001422367 2082 Yes PKS other NH Mycobacterium c_000000558373 14639 Yes PKS other NH Illumatobacter c_000001553214 13484 Yes RiPPs NH Illumatobacter c_000001430076 2544 Yes NRPS NH Kitasatospora	c_000001582133	1455	Yes	RiPPs	NH	Acidiferrimicrobium
c_000001422367 2082 Yes PKS other NH Mycobacterium c_000000558373 14639 Yes PKS other NH Illumatobacter c_000001553214 13484 Yes RiPPs NH Illumatobacter c_000001430076 2544 Yes NRPS NH Kitasatospora	c_000000721337	3679	Yes	PKS other	NH	llumatobacter
c_000000558373 14639 Yes PKS other NH Illumatobacter c_000001553214 13484 Yes RiPPs NH Illumatobacter c_000001430076 2544 Yes NRPS NH Kitasatospora	c_000000056155	14612	Yes	RiPPs	NH	NA
c_000001553214 13484 Yes RiPPs NH Illumatobacter c_000001430076 2544 Yes NRPS NH Kitasatospora	c_000001422367	2082	Yes	PKS other	NH	Mycobacterium
c_000001430076 2544 Yes NRPS NH <i>Kitasatospora</i>	c_000000558373	14639	Yes	PKS other	NH	llumatobacter
	c_000001553214	13484	Yes	RiPPs	NH	llumatobacter
c_000000728431 18356 Yes NRPS NH NA	c_000001430076	2544	Yes	NRPS	NH	Kitasatospora
	c_000000728431	18356	Yes	NRPS	NH	NA

c_000000884209	4597	Yes			
		165	RiPPs	NH	Nocardioides
c_000000419696	8612	Yes	RiPPs	NH	Actinomarinicola
c_000001169071	1080	Yes	PKS other	NH	Nakamurella
c_000000478137	6307	Yes	PKS other	NH	Nakamurella
c_000000369796	3709	Yes	PKS other	NH	Mycobacterium
c_000001567333	1407	Yes	NRPS	NH	Streptomyces
c_000000630525	10930	Yes	Others	NH	lamia
c_000001470970	1820	Yes	NRPS	NH	Planomonospora
c_000000114761	30872	Yes	NRPS	NH	NA
c_000000457577	3476	Yes	PKS other	NH	Nakamurella
c_000000987961	15801	Yes	Others	NH	llumatobacter
c_000000879857	1105	Yes	PKS other	NH	llumatobacter
c_000000092357	1424	Yes	PKSI	NH	Labedaea
c_000000063584	11277	Yes	Others	NH	NA
c_000000072416	2639	Yes	PKSI	NH	Nakamurella
c_000000484653	2975	Yes	PKSI	NH	Sinosporangium
c_000000873538	5075	Yes	Others	NH	Brachybacterium
c_000000334014	12474	Yes	RiPPs	NH	NA
c_000000487468	19891	Yes	Others	NH	NA
c_000000937396	8547	Yes	RiPPs	NH	NA
c_000000773691	26497	Yes	NRPS	NH	NA

c_000000569321	1054	Yes	NRPS	NH	NA
c_000001406901	31944	Yes	NRPS	NH	NA
c_000001001163	1376	Yes	NRPS	NH	NA
c_000000907367	3053	Yes	PKS other	NH	NA
c_000000336092	5341	Yes	NRPS	NH	NA
c_000000885165	10932	Yes	RiPPs	NH	NA
c_000001032322	7370	Yes	RiPPs	NH	NA
c_000000534957	1807	Yes	NRPS	NH	NA
c_000000266058	6019	Yes	NRPS	NH	NA
c_000001220846	5414	Yes	NRPS	NH	NA
c_000000442515	1337	Yes	PKS other	heterocyst glycolipids (28%) NH BGC0000869	NA

NH – No Hits NA – Not Available

Table S10. List of BGCs recovered from *C. tomentosum* sample.

Contin	BGC length (bp)	Contig edge	BCG class	KnownClusterBlast	Taxonomic assignment
Contig					(genusNHlevel)
c_000000266856	17362	Yes	NRPS	NH	Streptomyces
c_000000640643	2899	Yes	NRPS-like	NH	Streptomyces

NH – No Hit

APPENDIX IV

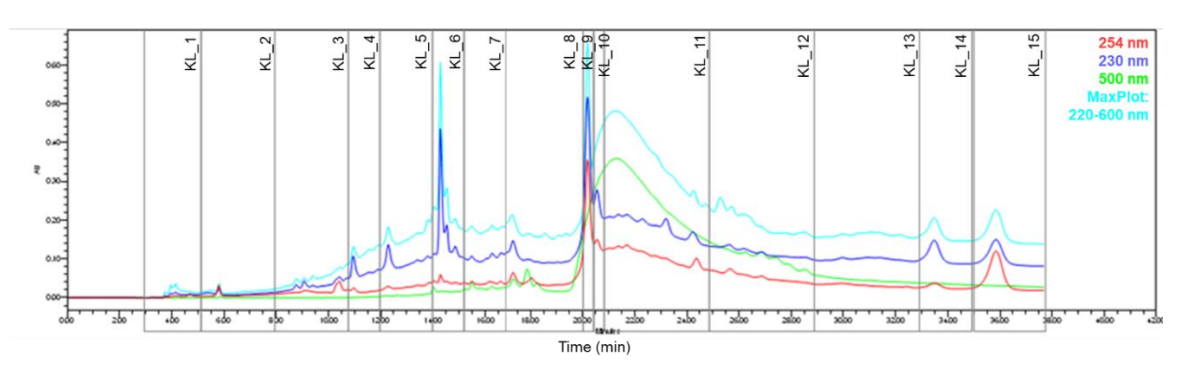


Figure S6. Reverse-phase HPLC chromatogram of CT-F6_KL sample with the indication of the recovered fractions.

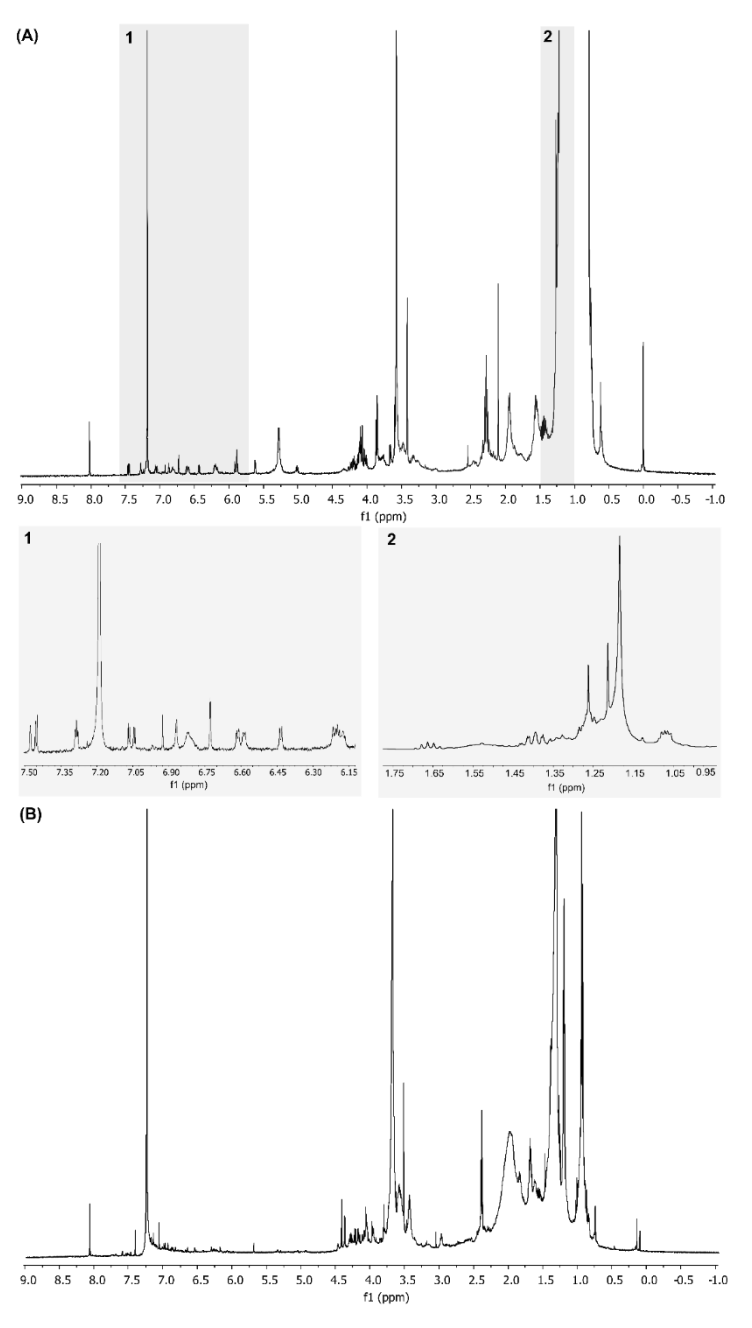


Figure S7. ¹H NMR (600 MHz, chloroform-*d*,) spectrum of fraction KL_9 containing semipurified **1**, highlighting the typical prodigiosin signals δ_H 7.5-6.20, associated to the pyrrole rings (**A1**) and δ_H 1.29-1.25, consistent with a large methylene envelope (**A2**). ¹H NMR (600 MHz, chloroform-d) spectrum of the most purified fraction (KL_9-10_A) containing **1** (**B**).

Table S11. Reverse-phase VLC conditions used to fractionate CT-F61 crude extract. The solvent mixture used to obtain each fraction is shown as well as the yielded mass (mg).

Fraction	MeOH (%)	H ₂ O (%)	Volume (mL)	Mass (mg)
А	5	95	500	2137.05
В	10	90	500	737.18
С	20	80	500	158.62
D	30	70	500	36.59
E	40	60	500	33.49
F	50	50	500	29.10
G	70	30	500	29.37
Н	90	10	500	111.74
1	100	0	750	1667.74
J	100 IPA	-	1000	50.94
K	100 DCM	-	1000	18.88
L	100 AC	-	500	6.21
M	100	0	750	24.94

MeOH: metanol; H₂O: water: IPA: isopropanol;

DCM: dichloromethane; AC: acetone

Table S12. Reverse-phase semi-preparative HPLC conditions used to fractionate CT-F61 KL sample.

Time (min)	% H₂O	% MeOH	% IPA
0.00	70	30	0
12.00	0	100	0
25.00	0	30	70
27.00	0	20	80
42.0	0	20	80
44.0	0	100	0
45.0	7	30	0
46.0	70	30	0

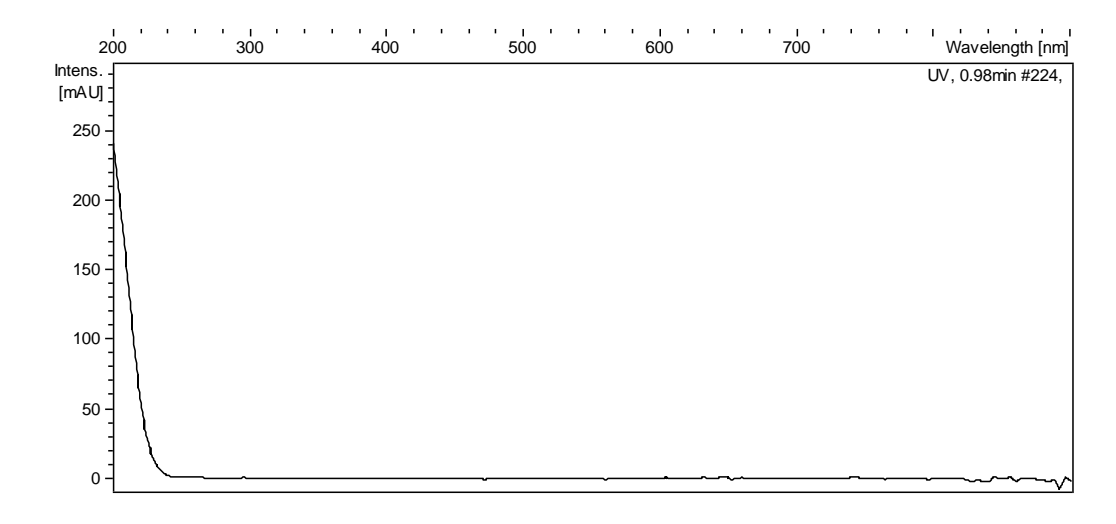
MeOH: metanol; H₂O: water; IPA: isopropanol

Table S13. Reverse-phase analytical HPLC conditions used to fractionate CT-F61 KL_9-10 sample.

Time (min)	% H₂O	% MeOH	% IPA
0.01	50	50	0
18.00	0	100	0
23.00	0	70	30
30.00	0	70	30
33.0	50	50	0
37.0	50	50	0

MeOH: metanol; H₂O: water; IPA: isopropanol

APPENDIX V



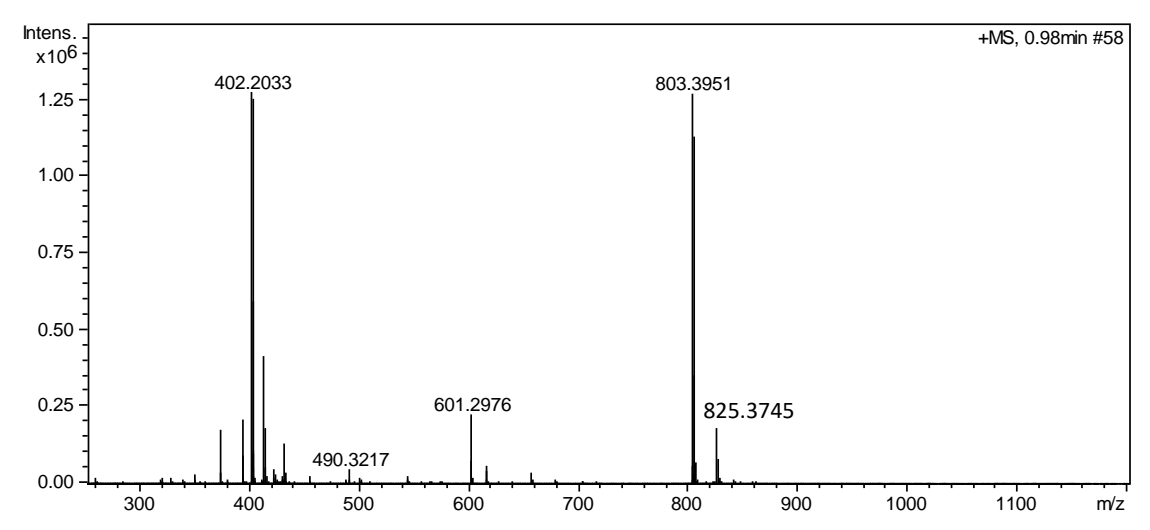


Figure S8. UV and (+)-ESI-TOF spectra of cellulamide A (2).

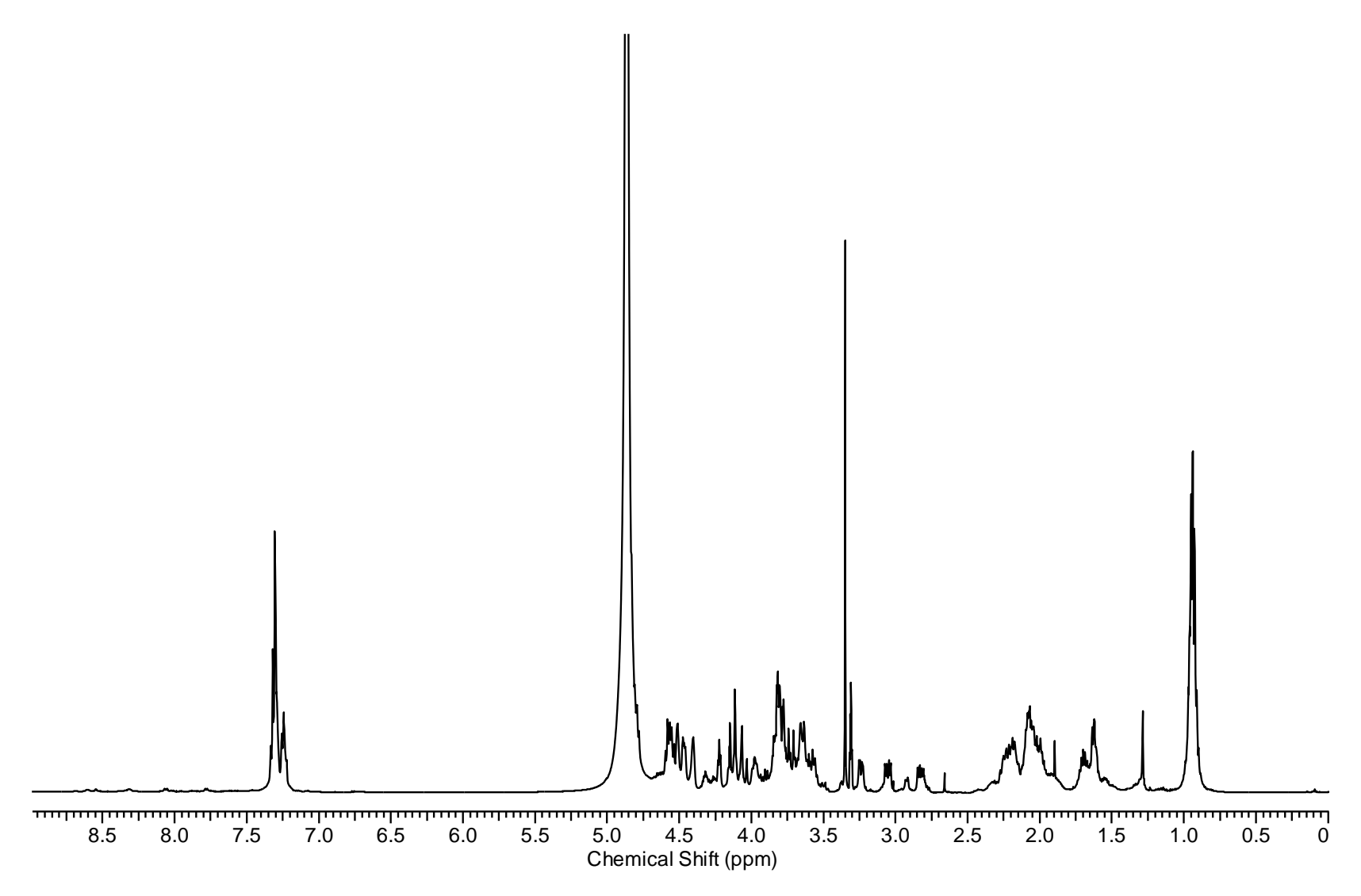


Figure S9. ¹H-NMR (500 MHz, CD₃OD) spectrum of cellulamide A (2).

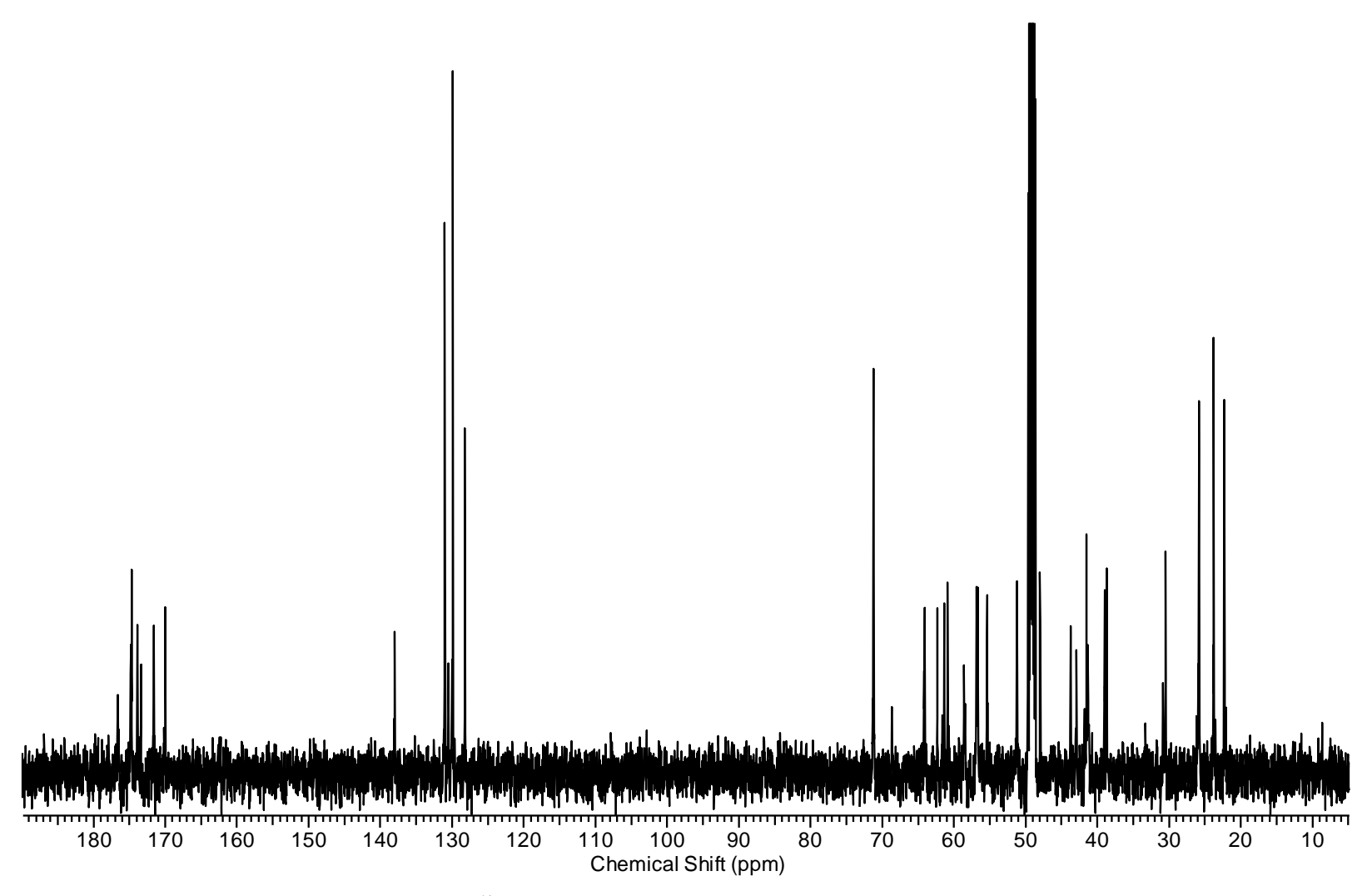


Figure S10. ¹³C-NMR (125 MHz, CD₃OD) spectrum of cellulamide A (2).

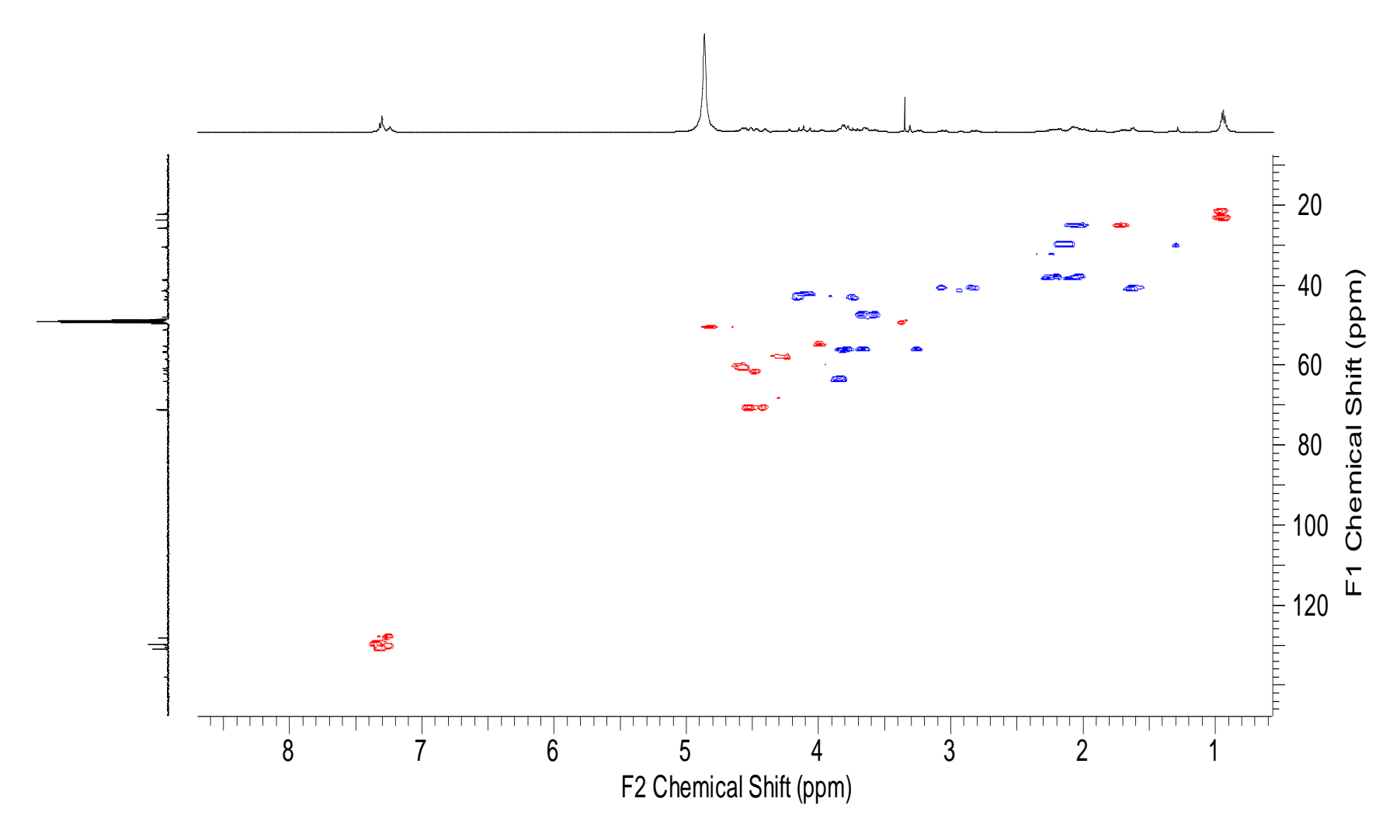


Figure S11. HSQC (CD3OD) spectrum of cellulamide A (2).

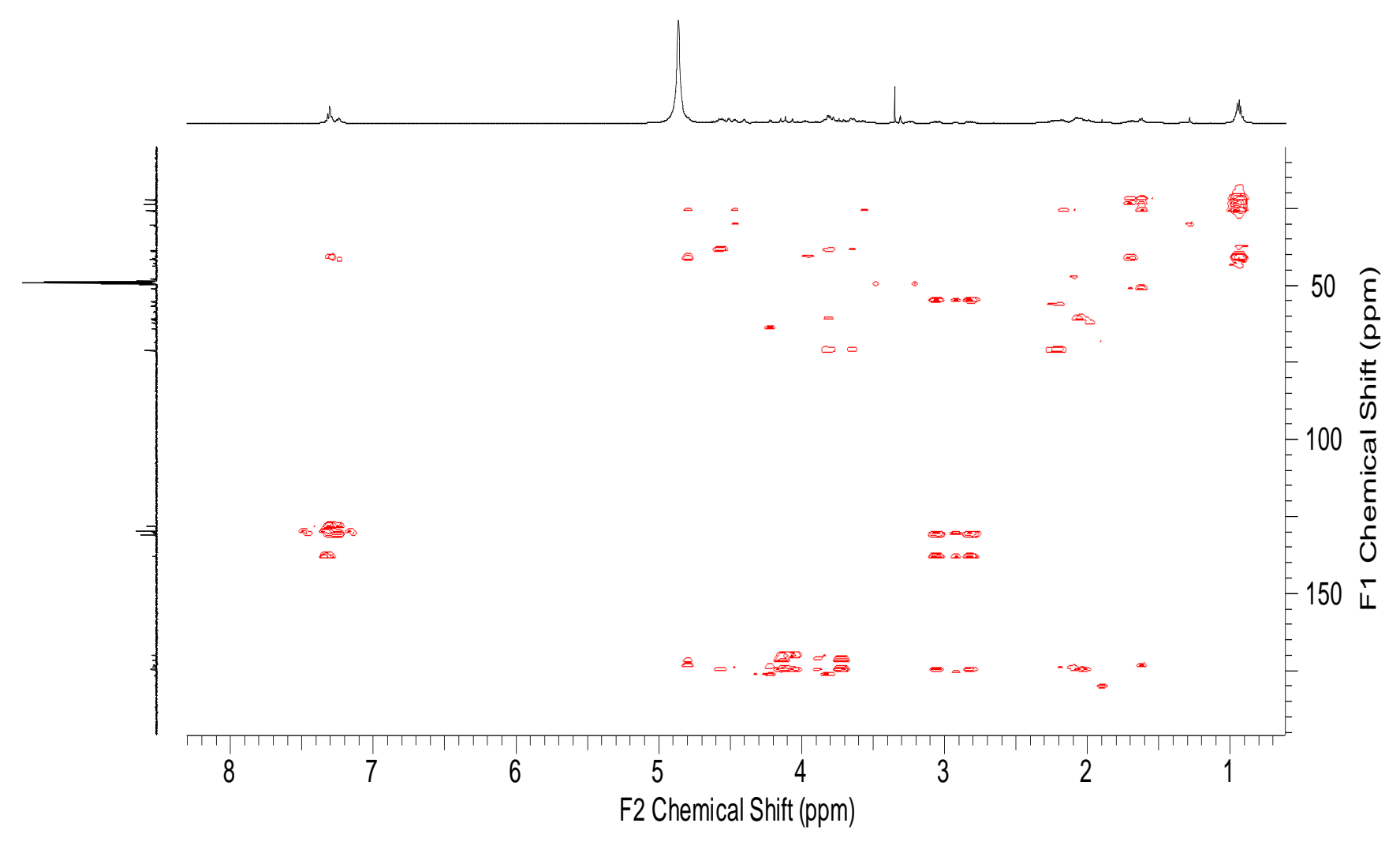


Figure S12. HMBC (CD₃OD) spectrum of cellulamide A (2).

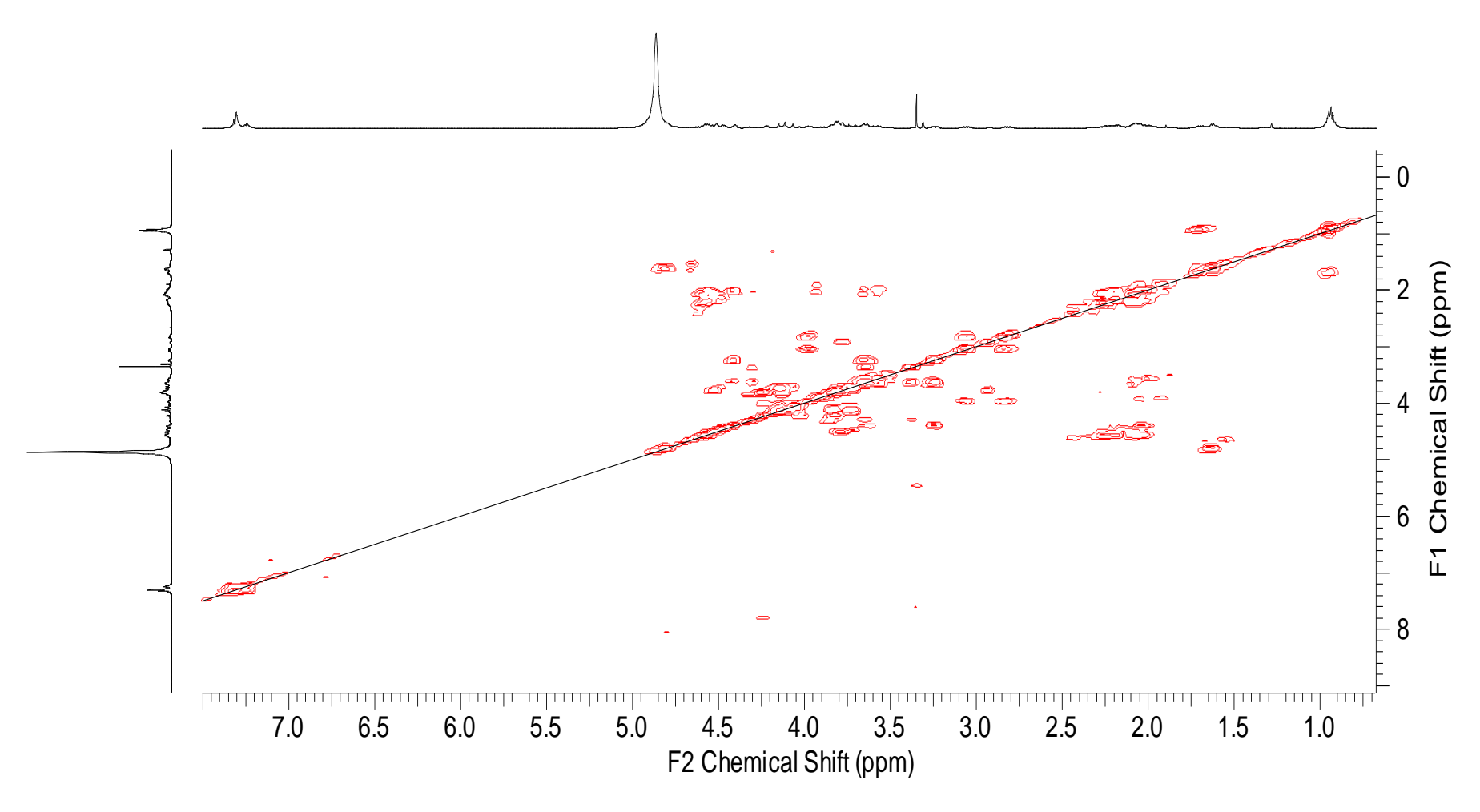


Figure S13. COSY (CD₃OD) spectrum of cellulamide A (2).

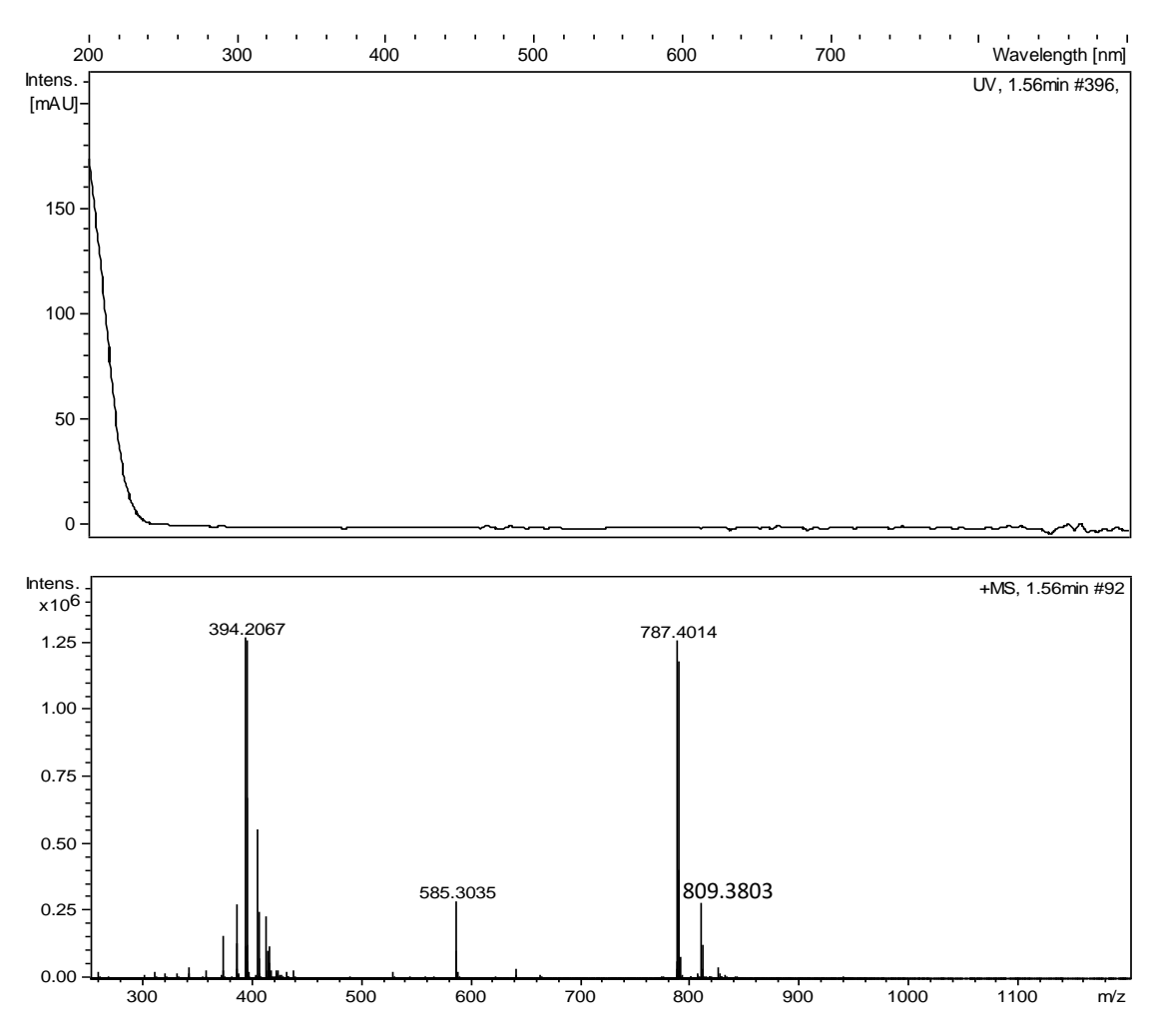


Figure S14. UV and (+)-ESI-TOF spectra of cellulamide B (3).

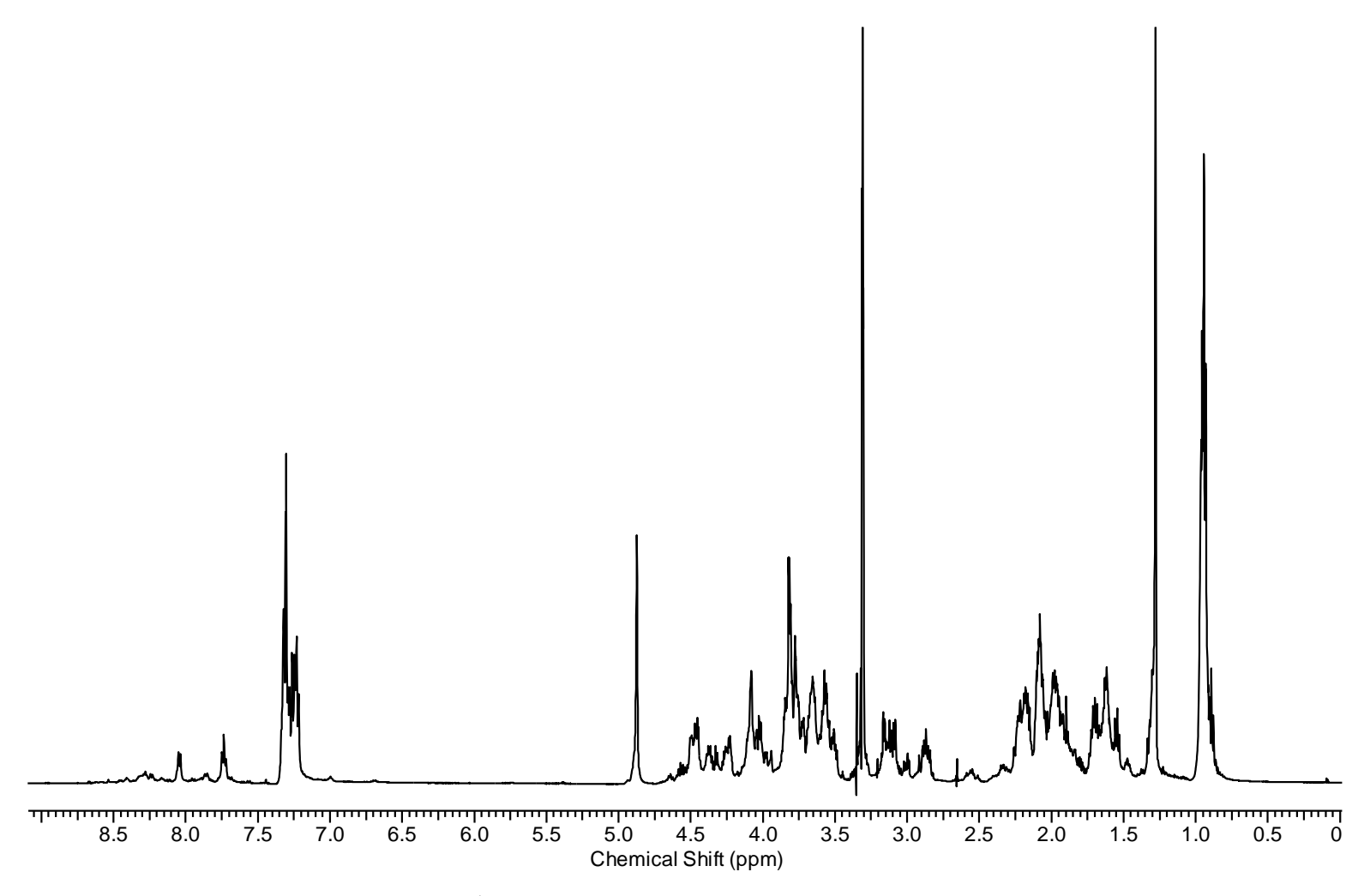


Figure S15. ¹H-NMR (500 MHz, CD₃OH) spectrum of cellulamide B (3).

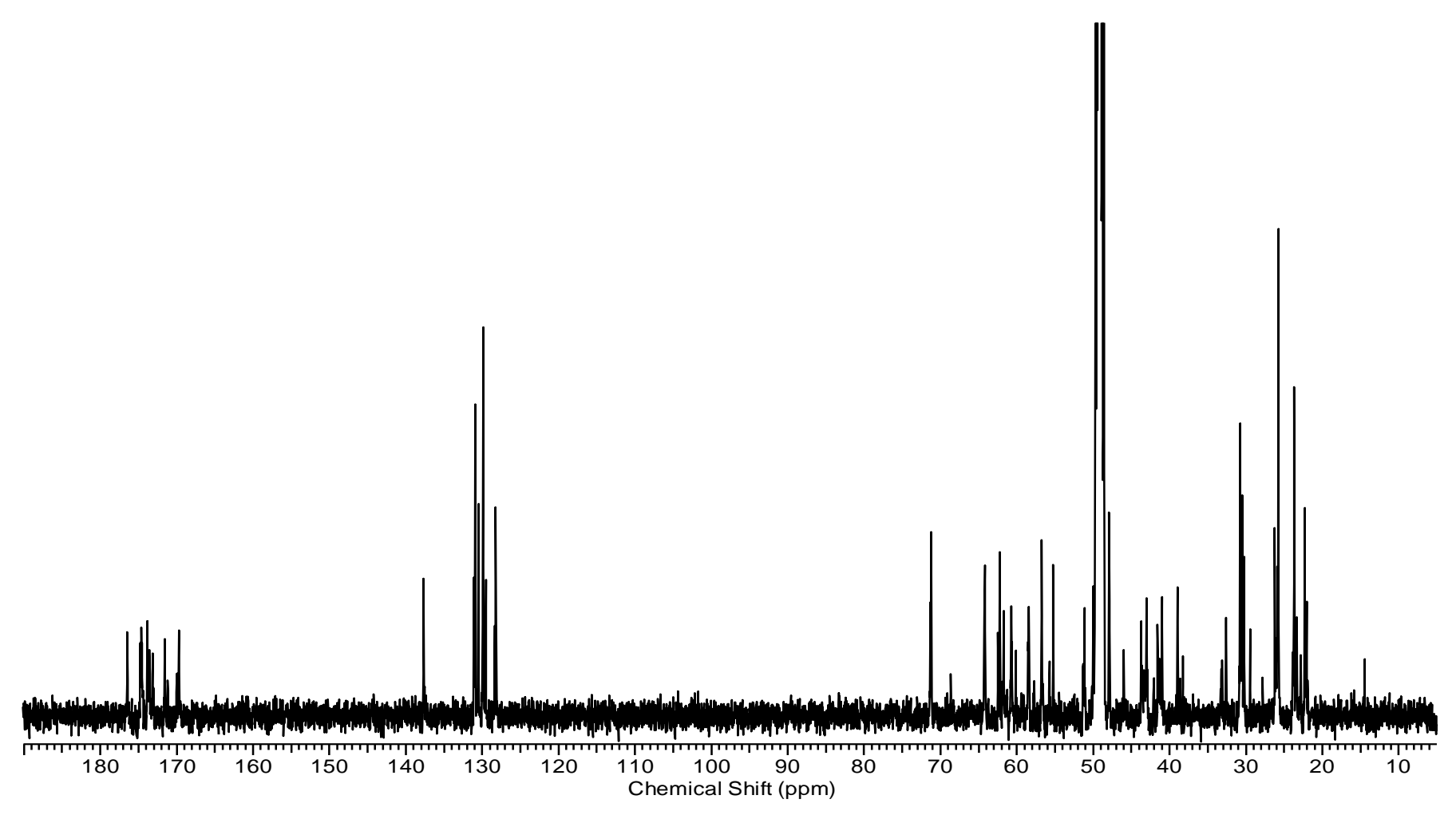


Figure S16. ¹³C-NMR (125 MHz, CD₃OH) spectrum of cellulamide B (3).

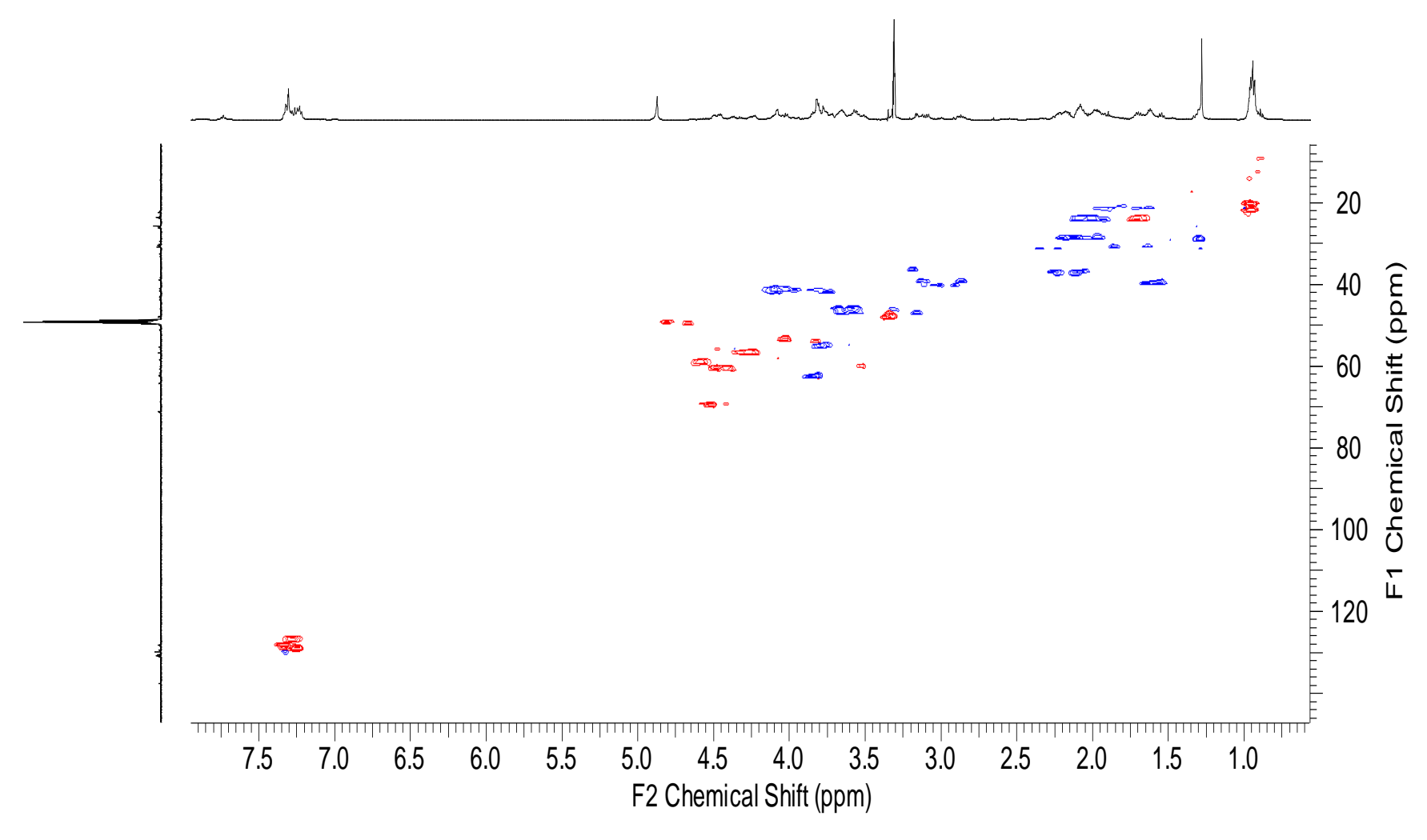


Figure S17. HSQC (CD₃OH) spectrum of cellulamide B (3).

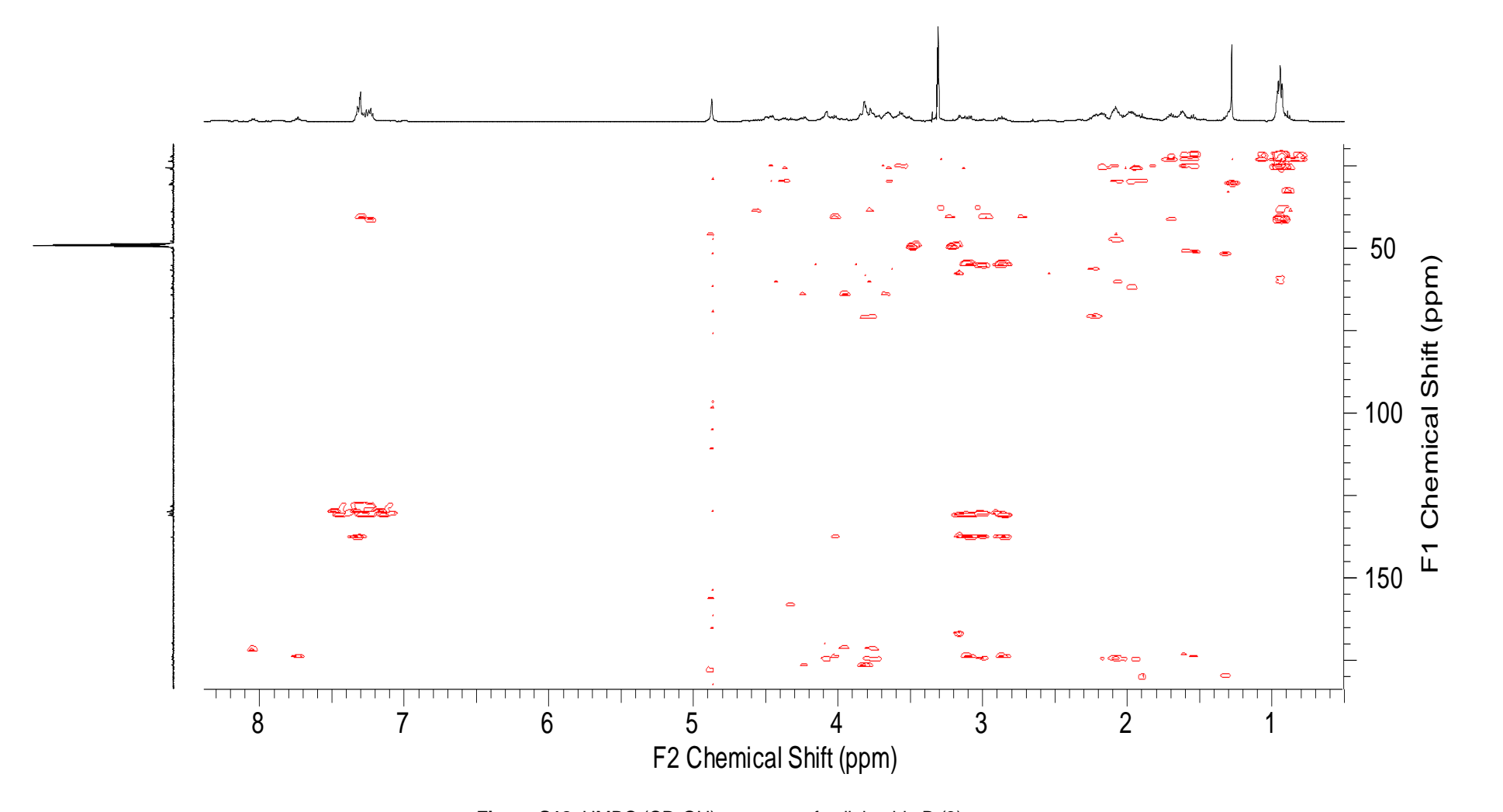


Figure S18. HMBC (CD₃OH) spectrum of cellulamide B (3).

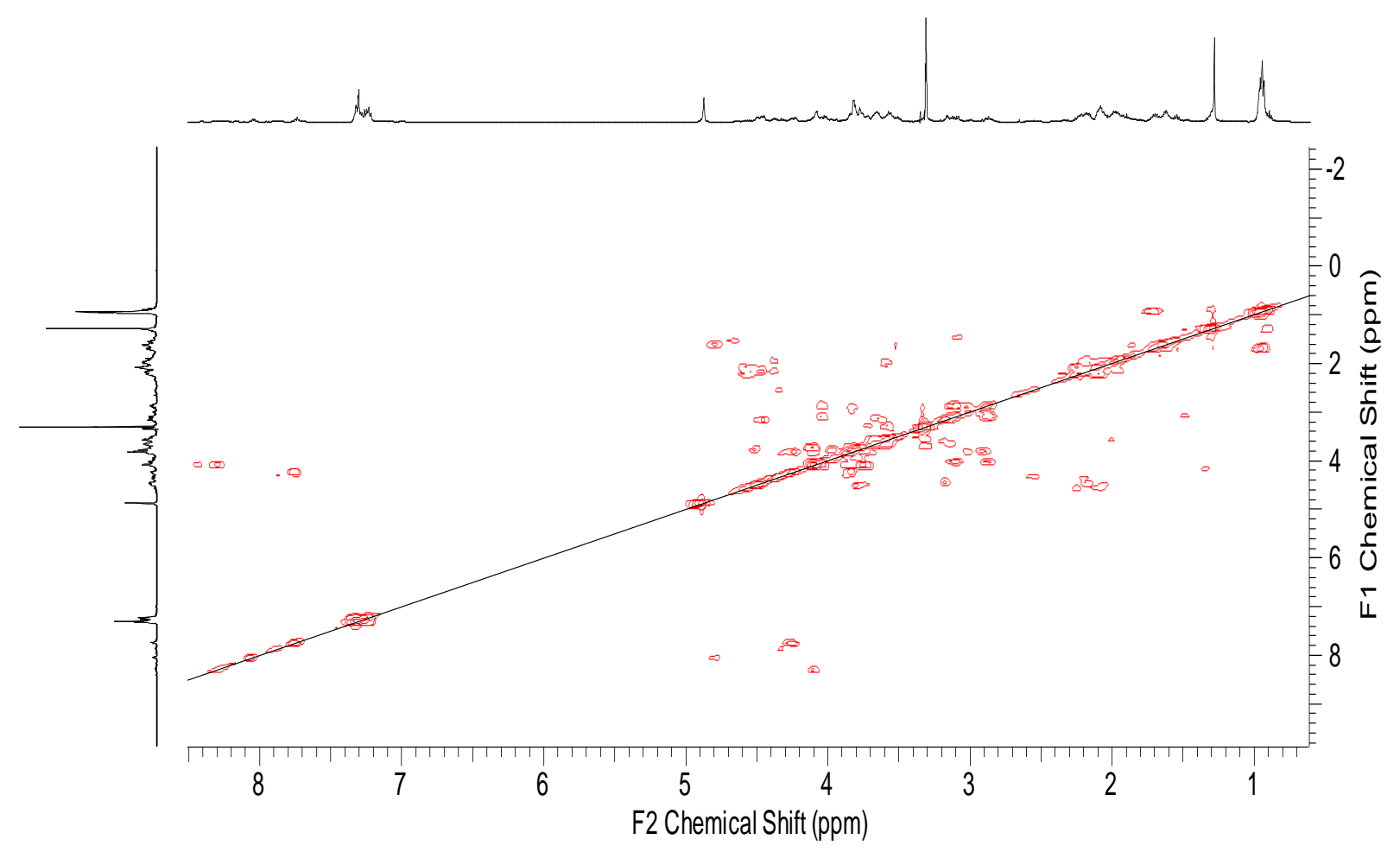


Figure S19. COSY (CD₃OH) spectrum of cellulamide B (3).

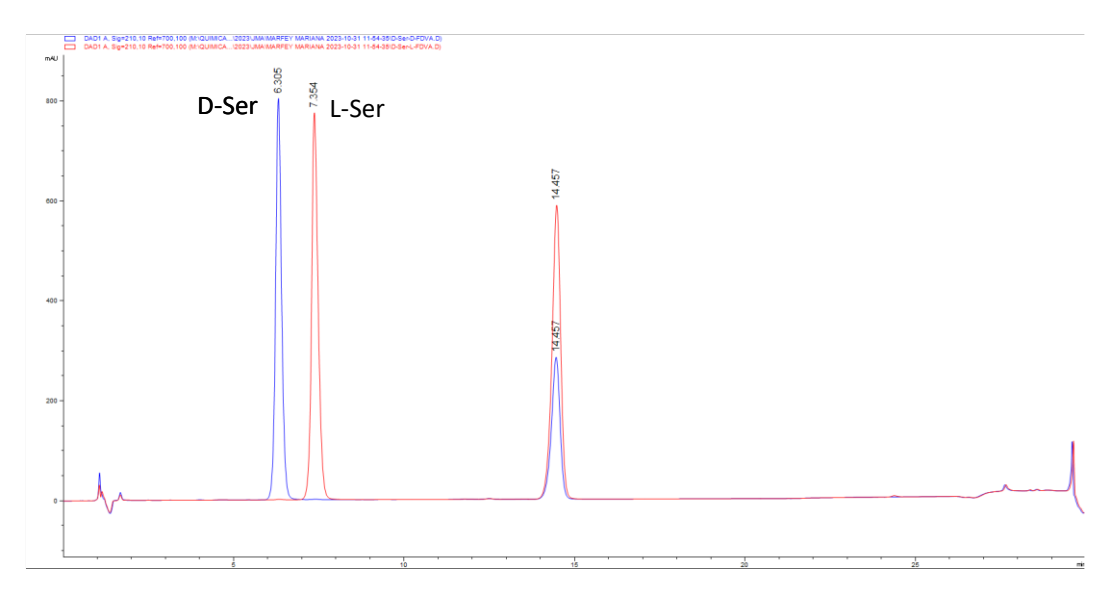


Figure S20. HPLC traces at 210 nm of the D-FDVA derivatives of Ser.

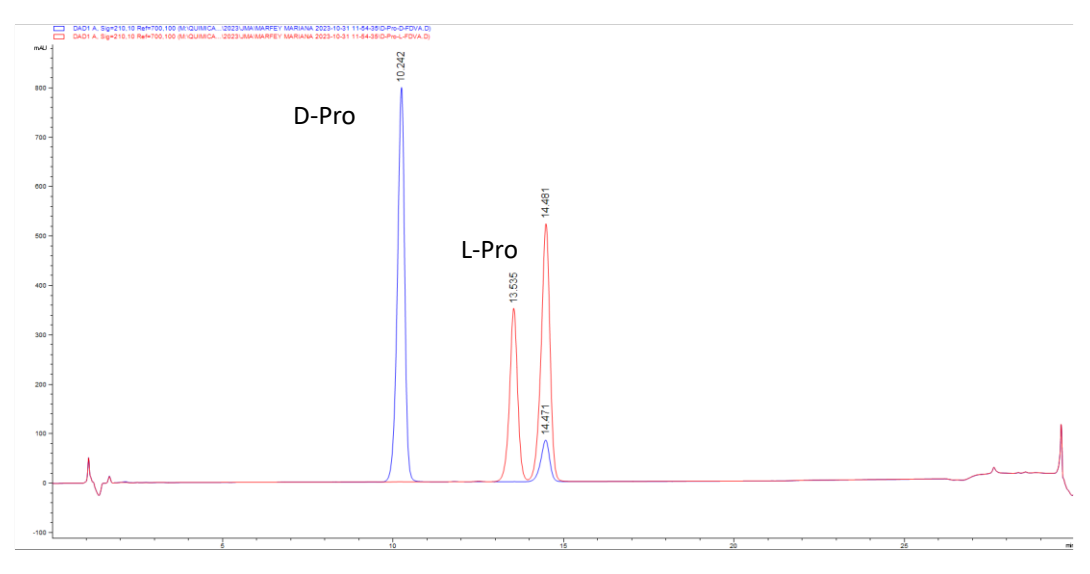


Figure S21. HPLC traces at 210 nm of the D-FDVA derivatives of Pro.

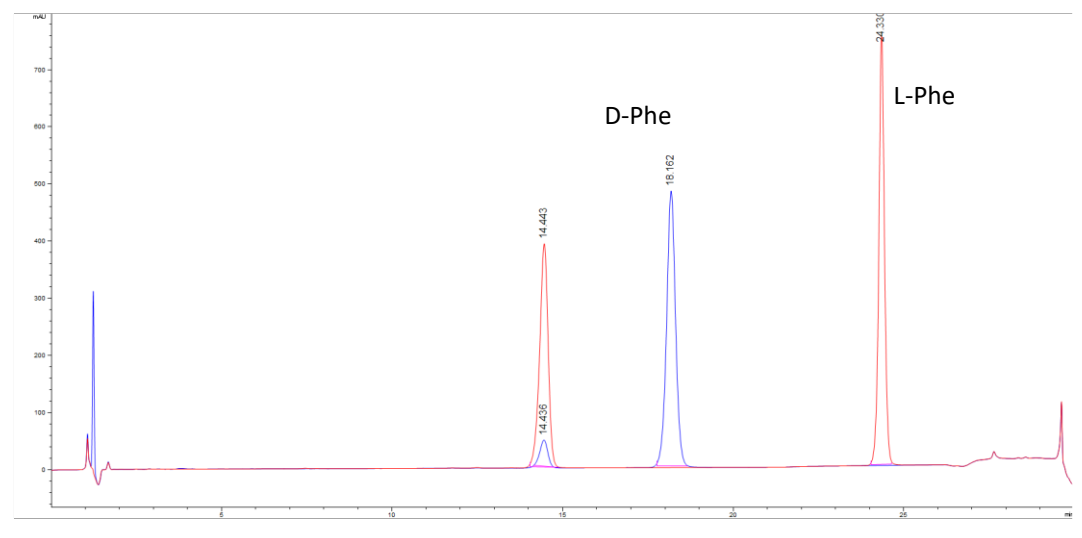


Figure S22. HPLC traces at 210 nm of the D-FDVA derivatives of Phe.

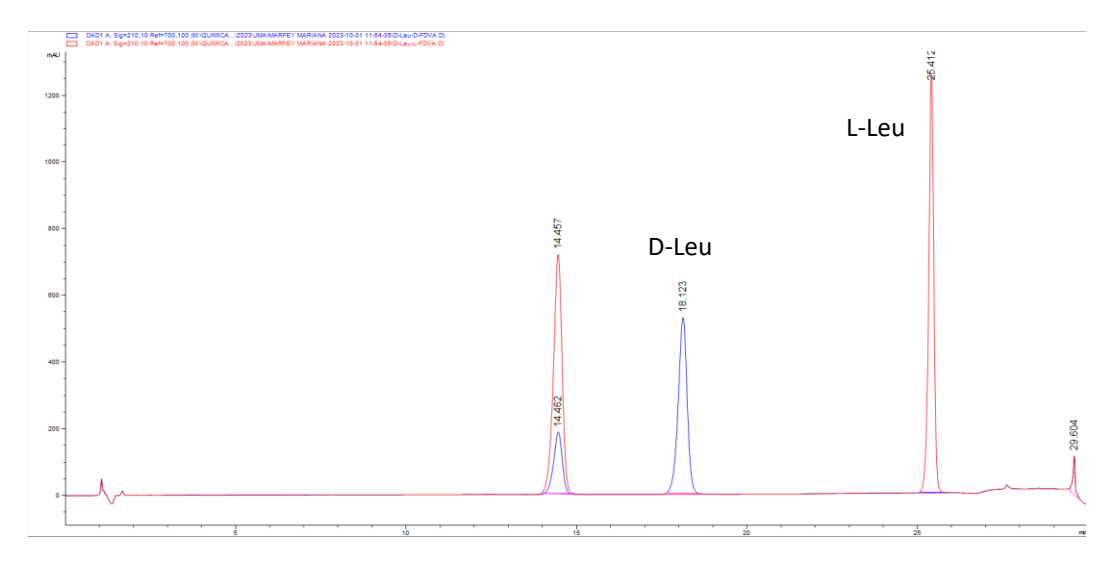


Figure S23. HPLC traces at 210 nm of the D-FDVA derivatives of Leu.

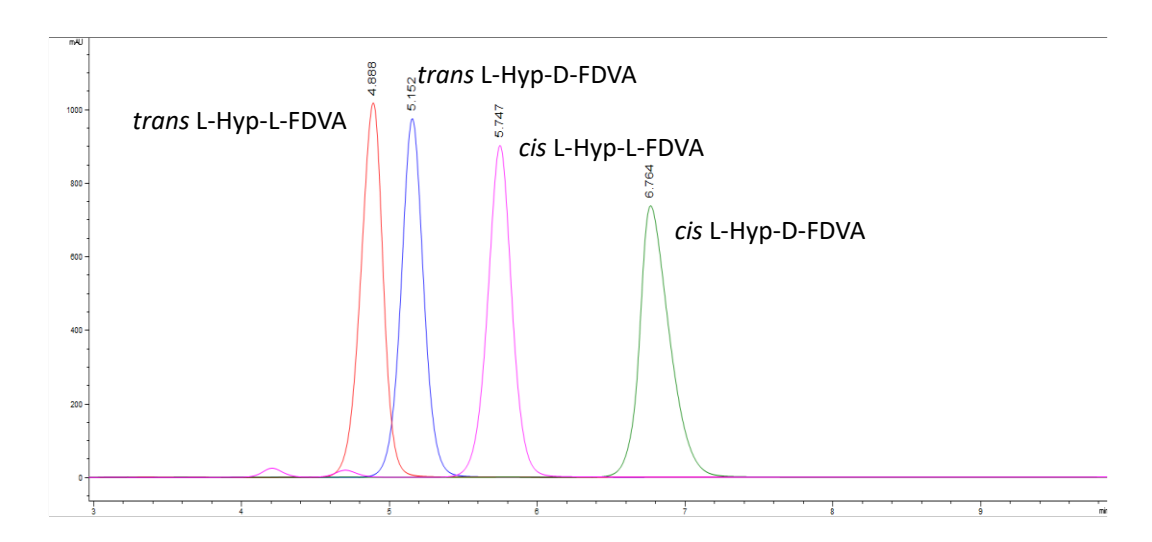


Figure S24. HPLC traces at 210 nm of the D and L-FDVA derivatives of cis and trans L-Hyp.

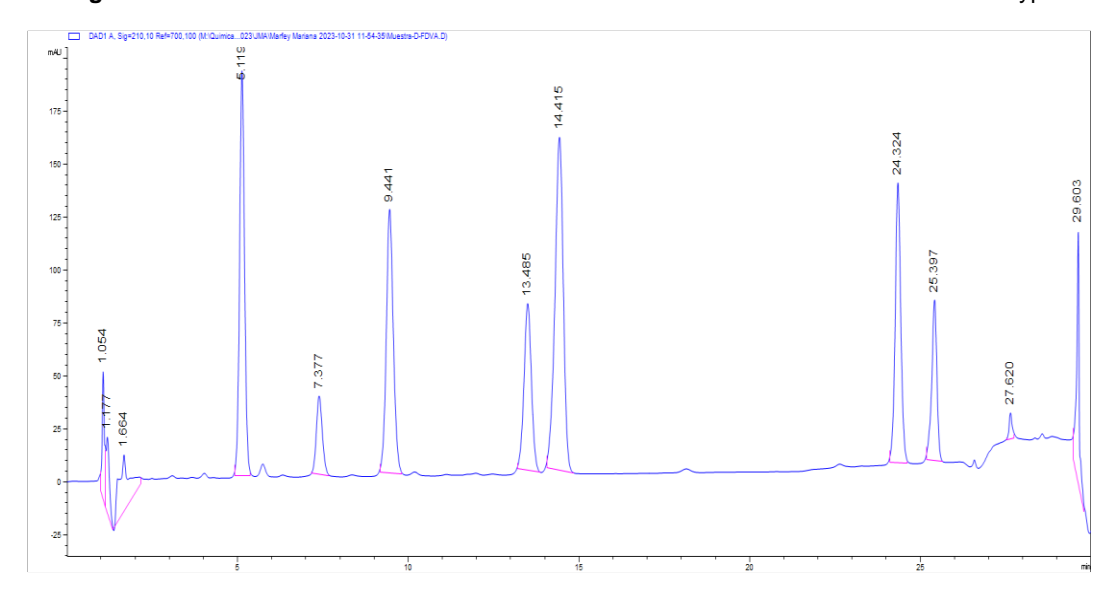


Figure S25. HPLC trace at 210 nm of the D-FDVA derivatives of the hydrolyzate of cellulamide A (2).

APPENDIX IV

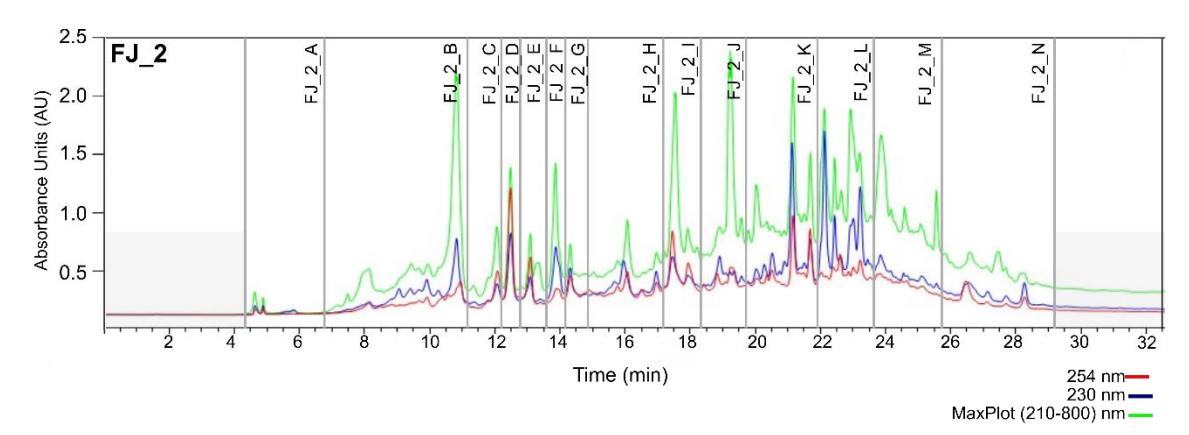


Figure S26. Reverse-phase semi-preparative HPLC chromatogram of CT-F61 FJ_2 sample with the indication of the recovered fractions. The darkest shaded zone corresponds to the baseline, collected separately.

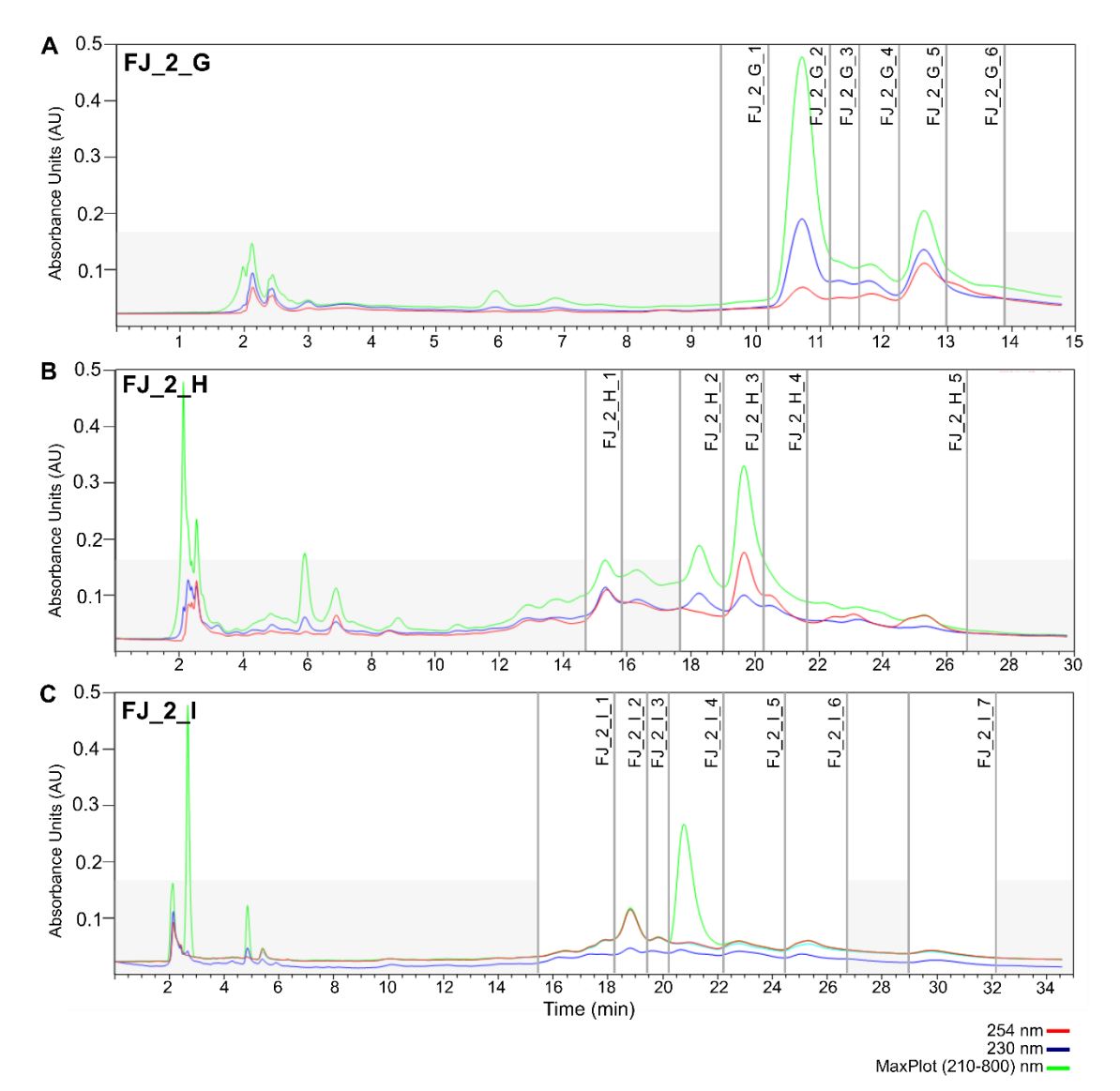


Figure S27. Reverse phase HPLC chromatogram of CT-F61 (**A**) FJ_2_G, (**B**) FJ_2_H and (**C**) FJ_2_I samples with the indication of the recovered fractions. The darkest shaded zone corresponds to the baseline, collected separately.

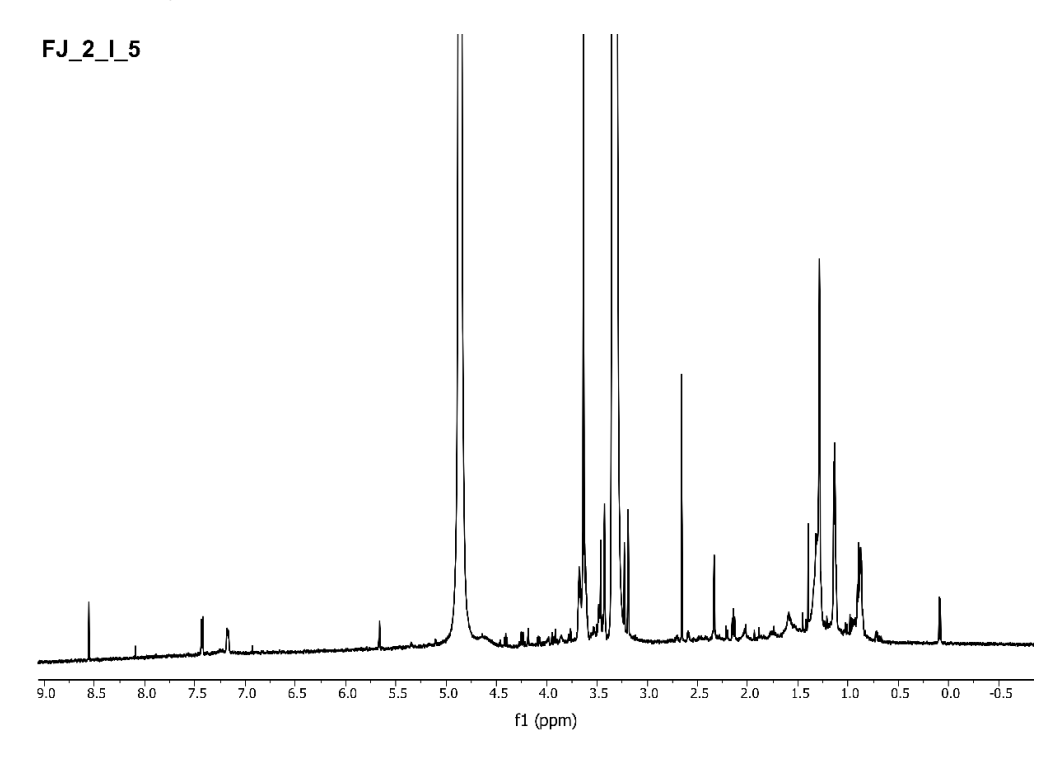


Figure S28. ¹H-NMR (600 MHz, CD₃O) spectrum of fraction FJ_2_I_5 containing the putative novel compound *m/z* 539.35605 [M+Na]⁺ (4).

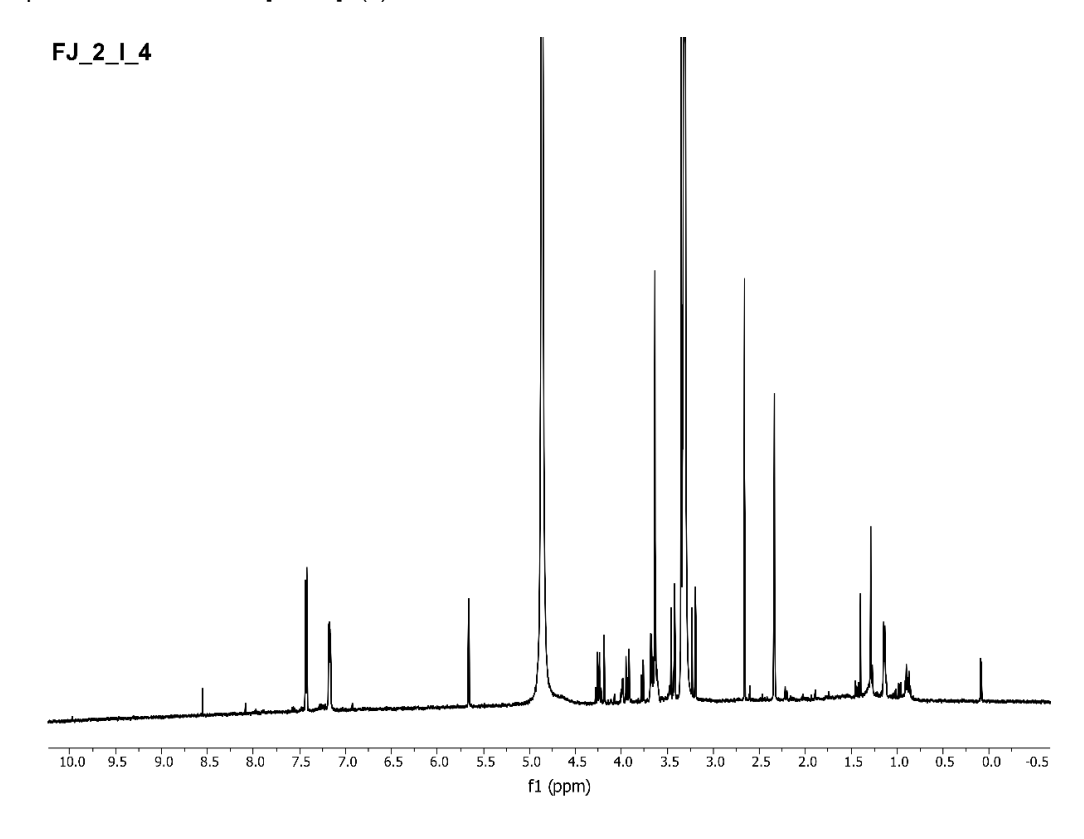


Figure S29. ¹H-NMR (600 MHz, CD₃OH) spectrum of fraction FJ_2_I_4 containing the pure putative novel compound m/z 387.18048 [M+H]⁺ (5).

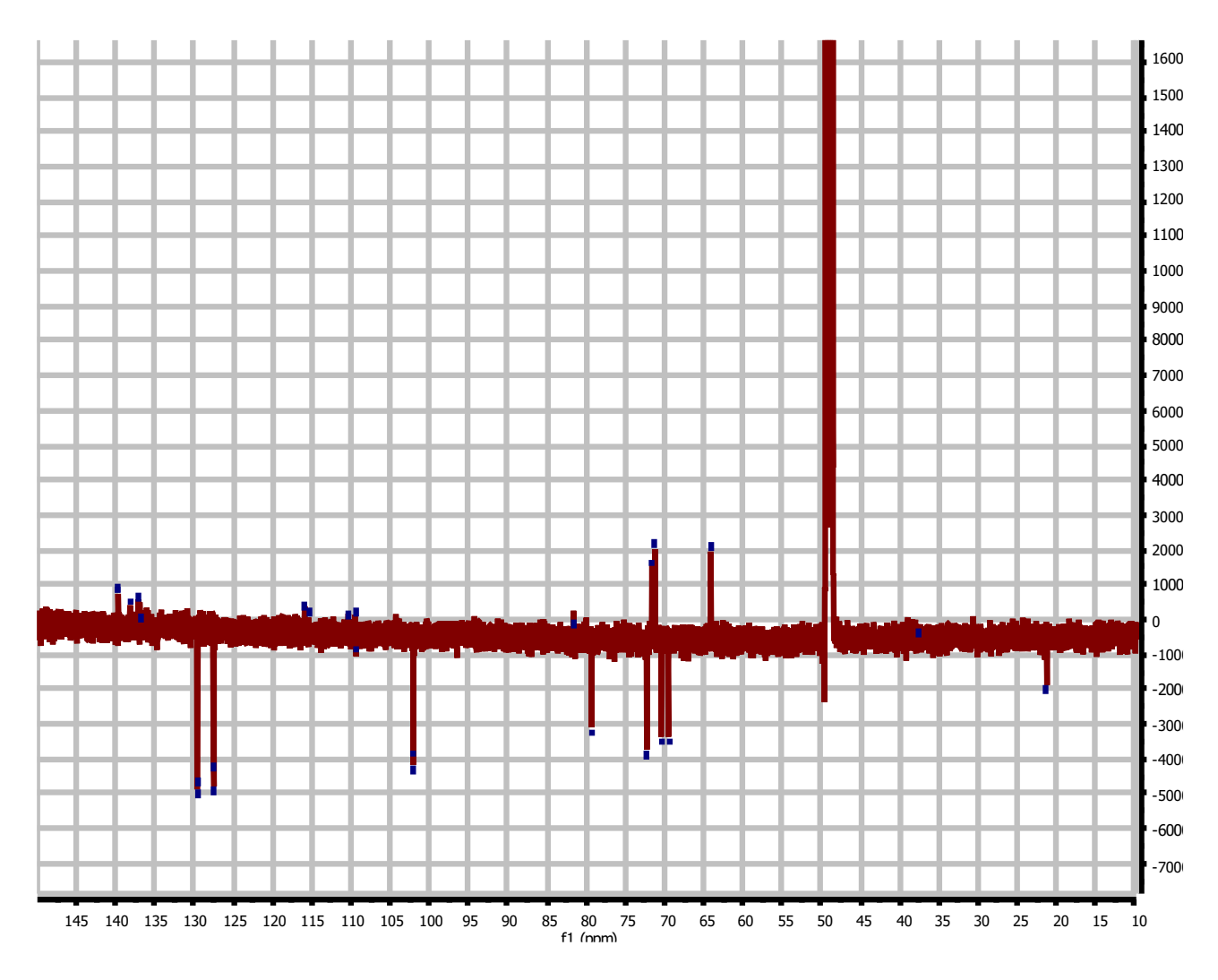


Figure S30. ¹³C-NMR (600 MHz, CD₃OH) spectrum of fraction FJ_2_I_4 containing the pure putative novel compound *m/z* 387.18048 [M+H]⁺ (5).

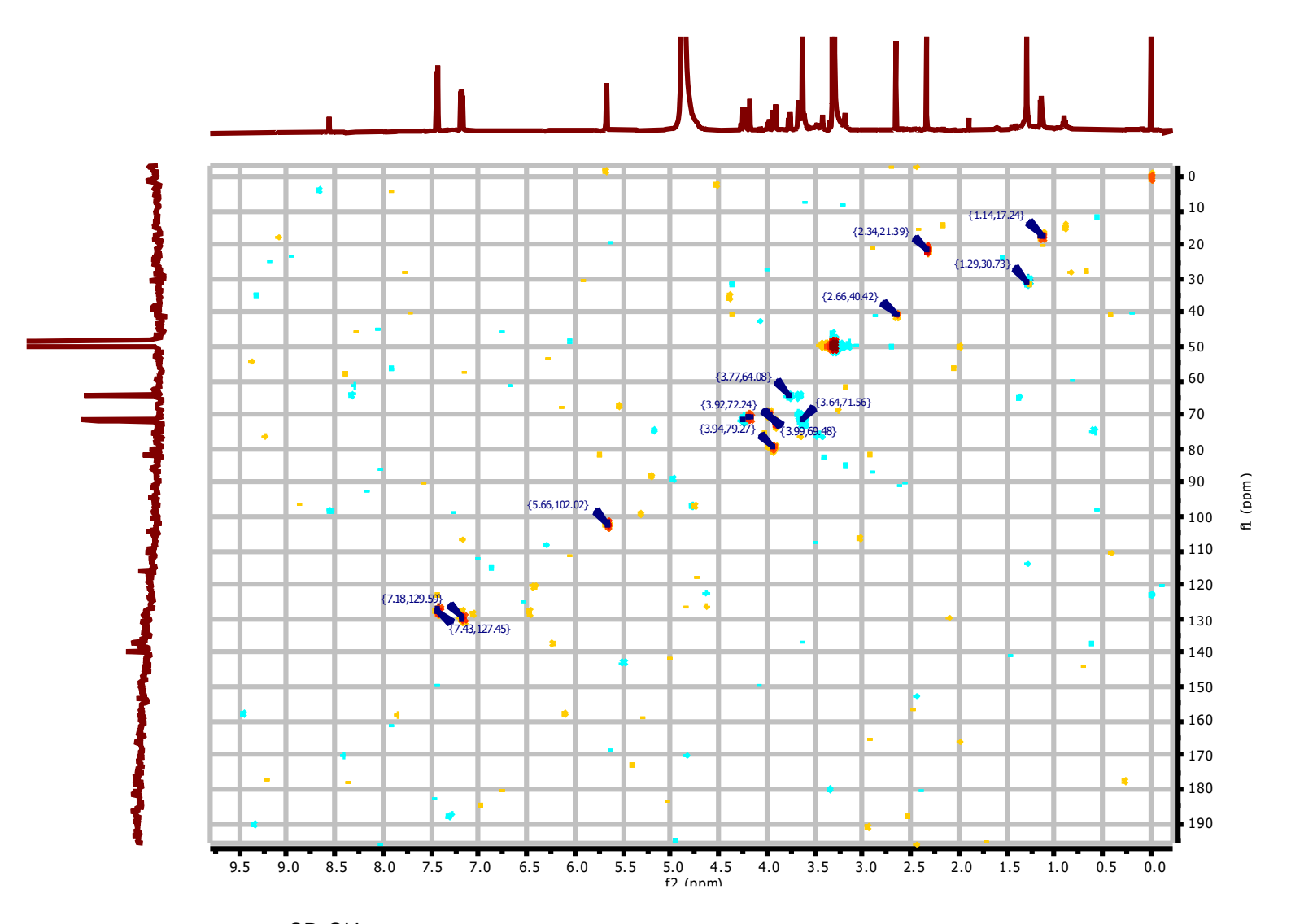


Figure S31. HSQC (600 MHz, CD₃OH) spectrum of fraction FJ_2_I_4 containing the pure putative novel compound *m/z* 387.18048 [M+H]⁺ (5).

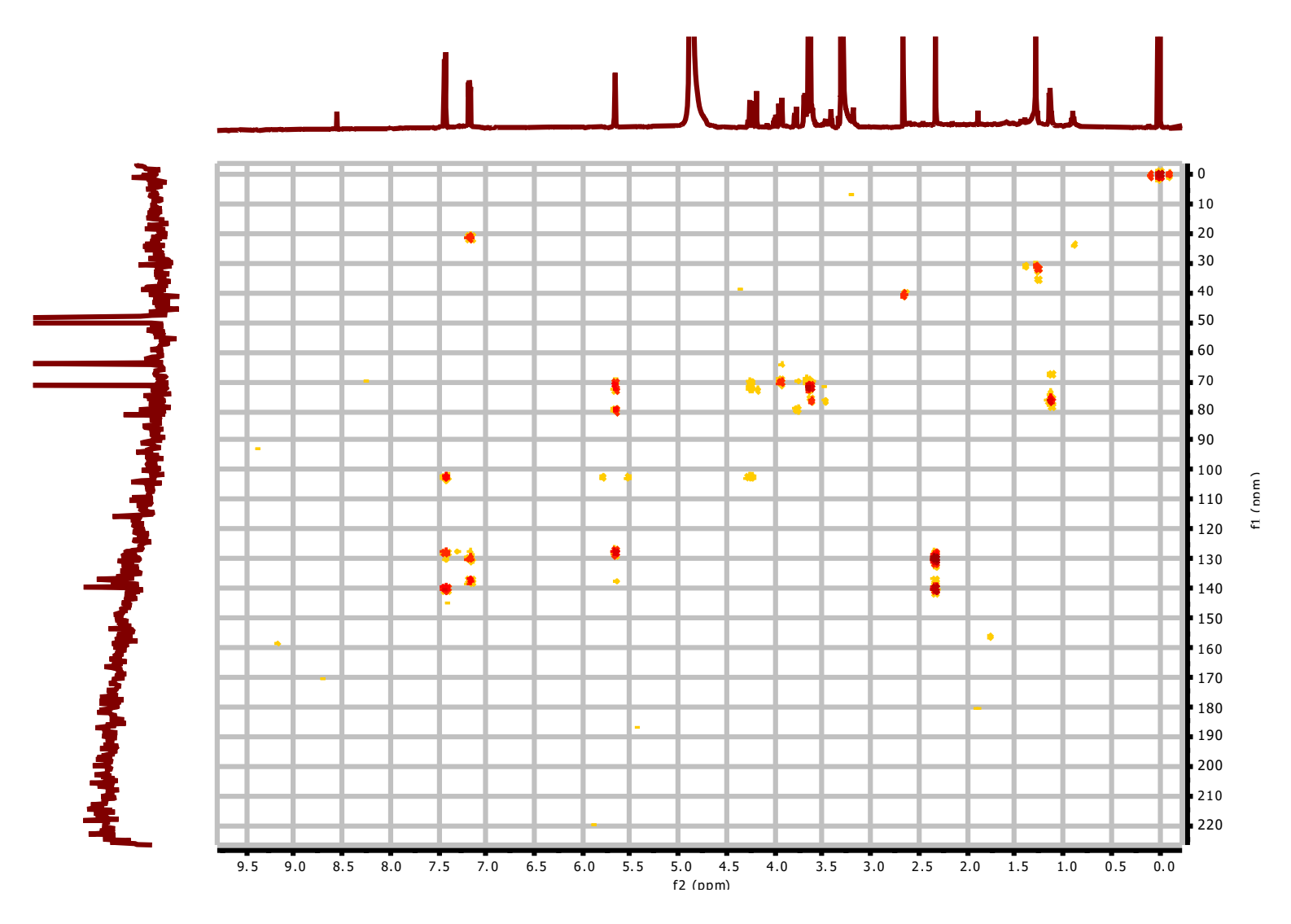


Figure S32. HMBC (600 MHz, CD₃OH) spectrum of fraction FJ_2_I_4 containing the pure putative novel compound *m/z* 387.18048 [M+H]⁺ (5).

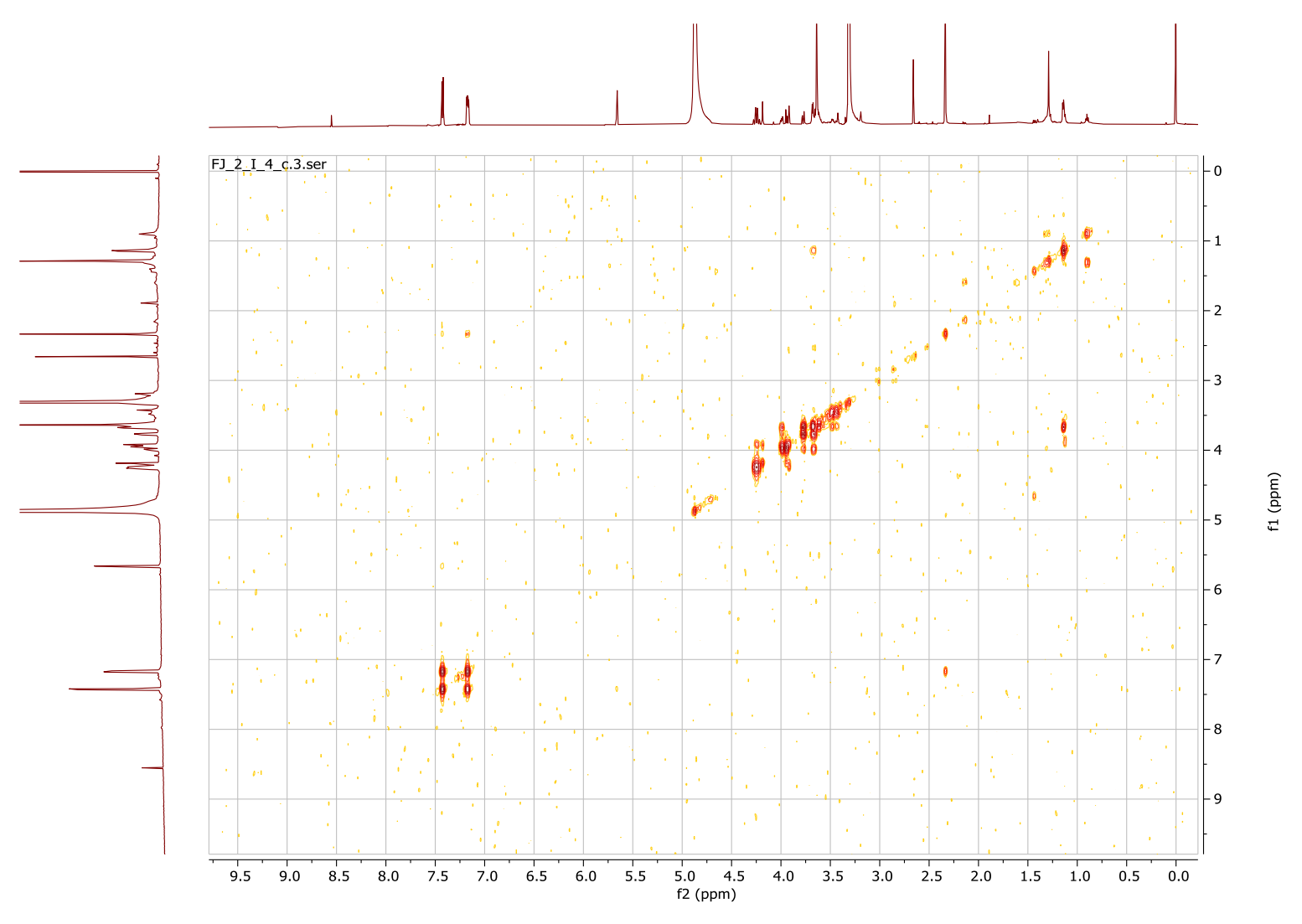


Figure S33. COSY (600 MHz, CD₃OH) spectrum of fraction FJ_2_I_4 containing the pure putative novel compound *m/z* 387.18048 [M+H]⁺ (5).

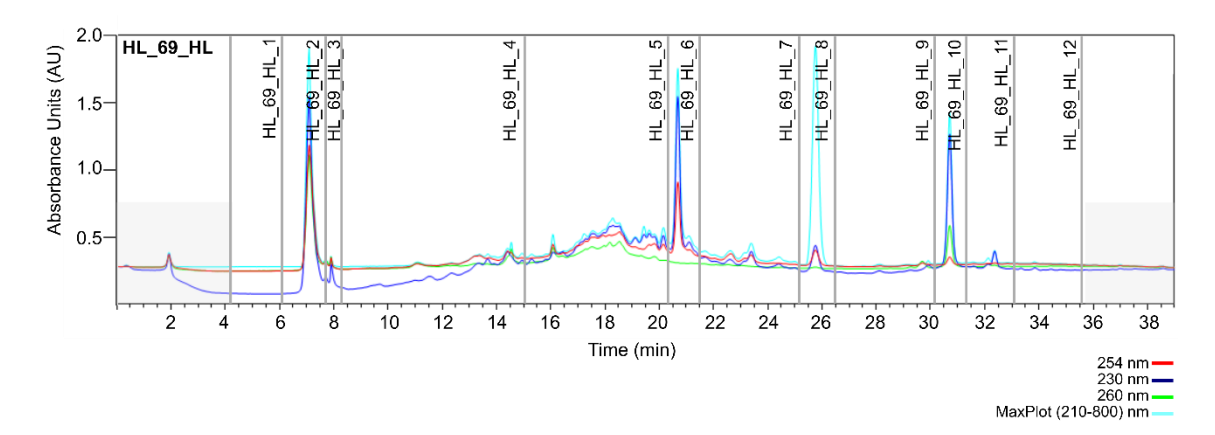


Figure S34. Reverse-phase semi-preparative HPLC chromatogram of CC-F88 HL_69_HL sample with the indication of the recovered fractions. The darkest shaded zone corresponds to the baseline, collected separately.

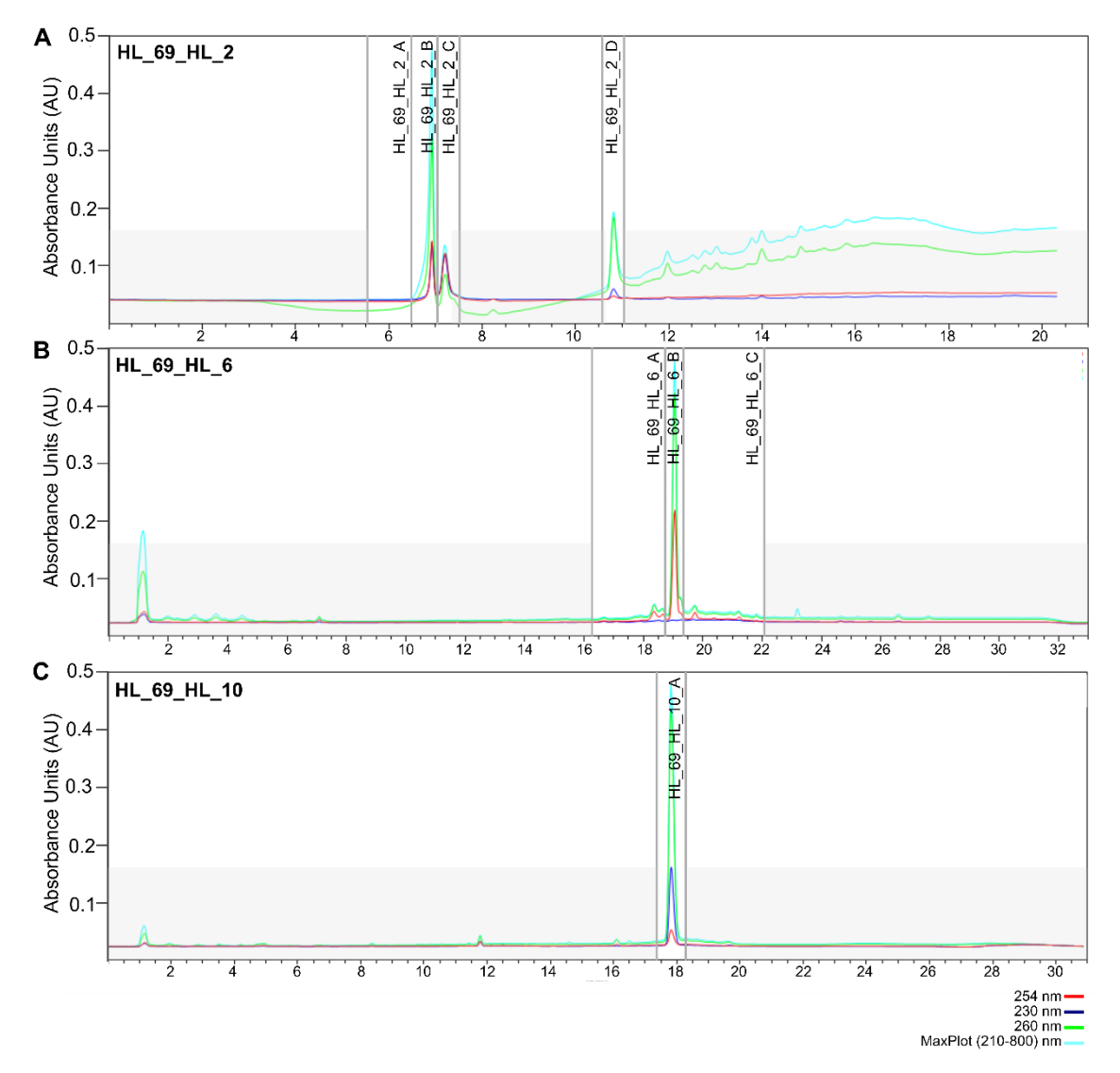


Figure S35. Reverse phase HPLC chromatogram of CC-F88 (**A**) HL_69_HL_2, (**B**) HL_69_HL_6 and (**C**) HL_69_HL_10 samples with the indication of the recovered fractions. The darkest shaded zone corresponds to the baseline, collected separately.

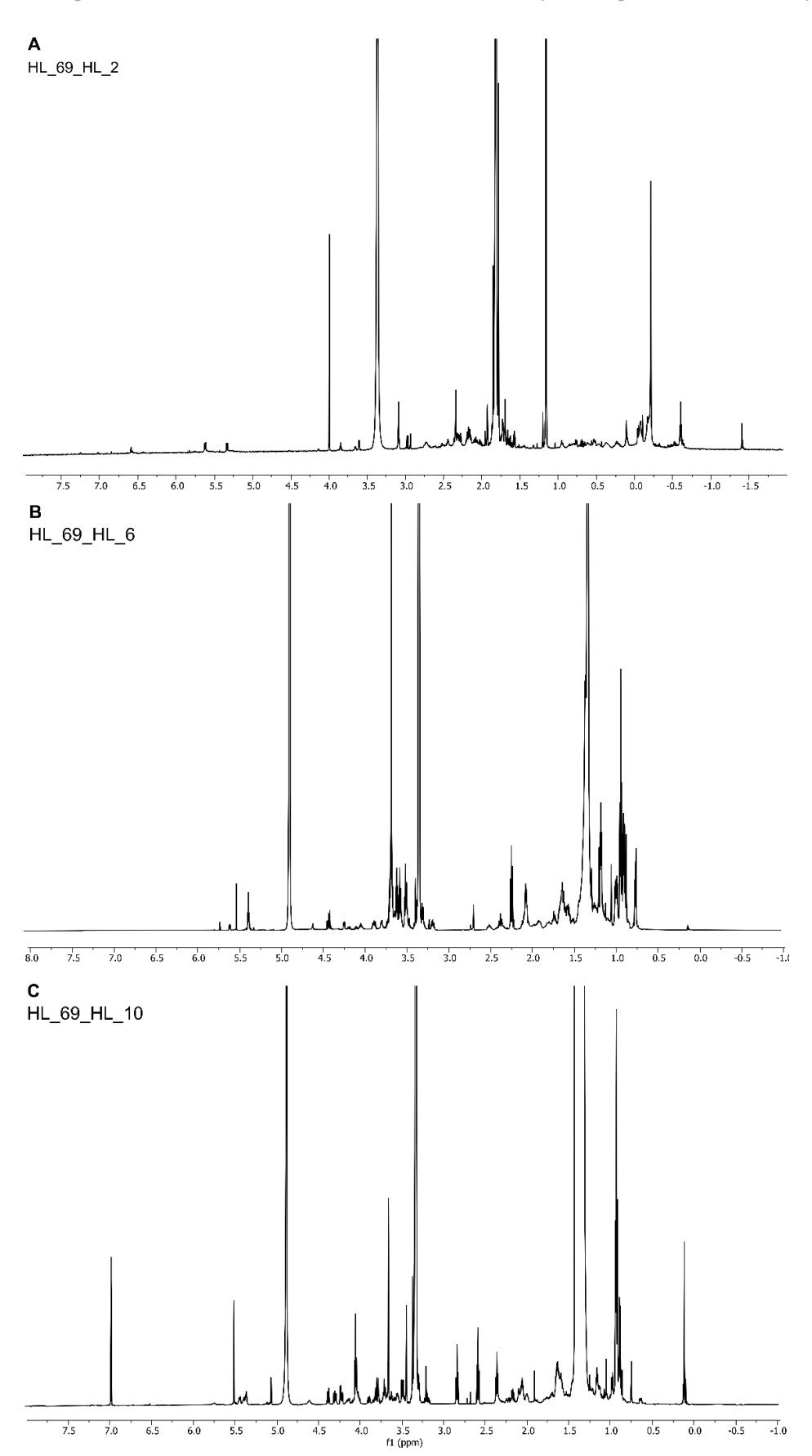


Figure S36. 1 H-NMR (600 MHz, CD₃OD) spectra of fractions (**A**) HL_69_HL_2, (**B**) HL_69_HL_6 and (**C**) HL_69_HL_10.

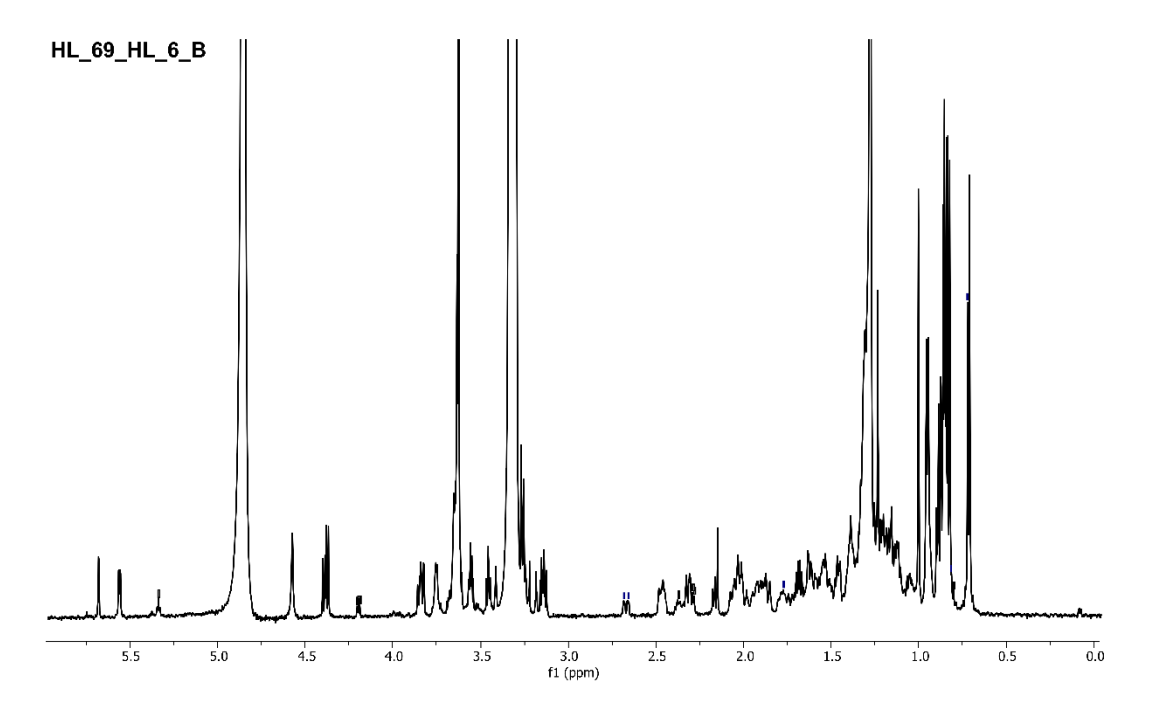


Figure S37. 1 H-NMR (600 MHz, CD₃OD) spectrum of fraction HL_69_HL_6_B containing the pure putative novel compound m/z 635.41809 [M-H] $^{-}$ (6).

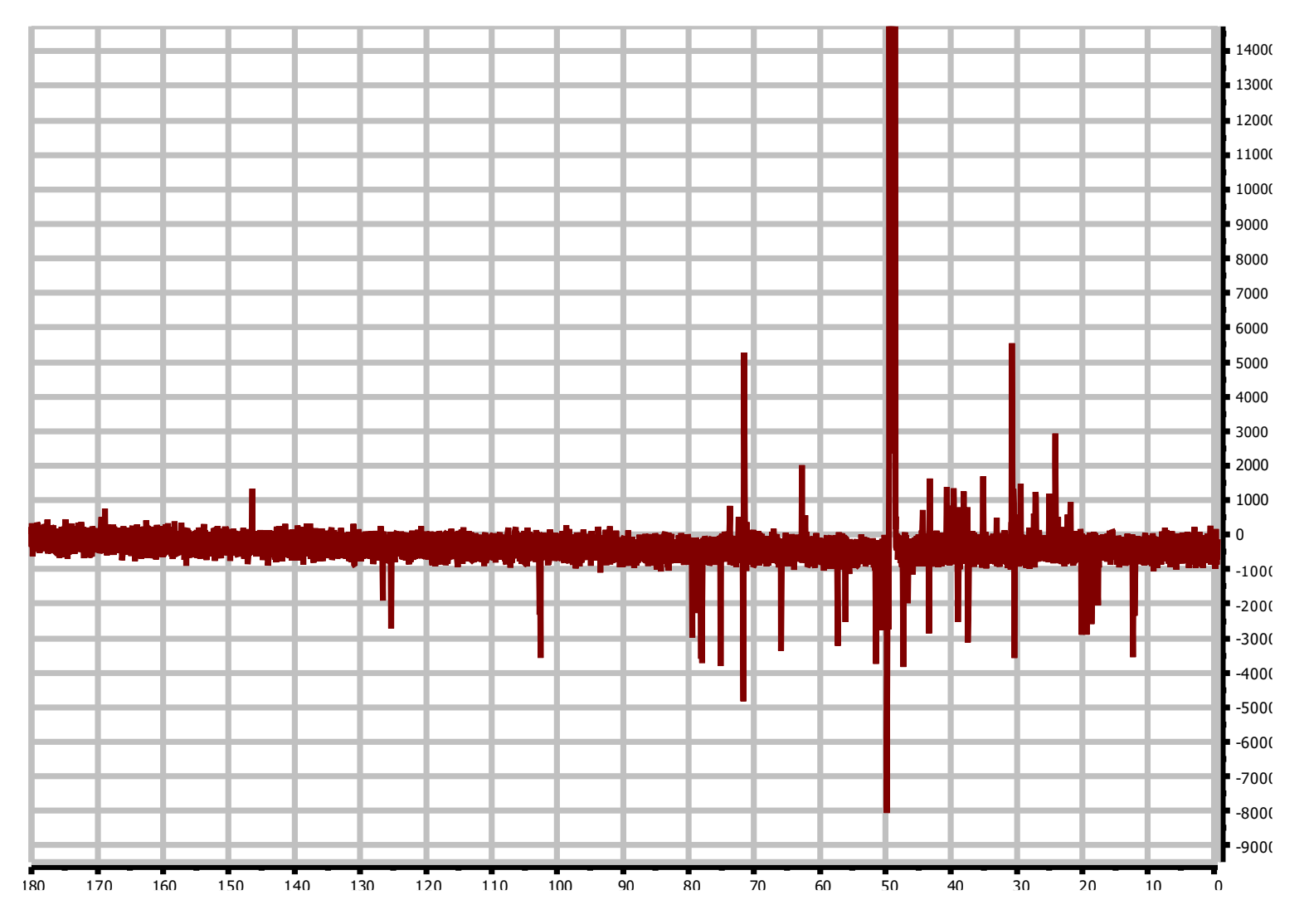


Figure S38. ¹³C-NMR (600 MHz, CD₃OH) spectrum of fraction HL_69_HL_6_B containing the pure putative novel compound *m/z* 635.41809 [M-H]⁻ (6).

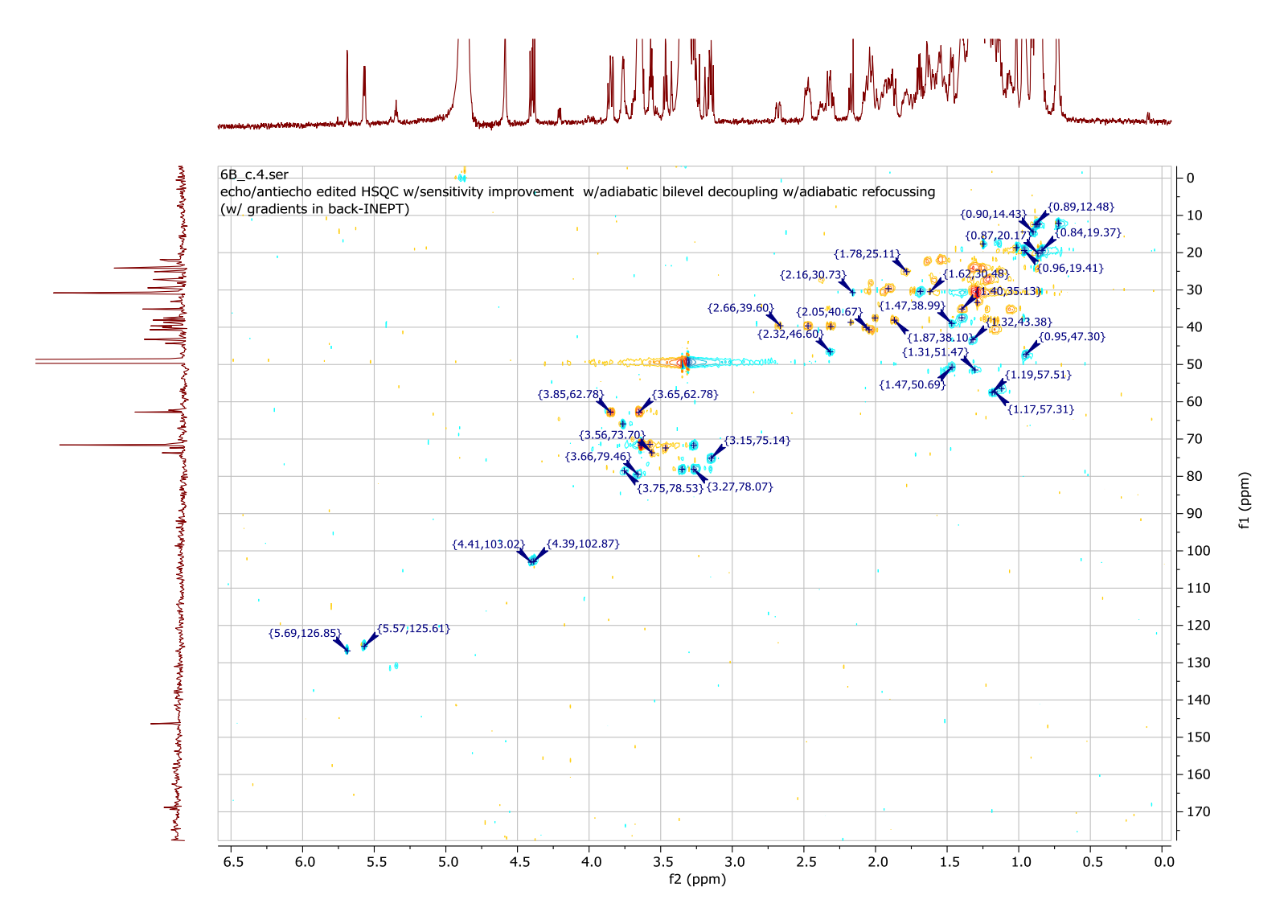


Figure S39. HSQC (600 MHz, CD₃OH) spectrum of fraction HL_69_HL_6_B containing the pure putative novel compound *m/z* 635.41809 [M-H]⁻ (6).

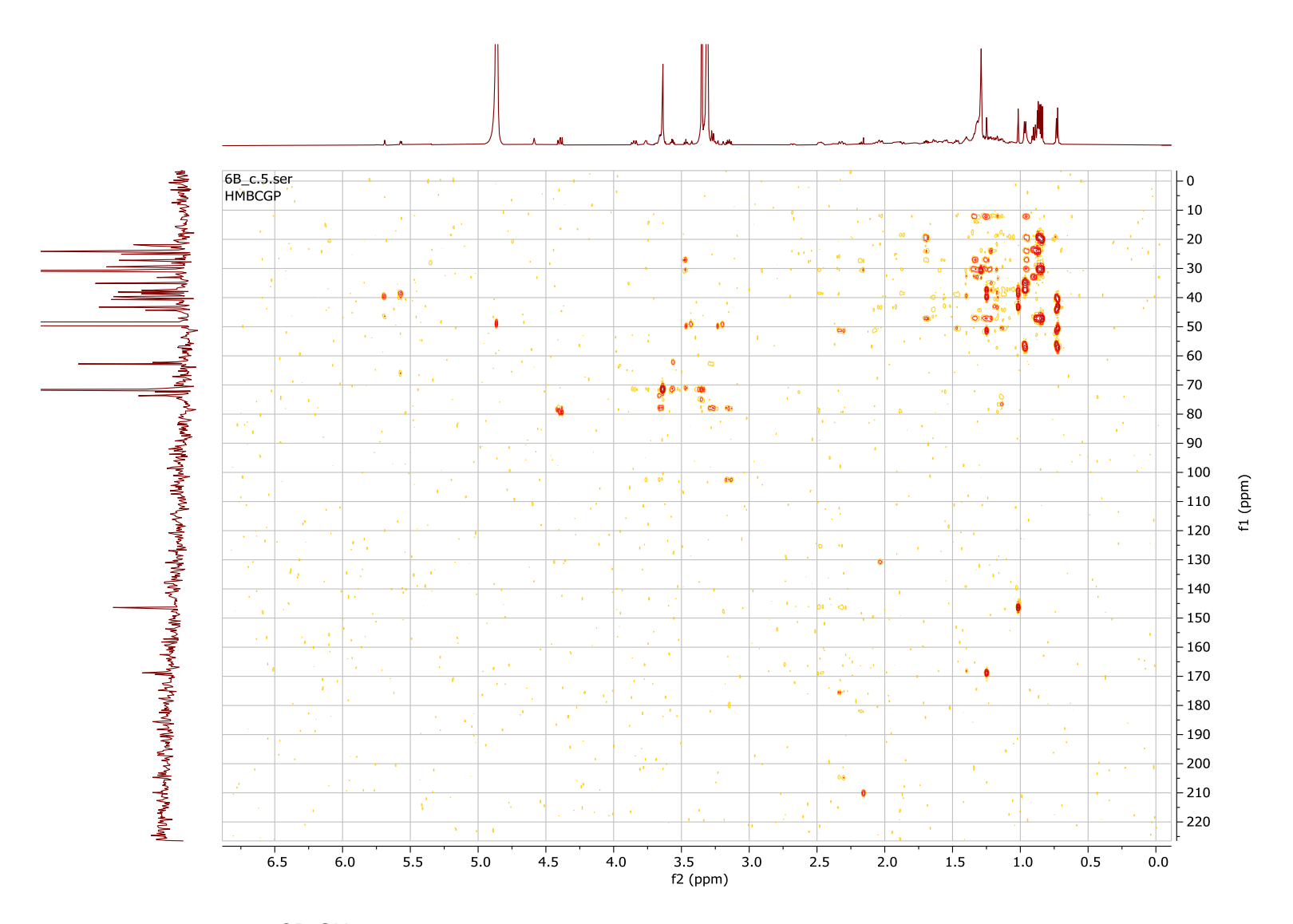


Figure S40. HMBC (600 MHz, CD₃OH) spectrum of fraction HL_69_HL_6_B containing the pure putative novel compound *m/z* 635.41809 [M-H]⁻ (6).

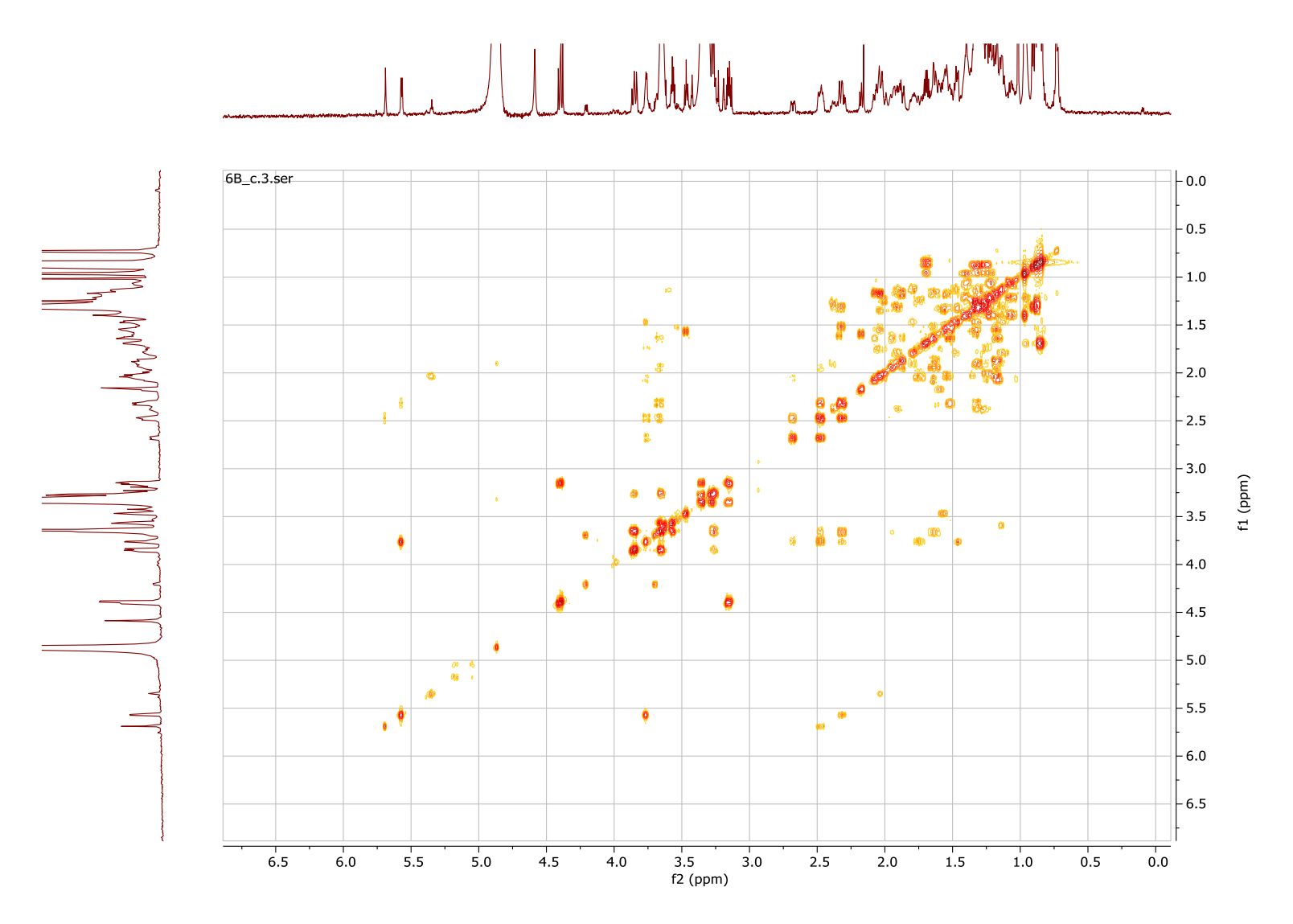


Figure S41. COSY (600 MHz, CD₃OH) spectrum of fraction HL_69_HL_6_B containing the pure putative novel compound *m/z* 635.41809 [M-H]⁻ (6).

Table S14. Normal-phase FC conditions used to fractionate CT-F61 FJ sample. The solvent mixture is presented, as well as the volume used and the corresponding collection tubes.

Eluents Mixture	Volume (mL)	Tubes
100% CH ₂ Cl ₂	250	1-4
99% CH ₂ Cl ₂ : 1% MeOH	100	5-12
98% CH ₂ Cl ₂ : 2% MeOH	100	13-19
97% CH ₂ Cl ₂ : 3% MeOH	100	20-27
96% CH ₂ Cl ₂ : 4% MeOH	100	28-38
95% CH ₂ Cl ₂ : 5% MeOH	100	39-43
94% CH ₂ Cl ₂ : 6% MeOH	100	44-52
93% CH ₂ Cl ₂ : 7% MeOH	100	53-60
92% CH ₂ Cl ₂ : 8% MeOH	100	61-67
91% CH ₂ Cl ₂ : 9% MeOH	100	68-76
90% CH ₂ Cl ₂ : 10% MeOH	100	77-82
88% CH ₂ Cl ₂ : 12% MeOH	50	83-85
86% CH ₂ Cl ₂ : 14% MeOH	50	85-89
85% CH ₂ Cl ₂ : 15% MeOH	100	90-95
70% CH ₂ Cl ₂ : 30% MeOH	100	96-104
50% CH ₂ Cl ₂ : 50% MeOH	250	105-124
30% CH ₂ Cl ₂ : 70% MeOH	100	125-132
100% MeOH	200	RB 1
90% MeOH: 10% H ₂ O	100	RB 2
50% MeOH: 50% H ₂ O	200	RB 3

MeOH: methanol; H₂O: water; RB: round bottom balloon

Table S15. Normal-phase FC fractions of CT-F61 FJ sample. The collection tubes corresponding to each fraction are presented, as well as the yielded mass (mg).

Fraction	Tubes	Mass (mg)
FJ_1	1-55	13.94
FJ_2	56-66	68.35
FJ_3	67-75	609.23
FJ_4	76-90	117.79
FJ_5	91-100	43.25
FJ_6	101-109	62
FJ_7	110-117	419.11
FJ_8	118-132	152.87
FJ_9	RB 1	35.58
FJ_10	RB 2	25.49
FJ_11	RB 3	74.24

RB: round bottom balloon

Table S16. Reverse-phase semi-preparative HPLC conditions used to fractionate CT-F61 FJ_2 sample.

Time (min)	MeOH (%)	H ₂ O (%)
0	30	70
20	100	0
30	100	0
32	30	70
34	30	70

MeOH: methanol; H₂O: water;

Table S17. Reverse-phase HPLC fractions of CT-F61 FJ_2 sample with the indication of the yielded mass (mg).

Fraction	Mass (mg)
FJ_2_A	1.05
FJ_2_B	1.34
FJ_2_C	1.44
FJ_2_D	0.31
FJ_2_E	0.38
FJ_2_F	0.97
FJ_2_G	1.01
FJ_2_H	1.58
FJ_2_I	3.45
FJ_2_J	8.73
FJ_2_K	30.63
FJ_2_L	3.48
FJ_2_M	3.48
FJ_2_N	4.96
BL	1.77
BL – baseline	

Table S18. Reverse-phase HPLC fractions of CT-F61 FJ_2_G, FJ_2_H and FJ_2_I samples with the indication of the yielded mass (mg).

Fraction	Mass (mg)	Fraction	Mass (mg)	Fraction	Mass (mg)
FJ_2_G_1	0	FJ_2_H_1	0.13	FJ_2_l_1	0.22
FJ_2_G_2	0.11	FJ_2_H_2	0.81	FJ_2_I_2	0.17
FJ_2_G_3	0.08	FJ_2_H_3	0	FJ_2_I_3	0.31
FJ_2_G_4	0.12	FJ_2_H_4	0.25	FJ_2_I_4	0.30
FJ_2_G_5	0.60	FJ_2_H_5	0.24	FJ_2_I_5	0.21
FJ_2_G_6	0.19	FJ_2_H_BL	0.61	FJ_2_I_6	0.72
FJ_2_G_BL	0.17			FJ_2_I_7	0.96
				FJ_2_I_BL	0.88

BL – baseline

Table S19. Reverse-phase VLC conditions used to fractionate CC-F88 crude extract. The solvent mixture used to obtain each fraction is shown, as well as the yielded mass (mg).

Fraction	MeOH (%)	H ₂ O (%)	Volume (mL)	Mass (mg)
Α	5	95	1000	3675.8
В	10	90	500	590.1
С	20	80	500	134.49
D	30	70	500	29.66
E	40	60	500	31.39
F	50	50	500	27.31
G	70	30	500	17.58
Н	90	10	500	350.92
I1	100	0	1000	844.71
12	100	0	1000	160.75
J	100 AC	-	500	40.44
K	100 DCM	-	500	523.71
L	100	0	1000	59.54

MeOH: methanol; H₂O: water; AC: acetone; DCM: dichloromethane

Table S20. Normal-phase FC conditions used to fractionate CC-F88 HL sample. The solvent mixture used to obtain each fraction is shown as well, as the yielded mass (mg).

Fraction	MeOH (%)	Hex (%)	EtOAc (%)	Volume (mL)	Mass (mg)
HL_1	-	90	10	400	202.4
HL_2	-	70	30	150	36.26
HL_3	-	50	50	150	41.28
HL_4	-	30	70	150	45.2
HL_5	-	0	100	150	20.23
HL_6	10	-	90	150	5.78
HL_7	30	-	70	150	28.50
HL_8	50	-	50	150	84.31
HL_9	70	-	30	150	262.62
HL_10	90	-	10	150	224.95
HL_11	100	-	-	150	114.35
HL_12		1:1 MeOH+DCI	М	400	27.56

MeOH: methanol; Hex: hexane; EtOAc: ethyl acetate; DCM: dichloromethane

Table S21. Reverse-phase FC conditions used to fractionate CC-F88 HL_69 sample.

Time (min)	H ₂ 0 (%)	MeOH (%)	Isopropanol (%)
0	70	30	-
45	0	100	-
55	0	100	-
75	-	10	90
80	-	10	90

MeOH: methanol; H₂O: water

Table S22. Reverse-phase FC fractions of CC-F88 HL_69 sample, with the indication of the corresponding collection tubes and yielded mass (mg).

Fraction	Collection Tubes	Mass (mg)
HL_6-9_A	2-3	9.91
HL_6-9_B	4-6	1.44
HL_6-9_C	7-9	1.32
HL_6-9_D	10-16	2.04
HL_6-9_E	17-21	2.28
HL_6-9_F	22-32	114.61
HL_6-9_G	33-39	100.57
HL_6-9_H	40-47	20.78
HL_6-9_I	48-56	8.88
HL_6-9_J	57-64	8.86
HL_6-9_K	65-2'	9.68
HL_6-9_L	2'-6'	0.98
HL_6-9_M	7'-10'	0.80
HL_6-9_N	11'-39'	2.96
HL_6-9_wash	-	8.46

Table S23. Reverse-phase semi-preparative HPLC conditions used to fractionate CC-F88 HL_69_HL sample.

Time (min)	MeOH (%)	H ₂ O (%)	Isopropanol (%)
0	60	40	0
10	100	0	0
20	100	0	0
30	20	0	80
35	20	0	80
37	60	40	0
39	60	40	0

Table S24. Reverse-phase semi-preparative HPLC fractions of CC-F88 HL_69_HL sample, with the indication of the corresponding yielded mass (mg).

Fraction	Mass (mg)	Mass (%)
HL_69_HL_1	0.77	1.42
HL_69_HL_2	1.69	3.12
HL_69_HL_3	3.74	6.90
HL_69_HL_4	3.32	6.12
HL_69_HL_5	22.51	41.52
HL_69_HL_6	3.52	6.49
HL_69_HL_7	3.5	6.46
HL_69_HL_8	2.47	4.56

HL_69_HL_9	2.61	4.81
HL_69_HL_10	1.9	3.50
HL_69_HL_11	1.66	3.06
HL_69_HL_12	2.69	4.96
HL_69_HL_13	3.83	7.07

Table S25. Reverse-phase analytical HPLC conditions used to fractionate CC-F88 HL_69_HL_2, HL_69_HL_6 and HL_69_HL_10 samples.

	Time (min)	H20 (%)	MeOh (%)	Isopropanol (%)
HL_69_HL_2	0	40	60	0
	10	0	100	0
	18	0	100	0
	20	40	60	0
	21	40	60	0
HL_69_HL_6	0	30	70	0
	20	0	100	0
	35	0	100	0
	36	30	70	0
	40	30	70	0
HL_69_HL_10	0	30	70	0
	10	0	100	0
	20	0	100	0
	25	0	20	80
	27	30	70	0
	31	30	70	0

MeOH: methanol; H₂O: water

Table S26. Reverse-phase analytical HPLC fractions of HL_69_HL_2, HL_69_HL_6 and HL_69_HL_10 samples with the indication of the yielded mass (mg).

Fraction	Mass (mg)	Fraction	Mass (mg)	Fraction	Mass (mg)
HL_69_HL_2_A	0.16	HL_69_HL_6_A	1.08	HL_69_HL_10_A	0.6
HL_69_HL_2_B	0.79	HL_69_HL_6_B	0.4	HL_69_HL_6_BL	1.03
HL_69_HL_2_C	0.43	HL_69_HL_6_C	1.33		
HL_69_HL_2_D	0.2	HL_69_HL_6_BL	0.43		
HL_69_HL_2_BL	1.4				

BL - baseline